Ligand regulation of muscarinic acetylcholine receptor organisation

A thesis presented for the degree of Doctor of Philosophy in Biochemistry and Molecular Biology

Despoina Aslanoglou

Division of Biochemistry and Molecular Biology
Institute of Molecular, Cell and Systems Biology

University of Glasgow

December 2015

UNIVERSITY
of
GLASGOW

Abstract

Muscarinic acetylcholine receptors (M_1-M_5) belong to the class A family of transmembrane G protein coupled receptors (GPCRs) and mediate various signalling processes. M_1, M_3 and M_5 predominantly couple to G_q and promote intracellular calcium ion release from the endoplasmic reticulum. M_2 and M_4 preferentially couple G_i inhibiting adenylyl cyclase activity to thus decrease cAMP production and acting to regulate various ion channels. There is growing evidence that many GPCRs can exist as dimers or higher-order oligomers (Milligan, 2013) and muscarinic receptors are no exception (Alvarez-Curto *et al.*, 2010). Herein, combinations of homomers and heteromers of co-expressed human M_2 (hM_2WT) and a RASSL (Receptor Activated Solely by Synthetic Ligand) form of the human M_3 receptor (hM_3RASSL) (Alvarez-Curto *et al.*, 2011) were demonstrated to occur using N-terminal SNAP and CLIP tags in combination with homogeneous time resolved FRET (htrFRET).

Stable Flp-In™ T-REx™ 293 cell lines able to inducibly express each of these receptor forms upon addition of doxycycline, and a cell line able to express both the hM_3RASSL constitutively and hM_2WT in a doxycycline inducible manner were generated. In these cells both hM_3RASSL and hM_2WT were detected after treatment with different concentrations of doxycycline via Western blots using tag-specific antibodies. Radioligand binding using [^{3}H]-QNB indicated that similar amounts of hM_2WT and hM_3RASSL were expressed following induction with 5 ng.ml^{-1} doxycycline in the cells co-expressing the two receptors. Expression of the receptors was observed at the surface of live cells following labelling of the expressed receptors with SNAP and CLIP-specific cell impermeant substrates. Following induction with doxycycline each of hM_2WT and hM_3RASSL homomers and hM_2WT-hM_3RASSL heteromers were identified. Detection of oligomers was achieved following co-labelling with htrFRET-compatible substrates. Occupancy of hM_2WT-hM_3RASSL heteromers with the hM_2WT agonist carbachol resulted in a marked, time and concentration-dependent decrease in detected heteromers and a concomitant, concentration-dependent increase in hM_2WT homomers. The dynamics of interchange between heteromers and homomers was investigated by using a multiplex labelling approach and htrFRET. This method involved labelling with one energy donor and two energy acceptors capable of emitting at distinct wavelengths. Results confirmed the hM_2WT-hM_3RASSL heteromer to hM_2WT homomer transition upon selective carbachol-mediated activation of hM_2WT. A small increase in the hM_3RASSL homomer was detected upon activation of the hM_3RASSL with the selective agonist clozapine-N-oxide, but this was only observed in the absence of heteromers.

Despite the presence of hM_2WT-hM_3RASSL heteromers the functional pharmacology of hM_2WT and hM_3RASSL receptor specific agonists was largely unaltered.

Table of Contents

List of Figures

List of Tables

Acknowledgements

I would like to express my special appreciation to Professor Graeme Milligan for the opportunity he offered me to undertake this project and also for his guidance throughout the course of the PhD. I am also indebted to my co-supervisor Dr Elisa Alvarez-Curto for her guidance, support and her input into the project. I would also like to extend warm thanks to all the members of the Milligan lab, both past and present. In particular, I would like to thank Dr Brian Hudson, Dr Amanda Mackenzie, Laura Jenkins, Dr Richard Ward, Dr Sara Marsango, Dr Maria Jose Varela Liste, Dr Kenneth Watterson and all the PhD students in Lab 253. A special thanks to Dr John Pediani for his help with the microscopy work! I would like to express my gratitude to the Medical Research Council for funding my PhD.

I am grateful to my friends Maria, Aris, Christos and Emmanuela for their friendship and the great nights in the puband also for their support during the difficult times. I particularly want to thank my very good friend Aris for encouraging me during the write up of the Thesis.

Finally, I would like to dedicate this thesis to the best teachers in the world, my mother, Ioanna and my father, Dimitris.

Author’s Declaration

The work presented in this thesis was conducted by the author, unless otherwise stated. No part of the work has been previously presented for any degree either in this University or any other institution.

Definitions/Abbreviations

Ach: acetylcholine

ADP: adenosine diphosphate

ATP: adenosine triphosphate

Atr: Atropine; non-selective, orthosteric muscarinic antagonist

BCA: bicinchoninic acid

BN PAGE: Blue Native polyacrylamide gel electrophoresis

BRET: Bioluminescence resonance energy transfer

BSA: Bovine serum albumine

cAMP: cyclic adenosine monophosphate

Cch: carbachol; non-selective, orthosteric muscarinic agonist

CD86: cluster of differentiation 86

cDNA: complementary deoxyribonucleic acid

CNS: Central nervous system

CNO: clozapine-N-oxide

Co-IP: co-immuno-precipitation

C-terminus: carboxyl domain of a protein that lies in the cytosolic region of the cell in the case of GPCRs

DDM: n-dodecyl-β-D-maltoside

dNTP: deoxyribonucleotide

Dox: doxycycline

dpm: disintegrations per minute

DREADD: designer receptor exclusively activated by designer drugs

EDTA: ethylenediaminetetraacetic acid

FBS: fetal bovine serum

FlpIn™ TREx™ 293 cells: used for the generation of stable cell lines allowing homogeneous expression of the protein of interest from a FlpIn expression vector in the FRT site. Expression of protein is under the control of a tetracycline repressor protein (TREx)

fmol: fempto mol

FRT site: Flip recombination target

FRET: Forster resonance energy transfer; commonly known as fluorescence resonance energy transfer

FSK: forskolin

G protein: guanine nucleotide-binding protein

GDP: guanosinediphosphate

GTP: guanosine triphosphate

GPCR: G protein-coupled receptor

[^{3}H]-QNB: tritiated quinuclidinyl benzilate

HA: hemagglutinin epitope tag

HBSS: Hank's Balanced Salt solution

HEK 293: Human embryonic kidney cells

HEPES: 4-(2-hydroxyethyl)-1-piperazineethanesulfonic acid

htrFRET: homogeneous time-resolved fluorescence resonance energy transfer

IP-1: inositol monophosphate

IP: immuno-precipitation

IL3: third intracellular loop

Ki: dissociation constant

kDa: kilo Dalton

mAChR: muscarinic acetylcholine receptor

min: minute

nm: nano meter

nM: nano Molar

ng: nano gram

N-terminus: amino terminal domain of a protein that lies in the extracellular region in the case of GPCRs

PAGE: polyacrylamide gel electrophoresis

PBS: phosphate buffered saline

PLA: proximity ligation assay

r: Pearson's correlation coefficient

RASSL: receptor activated solely by synthetic ligand

RET: resonance energy transfer

RIPA: radioimmune precipitation assay buffer

SDS: sodium dodecyl sulphate

TM: transmembrane domain

Tun: tunicamycin

Chapter 1

Introduction

1.1 G protein-coupled receptors

G protein-coupled receptors (GPCRs) are a large and diverse family of plasma membrane proteins. They are highly conserved throughout evolution with approximately 1-2% of the human genome encoding for GPCRs. The evolution of multicellular organisms was partly dependent on the successful evolution of GPCRs, being able to transduce extracellular signals to intracellular functions, and thus, enabling cells to communicate with each other and with their environment (Bockaert and Pin, 1999). GPCRs are present in insects (Hill *et al.*, 2002) and plants (Insel *et al.*, 2012) and thus are considered to be of ancient origin (Perez, 2005). They are also present in nematodes with the *C.elegans* genome encoding more than 1000 GPCRs (Bargmann, 1998), in yeast (Versele *et al.*, 2001) and protozoa (Vernier *et al.*, 1995).

GPCRs are recognised by a vast variety of ligands, including ions, odorants, lipids, photons, amino acids, hormones and polypeptides (Kobilka, 2007) and are involved in several cell signalling transduction pathways that regulate numerous important cellular processes (Lagerstrom and Schioth, 2008), thus possessing a vital role in sensing environmental changes (Goddard and Watts, 2012). GPCR function is implicated in the regulation of various physiological systems and disease states such as cancer, pain, cardiovascular disorders, gastrointestinal disorders and conditions of the central nervous system. The complex signalling pathways that are mediated via GPCR activation, the generation of cell-based functional assays in combination with traditional radioligand binding assays and the novel structural information derived from crystal structures of several GPCRs have enabled the translation of fundamental biology into therapeutic applications (Milligan and McGrath, 2009). In addition, the cell membrane location of GPCRs and the diversity of tissue expression make GPCRs ideal targets for drug discovery. Not surprisingly, around 30% of drugs developed target GPCRs and there is still growing interest in this type of receptor both within the pharmaceutical industry and academia (Hill, 2006). Many diseases and disorders involving non-functional or constitutively activated receptors, changes in ligand binding specificity or improper receptor processing and cases where G proteins are inactive or constitutively active had generated the need for development of therapeutics to target either directly GPCRs or molecules that are involved in GPCR signalling pathways.

1.2 Structure of GPCRs

GPCRs possess a characteristic seven trans-membrane (7-TM) architecture and therefore they are also known as 7-TM receptors. Each TM domain is composed of 25-30 amino acid residues with a relatively high degree of hydrophobicity. Other common features of GPCRs include an N-terminal extracellular domain and a C-terminal cytoplasmic domain. The seven transmembrane domains are α-helices connected by six loops, three of which are intracellular and three extracellular (Perez and Karnik, 2005). Different types of GPCRs demonstrate sequence variations and differences in the length and the function of N-terminal, C-terminal domains and the intracellular loops (Bockaert and Pin, 1999). The common structure of a GPCR is illustrated in Figure 1.1.

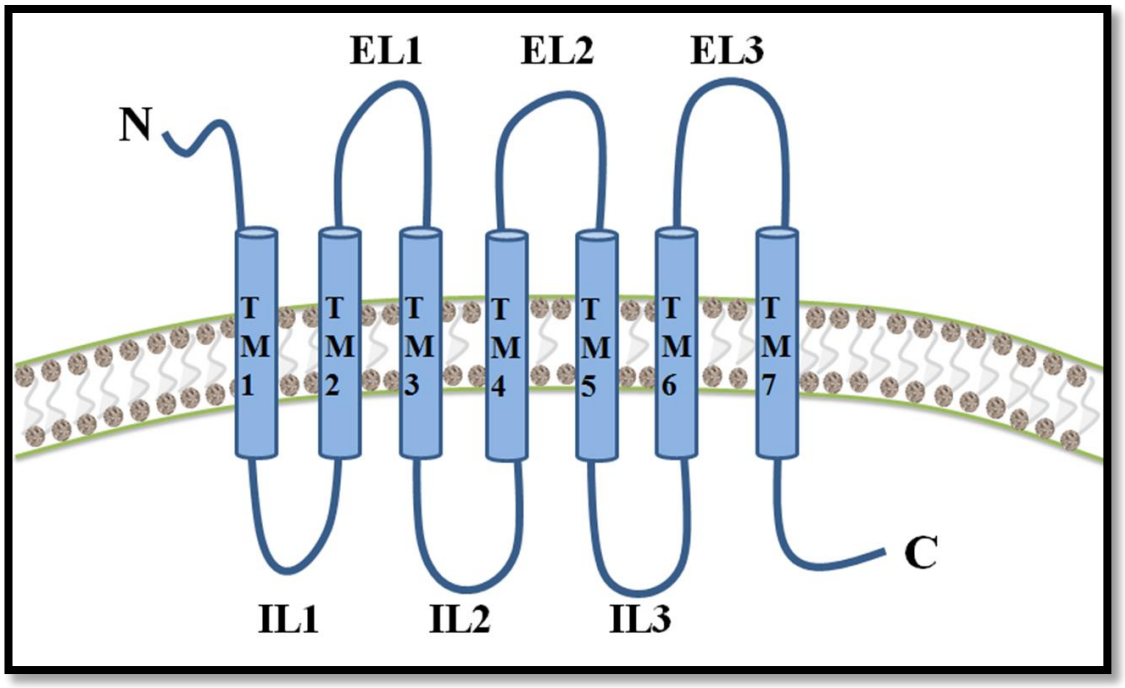

Figure 1.1 Topographic structure of a GPCR. GPCRs are composed of 7 transmembrane domains that consist of α-helices (TM1-TM7), 3 extracellular loops (EL1-EL3), an extracellular amino terminus (N-terminus), 3 intracellular loops (IL1-IL3), with IL3 possessing a key role in G protein binding and activation, and an intracellular carboxyl domain (C- terminus).

The majority of the information on GPCR structure was provided once the 3-D structure of rhodopsin was solved, by X-ray crystallography (Palczewski *et al.*, 2000). Rhodopsin is a visual pigment located in the photoreceptor cells of retina and is responsible for converting photons into chemical signals (Zhou *et al.*, 2012). The crystal structure of rhodopsin has served as a template for other GPCRs and the information obtained had greatly enriched

the understanding of GPCRs in terms of structure and function (Palczewski, 2006). The crystal structures of other GPCRs followed and these included the β_1-adrenoceptor (Warne *et al.,* 2008), β_2-adrenoceptor (Rasmussen *et al.,* 2007), A_{2A}-adenosine receptor (Jaakola *et al.,* 2008), the complex of β_2-adrenoceptor with its G protein (Rasmussen *et al.,* 2011), the human muscarinic M_2 receptor (Haga *et al.,* 2012) and the rat M_3 receptor (Kruse *et al.,* 2012). The 7-TM domain of rhodopsin is composed of α-helices arranged in a barrel-shaped, cylindrical formation connecting the three intracellular and three extracellular loops. The N-terminus is composed of a two-stranded β-sheet and it contains glycosylation sites (Asn2, Asn15) along with other amino acids that are important in the folding of the receptor (Thr4, Asn5, Thr17, Pro23, Asn28). The second extracellular loop (EL2) of rhodopsin extends between TM4 and TM5 and is crucial for ligand binding. The EL2 consists of a two-stranded β-sheet which is positioned at the opening of the ligand binding pocket and serves as a 'lid' blocking the exit of the bound ligand from the pocket. The stability of the β-sheet is enhanced by hydrophobic interactions between certain residues (Tyr178, Pro180, Met183, Cys185 and Cys187), by hydrogen bonding network involving Glu181, Tyr192 of the sheet and Tyr268 of TM6, and by a disulphide bridge between Cys187 of the β-sheet and Cys110 located on TM3. The presence of a salt bridge between the two strands of the β-sheet formed by Asp190 and Arg177 further maintains the conformational stability of the 'lid' structure (Zhou *et al.,* 2012). The ligand binding pocket is located on the extracellular part of the 7-TM domain and is surrounded by hydrophobic residues (Met207, Phe208, Phe212 on TM5 and Trp265, Tyr268 on TM6) stabilising the conformation which only undergoes dynamic changes upon receptor activation. Another salt bridge between Arg135 on TM3 and Glu247 on TM6 is formed and acts as an ionic lock blocking the G protein binding site of the receptor in its inactive conformation. The ionic lock breaks only upon photo-activation, with TM6 shifting away from the 7-TM core, thus creating a cavity on the cytoplasmic side of the receptor allowing for G protein binding and activation (Palczewski, 2006). A highly conserved NPXXY motif that is located on TM7 possesses a vital role in receptor activation through the shifting of the tyrosine residue towards TM6 further promoting the breakage of the ionic lock. The third intracellular loop (IL3) of rhodopsin is essential for interactions with G protein and arrestins. Lys296 acts as Schiff base to covalently link to 11-*cis*-retinal (prosthetic group), while Glu113 is essential for stabilising the interaction with the ligand (Palczewski, 2006). Other residues within the binding pocket of rhodopsin enable 11-*cis*-retinal to act as an inverse agonist and prevent receptor activation until a photon is absorbed and photo-activation occurs (Tsutsui and Shichida, 2010). Photo-activation

causes the isomerisation of 11-*cis*-retinal to the *trans*- isomer (*trans*-reinal), which is the full agonist of rhodopsin. The C-terminus of rhodopsin contains palmitoylation sites at residues Cys322 and Cys323, several serine and threonine residues that act as phosphorylation sites, and a VXPX motif important for receptor transport. Figure 1.2 shows the crystal structure of rhodopsin.

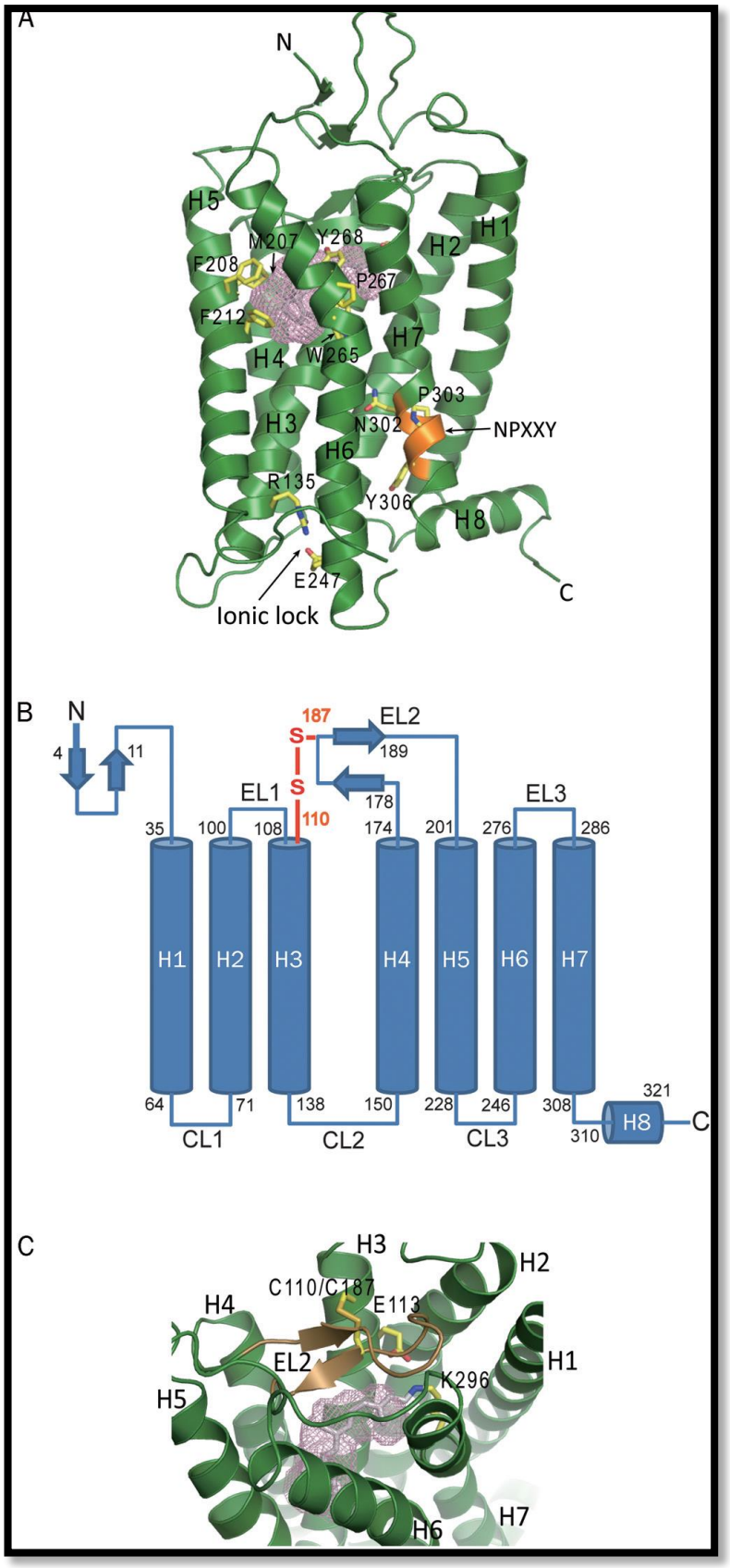

Figure 1.2 Crystal structure of bovine rhodopsin. (A) The 3-D structure of rhodopsin showing the 7-TM domain forming a cylindrical structure, the extracellular N-terminus and the intracellular C-terminus. Residues that are involved in the binding pocket architecture are shown in yellow. The ionic lock and the NPXXY motif are also shown. **(B)** The 2-D structure of rhodopsin demonstrating some of the secondary structural features such as the disulphide bridge connecting

the EL2 with TM3. **(C)** The 3-D structure of the ligand binding pocket with EL2 acting as a 'lid' for the pocket (Figure taken from Zhou *et al.,* 2012).

A lot of the structural features of rhodopsin are conserved in other GPCRs, but some differences exist especially in the binding pocket and also in the mechanism of receptor activation. Activation of rhodopsin requires that the ligand remains tightly held in the pocket and this is achieved by the EL2 domain adopting a conformation forming a tight 'lid' blocking the ligand in the pocket. Other GPCRs have a more flexible EL2 domain above the binding pocket (Zhou *et al.,* 2012).

Most GPCRs contain highly conserved disulphide bridges between cysteine residues in the EL2 and EL3, a bond that is essential for folding and packing of the receptor and for regulating the ligand binding site by stabilizing receptor conformation (Karnik and Khorana, 1990). The orthosteric binding site is often located deep in the pocket created by the TM domains. Based on biochemical and mutagenesis studies of the rhodopsin system and rhodopsin-like receptors, a switch from inactive to active conformation is associated with movement of the TM3 and TM6, upon ligand binding. The conformational changes namely the rotation of TM6 and the dissociation from TM3, in turns affect the conformation of the IL2 and IL3, making the G protein binding domain visible and available for recognition and binding by a G protein (Venkatakrishnan *et al.,* 2013).

Other ligand binding sites may exist, depending on the receptor and these are usually located on the extracellular loops. These differ from the orthosteric binding site and are called allosteric binding sites, allowing the binding of distinct ligands to the GPCR. The binding of allosteric ligands can influence the binding characteristics of orthosteric ligands and it may also induce activation of G-protein dependent pathways via GPCR allosteric activation (van der Westhuizen *et al.,* 2015).

1.3 Classification of GPCRs

GPCRs are classified into six groups (A to F) based on sequence homology and are also classified according to the endogenous ligands they bind to (Cherezov *et al.,* 2007). The A-F classification system covers all GPCRs and some of the classes are not found in humans. For example D and E represent fungal pheromone receptors and class F includes archaebacterial opsins (Fredriksson *et al.,* 2003).

The mammalian GPCRs are categorised in three main classes according to sequence similarity and these are: class A (rhodopsin-like receptor family), class B (secretin receptor family) and class C (family of metabotropic glutamate receptors) (Emami-Nemini *et al.,* 2013).

The rhodopsin-like (class A) family has more than 700 members that share high sequence similarity (Pal *et al.,* 2012) and share several structural characteristics with rhodopsin such as an NPXXY motif on TM7 and a DRY motif between TM3 and IL2 (Palczewski *et al.,* 2000). Ligand binding for most rhodopsin-like receptors takes place within a cavity formed between the TM region. Some important GPCRs that belong to class A family include muscarinic acetylcholine receptors, dopamine receptors, adrenergic receptors, opioid receptors, adenosine receptors and histamine receptors.

The secretin-like (class B) family consists of several members such as calcitonin receptor, corticotropin releasing hormone receptor, glucagon and glucagon-like receptor, growth hormone releasing receptor etc. This receptor family is characterised by binding to large peptide hormones (Pal *et al.,* 2012). The secretin receptor was the first to be cloned in the family and hence the name. The N-terminal domain is 60-80 amino acids long, containing cysteine residues that form disulphide bridges that play key roles in ligand binding. The secretin receptor and other members of this family play a key role in hormonal homeostasis with secretin receptor stimulating secretion of acid-neutralising fluids in pancreas and duodenum; growth hormone releasing hormone receptor mediating growth hormone secretion; glucagon and calcitonin receptors regulating glucose homeostasis (Pal *et al.,* 2012). Novel insights into the structure and function of class B receptor family was offered by publications of the crystal structures of the glucagon receptor and the corticotropin releasing factor receptor 1 (Hollenstein *et al.,* 2014).

The glutamate-like receptor (class C) family consists of metabotropic glutamate receptors (mGlu receptors), Ca^{+2} sensing receptors, γ-aminobutyric acid B receptors ($GABA_B$), sweet and amino acid taste receptors, pheromone receptors and some orphan receptors (Chun *et al.,* 2012). The N-terminus of glutamate receptor family members is 280-580 amino acids long and contains the ligand recognition domain generated by forming two lobes separated by a cavity in which glutamate binds to produce the so called 'Venus fly trap' or VFT domain. This extracellular domain is common to class C receptors and it is responsible for ligand recognition. The VFT domain may also accommodate allosteric binding sites and it is connected with the 7-TM core through a cysteine rich domain, which also plays a role in receptor activation (Chun *et al.,* 2012).

1.4 Signalling of GPCRs

GPCRs couple to and activate guanine nucleotide binding proteins (G proteins). G proteins are hetero-trimeric proteins that consist of three subunits (α, β and γ) which exist in a complex when inactive. The Gα is the largest subunit (40-45 kDa) in the heterotrimeric complex. It is composed of two domains (a GTPase domain and an α-helical domain) and is capable of forming a complex with one β (35 kDa) and one γ subunit (15 kDa), when in GDP-bound form (Malbon, 2005). Upon ligand mediated activation the receptor undergoes a conformational change leading to the exchange of GDP for GTP on the Gα subunit, which then dissociates from the Gβγ complex. The G protein subunits then act on downstream effectors and initiate signalling pathways. The GTPase activity (GTP-hydrolysing activity) of the Gα subunit hydrolyses GTP into GDP, leading to the termination of the G protein mediated downstream signalling and the different subunits re-associate back into the hetero-trimeric complex (Hamm, 2001). The Gβγ subunits can function independently from the Gα and activate a diverse range of effectors initiating signal transduction pathways (Sadja *et al.,* 2003). The Gβγ complex can interact with phospholipase Cβ (PLCβ) (Lin and Smrcka, 2011), G protein receptor kinase 2 (GRK2) (Evron *et al.,* 2012), G protein-regulated inwardly rectifying potassium channels (GIRK) (Luscher and Slesinger, 2010), N-type calcium channels (Brown and Sihra, 2008), adenylate cyclase (AC) isoforms (Sunahara and Taussig, 2002). Regulation of G protein function is mediated by accessory proteins e.g. activators of G protein signalling (AGS) which facilitate the exchange rate of GDP for GTP, and regulators of G protein signalling (RGS), that act by accelerating the rate of GTP hydrolysis on the Gα subunit, therefore, having a regulatory role in the duration of G protein activation (Traynor and Neubig, 2005).

There are four main classes of Gα subunits that have been identified based on sequence similarity (Neves *et al.,* 2002). These are: G_s (stimulates an increase in intracellular cyclic adenosine monophosphate (cAMP) levels by activating an AC), $G_{i/o}$ (inhibits AC which leads to a decrease in intracellular cAMP levels); $G_{q/11}$ (leads to an increase in intracellular calcium ion levels through the activation of PLCβ) and $G_{12/13}$ (regulation of Rho guanine nucleotide exchange factors, RhoGEF proteins).

In more detail, $G\alpha_s$ subunit activates the enzyme AC, which in turns catalyses the conversion of ATP into cAMP, resulting in increased cytosolic cAMP levels. Four molecules of cAMP are required for binding to the cAMP-dependent protein kinase, also known as protein kinase A or PKA. When PKA is activated it interacts with proteins to phosphorylate them on specific serine and/or threonine residues. The $G\alpha_{i/o}$ subunit has the

opposite effect compared to the $G\alpha_s$, since its activation leads to the inhibition of AC activity and thus, the reduction in cAMP production levels, which in turns results in a decrease in the PKA activity.

The $G\alpha_{q/11}$ subunit, once activated by a GPCR, activates the enzyme PLC. PLC hydrolyses phosphatidylinositol 4, 5 -bisphosphate (PIP_2) into diacylglycerol (DAG) and inositol 1,4,5-trisphosphate (IP_3). DAG remains bound to the membrane and acts as a second messenger by activating protein kinase C (PKC) which phosphorylates proteins. IP_3 diffuses in the cytosol and acts on IP_3 receptors located in the endoplasmic reticulum (ER), resulting in an increase in intracellular calcium ion levels. Calcium ions together with DAG work towards the activation of PKC.

The $G\alpha_{12/13}$ subunits act by activating Rho guanine nucleotide exchange factors (Rho-GEFs) which in turn activate the small cytosolic Rho-GTPase. The Rho-GTPase can activate numerous proteins such as Rho-kinase that are responsible for regulation of actin cytoskeletal remodelling in cells. A brief summary of the different G protein mediated pathways is included in Figure 1.3.

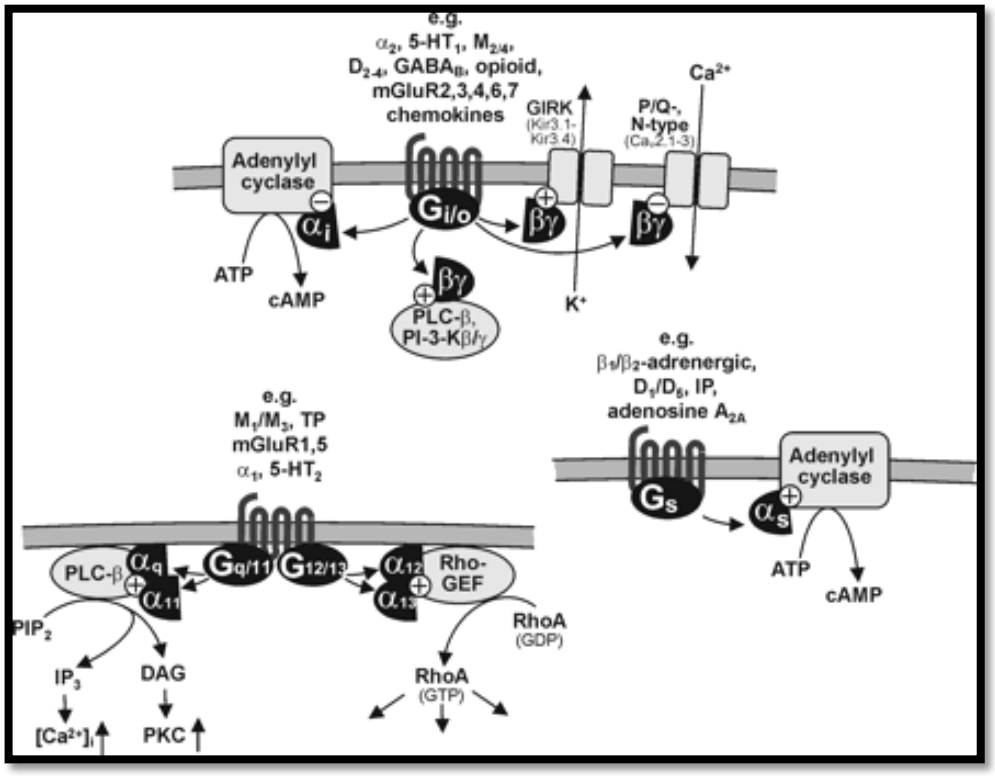

Figure 1.3 G protein coupling patterns. Examples of GPCRs that couple to different G protein types and mediate the different signalling pathways. (Figure taken fromWettschureck and Offermanns, 2005).

1.5 Regulation of GPCR signalling and G protein independent signalling pathways

Regulation of GPCR signalling occurs during three different processes: 1. Desensitisation, 2. Internalisation and 3. Down-regulation. The key element that is involved in these processes is a cytosolic protein called β-arrestin (Luttrell and Lefkowitz, 2002). Beta arrestins are multifunctional proteins acting as signal terminators, as adaptor proteins and as signal transducers (DeWire *et al.*, 2007; Shukla *et al.*, 2013). The roles of arrestins are listed in the schematic diagram in Figure 1.4.

The family of arrestins contains four members: two visual arrestins (arrestin 1 and 4) and two non-visual arrestins (arrestin2 and 3, also known as β-arrestin1 and β-arrestin2, respectively) (Lefkowitz and Shenoy, 2005). The visual arrestins restrict to binding to photoreceptors such as rhodopsin (Gurevich and Benovic, 1993). The two β-arrestins (1 and 2) although structurally similar to visual arrestins, are of broader importance in terms of GPCR signalling regulation. Crystal structures of arrestin molecules in their basal state have revealed an elongated molecule containing an N- and a C-domain, composed of antiparallel β-sheets, which are connected by a linker region made of 12 residues. The polar core is a region located between the two domains and is composed of a network of charged residues connected with hydrogen bonds (Han *et al.*, 2001). Arrestins bind to the ligand activated receptor once it has been phosphorylated at its C-terminal domain or intracellular loops by protein kinases such as GRKs (Kovoor *et al.*, 1999).Two types of interactions are involved in the binding of β-arrestin to a phosphorylated GPCR. Briefly, a phosphate sensor on β-arrestin interacts with the phosphorylated C- terminus or the IL3 of the receptor and a conformational sensor on rhodopsin recognises the agonist-induced active conformation of the receptor's core (Shukla *et al.*, 2013). Important information obtained from X-ray laser experiments have enabled the production of the first 3-D map of a pre-activated form of mouse visual arrestin bound to a constitutively active form of human rhodopsin (Kang *et al.*, 2015). According to this model rhodopsin uses TM7 and helix 8 to recruit arrestin, while arrestin undergoes conformational changes through rotating its N- and C-termini resulting in the opening of a cleft on arrestin allowing accommodation of the IL2 domain of rhodopsin (Kang *et al.*, 2015).

Following receptor stimulation for a prolonged period of time, receptor mediated signalling is attenuated i.e. the response to the persistent stimulus is decreased, via a process called desensitisation. Desensitisation begins with exposure of the receptor to agonist and it is initiated by the phosphorylation of key residues in the C tail and cytoplasmic loops of the receptor by protein kinases (e.g. PKA, PKC, GRKs).

The interaction between the receptor and β-arrestin that confers a series of conformational changes, upon the receptor, leads to dissociation of the receptor-G protein complex (via sterically blocking the G protein- receptor coupling) and thus, the termination of G-protein mediated signalling cascades. Therefore, β-arrestin possesses a role as signal terminator (Luttrell and Lefkowitz, 2002). This interaction initiates the process of receptor homologous desensitisation (mediated by agonist stimulation of the receptor and subsequent receptor phosphorylation by GRKs). Ligand binding is not always required for the process, since an unbound receptor can be desensitised by heterologous desensitisation (receptor phosphorylated by second messenger-dependent protein kinases) (Luttrell and Lefkowitz, 2002).

Arrestins also have the ability to act as adaptor proteins by binding to components of the endocytic machinery. The high affinity binding of β-arrestin to clathrin, dynamin and β2-adaptin subunit of the AP-2 adaptor protein results in a multi-complex formation linking the receptor-bound arrestin to the clathrin endocytic machinery. This process initiates receptor internalisation in clathrin coated pits, and subsequently in clathrin coated vesicles (Oakley *et al.,* 2000; Han *et al.,* 2001). Goodman *et al.,* (1996) demonstrated the co-localisation of β_2-AR with β-arrestin and clathrin, by immuno-fluorescence microscopy in live cells, suggesting arrestin possesses a role in endocytosis and trafficking of GPCRs (Goodman *et al.,* 1996).

β-arrestin can act as a multi-protein scaffold and has a role in the recruitment of specific signalling molecules to the receptor, thus conferring the role of signal transducer to β-arrestin, since it can re-direct signalling to alternate pathways (Gurevich and Gurevich, 2003; Kang *et al.,* 2015). Arrestin can recruit Src family kinases, components of extracellular signal regulated kinases ERK1/2, c-Jun N-terminal kinases (JNK3) and p38 kinases, re-directing the receptor signalling pathway towards mitogen activated protein kinase (MAPK) signalling cascades, leading to ERK1/2 phosphorylation, upon receptor internalisation (Calebiro *et al.,* 2010; Mundell and Benovic, 2000). MAP kinase pathway is regulated by a series of signalling cascades. The pathway is initiated by the activation of MAP kinase kinase kinases (MAPKKK) that in turn phosphorylate and activate MAP kinase kinases (MAPKK). MAPKK in turns phosphorylate and activate MAP kinases (MAPK) such as ERK1/2. Activated ERK1/2 acts by phosphorylating various cytoplasmic, nuclear and cytoskeletal components that are involved in cellular processes that regulate cell cycle (division and growth), apoptosis, cell differentiation, proliferation (Luttrell and Lefkowitz, 2002).

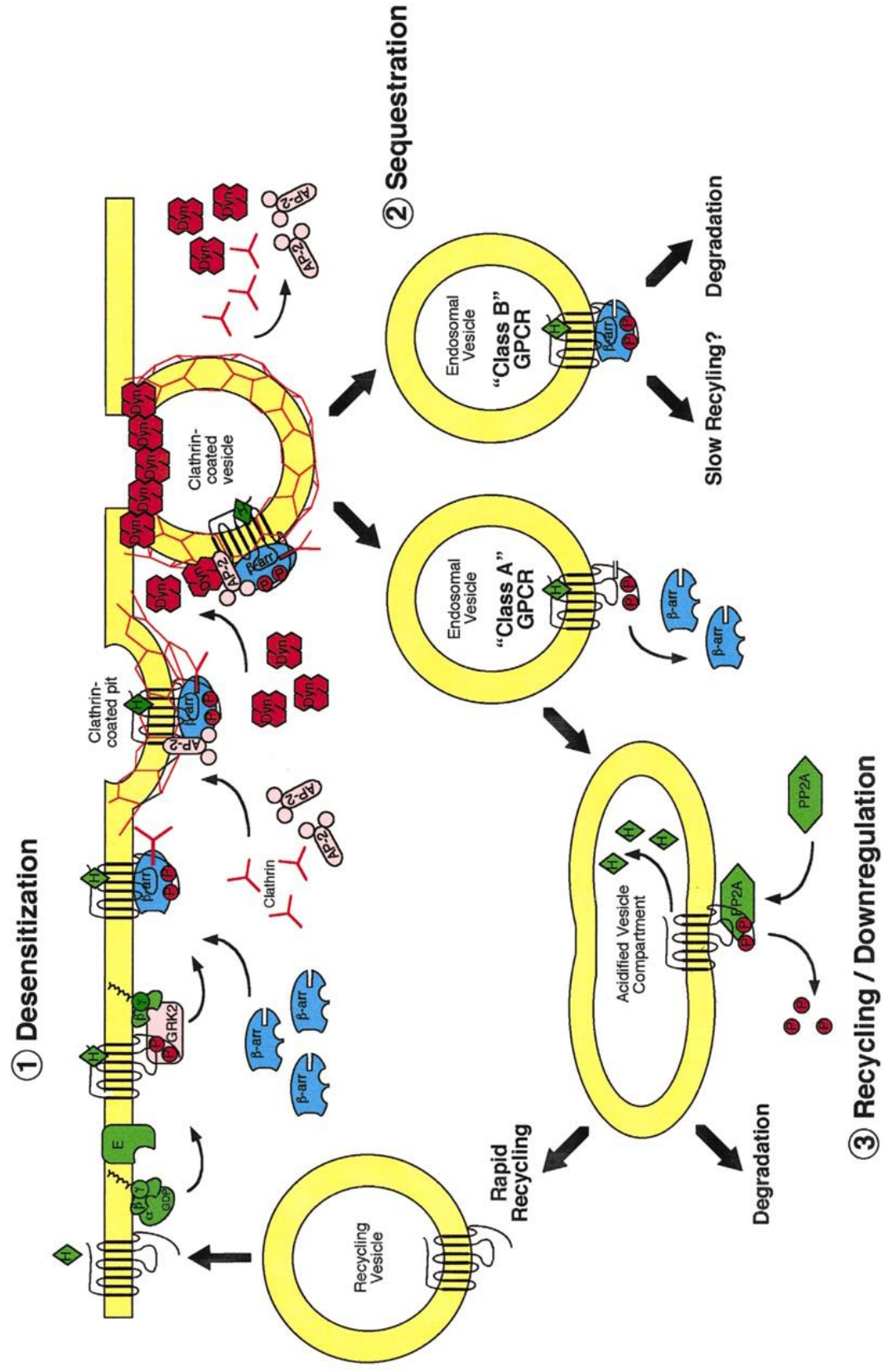
① Desensitization
② Sequestration
③ Recycling / Downregulation
Clathrin-coated pit
Clathrin-coated vesicle
Clathrin
Dyn
AP-2
β-arr
GRK2
Endosomal Vesicle
"Class A" GPCR
"Class B" GPCR
Slow Recyling?
Degradation
Recycling Vesicle
Rapid Recycling
Acidified Vesicle Compartment
PP2A

Figure 1.4 Roles of β-arrestin in the life cycle of GPCRs. The activation of a GPCR leads to its phosphorylation at specific serine and threonine residues by GRKs, resulting in the recruitment of β-arrestins at the cell membrane. 1. Binding of β-arrestin to the phosphorylated GPCR terminates G protein coupling, initiating receptor desensitisation process. 2. β-arrestin recruits proteins involved in the clathrin dependent internalisation of the receptor, a process that leads to 3. Receptor recycling or down-regulation, depending on the strength of interaction between the GPCR and arrestin molecules (Figure taken from Luttrell and Lefkowitz, 2002).

1.6 Muscarinic acetylcholine receptors

Muscarinic acetylcholine receptors (mAChRs) are a family of five closely related class A GPCRs. The five different sub-types denoted M_1-M_5 are encoded by CHRM1-CHRM5 and are highly conserved throughout evolution from fungi to humans. The mAChRs have been cloned, sequenced and studied thoroughly through the years and the muscarinic acetylcholine system is considered of great physiological importance with these receptors playing important roles in regulating numerous cellular functions. The natural ligand for mAChRs is acetylcholine, which is released from cholinergic nerve endings and non-neuronal cells. Acetylcholine-mediated activation of the receptors is responsible for G protein activation and the downstream signalling pathway that follows activation (Kurowski *et al.,* 2015).

The mAChRs may be sub-divided into two groups based on the preference for G protein coupling efficiency. M_1, M_3 and M_5 couple predominantly to $G_{q/11}$ proteins upon agonist activation of the receptor (Bymaster *et al.,* 2002). Activation of the $G_{q/11}$ protein is followed by activation of PLC and this in turns results in increased intracellular calcium ion release (Figure 1.5 A). The βγ subunits of the Gαq protein can regulate the function of certain ion channels including potassium or calcium channels (Beech *et al.,* 1992; Hille, 1992).

M_2 and M_4 muscarinic acetylcholine receptors show a preference for $G_{i/o}$ heterotrimeric G protein coupling and this leads to a negative effect on neurotransmitter release (Bymaster *et al.,* 2002). Activation of $G_{i/o}$ pathway is responsible for inhibition of adenylate cyclase activity resulting in a decrease of cAMP accumulation (Figure 1.5 B). The βγ subunits of the $G_{i/o}$ protein may also directly regulate potassium channels. This is a key pathway that follows activation of M_2 receptors in heart muscle (Krejci and Tucek, 2002). The M_2 receptor has also demonstrated the ability to activate alternate G proteins such as G_s resulting in a stimulatory effect on cAMP synthesis. This ability was shown to be

dependent on the agonist used, the duration of stimulation and the density of the receptors at the surface of the cells or tissues being examined.

Various studies have suggested that muscarinic receptors may also signal through G protein- independent pathways (Tobin and Budd, 2003; Billington and Penn, 2002). Changes in receptor localisation and trafficking have been reported following receptor modification through phosphorylation by protein kinases. The observation that β- arrestin recruitment is linked to receptor phosphorylation led to the hypothesis that these two functions may be ligand biased.

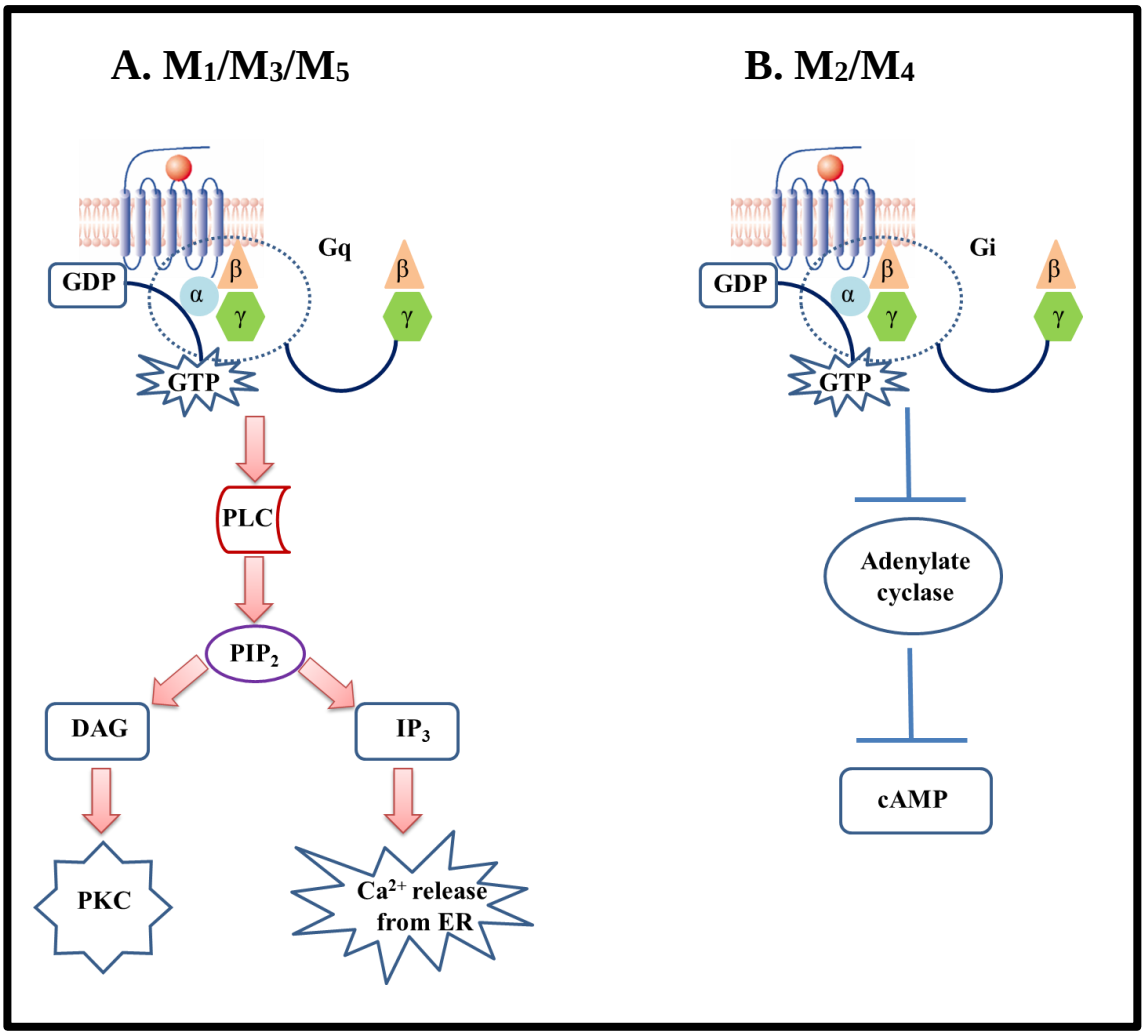

Figure 1.5 G protein mediated signalling of muscarinic acetylcholine receptor subtypes. (A) M_1, M_3 and M_5 couple to $G_{q/11}$ protein and induce activation of PLC, which catalyses PIP_2 into DAG and IP_3 resulting in the activation of PKC and calcium ion release from the ER. **(B)** M_2 and M_4 receptor subtypes preferentially couple to $G_{i/o}$, inhibiting the activation of AC and thus resulting in decreased cAMP levels.

1.7 Expression and function of mAChRs

The family of mAChRs plays an important role in the regulation of numerous essential functions of the central and peripheral nervous systems. The expression of these receptors is widespread in numerous tissues and organs as observed by immunological and immuno-cytochemical methods (Levey, 1993; Levey *et al.,* 1991), *in situ* hybridisation histochemistry (Weiner *et al.,* 1990) and generation and analysis of muscarinic *Chrm1-Chrm5* knock-out (KO) mice (Wess *et al.,* 2007). The generation of transgenic mAChR KO mice has offered insight into numerous muscarinic receptor-related functions (Matsui *et al.,* 2000; Wess, 2004). The mAChR KO mice were all viable, fertile and without signs of major physiological defects (Wess *et al.,* 2007).

The $G_{q/11}$ coupling group of mAChRs (M_1, M_3 and M_5) is expressed in post-synaptic terminals suggesting a role in the modulation of synaptic transmission. M_1 receptor is widely expressed in the major forebrain areas such as the cerebral cortex, striatum, and hippocampus but is also abundant in the periphery e.g. salivary glands and sympathetic ganglia. The M_1 KO mice demonstrated increased locomotor activity associated with memory and learning deficits (Miyakawa *et al.,* 2001). The M_1 receptor has been suggested to be implicated in Alzheimer's disease and related cognitive disorders and therefore identification or development of M_1 selective ligands could be advantageous in the treatment of such disorders. Studies in mouse models for Alzheimer's disease have demonstrated that M_1 deficiency increased the risk for development of Alzheimer's (Davis *et al.,* 2009) and further enhanced the severity of cognitive decline related with the disease (Medeiros *et al.,* 2011). M_3 receptor, apart from its wide expression in the CNS, is also found in smooth muscle of the gastrointestinal and urinary tracts and in exocrine glands and eyes. Activation of M_3 promotes smooth muscle contraction, salivary gland secretion and is involved in the stimulation of the parasympathetic system (Bubser *et al.,* 2012). The physiological role of M_3 receptor subtype has been extensively examined, since the receptor is widely expressed in CNS and periphery (Wess *et al.,* 2007). The study of the role of M_3 receptor was assisted by the generation of whole body M_3 receptor KO mice (Yamada *et al.,* 2001) and it was proposed that activation of M_3 is implicated in stimulation of smooth muscle contraction, in the promotion of glandular secretion and dilation of peripheral blood vessels. M_3 receptor KO mice demonstrated reduced body fat mass (Yamada *et al.,* 2001) and the activity of M_3 was linked to cancer with a proposed role of M_3 in tumour formation in the gastrointestinal tract (Raufman *et al.,* 2008). There has also been an association of M_3 receptor activation in β-pancreatic cells with glucose

homeostasis and promotion of insulin release (Gautam *et al.,* 2006; 2007). In an attempt to study this role of M_3 receptor, M_3 KO mice that lacked the receptor selectively in pancreatic β-cells were generated and these demonstrated impaired glucose tolerance and reduced insulin secretion (Nakajima *et al.,* 2013). On the other hand, transgenic mice over-expressing the M_3 receptor in β-cells displayed enhanced glucose tolerance and increased insulin release (Nakajima *et al.,* 2013). This finding is considered of great therapeutic importance offering a potential approach in the treatment of type 2 diabetes with the identification of compounds that can selectively activate M3 receptors (Kruse *et al.,* 2014). M_3 receptor demonstrated an ability to modulate appetite via regulating melatonin-concentrating hormone (MCH) neurones in hypothalamus, in a study using M_3 KO mice (Yamada *et al.,* 2001). Exocrine secretion of saliva was also found to be mediated by M_3 (Matsui *et al.,* 2000) as well as M_1 (Gautam *et al.,* 2004). The generation of M_5 KO mice revealed an important role of the M_5 receptor in the modulation of drug-addiction and drug-seeking behaviours (Wess *et al.,* 2007). M_5 expression has been detected in peripheral and cerebral blood vessels and also in brain regions including substantia nigra, hippocampus, hypothalamus, as well as at distinct midbrain dopamine cell body regions, a fact that implies co-localisation with dopamine receptor subtypes. Most neurons in substantia nigra especially in the region of ventral tegmental area co-express mRNA corresponding to both M_5 and D_2 receptors (Raffa *et al.,* 2009).

The $G_{i/o}$ coupling group of mAChRs (M_2 and M_4) generally confers an inhibitory effect on pre-synaptic terminals resulting in reduced neurotransmitter release. M_2 is abundant in the CNS, regulating acetylcholine release in the cortex and hippocampus. It is expressed in the body periphery, smooth muscle organs and it is the predominant muscarinic receptor in the heart. M_2 receptor is also abundant in the urinary bladder smooth muscle and activation of M_2 can cause contraction of the bladder in an indirect manner by reversing sympathetically-mediated relaxation (Hedge *et al.,* 1997). Mice deficient in M_2 receptor demonstrated decreased responses to cholinergic stimuli (Matsui *et al.,* 2002).Transgenic M_2 KO mice revealed that M_2 receptor has a role in the regulation of body temperature (Gomeza *et al.,* 1999) and also in controlling cardiac myocyte contraction (Wess, 2004). Although, M_3 receptor is thought to have a dominant role in inducing smooth muscle contraction, the M_2 receptor is suggested to play a modulatory role in the intracellular signalling of M_3 (Matsui *et al.,* 2002).

M_4 receptor is expressed in high concentrations in the periphery (e.g. lung, salivary glands and ileum) and shows similar expression levels as M_1 in brain regions (hippocampus, cerebral cortex, striatum), while showing low levels of expression in thalamus, cerebellum

and brainstem. M_4 proposed actions include regulation of locomotor activity, analgesia, auto-inhibition of acetylcholine and balancing dopaminergic activity (Bymaster *et al.,* 2002). M_4 KO mice showed an inhibitory effect on the striatal dopamine mediated locomotor activity (Bymaster *et al.,* 2002; Wess *et al.,* 2007).

Muscarinic receptors can modulate the action of ion channels such as K^+ and Ca^{2+} in striatal medium spiny neurons, a function that has been attributed to M_1 and M_4 receptor subtypes (Yan *et al.,* 2001). M_2 receptor-mediated activation of K^+ channels results in decreased heart rate. It is also known that muscarinic receptors can modulate striatal dopamine release. More specifically, stimulation of M_4 and M_5 seems to enhance striatal dopamine release, whereas, activation of M_3 receptors shows the opposite effect i.e. inhibition of dopamine release (Zhang *et al.,* 2002). Lack of M_1 and/or M_4 muscarinic receptors in KO mice resulted in hypersensitivity of dopamine phenotype which is associated with psychotic activity and schizophrenia (reviewed in Kruse *et al.,* 2014). A better understanding of the function and involvement of mAChRs in pathological conditions can enable the development of therapeutics to target diseases and disorders of the CNS and periphery.

1.8 Structural aspects of ligand binding to mAChRs

A number of muscarinic ligands exist that bind to the orthosteric binding site of mAChRs ranging from full (e.g. carbachol, oxotremorine) and partial (e.g. arecoline) agonists to antagonists (e.g. atropine, scopolamine) and inverse agonists (e.g. pirenzepine, tiotropium). Xanomeline is considered to be a M_1 and M_4 selective agonist with important advantages offered in the improvement of symptoms in Alzheimer's disease and schizophrenia (Bodick *et al.,* 1997; Grant *et al.,* 2010) but it has also demonstrated the ability to bind and activate M_3 receptor (Christopoulos *et al.,* 2001). Xanomeline is considered to be an orthosteric ligand but it also binds at a secondary site on the M_1 receptor (De Lorme *et al.,* 2007).

The orthosteric binding site of the muscarinic acetylcholine receptors is the site where the endogenous ligand, Ach, binds. The binding site is enclosed deep in a pocket that is formed by the TM domains of the receptor. Several models have been suggested and these were initially based on mutagenesis and molecular docking studies. Such studies have revealed that Ach binding to the receptor's binding pocket is enabled by amino acid residues in TM3, TM4, TM6 and TM7 domains (Jacobson *et al.,* 2010). The crystal structure of

bovine rhodopsin was used as a template for the generation of a homology model of the M_1 receptor in an attempt to investigate the components of the orthosteric binding site that were crucial for Ach binding. This investigation revealed that Asp105 was an essential residue for Ach binding, through the formation of a salt bridge with Ach (Hulme *et al.,* 2003; Jacobson *et al.,* 2010). Other residues in the binding pocket that were considered important for the M_1 interaction with Ach included: Trp101, Tyr404 andTyr408. Phe77, Tyr179 and Phe374 were identified as crucial residues for participating in the allosteric binding site for binding to allosteric ligands such as AC-42 and TBPB (Jacobson *et al.,* 2010). Crystal structures of muscarinic receptors were recently obtained for the human M_2 bound to the antagonist QNB (Haga *et al.,* 2012) and the rat M_3 bound to the inverse agonist tiotropium (Kruse *et al.,* 2012). The flexibility of the muscarinic receptors' due to the presence of a large and very flexible IL3 was a limiting factor in solving the crystal structures (Kow and Nathanson, 2012). This was solved by a modification that involved the removal of a large part of IL3, in both receptors, and the replacement with phage T4 lysozyme that enhanced crystal formation without affecting the receptors' binding properties (Haga *et al.,* 2012; Kruse *et al.,* 2012). The QNB was found to interact with Asp103 (TM3) that acts as a counter ion and Asn404 (TM6) forming a hydrogen bond with QNB. Both residues serve to orient the ligand into the hydrophobic cavity formed by aromatic residues. This aromatic cage engages the amine moiety of QNB and forms a 'lid' to prevent the ligand dissociating from the binding pocket. The residues important for interacting with QNB within the aromatic cage are: Tyr104, Tyr403 and Tyr423 (Haga *et al.,* 2012). Phe181 also interacts with QNB and this is the only amino acid in the orthosteric binding pocket of M_2 that differs from all the other mAChR sub-types. The rest of mAChRs have a leucine residue in the homologous position e.g. Leu225 in M_3 (Haga *et al.,* 2012; Kruse *et al.,* 2013). The binding pocket of M_2 receptor bound to QNB is shown in Figure 1.6 A.

The crystal structure of M_3 receptor bound to tiotropium is very similar to that of M_2. M_3 receptor also has a large extracellular vestibule, which like in M_2 it is a part of a hydrophilic channel that contains the orthosteric binding pocket of the receptor. The binding site is located deep in the TM domains and is covered by a 'lid' composed of tyrosine residues e.g. Tyr148, Tyr506 and Tyr529. Asp147 in M_3 interacts with the amine moiety of the ligand tiotropium and Asn507 forms hydrogen bonds with tiotropium's hydroxyl and carbonyl groups (Kruse *et al.,* 2012). The binding pocket of M_3 receptor bound to tiotropium is shown in Figure 1.6 B.

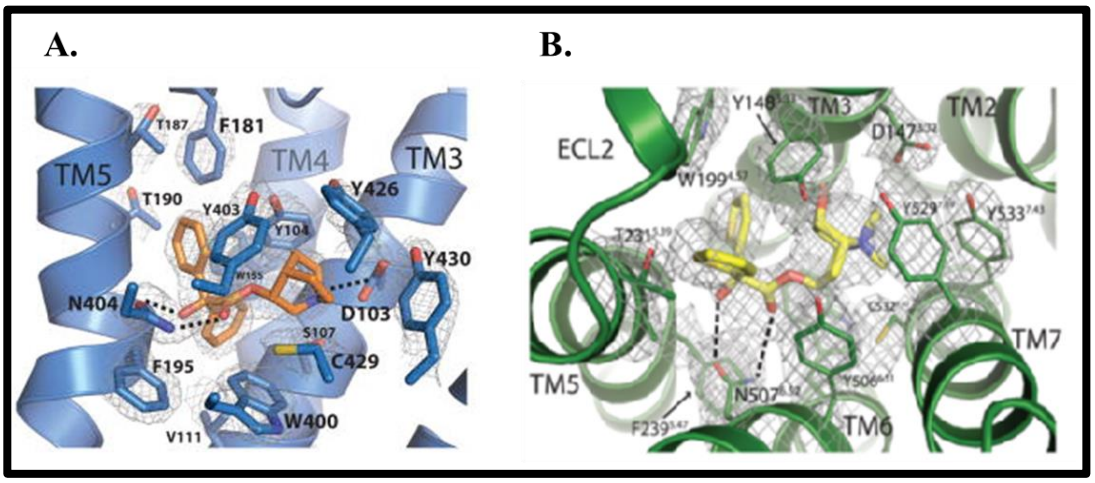

Figure 1.6 Crystal structures of mAChRs. (A) M_2 bound to QNB (Figure taken from Haga *et al.*, 2012) and (B) M_3 bound to tiotropium (Figure taken from Kruse *et al.*, 2012). The amino acid residues implicated in the interaction between the ligands and the binding pocket of each receptor are shown.

The orthosteric binding pocket of the mAChRs is characterised by a high degree of sequence homology across the different subtypes. This has been a limiting factor for the development of sub-type selective ligands for muscarinic receptors. This has attracted the focus on the discovery and development of allosteric modulators for mAChRs.

The secondary allosteric binding sites show greater divergence in homology among the different muscarinic receptor subtypes. The allosteric sites were not subjected to a strong evolutionary pressure as the orthosteric sites which were required to accommodate endogenous ligands (Smith and Milligan, 2010). Allosteric ligands cause conformational changes upon the receptor that either increases (positive allosteric modulator or PAM) or decreases (negative allosteric modulator or NAM) the binding and action of the orthosteric ligand to the receptor (van der Westhuizen *et al.*, 2015). Two types of allosteric modulators have been described for the M_1 receptor. These include allosteric agonists (able of activating the receptor even in the absence of an orthosteric ligand) and allosteric potentiators (require the presence of Ach to exert their function) (Jacobson *et al.*, 2010). The first allosteric agonist for the M_1 receptor was AC-42 and binding to the allosteric site was enabled by Tyr179 and Phe374 of the M_1 receptor. Phe77 (TM3) is also thought to be critical for maintaining AC-42 functional activity (Jacobson *et al.*, 2010).

Studies on the crystal structures of M_2 (Haga *et al.*, 2012) and M_3 (Kruse *et al.*, 2012) receptors have led to the identification of a large extracellular vestibule where allosteric ligands may bind. This domain is located above the orthosteric binding site and it is structurally coupled to the intracellular surface and the orthosteric binding domain and it is thought that this interaction allows allosteric ligands to affect the affinity and efficacy of

the orthosteric ligands and induce G protein activation (Gregory *et al.,* 2010; May *et al.,* 2007). The binding of M_2-bound to an orthosteric agonist iperoxo with a PAM, LY2119620, at the allosteric site was described by Kruse *et al.,* (2013a).
An allosteric agent (compound 16) that is able to specifically and selectively activate M_3 but not M_2 was identified, using structure-based molecular docking against M_2 and M_3 receptors and screening of large numbers of compounds (Kruse *et al.,* 2013 b). The identification of compound 16 as a partial agonist at M_3 (in a calcium mobilisation assay) and the inability to activate M_2 receptor (as demonstrated in an adenylyl cyclase inhibition assay) was very important as this was the first reported pharmacological agonist that showed sub-type selectivity at M_3 over M_2 receptor. In addition, compound 16 was able to stimulate insulin release in pancreatic β-cells (MIN6 insulinoma cells) a function linked to M_3 receptor activation (Gautam *et al.,* 2010). This could have an important impact in the development of novel therapeutics for the treatment of type 2 diabetes (Kruse *et al.,* 2013 b).

1.9 Generation and use of Receptors Activated Solely by Synthetic Ligands (RASSLs)

The importance of GPCRs in terms of therapeutics and their implication for various disorders of the periphery and CNS had pointed out the necessity for studying and understanding their function both *in vitro* and *in vivo* as well as the determination of the link between receptor activation and consequent physiological responses. The tools that have been employed to investigate receptor or pathway activation included the use of drug-like exogenous ligands targeting GPCRs and generation of gene knockouts (Conklin, 2007). Although, these methods were initially very useful in providing some information about receptor function, they lacked selectivity in terms of orthologous receptor-ligand pairs and showed a poor degree of spatiotemporal control of the GPCR-mediated signalling pathways. In addition, *in vivo* applications in studying GPCR function were problematic (Rogan and Roth, 2011). The ability to control GPCR signalling pathways, in order to investigate the effects of signalling *in vivo*, has been greatly complicated due to interference of the endogenous ligands with the system to be studied. These difficulties were the reason for turning towards a novel approach that involved building new GPCR pathways via creation of re-designed GPCRs.
The first efforts for selective GPCR activation began with the work of Strader *et al.,* (1991), which generated a mutated version of the β_2-adrenergic receptor, by site directed

mutagenesis. This resulted in a receptor unable to respond to natural adrenergic receptor ligands but could bind and be activated by a synthetic ligand unable to interact with the wild type receptors. Studies on the binding of agonists and antagonists, using this designer GPCR, had led to the determination of the role of ionic interactions between receptor and ligand in ligand binding specificity. A single amino acid substitution at the binding pocket region (i.e. replacement of the β-carboxymethyl side chain of Asp113 with the β-hydroxymethyl side chain of Ser) resulted in the genetically engineered β_2-adrenergic receptor able to respond potently and specifically to catechol ester or ketone ligands (Strader *et al.,* 1991) but not to adrenergic ligands. This work had only identified compounds with moderate affinities and unknown pharmacokinetics that were not suitable for *in vivo* applications, but had set the road for the new type of designer GPCRs (Rogan and Roth, 2011).

A similar approach to Strader *et al.,* (1991) involving rational design and mutagenesis of key amino acid residues involved in the ligand binding process, led to the generation of Receptors Activated Solely by Synthetic Ligands (RASSLs) using the human κ-opioid receptor as a template (Coward *et al.,* 1998). Two RASSLs were developed, Ro1 that contained the second extracellular loop domain from the δ-opioid receptor and Ro2 chimeric receptor also containing the same modification as Ro1 plus an amino acid substitution in the TM6 domain. The modified receptors were chosen based on the ability of the synthetic ligands spiradoline and bremazocine to bind and interact with extracellular loops of the receptors, and the preference of small molecules to interact with regions closer to the TM domains of the receptors. The redesigned receptors Ro1 and 2 were able to respond to and signal after activation with the synthetic small molecule ligands spiradoline and bremazocine, whilst, showing decreased affinity to natural opioid ligands such as dynorphin and enkephalin (Coward *et al.,* 1998). With this study Coward *et al.,* (1998) managed to demonstrate that GPCRs can be used as prototypes to generate RASSLs in order to selectively activate and investigate GPCR signalling. Ro1 and Ro2 RASSLs were the starting point for additional RASSL receptor generation, which showed unique features including altered internalisation and perturbed desensitisation properties (Scearse-Levie *et al.,* 2001; 2005; Pei *et al.,* 2008).

Other RASSLs were generated following the same approach. A mutation of Asp115 (a highly conserved residue between many GPCRs activated by biogenic amines that is critical for ligand binding to the orthosteric site) to glutamate of the G_q coupled serotonin receptor 5-HT_{2A} resulted in a RASSL (Kristiansen *et al.,* 2000). Another G_q coupled receptor, histamine H_1 receptor was made into a RASSL (Bruysters *et al.,* 2005) and the

first G_s coupled RASSL based on the melacortin receptor (MC4) (Srinivasan *et al.*, 2003) was developed. Claeysen *et al.,* (2003) used the 5-HT_4 receptor as a template to generate a family of designer GPCRs that could signal through the main three G proteins (G_q, G_s and G_i) (Claeysen *et al.,* 2003).

The first generation of RASSLs was based on pre-existing synthetic drugs that had known pharmacology and the side effects were considered negligible in animals. Some of the synthetic ligands show a degree of potency for the WT receptors. For example, spiradoline can activate the endogenous κ-opioid receptor (Coward *et al.,* 1998) and the synthetic ligand THIQ that targets the Rm1 and Rm2, is more potent at the parent receptor MC4 (Shrinivasan *et al.,* 2007). This points out the need for increased selectivity in activating designer receptors either by working in a KO background or by locally infusing the synthetic ligands to the tissue or organ site where only the RASSL is expressed. Another limitation of the first generation RASSLs was the lack of external control over the RASSL signalling due to constitutive activity of the RASSL. An example is the Ro1 receptor that showed no basal activity in tissue culture but had demonstrated a relatively high degree of constitutive activity *in vivo* (Coward *et al.,* 1998). It is not yet clear whether RASSL-linked basal activity originates from the RASSL-mediated signalling in the absence of ligand or from the over-expression of the receptor. Increased basal activity of a RASSL could be a result of the endogenous ligand-mediated activation (Conklin, 2007; Rogan and Roth, 2011).

The majority of the information on the roles and pharmacology of the mAChRs was obtained from studies that involved generation of KO and transgenic animals (Wess, 2012). The generation of RASSL variants of mAChRs by directed protein evolution was initiated by Armbruster *et al.,* (2007).This work involved the use of rat M_3 receptor as a template to generate a whole family of designer receptors exclusively activated by designer drugs (DREADDs). Repeated rounds of random mutagenesis and screening resulted in the identification and isolation of clones that were able to respond to the synthetic ligand clozapine-N-oxide (CNO) with increased affinity and potency, but were unable to respond to the endogenous muscarinic ligand Ach or related ligands such as carbachol (Cch). A mutated version of rat M_3 that lacked most of the IL3 ($rM_3\Delta3i$) to enhance expression in yeast, was used. This receptor was cloned into yeast expression vectors and the positive clones were selected based on the displayed desired pharmacological RASSL characteristics. The optimal mutation that conferred the RASSL characteristics to the receptor was Y148C. This was transferred to the equivalent and conserved residue at the

human M_3 receptor (Y149C) which was tested in combination with additional mutations. The optimal combination of mutations that were identified in the human M_3RASSL and conferred the ability to the receptor to respond to CNO and also caused loss of potency/affinity to Ach and Cch were: Y149C (TM3) and A239G (TM5). The hM_3RASSL potently enhanced levels of ERK1/2 phosphorylation through activation of MAPK proteins, in response to CNO but not acetylcholine (Armbruster *et al.*, 2007).

In order to investigate the conformational changes at the hM_3RASSL compared to the WT receptor, upon ligand-mediated activation, a FlAsH-CFP sensor was introduced at the receptor key points (i.e. FlAsH was introduced at IL3 and the CFP was placed at the C-terminus) to allow detection of conformational changes by intramolecular FRET (Alvarez-Curto *et al.*, 2011). A mutant containing the Y149C mutation did not respond to either CNO or Cch. The mutant containing the A239G mutation only responded to Cch but with slower kinetics and reduced potency compared to WT, but did not respond to CNO. The mutant containing both mutations was able to display the RASSL characteristics. Both Y149C and A239G mutations are required to generate the hM_3RASSL, by providing the suitable conformation within the receptor's binding pocket that allows binding to CNO. The key residues at the binding pocket that are thought to be interacting with CNO are Thr235 and Asp149. The three tyrosine residues in the hM_3WT receptor (Y149, Y507 and Y530) are thought to form a 'lid' structure above the binding pocket that maintains the required conformation for Ach binding. The Y149C mutation results in loss of the 'lid' structure in the hM_3RASSL conferring a more loose conformation of the binding pocket and thus, allowing CNO (which is more bulky than Ach and Cch) to bind and interact with Asp149. The binding of CNO to RASSL and the binding of Ach and Cch to the WT receptor result in similar conformational changes within the TM domains of both receptors according to the intramolecular FRET experiments described by Alvarez-Curto *et al.*, (2011). The molecular models that describe the binding of CNO to hM_3WT and to hM_3RASSL are shown in Figure 1.7. The hM_3RASSL elicited a potent calcium release through G_q coupling upon activation with CNO, similar to the response demonstrated by hM_3WT when activated by Ach or Cch. In addition, activation of ERK1/2 was observed upon CNO mediated activation of hM_3RASSL in a manner similar to that seen by hM_3WT upon addition of Ach or Cch (Alvarez-Curto *et al.*, 2011) (Figure 1.8).

The rest of the muscarinic family members (M_1, M_2, M_4 and M_5) were made into functional RASSL/DREADD receptors using hM_3RASSL as a template (Armbruster *et al.*, 2007). The generation of muscarinic RASSLs or DREADDs was a milestone and the validation of those designer receptors as valuable tools with defined ligand specificities

enabled studying specific functions of receptor sub-types (e.g. M_2 vs M_3) or general downstream signalling (e.g. G_q vs G_i). This is of great importance for *in vivo* and *in vitro* applications, especially for muscarinic receptors that share highly conserved residues in their orthosteric binding pocket (Hulme *et al.,* 2003). In addition, the designer receptors activated by CNO proved to be useful in numerous native and artificial cellular environments and have offered a novel approach in investigating receptor activation, function, signalling (Burstein *et al.,* 1995) and recently in the study of GPCR oligomerisation (Alvarez-Curto *et al.,* 2010; Aslanoglou *et al.,* 2015). Variants of the hM_3DREADD/RASSL receptor, termed hM_3Dq and rM_3/β_1D5 designer receptors were expressed in pancreatic β-cells and demonstrated the ability to modulate blood glucose levels and to mediate insulin secretion in response to CNO, suggesting clinical usefulness of the DREADDs in translational applications (Guettier *et al.,* 2009).

One of the main advantages of the second generation designer receptors is the lack of baseline activity (Armbruster *et al.,* 2007). In addition, the use of pharmacologically inert synthetic ligands, based on compounds with known pharmacology, offer the desired functional selectivity in the system studied. CNO, which is structurally similar to clozapine, is an inert ligand i.e. it does not target endogenous receptors and it is highly bioavailable in rodents and humans. Clozapine metabolism in the liver yields two main metabolites, CNO and N-desmethylclozapine, both of which show appreciable activation of the hM_3RASSL receptor (Sur *et al.,* 2003). N-desmethylclozapine was suggested to be a potent allosteric partial agonist of M_1 receptor (Sur *et al.,* 2003). CNO, despite its many advantages in the activation of DREADDs and RASSLs, is metabolised, to a small extent, to clozapine in the liver. Clozapine, is able to modulate neuronal activity by activating numerous receptors present the CNS, and this back metabolism effect can interfere with the selective activation of DREADDs and thus limits the translational application of the designer receptors. New evidence on the structure-activity relationship (SAR) between CNO and DREADDs was demonstrated by Chen *et al.,* (2015), where the DREADD hM_3Dq was used for studying the SAR between CNO and the receptor. This work led to the discovery of compounds demonstrating potent activation of the DREADD without activating the WT receptors. One of these compounds was the drug perlapine. Perlapine was proposed to be a novel hM_3Dq agonist with more than 10,000 fold selectivity for DREADD over the WT (Chen *et al.,* 2015).

A. **B.**

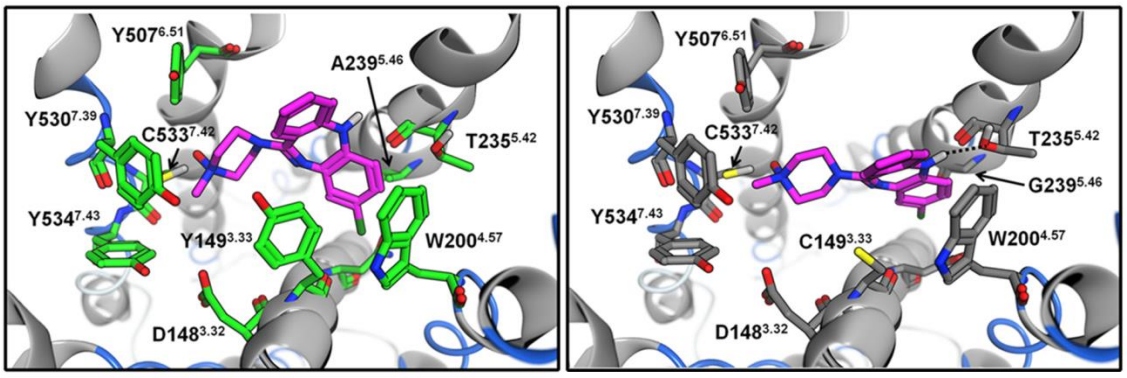

Figure 1.7 Molecular models of the binding mechanism of CNO to (A) hM$_3$WT and (B) hM$_3$RASSL. (A) Thr149 in M$_3$WT is essential for the 'lid' structure that confers a narrow conformation to the binding pocket allowing Ach and Cch, but not CNO to fit (CNO is a bulkier molecule than Ach and Cch). CNO thus, cannot interact with Thr235 and Asp149 within the binding site of the receptor. **(B)** The amino acid residues involved in the interaction between CNO and hM$_3$RASSL are labelled. The interaction of CNO with the Thr253 of the hM$_3$RASSL via a hydrogen bond is shown as a dotted line (Figures taken from Alvarez-Curto *et al.*, 2011).

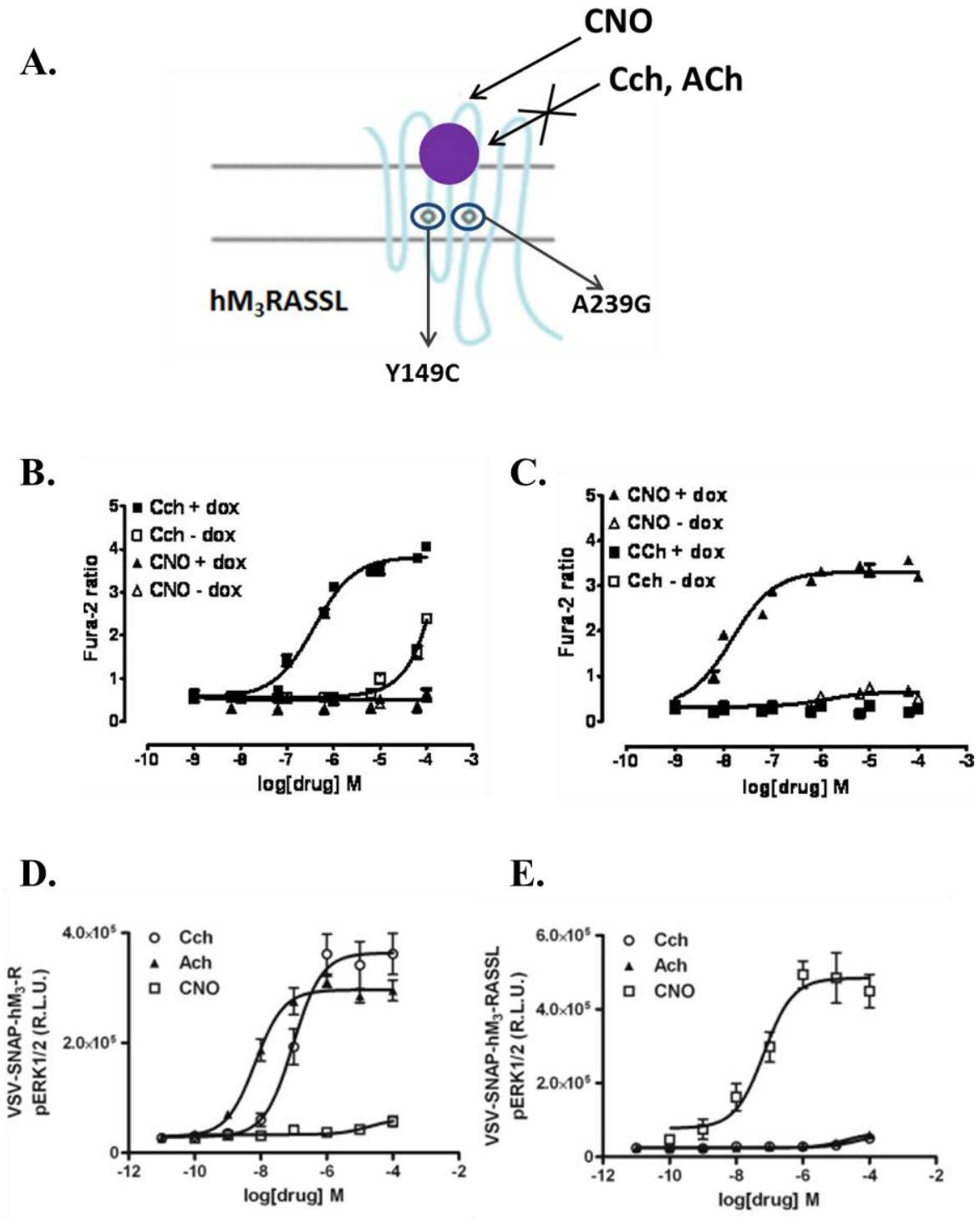

Figure 1.8 hM$_3$RASSL receptor activation in response to CNO. (A) The two point mutations (Y149C and A239G) on the hM$_3$WT that led to the generation of hM$_3$RASSL that cannot respond to natural muscarinic ligands such as acetylcholine or carbachol but only responds to the synthetic ligand CNO. Calcium mobilisation assay performed using cells stably expressing demonstrated that **(B)** carbachol but not CNO could elevate [Ca^{2+}]i levels via FLAG-hM$_3$WT-Citrine and **(C)** CNO but not carbachol could induce calcium release from ER via myc-hM$_3$RASSL-Cerulean (Alvarez-Curto *et al.*, 2010). Selective activation of ERK1/2 phosphorylation was achieved via **(D)** carbachol (but not CNO) mediated activation of VSV-SNAP-hM$_3$WT and **(E)** CNO (but not

carbachol) mediated activation of VSV-SNAP-hM_3RASSL (Figures taken fromAlvarez-Curto *et al.,* 2011).

1.10 Oligomerisation of GPCRs

1.10.1 Dimers versus monomers

The formation of biological complexes originating from proteins interacting with each other is termed oligomerisation. In an oligomer the interacting partner proteins (protomers) can be identical (forming homomers) or different (forming heteromers). The oligomerisation process is very common in many biological systems. A vast variety of proteins involved in numerous biological functions seem to be forming such complexes that are important for cellular function. Single transmembrane protein tyrosine kinase receptors, cytokine receptors, B and T cell receptors, various transcription factors, enzymes and nuclear hormone receptors are only some examples of protein types that exist and function as multimeric complexes or oligomers (Klemm *et al.,* 1998).
Initial studies on GPCRs proposed that monomeric receptors were able to bind and activate their G proteins (Whorton *et al.,* 2007). There is now growing evidence that supports the existence of GPCRs as dimers or higher order oligomers (Milligan, 2004, 2009, 2013; Javitch, 2004). The initial data suggesting the monomeric profile of GPCRs as functional units were the basis for the proposal of the receptor- G protein interaction/activation model (i.e. the 1:1 stoichiometry of receptor: G protein) (Terrillon and Bouvier, 2004). This model was re-examined because new evidence proposed a more consistent model, where a receptor dimer is capable of binding two ligand molecules and a G protein, changing the stoichiometry for ligand/dimer/G protein to 2:1:1 (Herrick-Davis *et al.,* 2005; Pellissier *et al.,* 2011). Initial evidence that supported the existence of functional monomeric GPCRs was demonstrated by the observation that monomeric rhodopsin in solution was able to activate its G protein (Ernst *et al.,* 2007) and to bind to arrestin in a 1:1 stoichiometry (Tsukamoto *et al.,* 2010; Bayburt *et al.,* 2011). Examples of purified receptors that were reconstituted into proteoliposomes capable of accommodating only monomers, demonstrated that monomeric GPCRs were able to activate their G proteins (Whorton *et al.,* 2007). On the other hand, there was a growing body of evidence clearly suggesting the existence of homomeric and heteromeric GPCR complexes and more importantly implying that those complexes are functional and potentially providing a regulatory role in many cellular processes (Milligan, 2009; Angers *et al.,* 2002; Klemm *et al.,* 1998).

Atomic force microscopy revealed the dimeric arrangement of rhodopsin in native mouse disc membranes (Fotiadis *et al.,* 2003) .The presence of rhodopsin dimers in native retinal membranes was demonstrated (Liang *et al.,* 2003), as well as the ability of the rhodopsin dimer to interact with a single G protein (Jastrzebska *et al.,* 2013). Crystal structures of the extracellular ligand binding regions of mGluR1 receptor in complex with glutamate and structures of the inactive state of the receptor showed the presence of receptor homodimers (Kunishima *et al.,* 2000). Information collected from crystal structures of chemokine CXCR4 receptor (Wu *et al.,* 2010), κ-opioid receptor (Wu *et al.,* 2012) and μ-opioid receptor (Manglik *et al.,* 2012) confirmed the ability of receptors to be arranged in a dimeric/oligomeric organisation. Different interfaces seemed to be involved in receptor oligomerisation. An example is the TM1-TM2-helix 8 interface that is observed in μ-opioid receptor homodimerisation (Manglik *et al.,* 2012), in κ-opioid receptor dimerisation (Wu *et al.,* 2012), in β_1-adrenergic receptor dimerisation (Huang *et al.,* 2013), in inactive rhodopsin (Park *et al.,* 2008) and rhodopsin bound to 11-*cis*-retinal (Ruprecht *et al.,* 2004) dimer formation. Another potential dimerisation interface that was revealed from studying crystal structures of CXCR4 and μ-opioid receptor involved TM5-TM6 interactions (Hiller *et al.,* 2013), while the role of TM5 seems to be important in the dimerisation of the dopamine D_2 receptor, muscarinic acetylcholine M_3 receptor and the 5-HT_{2C} receptor. TM6 domain was suggested to be involved in the homodimerisation interface of the β_2-adrenergic receptor (Hiller *et al.,* 2013).

Although solving the crystal structures of some GPCRs revealed valuable information about the oligomeric arrangement of the receptors, there was not a consensus dimeric/oligomeric interface common for all GPCRs or even common for the members of a group of GPCRs. In addition, the process of crystallisation is a complex and multi-step one, and it is not clear whether dimeric/oligomeric GPCR crystals have physiological relevance (Bouvier and Hebert, 2014).

1.10.2 Roles of oligomerisation

One of the initial reports of potential interactions between different GPCRs included functional cross-talk between α_2- and β_2-adrenoceptors demonstrated as an increase in α_2-adrenoceptor binding in cortical tissue after treatment with isoproterenol, a β_2-adrenoceptor agonist (Maggi *et al.,* 1980; reviewed in Gomez-Soler *et al.,* 2011). Various similar examples were reported but were considered as evidence of receptor signalling cross-talk rather than strong oligomerisation evidence. The first experiment that had pharmacological

significance was carried out by Jordan and Devi, (1999) who suggested the formation of a heterodimer between κ- opioid and δ-opioid receptors. Co-expression of both receptors resulted in decreased affinity of κ- or δ-opioid receptor selective ligands, when administered alone, but the affinity was restored when both ligands were added to the assay, suggesting the existence of heteromers, through the occurrence of positive co-operativity (Jordan and Devi, 1999). Another example whereby the formation of oligomeric complex confers pharmacological diversity to the receptor system is the observation of stable heteromers between the co-expressed orexin 1 (OX1) and cannabinoid 1 (CB1) receptors. The CB1 receptor antagonist, rimonabant, antagonises orexin A stimulation of ERK1/2 through OX1, when the two receptors are in a complex. The oligomeric profile of both receptors can be regulated by both OX1 and CB1 receptor ligands (Ellis *et al.*, 2006). This suggests that receptor heteromerisation can alter receptor pharmacology, probably by altering receptor-agonist recognition by the formation of a new binding site with unique pharmacology (Gomez-Soler *et al.*, 2011).

A very important example that attracted attention to GPCR oligomers was described in the work of Maggio *et al.*, (1993). This involved the generation of chimeric receptors combining features of the muscarinic M_3 and adrenergic α_{2C}-AR receptor to study oligomerisation using a functional complementation approach. A chimeric M_3/α_{2C}-AR was generated by combining the first five TM domains of M_3 (including the IL3) and the last two TM domains of the adrenergic receptor. An equivalent α_{2C}-AR/M_3 chimera involved the combination of the first 5 TM domains of the adrenergic receptor and the final two TM domains of the M_3, including the IL3 of M_3. The IL3 was included unaltered because it was considered to be essential for G protein coupling specificity. Treatment with the muscarinic agonist carbachol did not lead to muscarinic receptor-mediated signalling when each chimeric receptor was expressed alone. Co-expression of the chimeras resulted in a carbachol-mediated response, indicating that the muscarinic receptor function was rescued, potentially due to oligomerisation, thus, suggesting a role of receptor oligomerisation in receptor function (Maggio *et al.*, 1993; 1998). These examples support the hypothesis of class A receptors' ability to form oligomers (Milligan, 2013; Herrick-Davis, 2013).

Class C GPCRs form constitutive dimers/oligomers, with the $GABA_B$ receptor demonstrating the functional significance of oligomerisation, being able to activate G protein only when in hetero-dimeric form (Jones *et al.*, 1998; Kaupmann *et al.*, 1998). In the case of $GABA_B$ receptor heteromerisation is required for function (White *et al.*, 1998). $GABA_B$ consists of two subunits, the $GABA_{B1}$, that is capable of binding to the GABA

ligand, but cannot activate G protein and $GABA_{B2}$ which is responsible for G protein activation but not for binding to G protein (Jones *et al.,* 1998). Heteromerisation of the $GABA_{B1}$ and $GABA_{B2}$ results in the masking of the ER retention signal sequence of the $GABA_{B1}$ (Margeta-Mitrovic *et al.,* 2000) allowing the complex to reach plasma membrane and function. This suggests that oligomerisation possesses roles not just in the function and signal transduction but also in the trafficking of receptors (Pin *et al.,* 2007; Calebiro *et al.,* 2013), since neither of the protomers was able to function nor to travel to the plasma membrane alone. Additional evidence of dimer/oligomer formation in early protein synthesis was generated using a truncated version of β_2-AR where the C-terminal domain was replaced with the corresponding region of $GABA_{B1}$ receptor. This resulted in an ER export-deficient mutant that inhibited the cell surface trafficking/delivery of the wild type β_2-AR, when the two versions were co-expressed (Salahpour *et al.,* 2004). A similar approach was followed for co-expressed CXCR1 and CXCR2 receptors. The C-terminal domain of the CXCR1 was replaced with the ER retention motif sequence of the β_2-AR and a CXCR1 ER retention mutant was generated. Co-expression of the mutant with CXCR1 or CXCR2 WT prevented cell surface delivery of the WT receptors (Wilson *et al.,* 2005).This evidence suggests that formation of quaternary structure of GPCRs that leads to oligomerisation occurs early in biosynthesis of proteins (Milligan, 2004; Salahpour *et al.,* 2004). It is important to mention that the role of oligomerisation is also highly regulated in terms of protein folding, since misfolded proteins are unable to pass the cellular quality control and thus cannot traffic from ER to plasma membrane, but are processed for proteosomal degradation (Petaja-Repo *et al.,* 2001).

A role of oligomerisation in receptor internalisation has also been suggested since agonist mediated endocytosis has been documented for many heteromers including somatostatin SSTR1/SSTR5 heteromers (Rocheville *et al.,* 2000), α_{2A}/β_1-AR heteromers (Xu *et al.,* 2003) and δ-opioid/β_2-AR receptor heteromers, whereby stimulation of only one protomer was sufficient to cause co-internalisation of the complex. Homodimers of β_2-AR also internalised upon agonist binding (Sartania *et al.,* 2007).

Signalling of the receptors that participate in an oligomeric complex is affected in some cases, implying a role of oligomerisation in GPCR signalling cascades.

Oligomer formation can change G protein coupling preference and specificity, subsequently affecting GPCR signalling cascades. Dopamine D_1 and D_2 receptors signal through G_s and G_i, respectively, when in monomeric or homodimeric forms. The formation of a D_1/D_2 heteromer was followed by activation of G_q coupling, suggesting that heteromerisation can result in altered G protein coupling than that of the corresponding

monomers (Rashid *et al.,* 2007). This finding was opposed by Frederick *et al.,* (2015) who challenged the existence of the G_q signalling D_1/D_2 complex in mutant mouse models (behavioural pharmacological approach), in *ex vivo* analyses involving immunocytochemistry for investigating receptor co-localisation and proximity ligation assay (PLA) to assess proximity of receptors in brain slices and, finally, by BRET-based *in vitro* work (Frederick et al., 2015).

Interestingly, heteromerisation between muscarinic receptors M_3 and M_5, in cells co-expressing the receptors, demonstrated a negative regulatory role in receptor function. A peptide derived from the IL3 of M_5 that specifically targets heteromer formation without affecting receptor function, inhibited carbachol-mediated ERK1/2 activation and reduced the levels of heteromer formation between M_3 and M_5 (Borroto-Escuela *et al.,* 2010).

Dimers of GPCRs are considered as more appropriate scaffolds for binding to single arrestin molecules (Han *et al.,* 2001) resulting in the desensitisation of the GPCR dimer and leading to clathrin-mediated internalisation of the dimer (Milligan, 2004). It has been demonstrated that oligomerisation may alter the β-arrestin subtype -receptor interactions. Co-expressed thyroptropin releasing hormone TRH_1 and TRH_2 receptors demonstrated alternative patterns of β-arrestin subtype recruitment than that seen when each receptor was expressed alone (Hanyaloglu *et al.,* 2002). Co-expressed vasopressin V_2 and $V_{1\alpha}$ receptors were reported to behave in a similar manner in terms of β-arrestin recruitment (Terrillon *et al.,* 2004). Formation of oligomers in early stages of biosynthesis, was reported for vasopressin V_2 receptor (Morello *et al.,* 2000) and oxytocin receptors, using BRET (Terrillon *et al.,* 2003), as well as homomerisation and heteromerisation of opioid receptor subtypes (Wang *et al.,* 2005; Gomes *et al.,* 2013).

Oligomerisation of GPCRs can change the behaviour of the receptors and affect the plasma membrane diffusion, which may in turn affect the receptors' interactions with other cellular components including cytoskeletal, scaffolding proteins or the lipid molecules of the membrane (Gomes-Soler *et al.,* 2011). Receptor oligomerisation facilitates the proximity between two or more receptors, resulting in increased interaction probability but also in enhanced binding specificity through the formation of an enlarged interaction surface area (Klemm *et al.,* 1998) bringing potential stability to the complex.

1.10.3 Evidence of GPCR oligomers *in vivo*

Expression of receptors in heterologous cellular systems has been very useful in the investigation of GPCR oligomerisation, but it has been suggested that certain parameters such as the level of receptor expression may affect the interpretation of data and may lead to false conclusions about the oligomerisation of a receptor. Even if all the experimental conditions are controlled and all the assay controls are used, there are a number of factors that can affect the integrity of the results. Therefore, it is of great importance that experiments should be directed to *in vivo* studies in native tissues or even whole organisms, so that the functional relevance of GPCR oligomerisation can be validated. Some initial attempts to confirm the existence of oligomers in native tissues have been performed.

Homodimers of oxytocin receptors were identified using an htrFRET-based approach with fluorescently labelled antagonists, in mammary gland tissue of lactating rats (Albizu *et al.*, 2010). Functional complementation experiments using mutated receptors in the absence of functional LH receptors in mice confirmed the presence of LH receptor oligomers *in vivo* (Rivero-Muller *et al.*, 2010; Vassart, 2010).

Melatonin receptors MT_1 and MT_2 in rod photoreceptors were demonstrated to function as heterodimers. In a KO mouse study, the loss of either MT_1 or MT_2 receptors, or over-expression of a non-functional version of MT_2 receptor resulted in the inhibition of melatonin mediated signalling (Bouvier and Hebert, 2014).

Detection of constitutive serotonin 5-HT_{2C} receptor homomers in choroid plexus epithelial cells was achieved by employing a combination of fluorescence correlation spectroscopy (FCS) and photon counting histogram (PCH), using an anti-5-HT_{2C} fragment antigen binding protein to label native receptors in their native cellular environment (Herrick-Davis *et al.*, 2015).

A better understanding of the receptor expression and co-expression patterns in combination with the development of techniques that will enhance *in vivo* study of oligomerisation in native tissues would be advantageous in solving questions of GPCR oligomerisation and the physiological relevance and implications to disease.

1.10.4 Evidence of mAChRs oligomerisation

Following the observation of protein-protein interactions between the chimeric M_3/α_{2C}-AR and α_{2C}-AR/M_3 receptors that were attributed to the ability of muscarinic receptors to

dimerise via a domain swapping mechanism (Maggio *et al.*, 1993, 1998), other data emerged supporting oligomerisation of mAChRs.

The ability of mAChRs to form oligomers has been confirmed by various RET-based methods. For example, the use of two differentially tagged hM_1 receptors (hM_1-Rluc and hM_1-EYFP) generated BRET signal that was consistent with the formation of constitutive hM_1 homomeric complexes (Marquer *et al.,* 2010). Many variations of FRET have been utilised to study GPCR oligomerisation. Intra-molecular FRET has been used to study conformational changes within the receptor molecule (Vilardaga *et al.*, 2003). Inter-molecular FRET has been employed to study receptor dimerisation and also interactions between the M_1 receptor and ligand molecules (Ilien *et al.*, 2009). The stability and size of oligomers cannot be easily determined by conventional BRET and FRET-based approaches; hence a more specialised approach is required. For example, the dynamic interchange between M_1 monomers and dimers at the surface of live cells was determined using two-colour total internal reflection fluorescence imaging (TIRFM), which utilised a fluorescently labelled form of the muscarinic antagonist telenzepine. The results from this work were consistent with the presence of both M_1 dimers and monomers and it was proposed that, at steady state about 30% of the M_1 receptor population exists in a dimeric form (Hern *et al.*, 2010).

The oligomeric arrangement of M_2 receptor into homo-tetramers has been demonstrated in live cells by quantitative FRET (Pisterzi *et al.,* 2010) with the M_2 receptor tendency to form tetramers being confirmed by pharmacological studies (Redka *et al.,* 2014).

Zeng and Wess, (1999) had demonstrated the existence of M_3 in monomeric, dimeric and oligomeric forms, by subjecting lysates from COS-7 cells expressing the rat M_3 receptor to Western blot analysis under non-reducing conditions. Site directed mutagenesis using rat M_3 receptor as a template generated cysteine substituted M_3 mutants. This indicated two important cysteine residues (Cys140 and Cys220) with a key role in M_3 dimer formation. The results were confirmed by co-immunoprecipitation and immunological studies (Zeng and Wess, 1999). Disulphide cross-linking experiments under non-reducing conditions using these cysteine substituted mutants of the rat M_3 receptor led to the identification of some variants that exclusively existed in a constitutive dimeric form (Hu *et al.,* 2011). Results from these studies were consistent with the existence of two possible dimeric M_3 interfaces (e.g. TM4-TM5-IL2 through IL2-IL2 contacts and TM1-TM2-helix 8 through H8-H8 interactions) (Hu *et al.,* 2013). The formation of M_3 dimers or higher order oligomers has also been demonstrated by McMillin *et al.,* (2011) by saturation BRET experiments using Venus and luciferase tagged M_3 receptors (McMillin *et al.,* 2011).

Molecular modelling assisted by BRET data and mutagenesis of M_3 receptor's TM domains revealed the existence of four different dimeric arrangements characterised by four distinct interfaces involving: TM5-TM5, TM6-TM7, TM4-TM5 and TM1-TM2. The lowest energy model involved the TM5-TM5 interface and predicted that Tyr255 on a monomer of M_3 is responsible for interactions with Arg253, Lys256 and Lys260 residues on the adjacent M_3 monomer (McMillin *et al.,* 2011). A variant of FRET called homogeneous time-resolved FRET (htrFRET) has been used in combination with SNAP- and CLIP tagging of the N-terminus of receptors and labelling with SNAP and CLIP epitope specific fluorescent substrates (described in section 1.12), in the detection of homomers of the M_3 receptor (Alvarez-Curto *et al.,* 2010) and similarly in the detection of M_2 and M_3 homomers and heteromers in live cells (Aslanoglou *et al.,* 2015). The rhomboidal arrangement of M_3 tetramers was documented using quantitative FRET spectrometry and mathematical analysis of the FRET efficiencies obtained from spectral deconvolution (Patowary *et al.,* 2013). The above examples are shown in Figures 1.9 and Figure 1.10. In order to understand the basis of M_3 tetrameric interactions, a combination of site-directed mutagenesis and htrFRET was used (Varela Liste *et al.,* 2015). Molecular modelling studies assisted by alanine mutagenesis at residues within the TM domains of the VSV-SNAP-hM_3WT have pointed out the involvement of several TM domains of M_3 in the organisation of a tetramer. The TM domains involved were: TM1, TM4, TM5, TM6, TM7 and helix 8. Multiple residues on the TM domains were identified to play a role in the formation of oligomers and the molecular model generated was consistent with a dimer: dimer interface involving TM1-TM2-helix 8 interactions, with the presence of cholesterol molecules between the dimers of the receptor (Varela Liste *et al.,* 2015).

The ability of M_1, M_2 and M_3 receptors to form constitutive homomers was detected by quantitative BRET analysis using live HEK 293 cells expressing fluorescently tagged receptors. The presence of homomers of muscarinic receptors was demonstrated along with the existence of heteromers (M_1/M_2, M_2/M_3, M_1/M_3) by saturation BRET assays, suggesting that the dimer was the predominant receptor form (Goin and Nathanson, 2006). Maggio *et al.,* (1999) examined binding of two antagonists, pirenzepine and tripitramine, to M_2 and M_3 muscarinic receptors. The results revealed the existence of distinct receptor populations; the first corresponding to individual M_2 or M_3 receptors while the second population was consistent with heteromeric formation between M_2/M_3 (Maggio *et al.,* 1999). Biochemical data using co-immunoprecipitation and fluorescence microscopy experiments confirmed the M_2/M_3 heteromerisation and homomerisation of M_2 and M_3 and

suggested that β-arrestin 1 recruitment to M_3 required the paired activation of both receptor protomers that constitute the dimer (Novi *et al.*, 2005).

Saturation BRET in combination with co-immunoprecipitation experiments was carried out in order to study oligomerisation of M_3 and M_5 receptors (Borroto-Escuela *et al.*, 2010). This study suggested that M_3 and M_5 exist as constitutive homo-dimers and can also hetero-dimerise when expressed in the same cells. There is also evidence that suggest a key role of IL3 of M_5 in the modulation of dimerisation by possibly affecting the conformational rearrangement of M_3-M_5 hetero-dimer, in a G-protein independent fashion (Borroto-Escuela *et al.*, 2010).

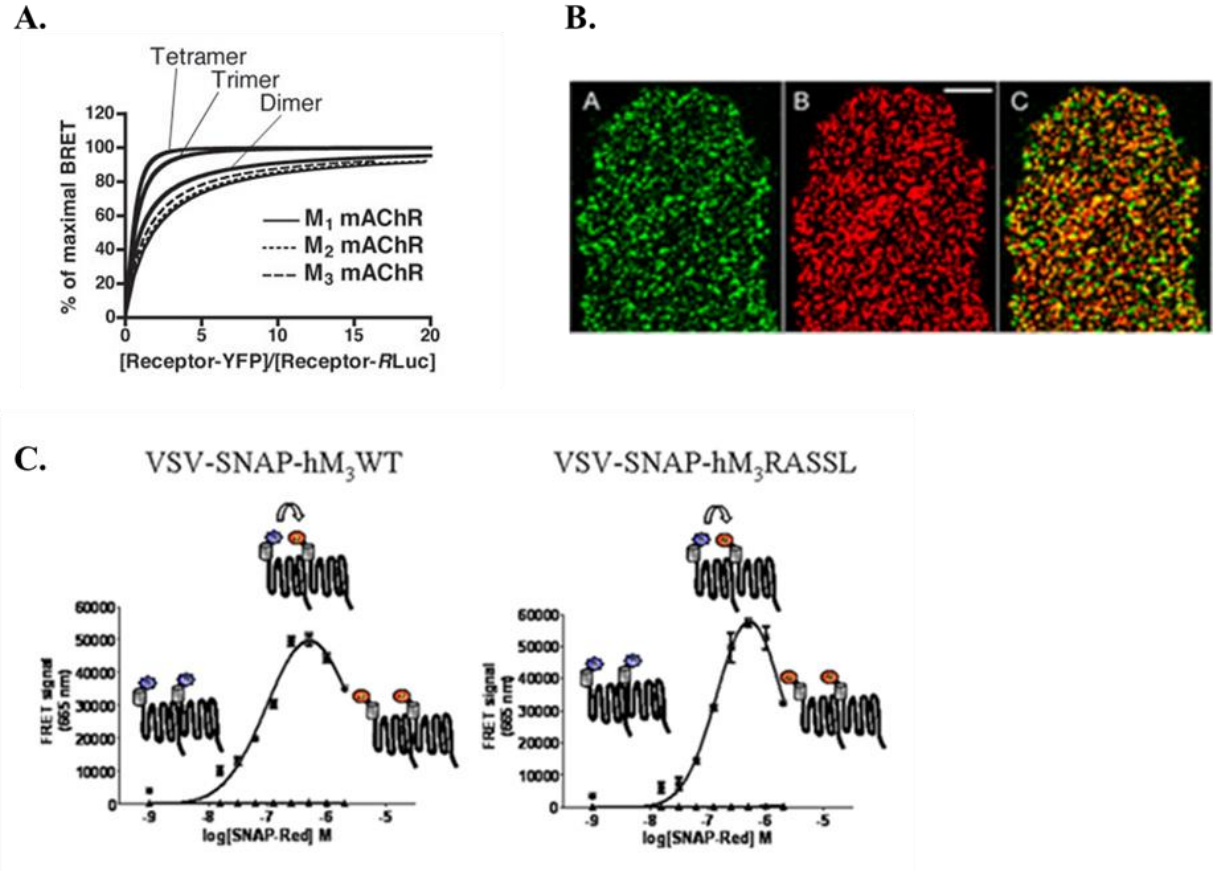

Figure 1.9 Muscarinic receptor oligomers. (A) A saturation BRET-based assay using transfected mammalian cells demonstrated the presence of homomers of M_1, M_2 and M_3 receptors (Figure taken from Goin and Nathanson, 2006). **(B)** Total internal reflection fluorescence microscopy carried out at single cell resolution utilising fluorescently tagged telenzepine successfully demonstrated the presence of M_1 dimers at the surface of live cells and proposed the dynamic interchange between monomers and dimers of M_1 receptor (Figure taken from Hern *et al.*, 2010). **(C)** Homogeneous time-resolved FRET signals that corresponded to the existence of VSV-SNAP-hM$_3$WT and VSV-SNAP-hM$_3$RASSL oligomers at the surface of live Flp-In™ T-REx™ 293 cells,

were obtained following labelling with SNAP-Lumi4 Tb and SNAP-Red substrates, acting as energy donor and acceptor, respectively (Figure taken from Alvarez-Curto *et al.*, 2010).

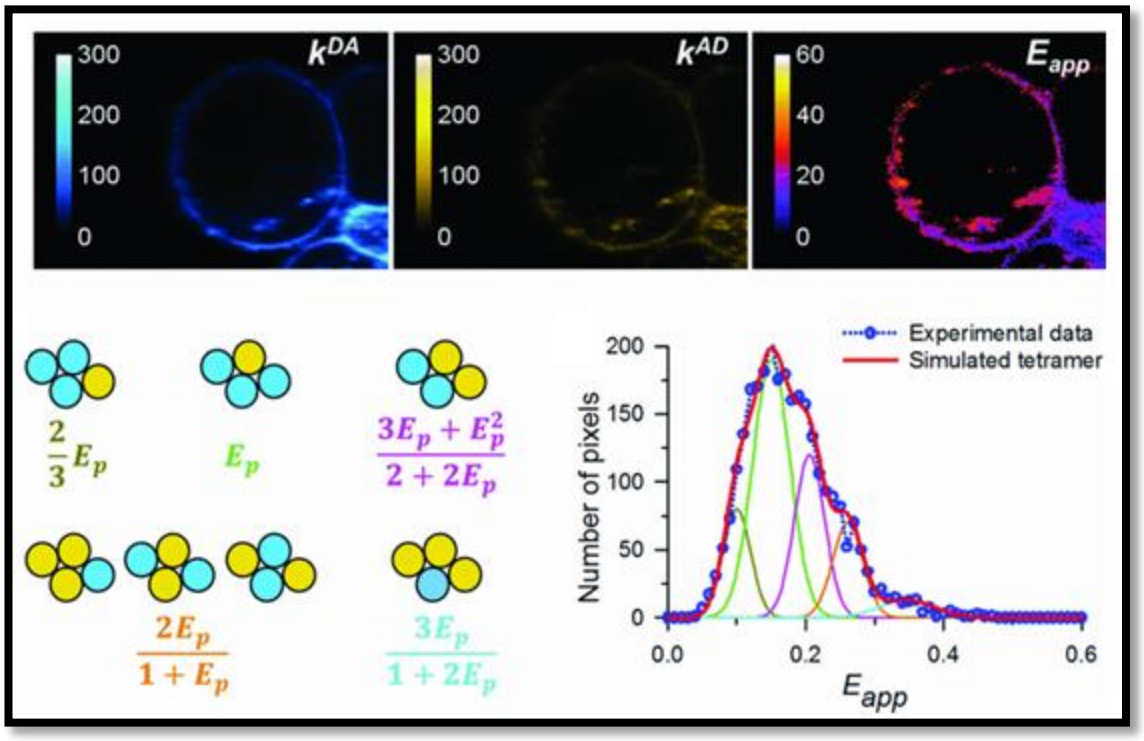

Figure 1.10 M_3 receptor is a tetramer of rhomboidal arrangement. FRET-based analysis of Flp-In™ T-REx™ 293 cells co-expressing myc-hM_3RASSL-Cerulean (inducible) and FLAG-hM_3WT-Citrine (constitutive) in combination with analysis within a theoretical framework of distributions of FRET efficiencies and spectral deconvolution of these efficiencies, suggested that the homomeric population of M_3 receptors is a mixture of dimers and rhombic tetramers (Figure taken from Patowary *et al.*, 2013).

Despite the growing evidence supporting GPCR oligomerisation, no general consensus on the mechanism that underlies this has been reached that could include all GPCRs. This could be due to structural differences between receptors, potentially requiring different dimer/oligomer interfaces. Many different methods have been used to investigate the oligomerisation of receptors. The different methods used provided a great degree of variation in the obtained outcomes in terms of oligomerisation and have not offered definitive answers on size, stability and regulation of receptor oligomerisation. This points out the importance for further investigation in the field of receptor oligomerisation in order to try and provide answers to questions regarding the size of the complexes formed, the

manner oligomerisation affects signalling and pharmacology of receptors and the nature of oligomerisation (constitutive or ligand-mediated).

1.11 Ligand regulation of oligomerisation

Several questions still remain unanswered about the size and stability of oligomeric complexes formed between GPCRs. In addition, ligand-mediated regulation of GPCR oligomerisation is still an area of great scientific debate. There is no consensus mechanism in terms of regulation of oligomerisation by ligands, but different observations have been encountered suggesting three possibilities. Firstly, if the receptor exists in a dimeric/oligomeric arrangement, it is possible that any ligand-mediated receptor activation may alter the conformation of the receptor and this can result in a change in the oligomeric profile of the receptor in question. Secondly, it is possible that no changes will be observed in receptor oligomerisation upon ligand binding. Finally, ligand activation may be a prerequisite for dimer/oligomer formation (Angers *et al.*, 2002).
Investigation of β_2-AR dimerisation suggested the dynamic interchange between monomeric and dimeric forms of the receptor upon ligand addition. More specifically, agonist (isoproterenol) stimulation of β_2-AR stabilised the dimeric formation whereas, inverse agonist (timolol) favoured the reversal of dimer formation into monomers (Hebert *et al.*, 1996). BRET-based assays that involved the stimulation of β_2-AR with a selective agonist, isoproterenol, resulted in an increase in the level of energy transfer consistent with either an increase in dimer formation or an intramolecular conformational change that altered the orientation of the energy donor and acceptor or their proximity (Angers *et al.*, 2000). More recent BRET-based experiments demonstrated physical and functional interactions between CB_1 cannabinoid receptors and β_2-AR in transfected cells and also in tissues co-expressing the receptors. Ligand regulation of oligomerisation affected the signalling and trafficking of the two receptors. The CB_1 receptor inverse agonist AM251 inhibited β_2-AR induced pERK signalling in cells co-expressing the receptors, while the CB_1 receptor neutral antagonist, O-2050, had no effect on the β_2-AR-related signalling pathways (Hudson *et al.*, 2010). Opioid agonists were documented to lead to a decrease in the dimer concentration of δ-opioid receptors (Cvejic and Devi, 1997). By contrast, constitutive BRET signal was observed indicating the dimerisation of δ-opioid receptor, but the oligomeric profile of the receptor was insensitive to agonist treatment (McVey *et al.*, 2001). The constitutive homomeric status of gonadotropin releasing hormone receptor,

as detected by FRET signal between the GFP and RFP tagged receptors, was increased upon agonist (buserelin) treatment in a concentration-dependent manner (Cornea *et al.*, 2000). However the heteromerisation between dopamine D_2 and somatostatin SST_5 receptors was promoted by antagonists rather than agonists (Rocheville *et al.*, 2000).
The dynamic interplay between $CXCR_1$ and $CXCR_2$ heteromers and their corresponding homomers was affected by the addition of the agonist CXCL8, which binds to both receptors, but shows greater affinity for $CXCR_2$. Changes in FRET signal were detected corresponding to a decrease of heteromers and increase in both $CXCR_1$ and $CXCR_2$ homomers. In addition, the expression of $CXCR_1$ interfered with the formation $CXCR_2$ homomers suggesting that receptor expression also plays a role in regulation of oligomerisation (Martinez-Munoz *et al.*, 2009).
A BRET-based approach to investigate the heteromerisation between α_1-AR and $CXCR_2$ receptors demonstrated that the constitutive heteromers formed were not affected by ligands (Mustafa *et al.*, 2012).
A combination of SNAP tag technology and TIRFM approach to detect individual receptors and oligomers of β_1-AR and β_2-AR receptors at the cell surface, allowed for single molecule tracking of individual GPCRs (Calebiro *et al.*, 2013). In addition, the detection and analysis of oligomers showed that β_1-AR was predominantly in a monomeric form at low receptor densities, but dimer formation was enhanced when receptor density increased. On the contrary, the β_2-AR showed a higher tendency towards forming dimers or higher order oligomers even at low receptor densities. The transient nature of the β_1/β_2-AR interaction was also demonstrated (Calebiro *et al.*, 2013). The method employed by Calebiro *et al.*, (2013) allowed for the dynamics and size of receptor complexes to be estimated, and enabled the monitoring of receptor mobility and finally was useful in assessing ligand regulation upon agonist binding (Calebiro *et al.*, 2013).

The issue of ligand regulation of muscarinic receptor oligomerisation is not yet clear. A series of contradicting results exists, with some indicating ligand-mediated regulation of the oligomeric status of muscarinic receptors and others supporting the inability of ligands to confer changes in the homomeric and/or heteromeric profile of muscarinic receptors. Some muscarinic ligands were documented to affect the oligomeric organisation of muscarinic receptors. Namely, pirenzepine induced M_1 dimerisation (Ilien *et al.*, 2009) and the orthosteric antagonist QNB stabilised pre-existing M_2 dimers (Park and Wells, 2003). The muscarinic toxin 7 (MT7), a highly M_1 selective allosteric peptide that is isolated from snake venom, seems to have the ability to bind and stabilise pre-existing dimeric forms of

M_1, probably by inducing conformational changes within the oligomer, without promoting new M_1 dimer formation. This was demonstrated by BRET-based assays, monitoring the BRET signal, indicative of the M_1-Rluc and M_1-EYFP interactions (Marquer *et al.*, 2010). Early biochemical data using mutants of the rat M_3 receptor lacking most of the IL3 resulted in non-significant changes in the muscarinic receptor oligomerisation upon treatment with carbachol (Zeng and Wess, 1999). On the other hand, Hu *et al.*, (2013) identified some cysteine substituted mutants of rat M_3 receptor where carbachol treatment resulted in a reduction of M_3 monomers and a simultaneous increase in dimeric form of M_3, in a concentration dependent manner (Figure 1.11) (Hu *et al.*, 2013).

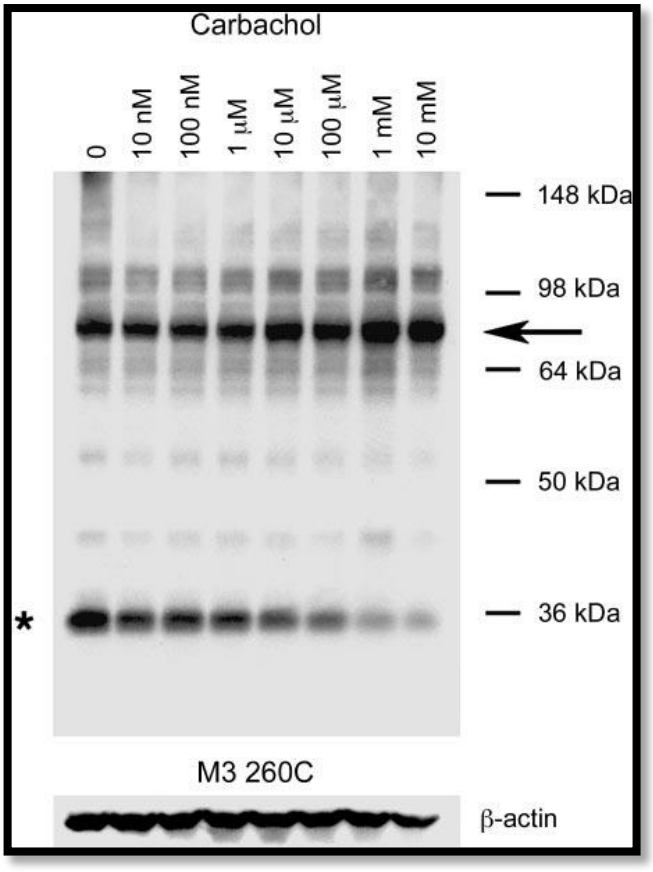

Figure 1.11 Carbachol regulates M_3 receptor dimerisation. Cysteine substituted rat M_3 receptor mutant (R260C) was used to perform cross linking experiments, assisted by incubation with copper phenanthroline (CuPhen). M_3 dimerisation increased in response to carbachol treatment (arrow) while at the same time there was a decrease in the monomeric form of the M_3 receptor (star) (Figure taken from Hu *et al.*, 2011).

Another BRET-based approach followed by Goin and Nathanson, (2006), demonstrated the existence of M_1, M_2, M_3 homomers and heteromers by quantitative saturation BRET analysis, but failed to show that short term carbachol treatment could regulate the oligomeric status of either homo- and hetero-mers between muscarinic receptors (Goin and

Nathanson, 2006). The ability of carbachol and atropine to regulate the homomeric arrangement of M_3WT receptor was demonstrated by htrFRET-based assays in combination with SNAP-tag technology, while the synthetic ligand CNO enhanced the dimerisation of the RASSL version of M_3, as described by Alvarez-Curto *et al.*, 2010 (Figure 1.12).

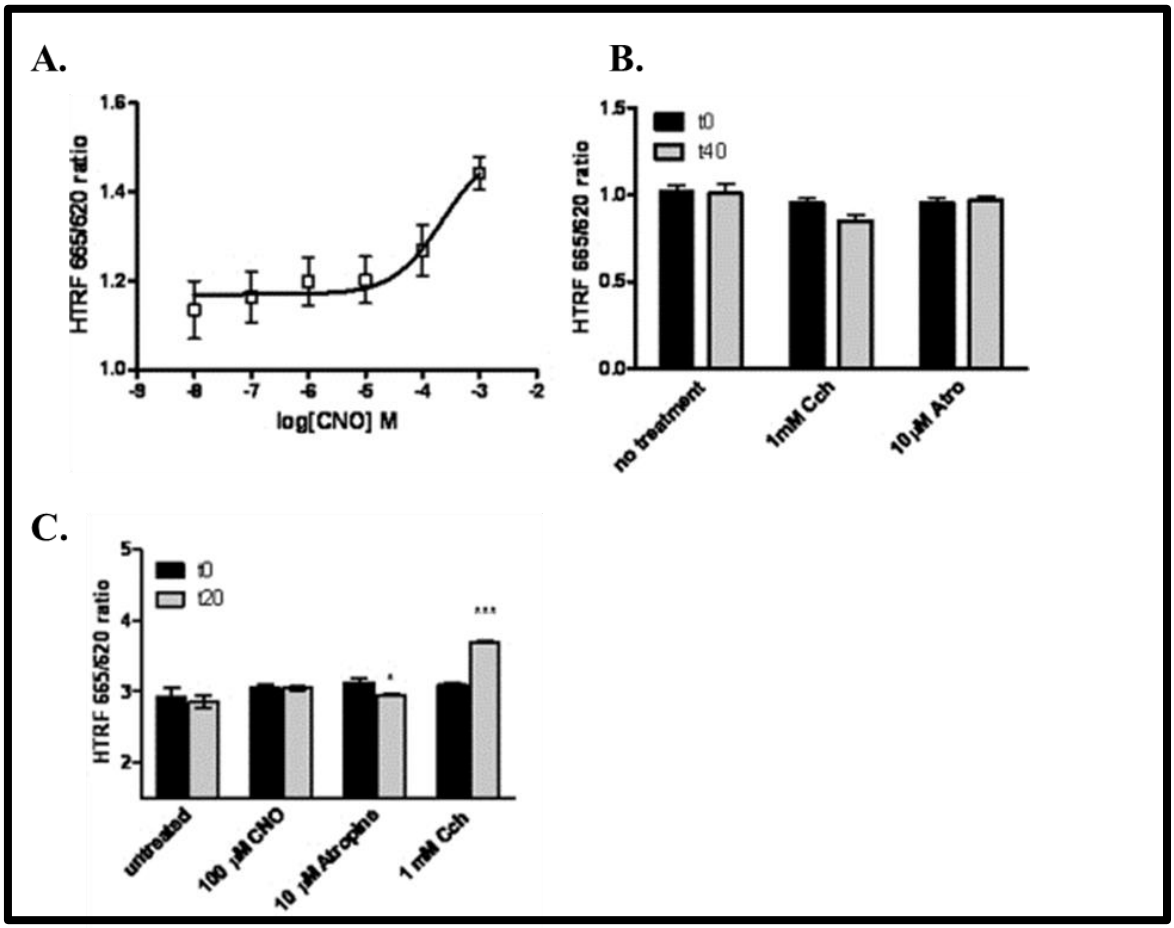

Figure 1.12 Agonists promote hM_3 receptor oligomerisation. Flp-In™ T-REx™ 293 cells inducibly expressing either the VSV-SNAP-hM_3RASSL (A and B) or the VSV-SNAP-hM_3W receptors were subjected to SNAP-Lumi4 Tb (donor) and SNAP-Red (acceptor) labelling and htrFRET was monitored upon ligand addition. (A) The synthetic ligand CNO induced an increase in homomerisation of VSV-SNAP-hM_3RASSL in a concentration dependent manner; (B) while Cch and atropine had no effect on the homomeric organisation of the receptor. (C) The agonist carbachol significantly increased the homomerisation of VSV-SNAP-hM_3WT, as demonstrated by an increase in htrFRET, while CNO had no effect on the homomeric profile of VSV-SNAP-hM_3WT (Figure taken from Alvarez-Curto *et al.*, 2010).

Recent data propose the ability of carbachol to induce changes in heteromerisation between M_2WT and M_3RASSL receptors in cells co-expressing both receptors. The heteromeric arrangement of M_2/M_3 was reduced upon carbachol treatment while at the same time the

M_2/M_2 homomerisation was increased, as detected by htrFRET. Although changes in M_2/M_3 heteromers and M_2 homomers were detected, the M_3 homomers seemed to remain unaffected by agonist treatment (Aslanoglou *et al.,* 2015).

The lack of a common theme for ligand-mediated regulation of GPCR oligomerisation may suggest that each receptor behaves in a unique manner in terms of interacting with other receptors. In addition, the experimental approach followed and the interpretation of the data obtained may be crucial for determining the role of ligands in regulating the oligomeric profile of receptors. Therefore, methods that offer enhanced resolution, high sensitivity and the appropriate controls (positive and negative) to ensure good quality data could be extremely advantageous.

Understanding and clarifying the role of ligands in the regulation of oligomeric state of GPCRs could contribute in the understanding of the actual role of oligomerisation.

1.12 Resonance energy transfer (RET) methods used to study GPCR oligomerisation

Novel advances in RET methods have revolutionised the development of htrFRET, a relatively new method that has been used for investigating protein-protein interactions, in live cell-based assay formats. htrFRET is based on the same principles of resonance energy transfer, as described by Theodor Förster in 1948 (that is the non-radiative energy transfer that occurs between two energy partners, one donor and one acceptor). The requirements for FRET energy donor and acceptor partners are: (A) energy compatibility; donor emission spectrum must overlap with the excitation spectrum of the acceptor, (B) compatible orientation of both donor and acceptor and (C) non-radiative energy transfer can occur only when the two energy partners (donor and acceptor) are in close proximity. The efficiency (E) of the transfer may be calculated using the equation below. Efficiency is inversely proportional to the sixth power of the distance (r):

$$E = \frac{Ro^6}{Ro^6 + r^6}$$

Where, E is the energy transfer efficiency and Ro is the Forster distance between donor and acceptor when the transfer efficiency is 50% (Förster, 1948).

Standard FRET experiments involve the fusion of fluorescent proteins to the receptor in question. Very popular combinations of fluorescent proteins for FRET experiments

includes variants of the GFP (CFP and YFP) incorporated into the receptor of interest by genetic engineering (Vilagarda *et al.*, 2009) (see Figure 1.13). Alternatives included a combination of CFP and FlAsH FRET sensor (Alvarez-Curto *et al.*, 2010). A conceptually similar RET-based method utilises the combination of a fluorescent protein and a luciferase has been extensively used to detect protein-protein interactions by monitoring BRET (Goin and Nathanson, 2006).

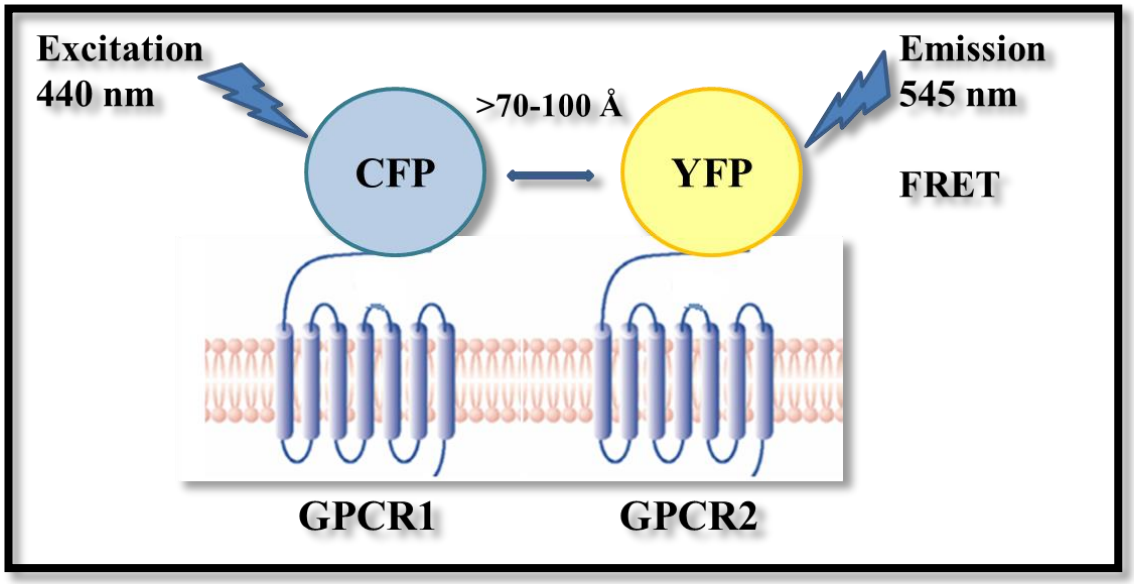

Figure 1.13 FRET between two GPCRs fused to CFP and YFP. Two spectrally compatible fluorescent proteins, such as CFP and YFP, can be fused at the C- or the N-terminus of two different GPCRs to investigate dimeric/oligomeric interactions between them. The FRET signal corresponds to the formation of a dimeric/oligomeric interaction between two GPCRs, as this brings the CFP and YFP into proximity.

htrFRET in combination with SNAP/CLIP tag fusions and TagLite® technology is based on the generation of protein fusions with epitope tags preferably at the extracellular N-terminus of the receptor expressed at the surface of live cells and labelled with FRET compatible fluorescent substrates. The SNAP tag is 20 kDa and is derived from O^6-guanine nucleotide alkyltransferase, an enzyme that is involved in the DNA repair mechanism in eukaryotic organisms. The SNAP tag can be specifically bound to any fluorophore that contains benzyl guanine (BG), resulting in a covalent interaction. A variant of SNAP tag, the CLIP tag can also be used. CLIP tag is of similar size and can also be fused at the receptor/protein of interest, without interfering with receptor function and it can be covalently labelled with benzyl cytosine conjugated fluorophore (Figure 1.14).
The main element in the htrFRET approach is the combination of energy donor and acceptor. Energy donors that can be used are either Europium cryptate (Eu^{3+} cryptate) or

Lumi4 terbium (Tb^{2+} cryptate). The rare earth cryptates belong to the family of lanthanides and they possess long fluorescent lifetime, a feature that is central to htrFRET. The long fluorescence lifetime allows the elimination of the background noise (non-specific signal originating from either auto-fluorescence or fluorescence coming from any remaining serum contained in the cell medium), by leaving a gap between the time of excitation and the time of FRET measurement, usually in the micro second scale. This allows for the specific FRET signal to be measured in a time-resolved manner. It is not necessary to separate free from bound and thus it is a homogeneous assay where washing steps are eliminated or limited.

Homogeneous time-resolved FRET offers flexibility and increased sensitivity, allowing for robust and reliable assays with high throughput potential and fewer false positive or negative results. SNAP and/or CLIP htrFRET compatible substrates allow measurement of emissions at two different and distinguishable wavelengths e.g. 620 nm donor and 665 nm acceptor (htrFRET signal) (Degorce *et al.*, 2009).

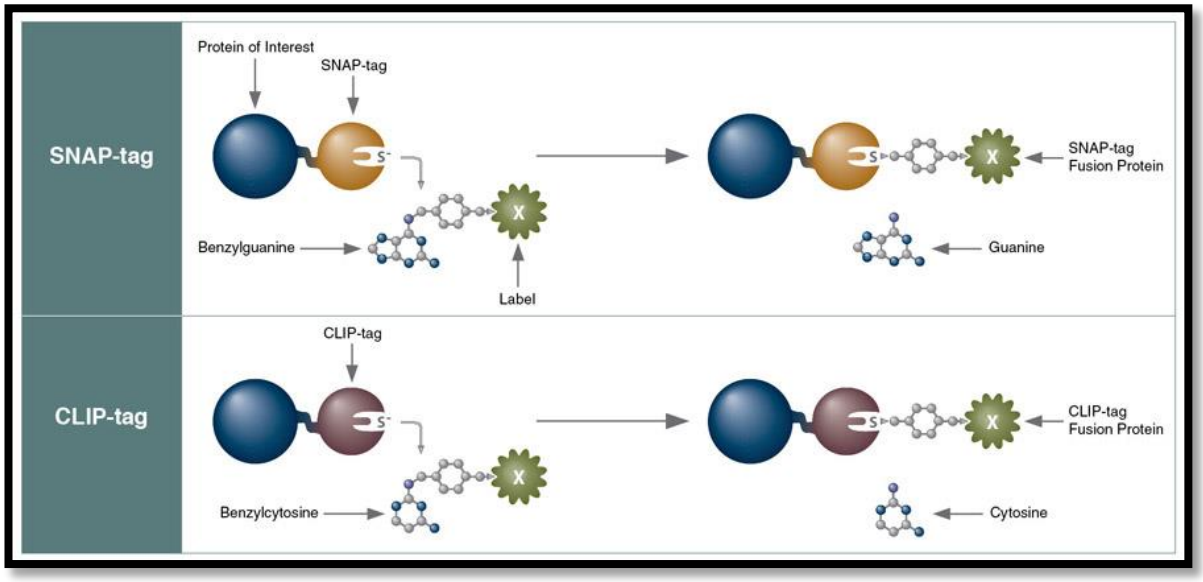

Figure 1.14 SNAP and CLIP tag labelling. The protein/receptor of interest can be tagged with a SNAP or CLIP tag by genetic engineering and once the fusion is expressed and trafficked to the cell surface, SNAP specific benzylguanine and CLIP specific benzylcytosine substrates can be used to label the tagged receptors. The SNAP and CLIP tags act as suicide enzymes by reacting with benzylguanine and benzylcytosine linked labels, to covalently bond the tags via a thio-ester linkage. The labelled SNAP or CLIP fusion protein, once labelled can be excited at a certain wavelength and then emits at a longer wavelength. (Figure from New England Biolabs https://www.neb.com/tools-and-resources/feature-articles/snap-tag-technologies-novel-tools-to-study-protein-function).

The first time that htrFRET methodology was used in combination with SNAP tag technology in detecting and analysing GPCR oligomers was described by Maurel *et al.*, (2008). This approach included generation of SNAP tagged $GABA_{B1}$ and FLAG tagged $GABA_{B2}$ receptors. The fused receptors were expressed at the surface of live HEK 293 cells and the SNAP-$GABA_{B1}$ was labelled with europium cryptate donor (BG-K) and the FLAG-$GABA_{B2}$ was labelled using anti-flag antibodies conjugated with d2 (acceptor), allowing the detection of TR-FRET signal consistent with the existence of receptor heterodimers at the surface of the cells. The maximal FRET signal was detected once the labelling conditions were optimised. Optimisation ensured equivalent labelling of SNAP tags with each fluorophore. The TR-FRET efficacy (ratio between the acceptor emission and amount of donor) was constant over a range of receptor density suggesting that the signal was due to actual protein-protein interactions rather than due to random collisions. Evidence demonstrating the existence of dimer of dimers organisation for $GABA_B$ receptors was also presented and this study constituted a very important contribution to the investigation of GPCR dimerisation (Maurel *et al.*, 2008).

Traditional approaches used for investigating GPCR oligomerisation such as ligand binding, co-immunoprecipitation and functional complementation have provided supporting evidence for the oligomerisation theory but cannot provide definitive proof of direct protein-protein interactions. In addition, such techniques cannot give answers about the size, the stability, regulation and more importantly about the role of oligomeric complexes (Cottet *et al.*, 2012). Other resonance energy transfer methods such as classical FRET using fluorescent proteins or BRET using luciferase and fluorescent protein fusions often require over-expression of the receptors in transfected cells. This often leads to difficulties in distinguishing RET signal corresponding to real protein interactions from signal obtained due to random collisions. In addition, the low noise-to-signal ratio that results from intrinsic fluorescence originating from the cells and/or the overlap between emission spectra of RET donor and acceptor is considered a drawback of these techniques. Although, RET-based methods present adequate spatial resolution that allows detection of interactions between proteins with relative precision, it is difficult to make conclusions on the amount or the order of oligomeric complexes e.g. dimer, trimer, tetramer or higher order oligomer.

The htrFRET approach offers great signal resolution and high signal-to-noise ratio. htrFRET does not demonstrate any dependence to the relative orientation of the fluorophore, since lanthanide emission is polarised, unlike in BRET or standard FRET.

The unique spectral properties of terbium cryptates (Lumi4 Tb) allow for multiplex labelling of the receptors using more than two fluorescent substrates that follow the rule of spectral compatibility, without any interference of their emission channels.

Fluorescently labelled ligands can be used in an htrFRET experimental design (Albizu *et al.*, 2010) and this may transfer the study of GPCR oligomerisation from heterologous expression systems to native tissues, which may potentially unravel the *in vivo* role of GPCR oligomers and establish the functional relevance of oligomers in native tissues. The use of ligands labelled with htrFRET compatible fluorophores may be a very useful alternative to fluorescently labelled antibodies used for studying receptors in native tissues. Antibodies can be target-specific but their size is a limiting factor since they generate steric hindrance in the vicinity of the receptors which can affect the binding of receptors. In addition, antibody binding to the epitope may be affected by possible conformational changes mediated by ligand induced receptor activation.
The combination of htrFRET with SNAP/CLIP tagging of receptors is a useful tool in detecting GPCR oligomers (Alvarez-Curto *et al.*, 2011; Pou *et al.*, 2012) at the surface of live cells (Figure 1.15), but it has also provided a novel approach in studying the dynamics of oligomerisation. One of the main disadvantages of any RET-based technique is the difficulty in reaching definitive conclusions about the order of oligomerisation i.e. the inability to distinguish dimers from higher order oligomers. Another drawback of the RET-based approaches is the inability to distinguish between cell-surface and intracellular receptors. In the case of htrFRET, this important issue was overcome, with the development of cell impermeant and cell permeable labelling substrates that allowed the specific labelling of either cell surface receptors or whole cell receptor population.

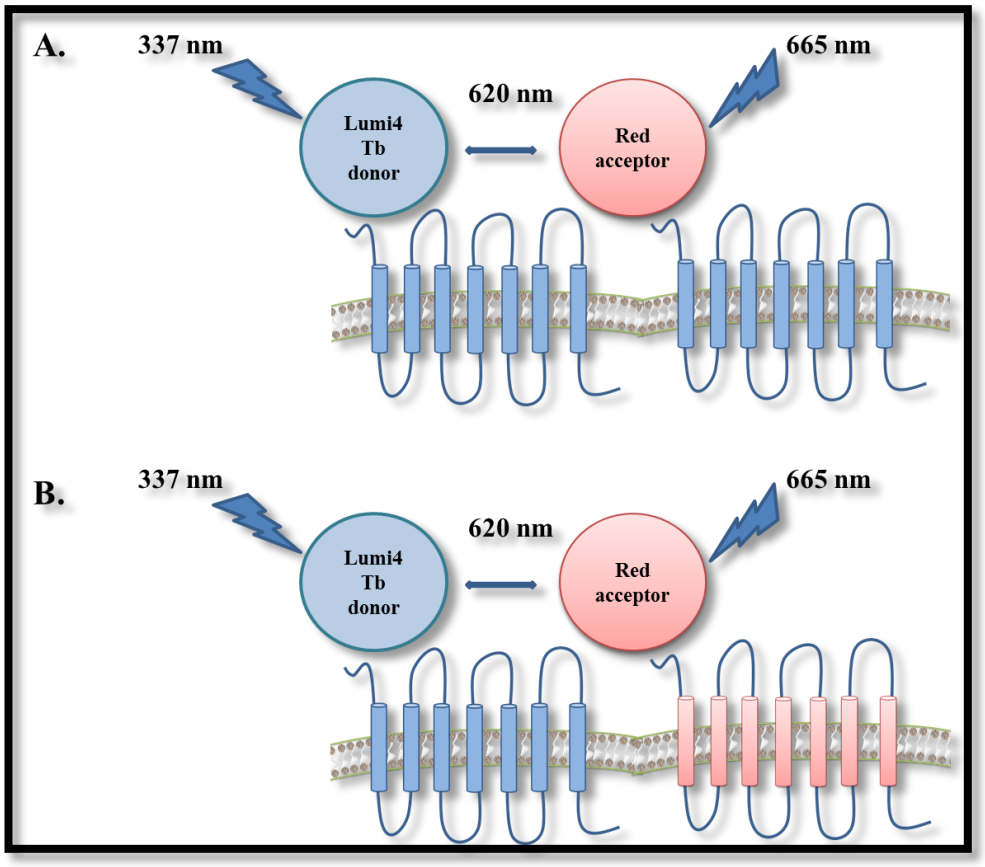

Figure 1.15 htrFRET based detection of GPCR homomers and heteromers. (A) Homomers between two N-terminally SNAP or CLIP tagged receptors can be detected at the cell surface, following labelling with SNAP or CLIP specific substrates. The SNAP/CLIP-Lumi4 Tb may be used as energy donor, emitting at 620 nm, and the SNAP/CLIP-Red as energy acceptor, emitting at 665 nm following transfer of energy from the donor. **(B)** Heteromers between SNAP and CLIP tagged receptors may be detected, following labelling with SNAP or CLIP Lumi4 Tb donor and CLIP or SNAP Red acceptor, respectively.

1.13 Aims of the project

The scope of this PhD project was to shed light into the field of muscarinic acetylcholine receptor oligomerisation and more specifically to look into the formation of homomers and heteromers between the human M_2WT (hM_2WT) and a genetically engineered variant of the human M_3WT, called hM_3RASSL, able to respond only to the synthetic ligand clozapine N-oxide (CNO). The debated topic of ligand regulation of receptor oligomerisation was another important topic to be tackled, since various observations have been reported on the subject, using different technical methods and various cellular expression systems. The aim was to investigate potential ligand-mediated regulation of hM_2WT and hM_3RASSL receptor oligomerisation. This employed an htrFRET approach in combination with SNAP-tag technology and heterologous expression of the receptors in Flp-In™ T-REx™-293 cells. An important aim was to assess the stability of any oligomeric complexes and the possible interchange between homomers and heteromers.

An understanding of oligomerisation of M_2 and M_3 receptors and ligand regulation of the oligomerisation profile would be advantageous in the study of the muscarinic receptors behaviour and in understanding of possible pathophysiology in tissues where the two receptors are co-expressed and co-localised (e.g. gastrointestinal and airway smooth muscle). In the long term, understanding of M_2/M_3 heteromer formation could lead to novel therapeutic approaches via the development of oligomer specific ligands that could modulate the pharmacology of the receptors in a complex and provide treatments with reduced side effects and increased selectivity and specificity.

Chapter 2

Materials and Methods

2.1 Materials

2.1.1 General reagents and kits

Agarose (Flowgen Biosciences, Nottingham, UK)

Bicinchoninic acid (BCA) reagent (Pierce, Tattenhall, UK)

Broad range Rainbow molecular weight protein marker (Life Technologies, Paisley, UK)

cAMP dynamic 2 kit (Cisbio Bioassays, Codolet, France)

Fluorescent dyes: SNAP-Surface 549, SNAP-Surface 488, CLIP-Surface 488, CLIP-Surface 547 (New England Biolabs, UK)

GF/C filters (Brandel Inc. Gaithersburg, MD)

Hank's Balanced Salt Solution (HBSS) (Life Technologies, Paisley, UK)

IP-One Tb kit (Cisbio Bioassays, Codolet, France)

NativePAGE™ Novex® 3-12% Bis-Tris Protein Gels (Life Technologies, Paisley, UK)

NuPAGE® Novex® 4-12% Bis-Tris Protein Gels (Life Technologies, Paisley, UK)

NuPAGE® MOPS SDS Running Buffer (20X) (Life Technologies, Paisley, UK)

Oligonucleotides for PCR reactions (Thermo Fisher Scientific, Ulm, Germany)

Polyethylenimine (PEI) (Sigma Aldrich, Poole, Dorset, UK)

Poly-D-Lysine (Sigma Aldrich, Poole, Dorset, UK)

Platinum® *Pfx* DNA polymerase (Life Technologies, Paisley, UK)

QIAfilter Plasmid Maxi kit (Qiagen, Crawley, UK)

QiaQuick gel extraction kit (Qiagen, Crawley, UK)

ReBlot Plus solution (Chemicon Europe Ltd., Chandlers Ford, UK)

Restriction endonucleases from Roche Applied Science (Lewes, East Sussex, UK), Promega, UK Ltd., (Southampton, UK), and New England Biolabs, UK)

SNAP/CLIP-Lumi4 Tb, SNAP/CLIP-Red and SNAP-Green (Cisbio Bioassays, Codolet, France)

Supersignal West Pico chemiluminescent substrate (Pierce, Perbio Science UK Ltd., Tattenhall, Cheshire, UK)

SYBR® Safe DNA Gel Stain (Life Technologies, Paisley, UK)

Tunicamycin (Sigma Aldrich, Poole, Dorset, UK)

Wizard Plus SV Miniprep kit (Promega, Southampton, UK)

X-ray film (Konika Europe, Hohenbrunn, Germany)

2.1.2 Tissue culture reagents

Dulbecco′s Modified Eagle′s Medium (DMEM), L-glutamine, 0.25% trypsin-EDTA, doxycycline- Sigma-Aldrich Company Ltd. (Poole, Dorset, UK)

Geneticin G418 and foetal bovine serum - Invitrogen (Paisley, UK)

Hygromycin B-Roche Applied Science (Lewes, East Sussex, UK)

Trypan Blue stain (0.4%) -Life Technologies (UK)

2.1.3 Ligands

Atropine methyl nitrate Sigma-Aldrich Company Ltd. (Poole, Dorset, UK)

Carbachol (Tocris Bioscience, UK)

Clozapine-N-Oxide (CNO) (Enzo Life Sciences, UK)

2.1.4 Radioligands

[^{3}H]-Quinuclidinyl benzilate (QNB) (Perkin-Elmer Life and Analytical Sciences, Beaconsfield, Buckinghamshire, UK)

2.1.5 Antisera

Rat anti-HA (Roche, UK)

Rabbit anti-VSV (in house)

Rabbit anti-SNAP (New England Biolabs, MA, USA)

Mouse anti-M_3 (Gift from Professor A. Tobin, University of Leicester)

Monoclonal anti-VSV-G agarose conjugate (Sigma Aldrich, UK)

Goat anti-mouse IgG HRP conjugate (GE Healthcare, UK)

Donkey anti-rabbit IgG HRP conjugate (GE Healthcare, UK)

Goat Anti-rat IgG HRP conjugate(GE Healthcare, UK)

Anti-goat IgG HRP conjugate (Sigma Aldrich, UK)

2.1.6 General buffers

Phosphate Buffered Saline – PBS (1X)

- 137 mM NaCl
- 2.7 mM KCl
- 1.5 mM KH_2PO_4
- 8 mM Na_2HPO_4

pH 7.4

Tris Buffered Saline –TBS (1X)

- 20 mM Tris-Base
- 150 mM NaCl

pH 7.4

Tris Buffered Saline-Tween 20 (TBS-T)

- TBS (1X)
- 0.1 % (v/v) Tween-20

Tris-EDTA (TE) buffer (1X)

- 10 mM Tris
- 1 mM EDTA

pH 7.4

Radioligand binding assay buffer (1X)

- 20 mM HEPES
- 100 mM NaCl
- 10 mM $MgCl_2$

pH 7.4

Radioimmune precipitation assay (RIPA) buffer (1X)

- 50 mM HEPES
- 150 mM NaCl
- 1% (v/v) Triton X-100
- 0.5% sodium deoxycholate
- 10 mM NaF
- 5 mM EDTA
- 10 mM Na_2HPO_4
- 5% (v/v) ethylene glycol

pH 7.4

Supplemented with Complete protease inhibitors mixture

Stored at 4 ˚C

Cell lysis buffer 1X (used for lysate preparation for Blue Native PAGE)

- 150 mM NaCl
- 0.01 mM Na_2HPO_4
- 2 mM EDTA
- 0.5% n-Dodecyl β-D-maltoside (DDM)
- 5% glycerol

Supplemented with Complete protease inhibitors mixture

Stored at 4 ˚C

Laemmli buffer (5X)

- 10% w/v sodium dodecyl sulphate (SDS)
- 10 mM dithiothreitol (DTT)
- 20% glycerol
- 0.2 M Tris-HCl
- 0.05% bromophenol blue

pH 6.8

2.1.7 Molecular biology solutions

TAE buffer (50X)

- 40 mM Tris-Base
- 5 mM EDTA
- 5.71 % (v/v) glacial acetic acid

Diluted 1:50 prior to use

DNA loading buffer (5X)

- 0.25 % (w/v) bromophenol blue
- 40 % (w/v) sucrose
- In water

Luria-Bertani (LB) broth

- 1% (w/v) bactotryptone
- 0.5% (w/v) yeast extract
- 1% NaCl

Dissolved in water and adjusted pH at 7.4

Sterilised by autoclaving

Ampicillin (100 $\mu g \cdot ml^{-1}$) was added for the preparation of LB ampicillin media, after the media was cooled down to 50˚C.

Luria-Bertani (LB) agar

- 1.5% (w/v) agar into LB broth

Ampicillin (100 $\mu g \cdot ml^{-1}$) was added for the preparation of LB ampicillin agar plates, after the media was cooled down to 50˚C. After gentle mixing, the agar was poured onto 10 cm^2 petri dishes and was left on bench to set before storing at 4˚C.

Solutions for generation of competent bacteria

Solution 1:

- 0.03 M (CH_3COOK)
- 0.1 M $RbCl_2$
- 0.01 M $CaCl_2$
- 0.05 M $MnCl_2$
- 15% glycerol

Adjusted pH at 5.8 with acetic acid and filter sterilised. Stored at 4˚C.

Solution 2:

- 10 mM MOPS (pH 6.5)
- 0.075 M $CaCl_2$
- 0.01 M $RbCl_2$
- 15% glycerol

Adjusted pH at 6.5 with HCl and filter sterilised. Stored at 4˚C.

2.2 Molecular Biology Methods

2.2.1 XL1 Blue Competent bacterial cells preparation

XL1-Blue cells were streaked onto an LB-agar plate that was incubated overnight at 37˚C. A single colony was used to inoculate 5 ml LB broth at 37˚C overnight. The overnight bacterial culture was used to inoculate 100 ml of LB broth and cells were allowed to grow until the optical density measured at 550 nm reached 0.45- 0.48. The culture was transferred into two 50 ml Falcon tubes, placed on ice for 5 minutes and subsequently centrifuged for 10 minutes at 4˚C at 2500 rpm. Cell pellets in each tube were gently resuspended in 10 ml Solution 1. The cell suspensions were incubated on ice for 5 minutes and then centrifuged for 10 minutes at 4˚C at 2500 rpm. The pellet was then resuspended

in 2 ml Solution 2 and incubated on ice for 15 minutes before aliquoting 220 µl cell suspension per tube and storing at -80˚C.

2.2.2 Transformation of competent bacterial cells

For the transformation of competent bacterial cells, XL1-Blue cells were thawed on ice. The DNA constructs (50-100 ng) or the ligation reaction (5 µl) was added to 50 µl of the competent cells and incubated on ice for 20 minutes. The bacteria were subjected to heat shock by incubating samples at 42 ˚C for 90 seconds. After the heat shock, cells were placed on ice for a further minute, before 1 ml of LB medium was added. The cells were allowed to recover at 37 ˚C in a shaking incubator for 1 h and then centrifuged for 1 minute at 14,000 rpm. The cell pellet was resuspended in 100 µl of LB and this was spread onto LB agar plates containing ampicillin (100 $\mu g \cdot ml^{-1}$). Plates were then incubated at 37 ˚C overnight to allow for selection of transformants.

2.2.3 Isolation and purification of plasmid DNA

For the extraction of the plasmid DNA from bacterial cells, the Wizard Plus SV Miniprep kit (Promega) was used. The QIAfilter Plasmid Maxi kit (Qiagen) was used to isolate and purify larger amounts of plasmid DNA. The kits were used according to manufacturer's instructions.

2.2.4 Quantification of DNA

Quantification of DNA was performed by measuring the absorbance of a DNA sample (1:100 dilution) at 260 nm using a spectrophotometer. Absorbance at 280 nm was also measured to assess the purity of the sample. This was carried out by calculating the ratio A_{260} / A_{280}. Samples with a ratio between 1.7 and 2 were considered pure enough for use. DNA samples used in ligation reactions were quantified by running the DNA samples on a 1% agarose gel, alongside with 5 µl of the DNA molecular marker (HyperLadder ™) and the sizes of the DNA fragments in question were compared to the molecular marker's fragments with known sizes.

2.2.5 Digestion of DNA with restriction endonucleases

30 µl final volume digestion reactions were performed by mixing up to 1µg DNA, 1-2 units of the selected restriction enzyme or combination of two compatible enzymes, 3 µl of the appropriate 10X restriction buffer, and sterile water. The digestion reactions were incubated at 37˚C for 1-4 hours depending on the amount of the DNA.

2.2.6 DNA gel electrophoresis

DNA constructs, PCR reaction products and digested DNA samples were analysed using 1% agarose gel electrophoresis. The samples were diluted in 5X DNA loading buffer and made up to 10 µl with water. The gel was prepared by adding 0.3 mg agarose to 30 ml 1x TAE buffer that was heated in the microwave until the agarose was melted. 3 µl SYBR® Safe DNA Gel Stain was added (1:1000 dilution) and the gel was gently mixed before it was poured onto the gel tank, left to set and then immersed in 1x TAE buffer. After loading of DNA samples gels were allowed to run at 50-100 mA for 30 minutes. The DNA fragments were visualised using ultraviolet (UV) light. The sizes of the DNA fragments were compared to the fragments on the DNA molecular marker (HyperLadder ^{TM}).

2.2.7 DNA purification from agarose gels

For cloning purposes, the DNA fragments that were required for the generation of constructs were excised from the gel and were purified using the QiaQuick gel extraction kit according to the manufacturer's instructions. The DNA was eluted in 30-50 µl sterile water and the concentration of DNA was measured using a spectrophotometer (section 2.2.4).

2.2.8 Ligation of DNA

The generation of constructs was carried out by ligating the appropriate plasmid vector with the desired DNA insert using T4 DNA ligase. Once the concentrations of the vector and insert DNA were determined by spectrophotometer or by agarose gel electrophoresis, various vector: insert ratios were tested, in order to identify the optimum ratio for each particular vector- insert pair. The vector: insert ratios mostly used were 6:1 and 4:1 and were calculated according the following formula:

$$ng\ of\ insert = molar\ ratio \frac{insert}{vector}\ X\ \frac{length\ of\ insert\ (kb)}{length\ of\ vector\ (kb)}$$

Ligation reaction

- 1 µl T4 DNA ligase
- 1 µl T4 DNA ligase buffer
- X µl Vector
- Y µl insert
- Water up to 10 µl

The reaction was incubated overnight on ice. Ice was placed in a 5 L beaker and was gradually allowed to melt to create a temperature gradient. After incubation, 5 µl of the reaction was used for bacterial transformation.

2.2.9 Polymerase chain reaction (PCR)

PCR was used to amplify the target fragments of DNA and to introduce restriction sites for the generation of fusion proteins. The high fidelity Platinum® *Pfx* DNA polymerase was used.

<u>50 µl Reaction components</u>

Template DNA: 50 ng/µl	1 µl
Primer (sense and antisense): 25 pmol/µl each	1.5 µl each
Platinum® *Pfx* DNA polymerase: 1 U	1 µl
Pfx polymerase buffer (10x)	5 µl
Enhancer buffer (10x)	5 µl
Mg_2SO_4: 50 mM	6 µl
dNTP mix: 0.25 mM each dNTP (dTTP, dATP, dGTP, dCTP)	1.5 µl
water	27.5 µl

<u>PCR protocol</u>

- 94˚C for 5 minutes to activate the Pfx polymerase
- Denaturing step: 94˚C for 30 seconds
- Annealing step: 55˚C for 30 seconds

- Extending step: 68˚C for 1.5 minutes

Repeat 30 cycles

2.2.10 DNA sequencing

DNA sequencing was performed at the Sequencing Service, School of Life Sciences, University of Dundee, Scotland. The amount of DNA sent was 20 ng/µl and the primer's concentration was 3.2 µM per reaction as instructed by the sequencing service.

2.2.11 Cloning- Generation of VSV-SNAP-hM$_2$WT, HA-CLIP-hM$_3$RASSL, VSV-SNAP-hM$_3$RASSL fusion constructs

The plasmids pSEMS1-26m (SNAP tag) and pCEMS1-CLIP10m (CLIP tag), supplied by Covalys Biosciences AG (Witterswil, Switzerland), were modified by the addition of a small linker region encoding for the metabotropic glutamate receptor 5 (mGluR5) signal sequence. An epitope tag, either HA or VSV-G, was also incorporated between the ClaI and EcoRI restriction sites of the multiple cloning site upstream of SNAP or CLIP tags. The linker was made by annealing two complementary primers containing the sequences described above with the addition of a Kozak sequence, start codon, and appropriate nucleotides to generate ClaI and EcoRI "sticky" ends. The primers were annealed by combining 1 ng of each with 1 X "multicore" buffer (Promega Corp.) in a final volume of 50 µl. This was then heated to 100 °C in a boiling water bath for 5 min, after which the bath was then turned off and allowed to cool overnight. The annealed fragment was then purified by gel extraction and ligated into the plasmid by standard techniques. The receptor sequences were PCR-amplified using primers designed to add BamHI (5'-CGCGGATCCGCCACCATGACCTTGCACAATAACAGT-3') and NotI (5'-TTTTCCTTTTGCGGCCGCCTACAAGGCCTGCTCGGGTGC-3') sites to the fragment termini. These were then ligated into the multiple cloning site downstream of SNAP or CLIP tags of the modified plasmids described above. To create constructs that could be used to make Flp-In™ T-Rex™ 293-inducible stable cell lines of these constructs, the entire insert from the ClaI site to the NotI site was cut out and ligated into a modified version of pcDNA5/FRT/TO (Invitrogen) with a ClaI site added to the multiple cloning site using a linker formed from two annealed primers as described previously (Alvarez-Curto et al., 2010). This work was previously carried out by Dr. Elisa Alvarez-Curto.

2.3 Cell culture Methods

2.3.1 Cell maintenance

All cells were maintained in an incubator at 37˚C in a humidified atmosphere with 5% CO_2.

2.3.2 HEK 293 cells

HEK 293 cells were maintained in Dulbecco's modified Eagle's medium-DMEM supplemented with 10 % foetal bovine serum (FBS), 2 mM L-glutamine, 1% antibiotic mixture (100 $U \cdot ml^{-1}$ penicillin and 0.1 $mg \cdot ml^{-1}$ streptomycin).

2.3.3 Flp-In™ T-REx™-293 cells

This cell line may be used as a host for the generation of stable cell lines expressing the gene of interest (GOI); it expresses the tetracycline repressor protein (tet repressor) and contains an FRT integration site.

Flp-In™ T-REx™-293 cells were maintained in DMEM supplemented with 10 % FBS, 1% antibiotic mixture (100 $U \cdot ml^{-1}$ penicillin and 0.1 $mg \cdot ml^{-1}$ streptomycin) and 100 $\mu g \cdot ml^{-1}$ zeocin.

Single stable Flp-In™ T-REx™-293 cells lines were maintained in DMEM with high glucose, supplemented with 10 % FBS, 1% antibiotic mixture (100 $U \cdot ml^{-1}$ penicillin and 0.1 $mg \cdot ml^{-1}$ streptomycin), 10 $\mu g \cdot ml^{-1}$ blasticidin and 200 $\mu g \cdot ml^{-1}$ hygromycin, which from now on will be referred to as complete DMEM. Double stable cell lines were maintained in complete DMEM supplemented with 1 $mg \cdot ml^{-1}$ geneticin (G-418).

2.3.4 Passaging of cells

Cells were passaged when 80-90% confluence was reached. Medium was removed and cells were washed once with sterile 1x PBS to remove any traces of growth medium. 0.25 % Trypsin-EDTA was then added to the cells for 2-3 minutes and the flask was shaken by hand until the cells were detached from the flask surface. Cells were then harvested in growth medium and centrifuged for 5 minutes at 1,300 rpm. The cell pellet was

resuspended in fresh growth medium and the suspension was added into flasks, dishes, plates or cover-slips, at the required dilution.

2.3.5 Transient transfection of HEK 293 cells using Polyethylenimine (PEI)

HEK 293 cells were plated in 10 cm dishes (2.5 x10^6 cells per dish) and grown to 70% confluence before they were ready for transfection with PEI. 250 µl of 150 mM NaCl sterile solution containing 5 µg of the DNA construct was mixed with 250 µl of solution containing 30 µl of PEI (at 1µg·µl^{-1}) and 220 µl 150 mM NaCl. The PEI: DNA ratio used for all the transfections was 6:1. The final solution was then incubated for 10 minutes at room temperature, allowing the PEI to coat the DNA with positively charged particles to enable introduction through the cell surface via endocytosis. The solution was then carefully pipetted onto the cells and incubated for 24 hours.

2.3.6 Generation of Flp-In™ T-REx™-293 cell lines expressing the receptor of interest

Flp-In™ T-REx™-293 cells were used as hosts for the generation of single stable cell lines expressing the receptor of interest in a doxycycline inducible manner. Flp-In™ T-REx™-293 cells stably express a tetracycline repressor protein and also contain an FRT (flippase recognition target) integration site. The GOI was sub-cloned into pcDNA5/FRT/TO (confers resistance to hygromycin). Flp-In™ T-REx™-293 cells were co transfected with pcDNA/FRT/TO-GOI construct and the pOG44 vector expressing the Flp recombinase. The resulting cells, with the integrated pcDNA5/FRT/TO GOI into the FRT site, were hygromycin resistant and sensitive to zeocin. The expression of the GOI was regulated by the tetracycline repressor (tet repressor) protein which in the presence of tetracycline or doxycycline (tetracycline analogue) was released from the operator sequence allowing the transcription and translation of the GOI.

Steps followed for the generation of Flp-In™ T-REx™-293 cells stably expressing VSV-SNAP-hM_2-WT or HA-CLIP-hM_3-RASSL receptors:

1. The GOI was sub-cloned into the pcDNA5/FRT/TO vector
2. pcDNA5/FRT/TO GOI was co-transfected with pOG44 vector into parental Flp-In™ T-REx™-293 host cells. A ratio of 9:1 (w/w) pOG44: pcDNA5/FRT/TO GOI was used for the transfections with a total of 5 µg of DNA per transfection.

3. Transfected cells were maintained in DMEM supplemented with 10 % FBS, 1% antibiotic mixture (100 $U \cdot ml^{-1}$ penicillin and 0.1 $mg \cdot ml^{-1}$ streptomycin) and 10 $\mu g \cdot ml^{-1}$ blasticidin.
4. 24 hours post transfection the medium was replaced with fresh DMEM for another 24 hours.
5. 48 hours post transfection the cells were split into separate 100 mm dishes using 1:500 and 1:1000 dilutions and maintained in complete DMEM containing 10 % FBS, 1% antibiotic mixture (100 $U \cdot ml^{-1}$ penicillin and 0.1 $mg \cdot ml^{-1}$ streptomycin), 10 $\mu g \cdot ml^{-1}$ blasticidin and 200 $\mu g \cdot ml^{-1}$ hygromycin. Hygromycin allows for the selection of cells that have successfully integrated the GOI into their genome.
6. The medium was replaced with fresh every 2-3 days until colonies (foci) of cells started to appear.
7. Once the colonies started to grow, the complete population of cells was pooled.
8. The pooled isogenic population of single stable cells was then screened for tetracycline/doxycycline dependent expression of the protein of interest.
9. Doxycycline-dependent inducibility of receptor expression was screened either by western blotting or by fluorescence measurement, when a fluorescent tag was fused to the receptor of interest.

Generation of the cell lines described above was carried out by Dr. Elisa Alvarez-Curto.

2.3.7 Generation of Flp-In™ T-REx™-293 cell lines co-expressing two receptors

Generation of a double stable cell line expressing one receptor in a doxycycline inducible manner and the second receptor in a constitutive manner, involves the use of a single stable cell line with the receptor expression being regulated by the tet repressor, as a host cell line. The host cell line was used for the introduction of a second cDNA construct encoding the second receptor of interest that would be constitutively expressed allowing the generation of a double stable cell line.

The steps followed for the generation of a double stable cell line included:

1. The cDNA encoding the receptor to be expressed constitutively of interest was sub-cloned into pcDNA3.
2. The pcDNA3 containing the GOI was transfected into the host cells which were maintained in complete DMEM.
3. 24 hours post transfection the medium was replaced with fresh complete DMEM.

4. 48 hours post transfection, the cells were split (1:500 and 1:1000 dilutions) into separate dishes and were maintained in complete DMEM for another 24 hours, until the cells were attached to the dish's surface.
5. The medium was then replaced with complete DMEM supplemented with 1 $mg \cdot ml^{-1}$ G-418 (geneticin) for selection.
6. Medium was replaced every 2-3 days until individual colonies were seen.
7. Individual colonies were picked (using a cloning ring) and each colony was plated per well in a 24-well plate and cells were grown until ready for screening.
8. The clones were then screened for constitutive expression of the second receptor and for doxycycline dependent expression of the first receptor. Screening of the clones was carried out by Western blotting or by fluorescence measurement (when a fluorescent tag was fused to the receptor(s) of interest).

Generation of the cell lines described above was carried out by Dr. Elisa Alvarez-Curto.

2.3.8 Induction of receptor expression with doxycycline

Single or double stable Flp-In™ T-REx™-293 cells were plated in 96- well plates, 10 cm dishes, or flasks and were grown to 70-80% confluence in DMEM. In order to initiate the expression of the receptor(s), the medium was replaced with DMEM containing the antibiotic doxycycline and incubated for 24 hours (unless otherwise stated, depending on the requirements of the experiments) at 37˚C/ 5% CO_2. After optimisation experiments and receptor expression determination the concentrations of doxycycline for the different cell lines were defined. The double stable Flp-In™ T-REx™-293 cells constitutively expressing the HA-CLIP-hM_3RASSL receptor required 5 $ng \cdot ml^{-1}$ of doxycycline to express the VSV-SNAP-hM_2WT receptor at the desired amount. The single stable cell line expressing HA-CLIP-hM_3RASSL receptor required 10 $ng \cdot ml^{-1}$ doxycycline and the cell line expressing the VSV-SNAP-hM_2WT was treated with 5 $ng \cdot ml^{-1}$ of the antibiotic.

2.3.9 Cell number determination

Cells were trypsinised as described in section 2.3.4 and harvested in growth medium by centrifugation at 1300 rpm for 5 minutes. The cell pellet was the resuspended in the growth medium. Cell suspension (10 µl) was mixed in a tube with 10 µl of trypan blue stain (0.4%) to be analysed in a Countess® Automated cell counter. 10 µl of the mixture of stained cells was then loaded onto a cell counting chamber and the cells were counted

using the Countess® Automated cell counter (Life Technologies, UK) or a hemocytometer, manually counting the cells under a microscope.

2.3.10 Cell harvesting

After treatment of live cells with doxycycline or PEI transfection, to allow expression of the desired receptor, cells were washed twice in ice cold PBS and then harvested by centrifugation, for 5 minutes at 4 ˚C, at 4000 rpm. The cell pellet was stored for at least 45 min at -80 ˚C and then used for lysate or membrane preparation or was kept frozen until needed.

2.3.11 Treatment of cells with tunicamycin

Cells were plated in 10 cm dishes and when 70-80% confluence was reached, tunicamycin was added at a final concentration of 6 μM. Treatment with doxycycline, to allow for receptor expression, was carried out simultaneously. Incubation with tunicamycin was routinely carried out for 16 h (or a maximum of 24 h for time course experiments). After the treatment, the cells were washed and harvested in ice cold PBS.

2.4 Membrane and protein isolation, detection and quantification methods

2.4.1 Membrane preparation

Cells were grown to confluence, after appropriate manipulation to allow expression of the desired receptor i.e. PEI transfection of HEK 293 cells or doxycycline induction of Flp-In™ T-REx™-293 stable cells. Cells were harvested after 24 h of treatment (Section 2.3.10), in ice-cold 1X PBS and pelleted by centrifugation. Pellets were frozen at -80 ^{0}C for a minimum of 1 h. Pellets were thawed and resuspended in ice-cold TE buffer supplemented with Complete protease inhibitor mixture. Cells were passed through 25-gauge needle (5-10 times) and then homogenised on ice, by 50 strokes on a glass Teflon homogeniser. Homogenised cells were centrifuged at 1000 x g for 5 minutes at 4 ^{0}C. The supernatant fraction was removed and transferred to microcentrifuge tubes and subjected to further centrifugation at 50,000 x g for 45 minutes at 4 ^{0}C. The pellets were resuspended in TE buffer and protein concentration was assessed by BCA assay (section 2.4.3) Membrane preparations were either used directly or kept at -80 ^{0}C until required.

2.4.2 Cell lysates preparation

Cells were grown to confluence after treatment to allow expression of the receptor(s). The cells were then harvested and washed twice in ice cold 1X PBS, by centrifugation (section 2.3.10). The pellets were resuspended in 1X RIPA buffer supplemented with Complete protease inhibitors mixture or cell lysis buffer for the preparation of lysates for Blue Native PAGE. Resuspended cells were then placed on a rotating wheel for 30-45 minutes at 4 ^{0}C, to allow further lysis, and then were centrifuged at 14,000 x g, for 15 minutes at 4 ^{0}C. The supernatant was then transferred to a clean tube and the protein concentration of the lysate was determined by BCA assay (section 2.4.3). Lysate preparations were either used directly or kept at -20^{0}C until required.

2.4.3 Determination of protein concentration using BCA assay

The BCA assay was used to determine the protein concentration of protein samples, from either lysates or membrane preparations. Two solutions were mixed for the assay. Solution A: bicinchoninc acid (BCA) and solution B: 4% copper sulphate solution in 50:1 ratio. Proteins reduce the Cu(II) to Cu(I) in a concentration-dependent manner and then the Cu(I) binds to BCA causing a colour change with an absorption of 562 nm. A standard curve was plotted using samples of bovine serum albumin (BSA) with known amount, allowing the determination of the concentrations of the protein samples in question. In a 96-well ELISA plate, 10 µl of the BSA samples and the protein samples with unknown concentration were plated and 200 µl of the mixed reagents A and B were added per well. The plate was incubated for 15-30 minutes at 37˚C. The absorbance at 562 nm was then read on a PheraStar FS plate reader and the protein concentration of the samples was calculated using Graph Pad software.

2.4.4 Sodium dodecyl sulphate polyacrylamide gel electrophoresis (SDS-PAGE)

Protein lysate samples or membrane preparation samples were heated at 60-65 ^{0}C in 5 x Laemmli buffer (10% w/v SDS, 10 mM DTT, 20% v/v glycerol, 0.2 M Tris-HCl at pH 6.8, 0.05% w/v bromophenol blue) for 5 minutes. The required amount of protein lysate or membrane preparation (usually 10-20 µg protein per well) was loaded on NuPAGE® Novex® 4-12% Bis-Tris Protein Gels (Life Technologies, UK) and run in 1x NuPAGE® MOPS SDS Running Buffer (Life Technologies, Paisley, UK). Proteins were then electrophoretically transferred onto a nitrocellulose membrane, and then were blocked for 1 h in 5% fat-free milk in 1 x TBST (2 mM Tris-Base, 15 mM NaCl, pH7.4 and 0.1% (v/v) Tween 20) and subsequently incubated with the primary antibody in 5% fat-free milk TBST at 4 ^{0}C, overnight. After 5 x 5 minutes washing steps with TBST, the appropriate horse radish peroxidase-conjugated IgG secondary antibody was incubated with the membrane at room temperature for 1 h. Immunoblots were developed using enhanced chemiluminescence solution (Pierce, UK).

2.4.5 Blue Native Polyacrylamide gel electrophoresis (BN-PAGE)

Cells were harvested and washed twice in ice-cold PBS (section 2.3.10) and the pellets were resuspended in lysis buffer: 150 mM NaCl, 2 mM EDTA, 0.01 mM Na_2HPO_4, 0.5%

DDM, 5% glycerol, supplemented with Complete protease inhibitors mixture, as described in section 2.4.2 on the preparation of lysates for Blue Native PAGE. Lysates were prepared and protein was quantified by BCA assay. Samples were prepared by adding 3 x G-250, Native PAGE sample buffer (Native PAGE Sample prep kit, Life Technologies). Some samples were also treated with 1% SDS, for 10 minutes at room temperature, and were run alongside with the un-treated samples. The samples were loaded on 10 well NativePAGE™ Novex® 3-12% Bis-Tris Protein Gels, 1.0 mm (Novex, Life Technologies, UK). The Native PAGE™ Running Buffer (20X) was used to prepare the (anode) 1x running buffer, placed in the outer chamber of the gel tank, and the two cathode running buffers. The dark blue- cathode running buffer was prepared by adding 0.2% (v/v) of the Native PAGE™ Cathode buffer additive (20X) in the 1x running buffer. The light blue-cathode buffer was prepared by adding 0.02% of the Native PAGE™ Cathode buffer additive (20X). The gels were run in the dark blue cathode buffer for 30 minutes and then the dark blue cathode buffer was replaced with the light blue cathode buffer and gels were run for another 1 hour at 250 mV, while the gel tank was transferred on ice.

Proteins were then transferred onto PVDF membranes and were subsequently fixed by incubating with 8% acetic acid for 15 minutes at room temperature. PVDF membranes were subsequently processed with the appropriate antibodies and developed as described in the section 2.4.4.

2.4.6 Co-immunoprecipitation

Cells were harvested (section 2.3.10) and were lysed in cell lysis buffer (section 2.4.2). The cell pellet in lysis buffer was placed on a rotating wheel for 45 minutes at 4˚C and then centrifuged for 30 minutes at 100,000 g at 4˚C and the supernatant-clear lysate was transferred to a clean tube. The protein concentration was determined by BCA assay. The lysate was incubated with anti-VSV agarose beads or anti-HA beads in 1:1 v/v, at 4˚C, rotating overnight. Samples were then washed four times in lysis buffer by centrifugation at maximum speed for 1 minute and the supernatant was discarded. The bound receptors were then eluted with 2 mg/ml VSV-peptide or HA-peptide by rotating on a wheel for 1 hour at 4˚C and the eluates were then collected by spinning at maximum speed for 1 minute at 4˚C. The protein concentration was calculated again to determine the recovery of the protein after the immunoprecipitation. Eluates were then prepared for separation on an SDS-PAGE or a Blue Native PAGE as described before (sections 2.4.4 and 2.4.5 respectively).

2.5 Radioligand Binding

2.5.1 Radioligand saturation binding experiments

Saturation binding data was determined by adding varying concentrations of the radioligand to 5 µg protein. A working stock of [^{3}H]-quinuclidinyl benzilate (QNB) was used to prepare the 10x dilutions at different concentrations to be added to the assay (100 µl per reaction). Atropine at a final concentration of 10 µM was used to determine non-specific binding. The final volume was 1 ml per reaction. The reactions were incubated at 30˚C for 2 hours before the bound ligand was separated from free by vacuum filtration through GF/C filters (Brandel Inc. Gaithersburg, MD) after two steps of washing with ice cold radioligand binding assay buffer. Bound ligand was estimated by liquid scintillation spectrometry.

2.5.2 Radioligand single point binding experiments

Single point binding using a single close to saturating concentration of [^{3}H]-QNB was carried out using 5 µg membrane protein per reaction in radioligand binding assay buffer, reaching up to 1 ml of final concentration. The concentration of the radioligand was dependent on the receptor being examined. The muscarinic ligand QNB has a lower affinity for the hM$_3$RASSL receptor with a K_D=2.44 nM (Alvarez-Curto *et al.*, 2011) therefore, higher concentrations of radioligand were required (up to 20 nM). The K_D of QNB for the hM$_2$WT was found to be around 0.4 nM, so lower radioligand concentrations were used (up to 3 nM). Atropine was used to define the non-specific binding at a final concentration of 10 µM. Reactions were incubated for 2 h at 30 ^{0}C. Bound ligand was separated from free by vacuum filtration through GF/C filters (Brandel Inc. Gaithersburg, MD). The filters were washed twice with assay buffer and bound ligand was estimated by liquid scintillation spectrometry.

2.5.3 Competition binding experiments

Competition binding assays were carried out by adding varying concentrations of the ligands to be tested e.g. acetylcholine, carbachol, clozapine-N-oxide or atropine in the presence of a single concentration of [^{3}H]-QNB. Non-specific binding was determined in the presence of 10 µM atropine. Reactions were incubated for 2 h at 30 ^{0}C. Bound ligand was separated from free by vacuum filtration through GF/C filters (Brandel Inc. Gaithersburg, MD). The filters were washed twice with assay buffer and bound ligand was estimated by liquid scintillation spectrometry.

2.6 Resonance Energy Transfer (RET) Methods

2.6.1 Detection of cell surface receptor expression and oligomerisation by htrFRET

Cells were grown to 100,000 per well on poly-$_D$-lysine pre-treated 96-well solid black bottom plates (Greiner Bio-one, UK). Cells were induced with doxycycline at the stated concentrations (see Results) for 24 h to express the receptor of interest. After doxycycline induction, cell surface receptor expression was monitored by adding 10 nM SNAP-Lumi4 Tb or 20 nM CLIP-Lumi4 Tb. After incubation at 37 ˚C/ 5 % CO_2 for 1 h, cells were washed three times with 1 x FRET labelling media (Cisbio Bioassays, France) and the fluorescence was read at 620 nm on a PheraStar FS.

For the htrFRET experiments, a combination of donor: acceptor pair was used to detect either homomers or heteromers. Detection of VSV-SNAP-hM_2WT homomers was carried out by labelling with 5 nM SNAP-Lumi4 Tb with varying concentrations of SNAP-Red. The HA-CLIP-hM_3RASSL homomers were detected by labelling with 10 nM CLIP-Lumi4 Tb and varying concentrations of CLIP-Red. Heteromeric interactions between VSV-SNAP-hM_2WT and HA-CLIP-hM_3RASSL were detected using 5 nM SNAP-Lumi4 Tb and varying concentrations of CLIP-Red, or the reverse combination, 10 nM CLIP-Lumi4 Tb with varying concentrations of SNAP-Red. The substrates were prepared to the appropriate concentrations in 1 x FRET labelling media (Cisbio Bioassays, France) and the labelling reaction was carried out for 1 h at 37 ^{0}C, 5% CO_2. Cells were then washed three times with 100 µl per well 1 x labelling media and plates were either read directly (once or

repeatedly for the requirements of the kinetic htrFRET experiments) after this or further processed to test the effect of receptor ligands. For the kinetic htrFRET experiment, ligands were added to the plates, dissolved in 1x FRET labelling medium; they were subsequently incubated at set temperatures and times and read out on a PheraStar FS HTRF compatible reader. Both the emission signal from the SNAP-Lumi4-Tb or CLIP-Lumi4 Tb (620 nm) and the FRET signal resulting from the acceptor SNAP-Red or CLIP-Red (665nm) were recorded. Finally, the specific fluorescent signal was calculated by subtracting from the total 665 nm signal that was obtained from cells labelled but not expressing the receptor (non-induced cells), and calculating the 665:620 ratio.

2.6.2 Monitoring ligand regulation of receptor oligomerisation by triple labelling htrFRET

Triple labelling experiments involved the simultaneous labelling of the cells with three different but spectrally compatible substrates. The substrate used as donor e.g. Lumi4 Tb, possesses certain spectral properties, demonstrating four distinct emission peaks upon excitation at 337 nm one of which (495 nm) is able to excite green region-emitting substrates/acceptors, whilst, the 620 nm emission peak can excite red region-emitting substrates/acceptors. It was this property that was utilised in the multiplex labelling (or multi-labelling) of the receptors, using one donor (Lumi4 Tb) and two acceptors able to emit at different and distinguishable wavelengths (i.e. red emitting at 665 nm and green emitting at 520 nm).

Cells were grown to 100,000 per well on poly-$_D$-lysine pre-treated 96-well solid black bottom plates (Greiner Bio-one, UK) and then receptor expression was induced by the addition of the appropriate concentration of doxycycline. After 24 hour of induction, cells were labelled with the three different substrates by incubating at 37˚C, 5% CO_2 for 1 hour. One set of experiments involved addition of 5 nM SNAP-Lumi4 Tb as donor and 100 nM CLIP-Red and 100 nM SNAP-Green as acceptors. The other set of experiments utilised CLIP-Lumi4 Tb at final concentration of 10 nM as a donor and 100 nM of SNAP-Green and 100 nM of CLIP-Red as acceptors. After the labelling step, cells were washed three times in 1x HBSS and 100 µl of 1x FRET labelling medium was added per well for the analysis. Two different protocols were used for the each utilising a different set of dichroic filters for the measurement of the three different wavelengths (620 nm, 665 nm and 520 nm).

The specific fluorescent signal was calculated by subtracting from the total FRET 665 nm or 520 nm signal that was obtained from cells labelled but not expressing the receptor (non-induced cells) and calculating the 665:620 ratio or the 520: 620 ratio.

2.6.3 Tag-Lite® internalisation assay

Cells were plated in a black-bottom 96-well plate and induced with doxycycline for 24 hours. Cells were labelled with 100 nM SNAP-Lumi4 Tb (for SNAP tagged receptors) and 200 nM CLIP-Lumi4 Tb (for CLIP tagged receptors). After 1 hour labelling at 37˚C, 5% CO_2 the plates were washed three times with 1x HBSS. Ligands were prepared at the final concentrations in Tag-lite® internalisation assay buffer (Cisbio Biosciences, France) and 100 µl of the ligand preparations were added per well. The Tag-lite® internalisation assay buffer may act as a FRET acceptor, when excited by one of the four emission peaks (490 nm) of the Lumi4 Tb donor. The assay buffer, once excited, emits at 520 nm. FRET measurements, using PheraStar FS, were carried out at set time points to allow kinetic determination of receptor internalisation in response to ligand mediated activation. The FRET ratio was calculated as a ratio of 620/520 and that was plotted over time, using Graph Pad software.

2.7 Functional assays

2.7.1 Calcium mobilisation assay

Cells (50,000 per well) were seeded in a pre-coated with poly-$_D$-lysine clear bottom black 96-well plate. Receptor expression was induced by adding doxycycline and incubating for at least 16 hours. After induction of receptor expression, the cells were incubated with Fura-2 AM for 45 minutes at 37˚C. After the labelling step was completed the Fura-2 AM was removed from the wells, and the cells were washed twice with 1x HBSS buffer and finally incubated in 100 µl 1x HBSS per well for 15 minutes. The compound serial dilutions were prepared in a separate 96-well ELISA plate. The plate containing the labelled cells and the plate with compound serial dilutions were then transferred to the Flex

Station (Molecular Devices) and the calcium concentration was measured. The data were plotted using Graph Pad software.

2.7.2 Inositol monophosphate (IP-1) accumulation

Cells were plated in 10 cm dishes and when 70-80% confluence was reached they were treated with doxycycline to induce receptor expression. A suspension of 10,000 cells per assay point was prepared in stimulation buffer and incubated with ligands for 1 hr at 37 ˚C, 5 % CO_2 in a white Proxiplate-384 Plus (PerkinElmer, Inc. USA). After ligand stimulation, cells were lysed in a mixture of detection reagents prepared in lysis buffer according to the manufacturer's instructions (IP-One Tb kit, Cisbio Bioassays, France) and subsequently incubated for a further 1 h at room temperature. FRET signal was then measured using a PheraStar FS and final IP1 concentrations were calculated as ratio of 665/620 nm.

2.7.3 Cyclic adenosine monophosphate (cAMP) detection

Cells were plated in 10 cm dishes and when 70-80% confluence was reached, they were treated with doxycycline to induce receptor expression. A suspension of 4,000 cells per assay point was prepared in 1x HBSS. The cells were co-incubated with the optimal concentration of forskolin (1 µM) and with ligands for 30 minutes in white, 384-well Proxiplate. This step was followed by lysis of cells using a mixture of detection reagents prepared in lysis buffer according to manufacturer's instructions (cAMP dynamic 2 kit, Cisbio Bioassays, France) and incubation for 1 h at room temperature. FRET signal was measured on a PheraStar FS and the inhibition of cAMP levels was calculated as ratio of 665/620 nm.

2.8 Epi-fluorescence imaging of live cells

Live cells (300,000 per well) were plated in a 6-well plate, on poly-$_D$-lysine pre-coated cover-slips (0.0 mm thickness) and they were incubated overnight in complete DMEM. The medium was removed the next day and fresh medium containing the appropriate

concentration of doxycycline was added for 24 hours. Labelling was performed 24 h post-induction, using the appropriate cell impermeable fluorescent dyes.

HA-CLIP-hM_3RASSL receptor was labelled with 5 µM CLIP- Surface 488 and the VSV-SNAP-hM_2WT was labelled with 5 µM SNAP-Surface 549. For the visualization of receptors in cells expressing both receptors, both dyes were added simultaneously.

Cells were incubated with the fluorescent dye for 30 min at 37 °C, 5% CO_2. After three washes with DMEM, fresh medium was added and the cells were further incubated for 30 min. Cells on cover-slips were then washed with 1x HBSS. Cover-slips were then transferred to a microscope chamber where they were imaged using an inverted Nikon TE2000-E microscope (Nikon Instruments, Melville, NY) equipped with a 40x (numerical aperture-1.3) oil-immersion Pan Fluor lens and a cooled digital photometrics Cool Snap-HQ charge-coupled device camera (Roper Scientific, Trenton, NJ). Ligands diluted in 1x HBSS were used for studying receptor internalisation upon agonist-induced receptor activation.

2.9 Statistical analysis

Data analysis and curve fitting were carried out using Graph Pad Prism 5 Software. The results were presented as means ± SEM of three independent replicates, unless otherwise stated, or as means ± range of two independent replicates (n=2). Statistical significances were tested using a two-paired t-test at $P<0.05$, as specified for each experiment. Concentration response curves were fitted to a non-linear regression equation using the three parameter fit. All graphs were created using GraphPad Prism 5 Software.

Chapter 3

Characterisation of cell lines used for studying oligomerisation of hM_2 and hM_3 muscarinic receptors

3.1 Introduction

The tools used for studying receptor oligomerisation are very important as they may determine the effectiveness of the approach followed as well as the quality of the outcome. In order to study the homomerisation and heteromerisation of the human M_2WT and M_3RASSL an htrFRET approach was used in combination with Tag-lite® technology. The htrFRET technique in combination with Tb^{3+} cryptate energy donors, utilised by Tag-lite® technology, has been helpful in probing molecular interactions (Bazin *et al.*, 2001) and has been used as a strategy to study receptor oligomerisation (Cottet *et al.*, 2012). Similar live cell-based htrFRET methods have been previously used to study heteromerisation between D_2 and D_3 dopamine receptors (Pou *et al.*, 2012) and the oligomerisation between metabotropic glutamate receptors (Doumazane *et al.*, 2011), as well as M_3 muscarinic receptor homomerisation (Alvarez-Curto *et al.*, 2010). This experimental approach requires the combination of three different parameters. Firstly, the fusion of the receptors with SNAP or CLIP epitope tags, preferably at the N-terminal domain of the receptor to allow extracellular labelling and detection. Secondly, use of the Tag-lite® labelling of the tagged receptors using htrFRET compatible substrates to specifically label the SNAP and/or CLIP-tagged receptors. Finally, a cellular expression system based on the generation of Flp-In™ T-REx™-293 stable cell lines can ensure consistent receptor expression at the cell surface.

The initial steps of the project involved the fusion of SNAP and CLIP epitope tags to the extracellular N-terminus of the hM_2WT and hM_3RASSL receptors, respectively. The additional HA and VSV-G epitope tags were also fused at the N-terminus of the receptors, upstream of the SNAP and CLIP tags, respectively. This allowed the use of tag specific antisera to detect the expressed receptors by immunoblotting and also to enable detection of receptor-receptor interactions via co-immuno-precipitation. In addition, the mGluR5 signal sequence was included in the fusion construct and it was cloned upstream of the receptor and the tag sequences, to enhance cell surface delivery of the expressed fusions (Figure 3.1).

The SNAP tag is a small (about 20 kDa) protein, based on O^6-alkylguanine DNA alkyltransferase that has the ability to be modified upon binding to fluorescent labels based on O^6-benzylguanine derivatives (Maurel *et al.*, 2008). The CLIP tag is a modified version of the SNAP tag that specifically reacts with O^6-benzylcytosine derivatives (Maurel *et al.*, 2008). A variety of substrates are available for specific SNAP or CLIP-tag labelling. These substrates allow covalent epitope tag to substrate labelling in a 1:1 ratio. The substrates used for htrFRET assays are cell impermeant, allowing the detection of cell surface

receptor expression and receptor-receptor interactions. The htrFRET donor/acceptor partners must fulfill the spectral compatibility criteria i.e. the emission spectrum of the donor must overlap with the excitation spectrum of the acceptor and additionally, the emission spectra of donor and acceptor must not overlap. The long half-time emission fluorescence of terbium cryptate in combination with the time-resolved FRET i.e. introducing a time delay between excitation and measurement, allows the elimination of short lived background fluorescence and offers a high signal-to-noise ratio. Labelling substrates such as SNAP-Lumi4 Tb and CLIP-Lumi4 Tb may be used as energy donors. The Lumi4 Tb donors emit at four different wavelengths upon excitation at 337 nm. The emission at 620 nm may in turns excite a nearby red energy acceptor, which will sequentially emit at 665 nm. This FRET signal, if detected, would suggest an interaction between the donor and acceptor species and could correspond to a possible protein-protein interaction. In the absence of a FRET acceptor partner, the fluorescence emission at 620 nm corresponds to the expression of the cell surface labelled receptor (Figure 3.2 A, B). The spectral properties of the htrFRET reagents are shown in Figure 3.2 C, demonstrating the overlap of the donor's emission and the acceptor's excitation spectra.

A cellular expression system that would allow the heterologous expression of the receptors at levels close to the physiological ones and that would enable the study of the receptors at the surface of live cells was required. This led to the generation of cell lines based on the Flp-In™ T-REx™-293 cells that allowed the expression of each of the VSV-SNAP-hM_2WT or HA-CLIP-hM_3RASSL receptors individually. The Flp-In™ T-REx™ -293 cells stably express the protein of interest in an isogenic and inducible manner. The level of expression of the protein of interest can be regulated by varying concentrations of doxycycline. A Flp-In™ T-REx™-293 cell line was also developed allowing the co-expression of both receptors, with the HA-CLIP-hM_3RASSL being expressed constitutively, while the VSV-SNAP-hM_2WT being expressed in a doxycycline inducible manner. Once the cell lines were established they were fully characterised in terms of receptor expression, cell surface delivery and function.

The high structural homology of the orthosteric binding site shared by all five muscarinic sub-types is responsible for the lack of selective muscarinic ligands (Wess, 2004). For this reason, a chemically engineered version of the M_3 receptor described as Receptor Activated Solely by Synthetic Ligand or RASSL that is not able to respond to acetylcholine or other muscarinic agonists, but is activated by the synthetic ligand CNO,

was developed (Armbruster *et al.*, 2007) and used instead of the wild type M_3 receptor (Alvarez-Curto *et al.*, 2011). This allowed the differential activation of the two receptors, hM_2WT and hM_3RASSL, when these were co-expressed.

The necessity of studying GPCR signalling *in vivo* without the complicating effects of endogenous ligands was one of the reasons that had led to the development of RASSLs and DREADDs (Coward *et al.*, 1998). The first RASSL that was generated was a mutant version of the β_2- adrenergic receptor that was unable to respond to its native ligands but was activated by non-natural ligands with low potency (Strader *et al.*, 1991). Generation of more RASSLs followed, such as the human κ opioid RASSL receptors (Coward *et al.*, 1998). Additional RASSLs were created that contained fluorescent tags or ones that demonstrated different internalisation and desensitisation properties (Scearce-Levie *et al.*, 2001, 2005; Pei *et al.*, 2008; Rogan and Roth, 2011). Muscarinic RASSLs were developed by Armbruster *et al.*, (2007) by selecting between libraries of randomly mutated M_3 receptors in yeast cells, during directed molecular evolution for the synthetic ligand CNO (Armbruster *et al.*, 2007). The hM_3RASSL contains two single mutations at the third (Y149C) and fifth (A239G) transmembrane domains. The hM_3RASSL binds to and responds to CNO with nanomolar potency, but is unresponsive to carbachol. Once activated by CNO, the M_3RASSL activates the G_q protein dependent pathway in a similar way as the hM_3WT, resulting in calcium ion release from the ER, activation of ERK1/2 phosphorylation pathway, β-arrestin recruitment and subsequent internalisation of the receptor (Alvarez-Curto *et al.*, 2011).

Aims of this chapter

- Determination of the total and cell surface expression levels of VSV-SNAP-hM_2WT and HA-CLIP-hM_3RASSL, in cells expressing each receptor individually and in cells co-expressing both receptors.
- Identification of the doxycycline concentrations that allow for similar expression levels of the receptors in cells expressing each of the receptor individually and in cells co-expressing the receptors.
- Investigation of the localisation, functionality and pharmacology of the expressed receptors.

3.2 Flp-In™ T-REx™-293 cell lines express each of the receptors, VSV-SNAP-hM_2WT or HA-CLIP-hM_3RASSL, at the cell surface in a doxycycline-dependent manner.

The doxycycline-dependent regulation of receptor expression in Flp-In™ T-REx™-293 cell lines was assessed by three different approaches. The first approach involved immuno-detection with anti-SNAP/CLIP antibody (able to recognise both SNAP and CLIP tags) against lysates of cells treated with different doxycycline concentrations. The anti-SNAP/CLIP antiserum was able to detect the HA-CLIP-hM_3RASSL at the regions of 100 kDa corresponding to the un-glycosylated version of the receptor and just above the 100 kDa (around 120 kDa) corresponding to the glycosylated version of the same receptor (Figure 3.3 A). The anti-HA antibody was able to detect only the un-glycosylated HA-CLIP-hM_3RASSL at 100 kDa (Figure 3.3 B). In a similar manner, the VSV-SNAP-hM_2WT was detected using the anti-SNAP/CLIP antibody and its molecular mass was identified at above 70 kDa (Figure 3.4). There was no receptor expression detected in the samples prepared using cells not treated with doxycycline, or in the samples prepared from non-transfected parental Flp-In™ T-REx™-293 cells. Therefore, it can be suggested that the polypeptides detected were specific and they corresponded to the receptors in question. In both cell lines expressing each receptor individually, receptor expression was increased with increasing doxycycline concentrations. Using the anti-SNAP/CLIP antibody in immuno-blotting experiments, it was demonstrated that two different forms of the receptors were detected, the glycosylated and non-glycosylated that appeared as slightly lower molecular mass polypeptides. To further explore this, cells expressing each of the receptors upon doxycycline induction were treated with tunicamycin and the lysates prepared were resolved on SDS-PAGE (Figure 3.5). Tunicamycin is a mixture of antibiotics that inhibit N-linked glycosylation by blocking GlcNAc phosphotransferase (GTP), in early stages of protein synthesis, thus leading to cell cycle arrest in G1 phase, which in turns results in apoptosis (Wheatley and Hawtin, 1999). Cells that were simultaneously treated with doxycycline to induce receptor expression and tunicamycin to block N-linked glycosylation appeared to express only the non-glycosylated version of the receptor, with lower molecular mass compared to the glycosylated form (Figure 3.5). Glycosylation of a protein confers an increase in the protein's molecular mass and in the case of the two receptors studied here, the molecular masses of the glycosylated HA-CLIP-hM_3RASSL and VSV-SNAP-hM_2WT were above 100 kDa and 70 kDa, respectively, as opposed to the lower molecular masses detected for each receptor i.e. 80-85 kDa for HA-

CLIP-hM$_3$RASSL (Figure3.3) and 60-65 kDa for VSV-SNAP-hM$_2$WT (Figure 3.4), when non-glycosylated. The treatments with tunicamycin were carried out for 16 hours, in order to maintain the levels of cell death due to apoptosis as low as possible, and inhibition of glycosylation effective enough.

In order to confirm the doxycycline-dependent inducible expression of receptors, but also the successful cell surface delivery of the expressed receptors, labelling of live cells was performed using cell impermeant substrates. HA-CLIP-hM$_3$RASSL was labelled with 20 nM CLIP-Lumi4 Tb and VSV-SNAP-hM$_2$WT was labelled with 10 nM SNAP-Lumi4 Tb in intact cells. Fluorescence emission at 620 nm was monitored following excitation at 337 nm (Figure 3.6 A and B). Receptors were only labelled with the energy donors (as described in Figure 3.2 B) in the absence of an energy acceptor, therefore, the fluorescence at 620 nm corresponded to the total expression of the cell surface labelled receptors at that particular concentration of doxycycline and Lumi4 Tb. Increasing the receptor expression with varying concentrations of doxycycline resulted in an increase in the 620 nm fluorescence. The increase in 620 nm signal for both receptors HA-CLIP-hM$_3$RASSL (Figure 3.6 A) and VSV-G-SNAP-hM$_2$WT (Figure 3.6 B) were in agreement with the results observed in the immunoblotting experiments (Figures 3.3 and 3.4, respectively). Addition of increasing concentrations up to 30 nM of CLIP-Lumi4 Tb (Figure 3.6 C) or 40 nM of SNAP-Lumi4 Tb (Figure 3.6 D), did not lead to saturation of the corresponding cell surface receptors, suggesting that the range of substrate concentrations used in the experiments were not sufficient to label the totality of the cell surface receptors, but only a fraction. The concentrations of Lumi4 Tb required to achieve receptor saturation lie within the micromolar range (Doumazane *et al.*, 2011). However, using sub-saturating Lumi4 Tb concentrations (in the nanomolar range) has been shown to be sufficient to study cell surface receptor expression and oligomerisation (Pou *et al.*, 2010; Alvarez-Curto *et al.*, 2010) without achieving full coverage of the expressed receptors.
Cell surface delivery of the receptors was also monitored by epi-fluorescence microscopy. This involved labelling of intact cells with cell impermeant SNAP or CLIP specific fluorescent dyes (Figure 3.7). The SNAP-Surface 488 (green) was used for detecting the VSV-SNAP-hM$_2$WT receptor (Figure 3.7 A) and the CLIP-Surface 547 (red) was used for detecting the HA-CLIP-hM$_3$RASSL at the cell surface (Figure 3.7 B). Receptor expression was detected at the surface of doxycycline treated cells. No fluorescence was detected in cells that were maintained in medium without doxycycline, although background fluorescence was observed, probably corresponding to non-specific binding of the

fluorescent dyes or to auto-fluorescence background (noise) due to any remaining serum contained in the growth medium that cells were maintained in.

3.3 Pharmacological profile of receptors expressed individually in Flp-In™ T-REx™-293 cells.

In an attempt to quantify total receptor expression, binding of near saturating concentrations of the muscarinic antagonist [^{3}H]-QNB to membranes prepared from doxycycline treated cells was carried out. Radioligand binding data showed a pattern of receptor expression similar to that detected with the fluorescent measurement at 620 nm and a comparable profile (increased receptor expression levels with increasing doxycycline concentrations) to the immunoblotting experiments (see Figures 3.3 and 3.4). Saturating concentrations of the radioligand were used in an attempt to achieve maximal coverage of the receptor/binding sites. The radioligand concentrations used were determined by the previously reported K_D values of the radioligand for each of the receptors. The reported affinity of [^{3}H]-QNB for the hM$_3$RASSL receptor according to Alvarez-Curto *et al.,* (2011) was k_D=2.44 nM, lower than that for the hM$_2$WT, which was in the range of 0.16-0.2 nM (Peralta *et al.,* 1987; Norman *et al.,* 1989; Burstein *et al.,* 1996).
The HA-CLIP-hM$_3$RASSL receptor expression was determined using membranes prepared from cells treated with 10 ng·ml^{-1} doxycycline, for 24 hours and the Bmax at 1.46 ± 0.66 pmol·mg^{-1} protein was calculated. The range of radioligand concentration used for this set of experiments was between 14-20 nM (Figure 3.8 A). This measurement is not absolutely precise as the radioligand concentration used did not saturate the receptor according to the saturation binding experiments carried out (see example in Figure 3.8 C).
The VSV-SNAP-hM$_2$WT was expressed with a Bmax at 1.8 ± 0.35 pmol·mg^{-1} protein, in membranes prepared from cells treated with 5 ng·ml^{-1} doxycycline for 24 hours, and the range of radioligand concentration used was between 0.16-0.45 nM (Figure 3.8 B).

The hM$_3$RASSL receptor was engineered by introducing two single point mutations in the orthosteric binding site and resulted in the inability of the receptor to bind to the muscarinic ligand [^{3}H]-QNB as efficiently as the wild type receptor. Consequently, that had resulted in a significantly lower affinity of the radioligand for the receptor. The previously reported K_D value for the hM$_3$RASSL receptor was reported to be higher (K_D=2.44 nM) than that of the wild type hM$_3$ receptor (K_D= 35± 0.9 pM) (Alvarez-Curto *et*

al., 2011). This had caused a lot of difficulties in carrying out radioligand saturation experiments using HA-CLIP-hM_3RASSL enriched membrane preparations. The radioligand binding experiment conditions involving exceptionally high concentrations of [^{3}H]-QNB (20-40 nM) and the cost of the experiments were limiting factors for succeeding in the generation of saturation isotherms of HA-CLIP-hM_3RASSL and had led to failure in confirming the K_D of [^{3}H]-QNB for the hM_3RASSL receptor. A representative example shown in Figure 3.8 C corresponds to one experiment that failed to demonstrate saturation of the HA-CLIP-hM_3RASSL by the radioligand. VSV-SNAP-hM_2WT enriched membranes, prepared from single cells treated with 5 ng·ml^{-1} doxycycline, were used to measure the specific binding of varying concentrations of [^{3}H]-QNB, ranging from 0.05-0.5 nM. This resulted in the generation of a saturation isotherm (Figure 3.8 D) with a K_D obtained at 0.32 ± 0.07 nM. The expression level of the VSV-SNAP-hM_2WT receptor was also determined with Bmax= 3.07 ± 0.52 pmol·mg^{-1} protein.

Competition binding assays were carried out to test the affinity of carbachol, atropine and CNO for VSV-SNAP-hM_2WT. For these experiments, concentrations of [^{3}H]-QNB sufficient to give 90% receptor occupancy were used. The competition binding curves shown in Figure 3.9 A, B and C are representative experiments using 5 μg of membrane protein preparations from cells treated with 5 ng·ml^{-1} doxycycline to express VSV-SNAP-hM_2WT. Carbachol could bind to the orthosteric site of the VSV-SNAP-hM_2WT receptor (pK_i = 6.37 ± 0.13) displacing the radioligand (Figure 3.9 A), whereas, the synthetic ligand CNO did not demonstrate binding to the receptor (Figure 3.9 B). The antagonist atropine outcompeted the radioligand (pK_i = 8.74 ± 0.05) (Figure 3.9 C). The pK_i values shown in Figure 3.9 were obtained from individual experiments. However, the pK_i values from four different experiments were pooled and shown in Table 3.1.

VSV-SNAP-hM$_2$WT	pK$_i$ (n=4)
Carbachol (Cch)	**6.0 ± 0.2**
Atropine (Atr)	**8.6 ± 0.1**

Table 3.1 Calculated pK$_i$ values for carbachol and atropine as a measure of affinity for the VSV-SNAP-hM$_2$WT receptor. Pooled data from four experiments, carried out in triplicates (presented as Means ± SEM, n=4).

The competition binding experiments using membranes enriched with HA-CLIP-hM$_3$RASSL receptor prepared from cells treated with 10 ng·ml^{-1} doxycycline, failed to provide the pK$_i$ values of the ligands for the receptor, therefore, no conclusions could be made on the affinity of the ligands to bind the receptor (data not shown). Information on CNO and atropine affinity for the hM$_3$RASSL was based on previous studies on the hM$_3$RASSL receptor (Alvarez-Curto *et al.,* 2011). A similar approach to perform competition binding experiments was followed using cells able to express both receptors, the HA-CLIP-hM$_3$RASSL in a constitutive manner and the VSV-SNAP-hM$_2$WT in a doxycycline inducible manner, and this is described in detail in section 3.9 of this chapter.

3.4 Functionality of receptors expressed individually in Flp-In™ T-REx™-293 cells.

Receptor function and the ability to activate the corresponding G protein were assessed. The hM$_3$RASSL binds to G$_{q/11}$ proteins in a similar way as the hM$_3$WT, activating the enzyme PLCβ which in turns catalyses the production of IP$_3$ and DAG from PIP$_2$. IP$_3$ then diffuses in the cytoplasm and binds to IP$_3$ receptors, triggering release of calcium ions from the ER. The hM$_2$WT receptor, upon activation with agonist, binds to and activates G$_{i/0}$ proteins. This results in the inhibition of adenylate cyclase and in turns reduction in cAMP production (Figure 3.10).

Flp-In™ T-REx™-293 cells treated with doxycycline for 24 hours, to express the HA-CLIP-hM$_3$RASSL receptor, were employed in IP-One assays to assess whether the receptor was able to stimulate production of inositol monophosphate (IP1), through coupling to $G_{q/11}$ proteins in response to the synthetic ligand CNO. CNO mediated activation of HA-CLIP-hM$_3$RASSL and initiated the accumulation of IP1 with a potency described by a pEC_{50} value of 7.7 ± 0.18. The receptor did not respond to the muscarinic ligand carbachol (Figure 3.11). Addition of a monophosphatase inhibitor (lithium chloride) prevented the degradation of IP1 and allowed the accumulation of the IP1 molecule.
The carbachol mediated coupling of the VSV-SNAP-hM$_2$WT receptor to $G_{i/0}$ proteins was demonstrated by monitoring the inhibition of adenylate cyclase demonstrated as a decrease in forskolin-induced levels of cAMP (pEC_{50}= 5.6 ± 0.46) (Figure 3.12). CNO did not demonstrate hM$_2$WT receptor activation.

3.5 Screening of cell lines co-expressing HA-CLIP-hM$_3$RASSL and VSV-SNAP-hM$_2$WT receptors.

To explore the potential co-existence between M_2 and M_3 homomers but also M_2-M_3 heteromers, a cellular system that allowed the co-expression of both receptors was generated, based on the Flp-In™ T-REx™-293 cell lines. The cell line inducibly expressing the VSV-SNAP-hM$_2$WT receptor was transfected with a construct encoding for the HA-CLIP-hM$_3$RASSL receptor. This resulted in constitutive expression of the HA-CLIP-hM$_3$RASSL receptor. The process of generating a cell line able of co-expressing HA-CLIP-hM$_3$RASSL in a constitutive manner and VSV-SNAP-hM$_2$WT upon doxycycline treatment is fully described in section 2.3.7.
Several clones were selected and were primarily screened by immuno-blotting, to assess total receptor expression, using the anti-SNAP/CLIP antiserum (Figure 3.13). Lysate preparations from four different clonal cell lines (clones 8, 10, 15 and 20), grown in the absence and presence of doxycycline, were subjected to immuno-blotting against the anti-SNAP/CLIP antiserum. Clone 8 seemed to express the constitutive HA-CLIP-hM$_3$RASSL in lower levels compared to the rest of the clones (Figure 3.13 A) according to the intensity measurements of the polypeptide bands (Figure 3.13 B). Clone 10 seemed to express the VSV-SNAP-hM$_2$WT in the absence of doxycycline, and it was therefore excluded as a potential cell line to study receptor oligomerisation, as it would be impossible to manipulate the co-expression of receptors. Clones 15 and 20 demonstrated a similar

expression profile for both the constitutive and the inducible receptors, with the total expression of the constitutive receptor HA-CLIP-hM_3RASSL being higher compared to clone 8. The expression of the inducible VSV-SNAP-hM_2WT, upon addition of 5 ng·ml^{-1} doxycycline for 24 hour, was similar between clones 15 and 20, but higher than that seen in clone 8, under the same doxycycline treatment conditions. A representative example is shown in Figure 3.13.

In an attempt to quantify the total expression of each receptor, and compare between the different clones, binding of near saturating concentrations (16 nM) of the muscarinic antagonist [^{3}H]-QNB to membranes prepared from doxycycline treated cells showed a similar pattern of receptor expression between clones 8 and 10, whereas, clones 15 and 20 demonstrated a slightly lower expression for both receptors, contradicting the Western blot analysis (Figure 3.14).

The next step included assessing cell surface expression of the constitutive HA-CLIP-hM_3RASSL, by monitoring fluorescence at 620 nm, using cells treated or not with doxycycline. Cells were labelled with 20 nM CLIP-Lumi4 Tb. The expression of the constitutive HA-CLIP-hM_3RASSL was unaffected by the presence of VSV-SNAP-hM_2WT, in all cell lines examined (Figure 3.15 A). Expression of VSV-SNAP-hM_2WT at the cell surface was measured by monitoring fluorescence at 620 nm after labelling with 10 nM SNAP-Lumi4. There was no fluorescence detected in the absence of doxycycline treatment, but when cells were treated with 5 ng·ml^{-1} doxycycline fluorescence at 620 nm was detected corresponding to the cell surface expression of VSV-SNAP-hM_2WT (Figure 3.15 B).

Clone 8 was selected for further characterisation and was employed for investigating oligomerisation between hM_2WT and hM_3RASSL. There were various reasons that clone 8 was considered more suitable compared to the rest of cell lines. One of the reasons included the observation of VSV-SNAP-hM_2WT receptor expression in the absence of doxycycline in clone 10 according to the Western blot analysis. This would complicate further characterisation and would potentially interfere with oligomerisation studies. Therefore, clone 10 was excluded. Although, clones 15 and 20 demonstrated lower HA-CLIP-hM3RASSL expression, compared to clone 8, according to radioligand binding experiments and fluorescence readings at 620 nm, they had to be excluded because their growth pattern was very slow and there were inconsistencies in the morphology of the cells which also demonstrated low degree of viability. In addition, the expression levels of the constitutive receptor in clone 8 were not very different to the ones observed in clones 15

and 20 and the expression of VSV-SNAP-hM$_2$WT could be manipulated by addition of doxycycline.

3.6 Characterisation of the selected cell line able of co-expressing HA-CLIP-hM$_3$RASSL and VSV-SNAP-hM$_2$WT.

The selection of the most suitable cell line able of expressing the HA-CLIP-hM$_3$RASSL in a constitutive fashion and the VSV-SNAP-hM$_2$WT only upon doxycycline treatment was further characterised. The initial aim was focused on identifying the doxycycline concentration at which the inducible VSV-SNAP-hM$_2$WT receptor was produced in amounts close to the constitutively expressed HA-CLIP-hM$_3$RASSL, to ideally reach a 1:1 receptor ratio. This was initially approached by immuno-blotting of lysate preparations against the anti-SNAP/CLIP antiserum, as well as the anti-HA and anti-VSV anti-sera detecting the HA- and VSV-G- epitope tags, respectively (Figure 3.16). According to the results obtained from the immuno-detection and Western blot analysis the HA-CLIP-hM$_3$RASSL was expressed in the absence of doxycycline, as expected and its expression levels were unaffected by doxycycline addition. In addition, the expression of the VSV-SNAP-hM$_2$WT was doxycycline dependent, while, no polypeptide corresponding to the VSV-SNAP-hM$_2$WT was detected by anti-SNAP and anti-VSV antibodies in the absence of doxycycline. VSV-SNAP-hM$_2$WT was visible in lysates from cells treated with 2 ng·ml^{-1} doxycycline (as detected using the anti-SNAP antibody) and 5 ng·ml^{-1} doxycycline (as detected with anti-VSV antibody). The expression of VSV-SNAP-hM$_2$WT was increased with increasing concentrations of doxycycline (Figure 3.16).

Cell surface delivery of both receptors was assessed by monitoring the fluorescence at 620 nm, following labelling with SNAP and CLIP specific substrates (Figure 3.17). Labelling with 20 nM CLIP-Lumi4 Tb enabled the detection of the constitutively expressed HA-CLIP-hM$_3$RASSL which did not seem to be affected by addition of increasing concentrations of doxycycline. On the other hand, labelling with 10 nM SNAP-Lumi4 Tb of cells treated with increasing concentrations of doxycycline, resulted in a linear increase of the 620 nm signal corresponding to the increase in the expression of the inducible VSV-SNAP-hM$_2$WT (Figure 3.17).

Cell surface VSV-SNAP-hM$_2$WT and HA-CLIP-hM$_3$RASSL were imaged individually following co-labelling with the cell impermeant fluorescent dyes CLIP-Surface 488 (green)

and SNAP-Surface 549 (red) (Figure 3.18). The constitutively expressed HA-CLIP-hM_3RASSL was present in cells treated or not treated with doxycycline but the VSV-SNAP-hM_2WT receptor was only detected at the surface of cells treated with doxycycline. Merging the images resulted in a clear demonstration of co-localisation of the two receptors at the surface of live cells, at the resolution of light microscopy.

3.7 Pharmacological profile of co-expressed receptors.

In an attempt to quantify the total expression of HA-CLIP-hM_3RASSL and VSV-SNAP-hM_2WT in cells that co-express the two receptors, receptor enriched membrane preparations from cells treated with varying concentrations of doxycycline were assessed using a single [^{3}H]-QNB concentration. Total receptor expression was determined by calculation of the Bmax value that corresponded to the expression levels of the constitutively expressed HA-CLIP-hM_3RASSL in membranes from cells not treated with doxycycline (Bmax= 1.6 ± 0.65 pmol·mg^{-1} protein). Membranes from cells treated with 5 ng·ml^{-1} doxycycline demonstrated an increase in total protein expression with a Bmax obtained at 4.7 ± 1.5 pmol·mg^{-1} protein. The difference in Bmax values corresponds to the expression of VSV-SNAP-hM_2WT upon doxycycline treatment (Figure 3.19).

Competition binding assays using [^{3}H]-QNB concentrations sufficient to give 90% receptor occupancy, were used to assess the affinity of carbachol, CNO and atropine for the receptors. The data presented in Figure 3.20 were obtained from individual experiments representative of the competition assays carried out using cells that are able of co-expressing both the receptors. The pK_i values shown on each graph in Figure 3.20 are for n=1. The counts from different assays could not be pooled together due to variation in the added radioactivity between the experiments. The pK_i values obtained from four different experiments were pooled together and the means are shown in Table 3.2.
Membranes prepared from cells treated or not with doxycycline were employed against a single near saturating concentration of [^{3}H]-QNB and varying concentrations of the non-labelled ligands were added as competitors. The synthetic ligand CNO successfully outcompeted the radioligand with a pK_i= 6.70± 0.17 in membranes where only the HA-CLIP-hM_3RASSL was expressed (-Dox conditions) (Table 3.2). The pK_i= 6.12 ± 0.21 was obtained from one individual experiment (Figure 3.20 A). CNO showed a slightly different affinity (pK_i= 6.24 ± 0.31) in the presence of the doxycycline inducible VSV-SNAP-

hM_2WT (+ Dox) (Table 3.2). The pK_i value from one individual experiment was found to be 5.68 ± 0.39 (Figure 3.20 B). Carbachol did not bind HA-CLIP-hM_3RASSL in membranes prepared from cells not treated with doxycycline (Table 3.2 and Figure 3.20 C for a representative example), but successfully outcompeted the radioligand when membranes enriched in VSV-SNAP-hM_2WT were used, with a pK_i= 6.10 ± 0.70 (Table 3.2). The pK_i from one individual experiment was calculated at 6.38 ± 0.27 (Figure 3.20 D). The antagonist atropine bound to the HA-CLIP-hM_3RASSL successfully outcompeting the radioligand with pK_i (-Dox) = 8.20 ± 0.14 (Table 3.2) and pK_i (+Dox) = 7.65 ± 0.10 (Table 3.2). The affinity of atropine for HA-CLIP-hM_3RASSL from one individual experiment was determined with pK_i (-Dox) = 8.13 ± 0.12 (Figure 3.20 E) and pK_i (+Dox) =7.68 ± 0.05 (Figure 3.20 F). A second affinity measurement for atropine was recorded, which corresponded to the VSV-SNAP-hM_2WT receptor, in membranes prepared from cells treated with doxycycline, with pK_i = 8.53 ± 0.10 (Table 3.2). The affinity of atropine for VSV-SNAP-hM_2WT from one individual experiment was determined with pK_i= 8.56 ± 0.05 (Figure 3.20 F).

Ligands / pK_i	**VSV-SNAP-hM_2WT (+Dox)**	**HA-CLIP-hM_3RASSL (-Dox)**	**HA-CLIP-hM_3RASSL (+Dox)**
Carbachol	**6.10 ± 0.70**	**-**	**-**
CNO	**-**	**6.70 ± 0.17**	**6.24 ± 0.31**
Atropine	**8.53 ± 0.10**	**8.20 ± 0.14**	**7.65 ± 0.10**

Table 3.2 pKi values for carbachol, CNO and atropine obtained from competition binding experiments. Carbachol only binds to VSV-SNAP-hM_2WT receptor and the synthetic ligand CNO only binds to the HA-CLIP-hM_3RASSL. The antagonist atropine was able to bind to both receptors with nanomolar affinities. Data presented as Means ± SEM, n=3, experiments carried out in triplicates.

3.8 Assessing the function of receptors when these are co-expressed in the same cell line.

The function of the doxycycline inducible VSV-SNAP-hM_2WT and the constitutive HA-CLIP-hM_3RASSL was assessed, when both receptors were co-expressed in the same cell line. The ability of the HA-CLIP-hM_3RASSL to bind to and activate the $G_{q/11}$ protein was

confirmed by assessing the accumulation of IP1 and intracellular calcium ion release, in response to CNO (Figure 3.21). The CNO-mediated activation of the HA-CLIP-hM_3RASSL resulted in a potent increase in IP1 levels, in the absence of VSV-SNAP-hM_2WT with a pEC_{50} = 8.2 ± 0.3. The potency of CNO remained unaltered in the presence of both receptors with pEC_{50} = 8.2 ± 0.27. There was a trend towards an increase in the efficacy of CNO, when both receptors were co-expressed, suggesting a possible synergistic effect of the hM_2WT receptor on the function of hM_3RASSL or simply implying possible cross-talk between the two receptors' signalling pathways (Hornigold *et al.*, 2003), but this increase was not statistically significant (P>0.05). The HA-CLIP-hM_3RASSL was unresponsive to carbachol, as expected.

The possibility of a synergistic effect between the hM_2WT and hM_3RASSL, in response to CNO, was not detected in calcium mobilisation experiments (Figure 3.22). Cells expressing the HA-CLIP-hM_3RASSL receptor responded robustly to CNO in the absence or presence of the doxycycline inducible VSV-SNAP-hM_2WT, with pEC_{50} (-Dox) = 8.4± 0.08 and pEC_{50} (+Dox) = 8.3 ± 0.06, respectively. Carbachol did not activate the hM_3RASSL receptor.

The VSV-SNAP-hM_2WT mediated $G_{i/o}$ coupling, upon stimulation with carbachol, was assessed by measuring the inhibition of adenylate cyclase activity. This was carried out by monitoring the levels of cAMP, in response to agonist (Figure 3.23). Cells expressing the VSV-SNAP-hM_2WT along with the constitutively expressed HA-CLIP-hM_3RASSL, showed a potent inhibition of the forskolin-induced levels of cAMP in the presence of varying concentrations of carbachol (pEC_{50}= 6.9 ± 0.1). The synthetic ligand CNO did not inhibit adenylate cyclase activity and in turn had no effect on cAMP levels, and thus we can conclude an inability of CNO to bind to and activate the hM_2WT receptor.

3.9 Discussion

The choice of the Flp-In™ T-REx™-293 cellular system for expressing the receptors of interest at the cell surface and further on for studying receptor oligomerisation was an important step for the initiation of the project. There are many advantages of Flp-In™ T-REx™-293 cells stably expressing the receptor(s) of interest over transiently transfected HEK 293 cells. For example, Flp-In™ T-REx™-293 cells express receptors in an isogenic and inducible manner offering consistency of expression between different experiments.

Here, cell lines able to express HA-CLIP-hM_3RASSL or VSV-SNAP-hM_2WT receptors individually, upon treatment with doxycycline, were generated and characterised. An additional cell line capable of expressing both receptors was selected from a number of clonal cell lines and was also characterised. In the selected cell line the HA-CLIP-hM_3RASSL receptor was constitutively expressed, while, expression of VSV-SNAP-hM_2WT was initiated only upon doxycycline addition. The Flp-In™ T-REx™-293 cell-based expression system assured the successful delivery of the receptors at the cell surface with the addition of the mGluR5 signal sequence to the fusion constructs. Incorporation of the SNAP and CLIP tags allowed the detection of the expressed constructs at the cell surface of live cells and constituted a key element in studying oligomeric interactions between the receptors (see Chapters 4 and 5). Despite the relatively large size of the SNAP and CLIP tags (about 20 kDa) their introduction at the N-terminal domain of the receptors did not affect receptor pharmacology and signalling, as demonstrated by the radioligand binding experiments and by the functional assays.

The chemical biology approach that involved the use of a mutated version of the hM_3 receptor, called hM_3RASSL, allowed for the differential activation of each receptor subtype. The hM_3RASSL receptor is only activated by the synthetic ligand CNO and the hM_2WT receptor is only activated by classical muscarinic agonists such as acetylcholine or carbachol. A limitation that arose from the use of hM_3RASSL receptor involved the reduced affinity of the radiolabelled ligand [^{3}H]-QNB for the receptor that led to difficulty in saturating the hM_3RASSL receptor population and thus, resulting in the inability to confirm the previously reported affinity of [^{3}H]-QNB for the hM_3RASSL.

The radioligand binding using saturating concentrations of the muscarinic radioligand [^{3}H]-QNB allowed the quantification of the total receptor expression in cells expressing each of the receptor alone and in cells co-expressing both receptors.

An important step involved the identification of the doxycycline concentration required to treat the cells able of co-expressing both receptors, which would lead to equal expression, ideally to 1:1 ratio, between the constitutively expressed HA-CLIP-hM_3RASSL and the doxycycline inducible VSV-SNAP-hM_2WT. That was achieved by determining the total expression of both receptors by using a single concentration of [^{3}H]-QNB which would theoretically be enough to saturate both the receptors.

Competition radioligand binding experiments, using concentrations of [^{3}H]-QNB sufficient to give a 90% receptor occupancy were carried out to assess the binding of ligands to the expressed receptors. Those experiments confirmed binding of CNO to the hM_3RASSL receptor and binding of carbachol to the hM_2WT receptor with nanomolar affinities. The

muscarinic antagonist atropine demonstrated the ability to bind both receptors with similar affinity.

The cell surface expression of the two co-expressed receptors in cells that co-expressed both receptors was monitored by measuring fluorescence at 620 nm, following labelling of cells with Lumi4 Tb donors. Cell surface delivery of the receptors was confirmed by epi-fluorescence microscopy.

The doxycycline concentrations used for each cell line were determined according to total and cell surface receptor expression profiles of the receptors. The aim was to identify the concentration of doxycycline at which VSV-SNAP-hM_2WT and HA-CLIP-hM_3RASSL would be expressed at similar levels in cells expressing each of the receptors. In addition, doxycycline concentration which would allow similar expression of both receptors in cells co-expressing VSV-SNAP-hM_2WT and HA-CLIP-hM_3RASSL was also identified.

Function of the expressed receptors was also assessed. HA-CLIP-hM_3RASSL-mediated activation of $G_{q/11}$ protein pathways was monitored by measuring IP1 accumulation levels and calcium ion release from the ER upon agonist stimulation. Activation of the $G_{q/11}$ pathway is traditionally measured by detection of intracellular calcium using fluorescent calcium indicator dyes. Although, monitoring calcium mobilisation is easy, calcium flux is very rapid and transient and this limits the sensitivity of the assay. An alternative approach was used that involved measurement of IP1 production. The use of lithium chloride to inhibit IP1 degradation allowed for an accurate and robust measurement of IP1 accumulation enabling the determination of potency and efficacy of CNO for HA-CLIP-hM_3RASSL. IP-One is a cell-based, htrFRET-based, competition immunoassay. The IP1 produced by cells after agonist-induced receptor activation competes with an IP1 analog coupled to d2 fluorophore (acting as energy acceptor), for binding to an anti-IP1 monoclonal antibody labelled with Eu^{2+} cryptate (acting as energy donor). The resulting signal is inversely proportional to the IP1 concentration in the cells.

Activation of $G_{i/o}$ protein is traditionally monitored by [^{35}S]-GTPγ assay. This approach only assesses direct activation of the G protein without providing information about the downstream signalling cascade. An alternative approach was utilised to monitor the agonist-mediated hM_2WT activation through $G_{i/o}$ protein coupling and the subsequent negative regulation of adenylate cyclase that results in a decrease in cAMP levels. The cAMP assay is a cell-based, htrFRET-based method for monitoring cellular cAMP levels. The assay requires pre-stimulation of adenylate cyclase with forskolin. Addition of phosphodiesterase inhibitors is also required to inhibit the degradation of cAMP to AMP.

Measurement of cAMP levels is carried out using a competition assay in which cellular cAMP competes with an introduced cAMP analog conjugated to d2 fluorophore (energy acceptor) for binding to an anti-cAMP monoclonal antibody conjugated to Eu^{2+} cryptate (energy donor). The $G_{i/o}$ mediated decrease in intracellular cAMP levels is expressed as an increase in the htrFRET signal. This assay is simple and robust, allowing the determination of agonist potency and efficacy for the receptor. In addition, the signal-to-noise ratio is greatly enhanced due to signal amplification achieved by moving down the signal transduction pathway, in contrast to the [^{35}S]-GTPγS assay that is not subjected to signal amplification.

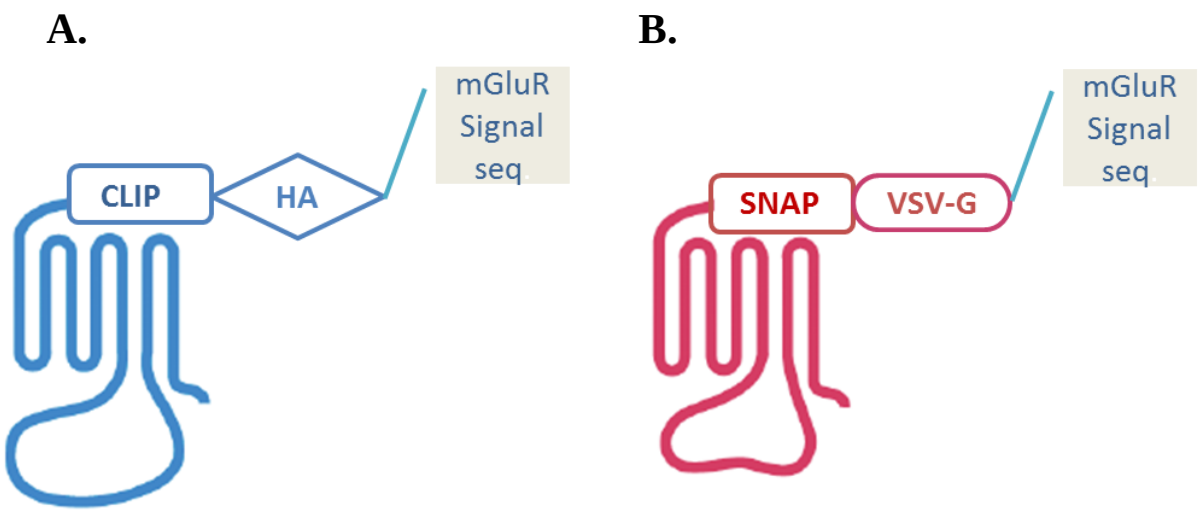

Figure 3.1 Schematic diagrams of the tagged receptors. (A) The N-terminal of the hM_3RASSL was fused with the CLIP tag and the HA epitope tag. **(B)** The VSV-G epitope tag was fused upstream the SNAP tag at the N-terminal sequence of the hM_2WT receptor. The mGluR5 signal sequence was also added to ensure cell surface delivery of the expressed receptors.

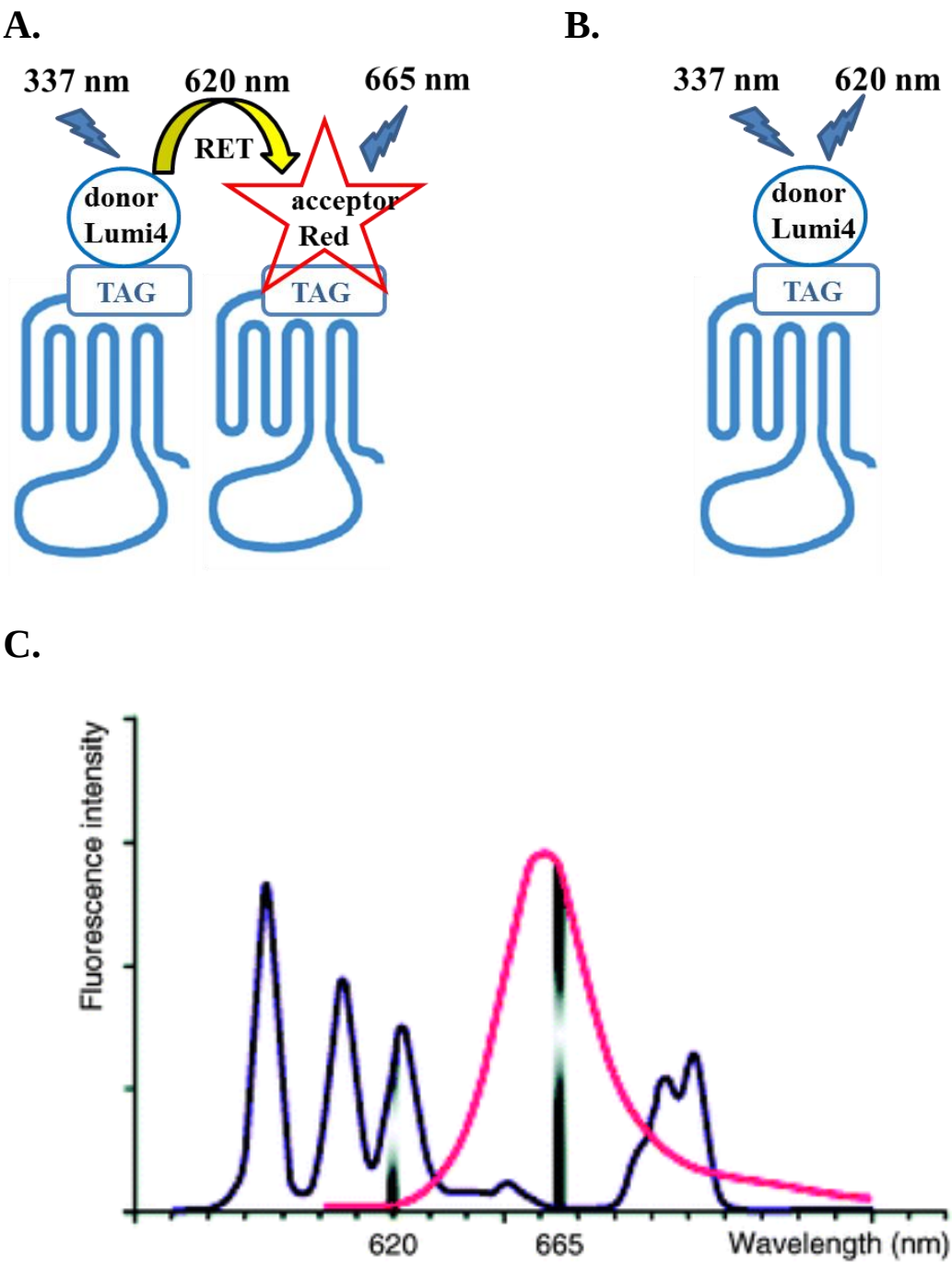

Figure 3.2 Tag-lite® technology to detect protein-protein interations by measuring htrFRET and to determine cell surface expression by measuring fluorescence at 620 nm. (A) When a terbium based htrFRET compatible donor (Lumi4) is excited at 337 nm, it emits at a higher wavelength, 620 nm, and given that the htrFRET compatible acceptor (d2-Red) is in close proximity, the emitted energy from the donor will excite the acceptor that will emit at 665 nm. This represents the FRET emission signal, and it is indicative of the close proximity of the donor/acceptor species. **(B)** In the absence of an acceptor, once the receptor labelled with a donor molecule is excited at 337 nm, energy is not trasferred but instead the donor emits at 620 nm. This fluorescence measurement can be used as a measurement of the total cell surface of expression levels of labelled receptors. **(C)** Diagram showing the spectral properties of htrFRET substrates. The emission spectra of the donor Europium cryptate (blue line) and the red acceptor (pink line) are the key elements allowing for the spectral selectivity between the acceptor fluorescence emission (665 nm) and the donor fluorescence emission (620 nm) (Diagram taken from Trinquet and Mathis, 2006).

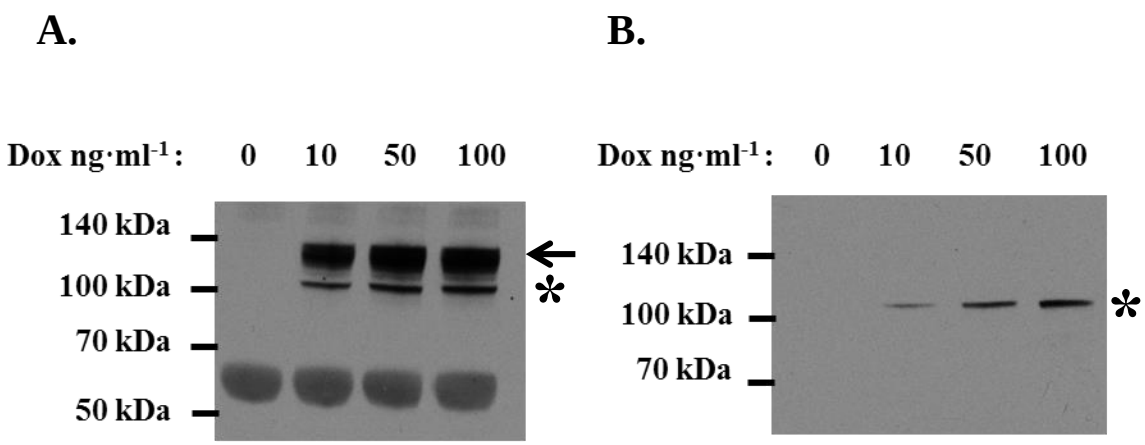

Figure 3.3 Immuno-detection of HA-CLIP-hM$_3$RASSL. Lysates were prepared from cells treated with the indicated concentrations of doxycycline to allow expression of the receptor. Samples (10µg protein per well) were immuno-blotted against **(A)** rabbit anti-SNAP antiserum and the polypeptides seen with molecular mass just below 140 kDa correspond to glycosylated HA-CLIP-hM$_3$RASSL receptor (arrow) and the polypeptides seen at 100 kDa correspond to the un-glycosylated receptor (star). The bands seen between 50-70 kDa correspond to non-specific binding. **(B)** Rat anti-HA antiserum was used against the same lysate sample preparations and the same specific polypeptide bands were detected corresponding to the un-glycosylated version of the receptor with molecular mass of 100 kDa (star). Samples prepared from cells not treated with doxycycline did not demonstrate receptor expression.

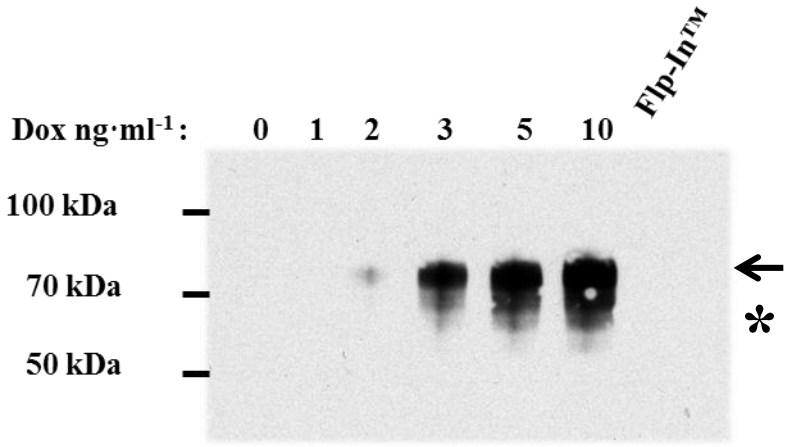

Figure 3.4 Immuno-detection of VSV-SNAP-hM$_2$WT. Lysates prepared from cells treated with the indicated concentrations of doxycycline to express the receptor were immuno-blotted against the rabbit anti-SNAP antibody, which specifically detected the VSV-SNAP-hM$_2$WT at 70 kDa (arrow). The expression of the receptor was increased with the increase in doxycycline concentration. Lysate samples prepared from cells not treated with doxycycline and those prepared from non-transfected Flp-In™ T-REx™-293 cells did not demonstrate receptor expression. The star indicates the presence of un-glucosylated receptor appearing as a lower molecular mass band. 10 μg of protein lysate were loaded per well.

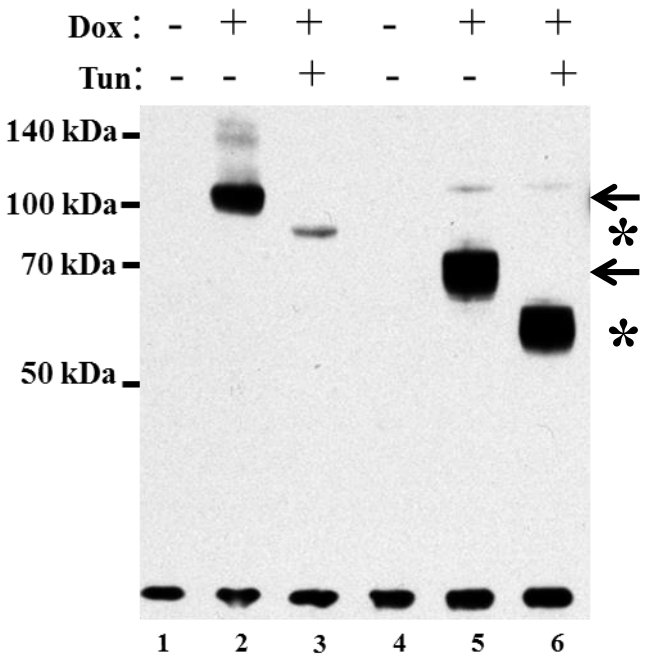

Figure 3.5 Treatment with tunicamycin inhibits receptor N-linked glycosylation. Flp-In™ T-REx™-293 cells stably expressing the HA-CLIP-hM_3RASSL (upon addition of 10 ng·ml^{-1} dox) or VSV-SNAP-hM_2WT (upon addition of 5 ng·ml^{-1} dox), were treated with 6 μM tunicamycin, for 16 hours. These cells were used to prepare the lysate samples that were subjected to SDS-PAGE and were immuno-blotted against the rabbit anti-SNAP antiserum. The glycosylated versions of HA-CLIP-hM_3RASSL (upper arrow) appeared to be of higher molecular mass compared to the non-glycosylated form of the receptor (upper star). The same pattern was seen in the glycosylated (lower arrow) and non-glycosylated (lower star) form of the VSV-SNAP-hM_2WT. Lanes 1 and 4 contain samples from non-induced Flp-In™ T-REx™-293 cells.

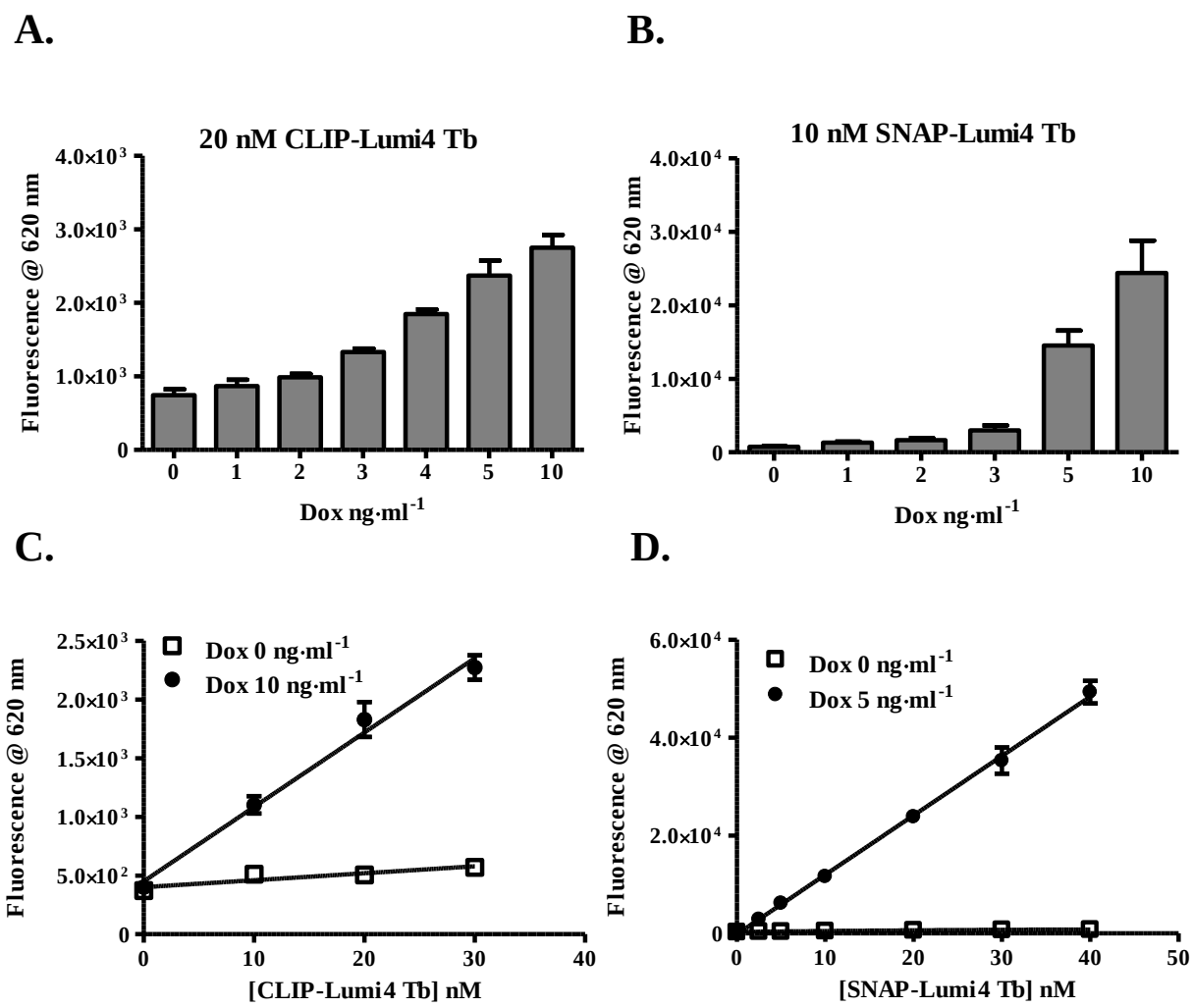

Figure 3.6 Fluorescence measurements at 620 nm showed that receptor expression at cell surface is doxycycline dependent. The expression of HA-CLIP-hM_3RASSL **(A)** was increased with the increase in doxycycline concentration, in live cells labelled with 20 nM CLIP-Lumi4 Tb. **(B)** The expression of the VSV-SNAP-hM_2WT was increased in the same fashion when cells were labelled with 10 nM SNAP-Lumi4 Tb. Increasing concentrations of the Lumi4 Tb substrates were used to label cells expressing **(C)** HA-CLIP-hM_3RASSL and **(D)** VSV-SNAP-hM_2WT, but without saturating the receptors, even at the higher concentrations used. (Data presented as Means ± Range, n=2 for A, C and D and Means ± SEM, n=3 for B, all experiments performed in triplicates).

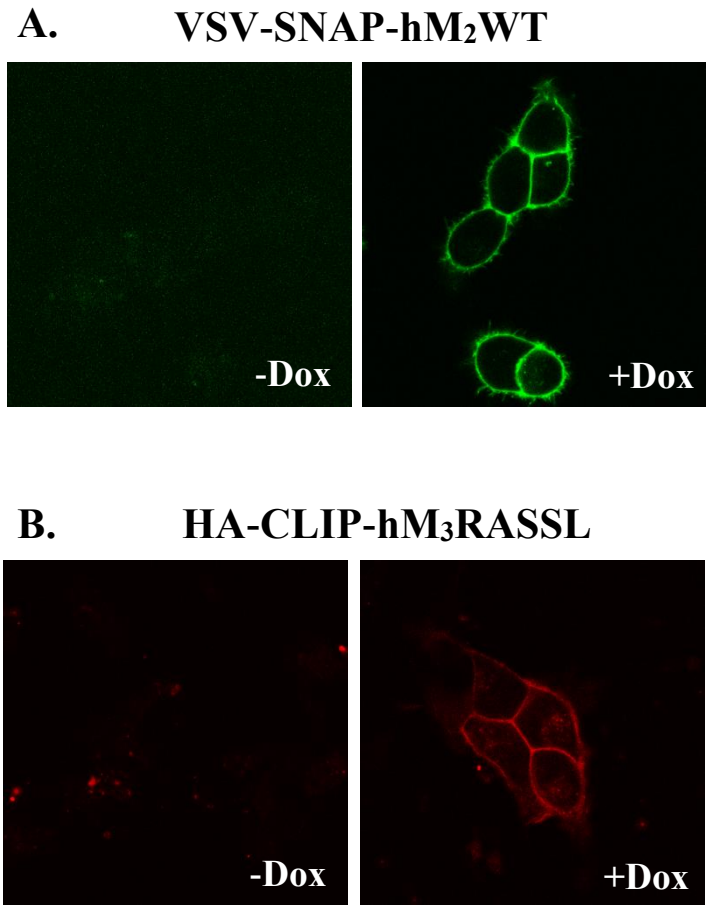

Figure 3.7 Live cell epi-fluorescence imaging demonstrates cell-surface receptor expression. Cells capable of expressing each of the receptors individually were grown on cover slips and were treated with doxycycline for 24 hours to induce receptor expression. Labelling of live cells was performed with cell impermeable fluorescent dyes that specifically recognised the SNAP or CLIP tags. **(A)** VSV-SNAP-hM_2WT labelled with 5 μM SNAP-Surface 488 (Green) and **(B)** HA-CLIP-hM_3RASSL labelled with 5 μM CLIP-Surface 547 (Red) were used for the labelling and fluorescence was monitored on an epi-fluorescence microscope. The expression of the VSV-SNAP-hM_2WT and HA-CLIP-hM_3RASSL was localised at the cell surface in cells treated with doxycycline (+Dox), but no fluorescence was seen in the cells grown in the absence of the antibiotic (-Dox).

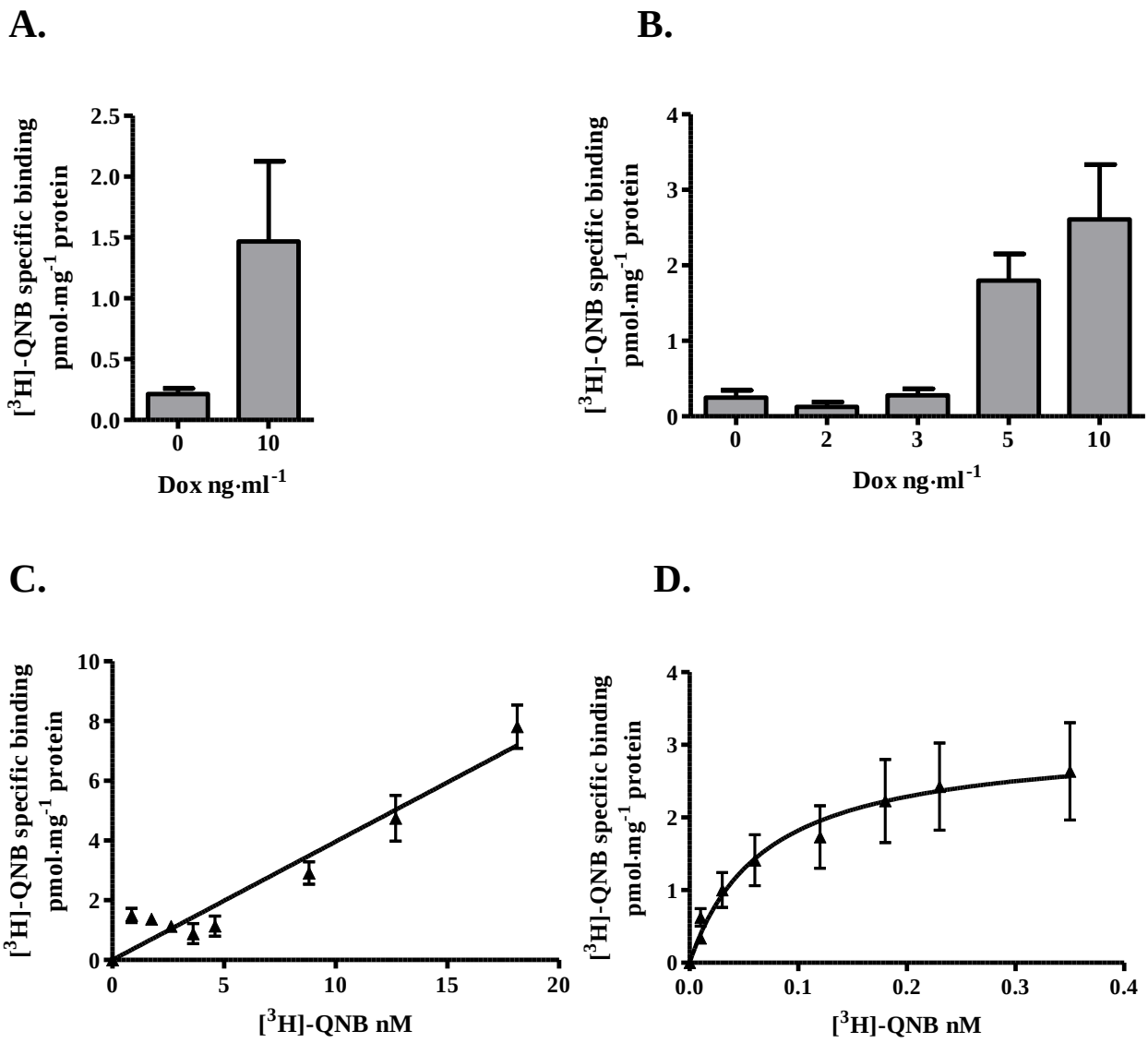

Figure 3.8 Total receptor expression determined by radioligand binding. Near saturating concentrations of [^{3}H]-QNB were used against membranes prepared from cells treated with doxycycline to induce expression of **(A)** HA-CLIP-hM$_3$RASSL (Data presented as Means ± Range, n=2, experiments in triplicates, radioligand concentration range 14-20 nM) and **(B)** VSV-SNAP-hM$_2$WT (Data presented as Means ± SEM, n=3, experiments in triplicates, radioligand concentration range 0.16-0.45 nM). **(C)** A representative example (n=1, experiment in triplicates) of an attempt to plot the saturation isotherm of the HA-CLIP-hM$_3$RASSL enriched membranes prepared from the cell line expressing the receptor upon treatment with 10 ng·ml^{-1} doxycycline failed to allow the calculation of K_D for the receptor. **(D)** Saturation isotherm of the VSV-SNAP-hM$_2$WT enriched membranes upon treatment with 5 ng·ml^{-1} doxycycline. A representative experiment is shown, as data from radioligand binding assays should not be pooled together due to differences in radioactivity added. The K_D and B_{max} were calculated from the pooled data from four independent experiments (n=4). The affinity of the radioligand as calculated by the dissociation constant (K_D= 0.32 ± 0.07 nM) and the expression levels (B_{max}= 3.07 ± 0.52 pmol·mg^{-1} protein) were determined as Means ± SEM, n=4, experiments in triplicates).

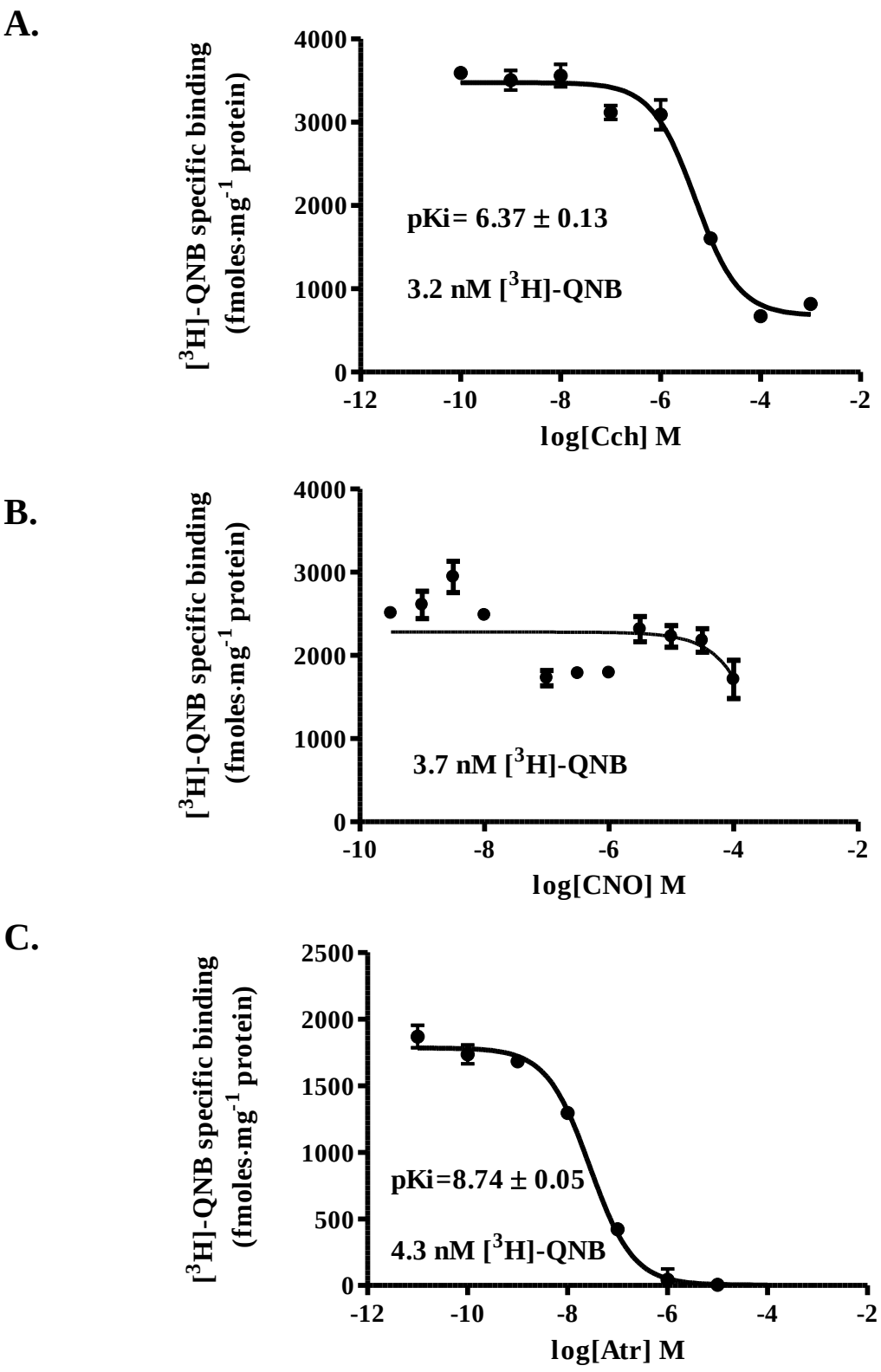

Figure 3.9 Competition binding data determined the K_i values of carbachol and atropine for the VSV-SNAP-hM_2WT receptor expressed in single stable cell line. The three figures are representative examples for the competition binding experiments carried out using 5 µg membrane protein per reaction and a set concentration of [^{3}H]-QNB, while adding increasing concentrations of the ligands Cch, CNO and atropine. **(A)** Carbachol competed with the added 3.2 nM [^{3}H]-QNB with a pK_i of 6.37 ± 0.13 calculated from this experiment. **(B)** The synthetic ligand CNO did not bind to hM_2WT receptor and therefore

could not compete with the added 3.7 nM [^{3}H]-QNB. **(C)** Atropine decreased the specific binding of the 4.3 nM [^{3}H]-QNB by displacing the radioligand with $pK_i = 8.74 \pm 0.05$. Data in the figure represent individual experiments carried out in triplicates. The pKi values shown in Table 3.1 (see page 98) represent the pooled data ffrom four different experiments and are presented as Means ± SEM, n=4 with each experiment carried out in triplicates.

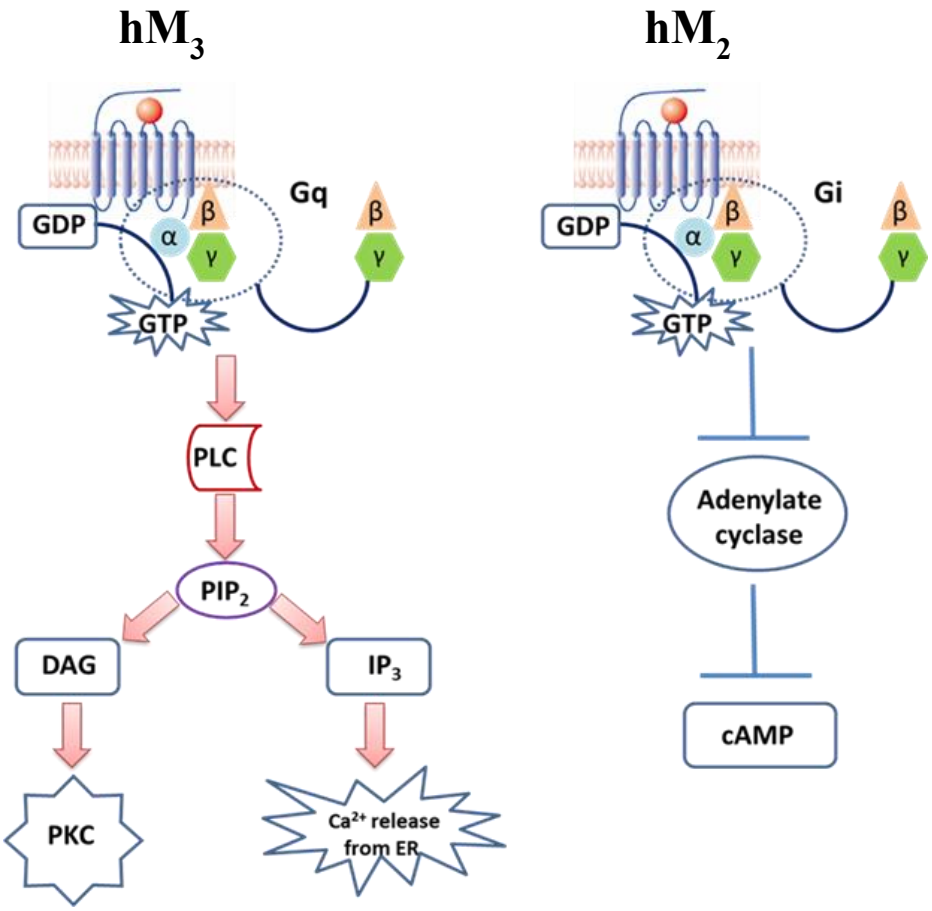

Figure 3.10 G protein coupling and signalling pathways of M_2 and M_3 receptors. M_3 receptor upon agonist mediated activation shows preference to $G_{q/11}$ coupling and this leads to activation of phospholipase Cβ (PLCβ), which in turns catalyses the formation of IP_3 and DAG)from PIP_2. IP_3 acts on IP_3 receptors in the ER and induces release of calcium ions. DAG while still bound on the membrane works to activate PKC. On the other hand, M_2 receptor, once activated by ligand, it binds to and activates the $G_{i/o}$ protein dependent pathway. $G_{i/o}$ acts by inhibiting the enzyme adenylate cyclase which catalyses the conversion of ATP to cAMP. Inhibition of adenylate cyclase, thus, leads to reduced intracellular cAMP levels.

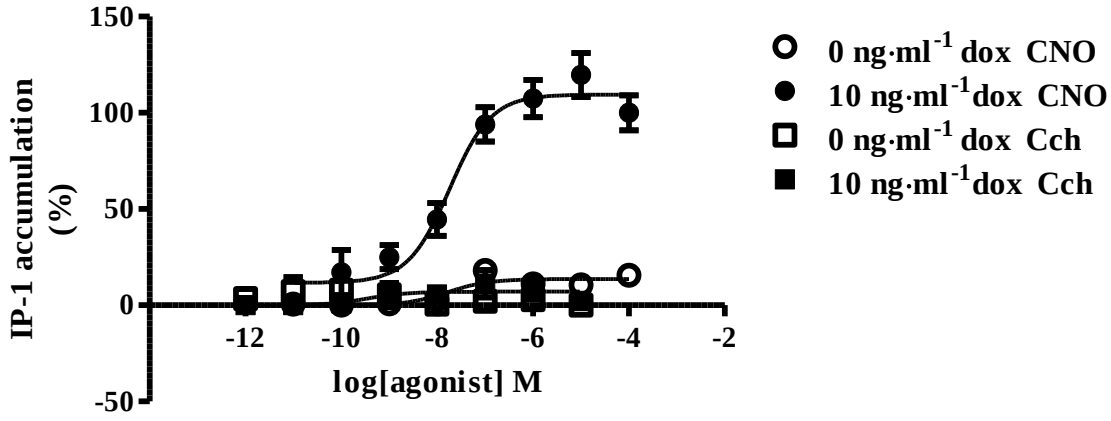

Figure 3.11 Accumulation of inositol monophosphate (IP1) upon CNO mediated activation of hM$_3$RASSL receptor. The HA-CLIP-hM$_3$RASSL receptor expressed in cells treated with 10 ng·ml^{-1} doxycycline was able to respond to the synthetic ligand CNO, which activated the receptor leading to $G_{q/11}$ protein coupling that potently resulted in the accumulation of IP1 (pEC_{50}=7.7 ± 0.18). The muscarinic agonist carbachol was unable to induce a $G_{q/11}$ coupling response, since it does not bind to the hM$_3$RASSL receptor. Data presented as Means ± SEM, n=4 and normalised to percentage, experiments carried out in triplicates.

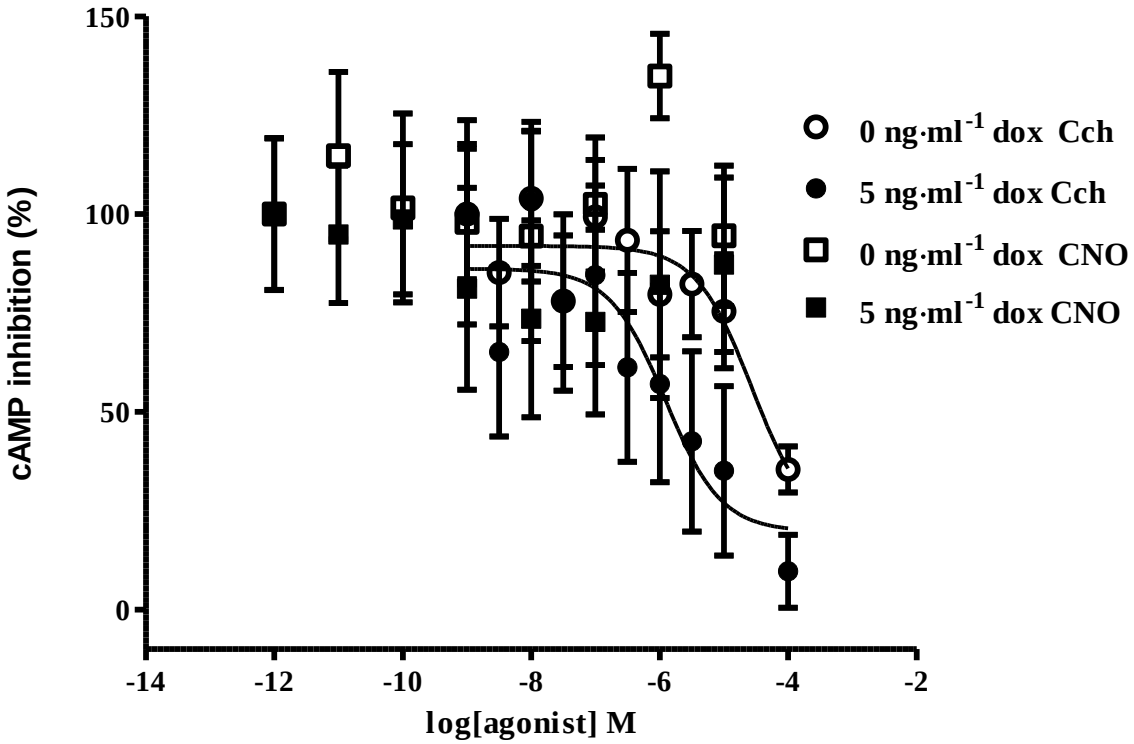

Figure 3.12 cAMP inhibition upon carbachol mediated activation of hM_2WT receptor. The VSV-SNAP-hM_2WT receptor expressed in cells treated with 5 $ng \cdot ml^{-1}$ doxycycline responded to carbachol by coupling to $G_{i/o}$ protein, and in turn inhibiting adenylate cyclase, resulting in a decrease in the cAMP levels (pEC_{50}= 5.62 ± 0.46). Cells not treated with doxycycline also showed a decrease in cAMP levels at the highest carbachol concentration, probably due to the low levels of endogenous muscarinic receptors present. VSV-SNAP-hM_2WT did not respond to the synthetic ligand CNO. Forskolin (1 μM) was used in the assay to initially activate adenylyl cyclase. IBMX at 0.5 mM was used to prevent degradation of cAMP to AMP. Data was normalised to percentage for the maximal forskolin response and presented as Means ± SEM, n=3, experiments in triplicates.

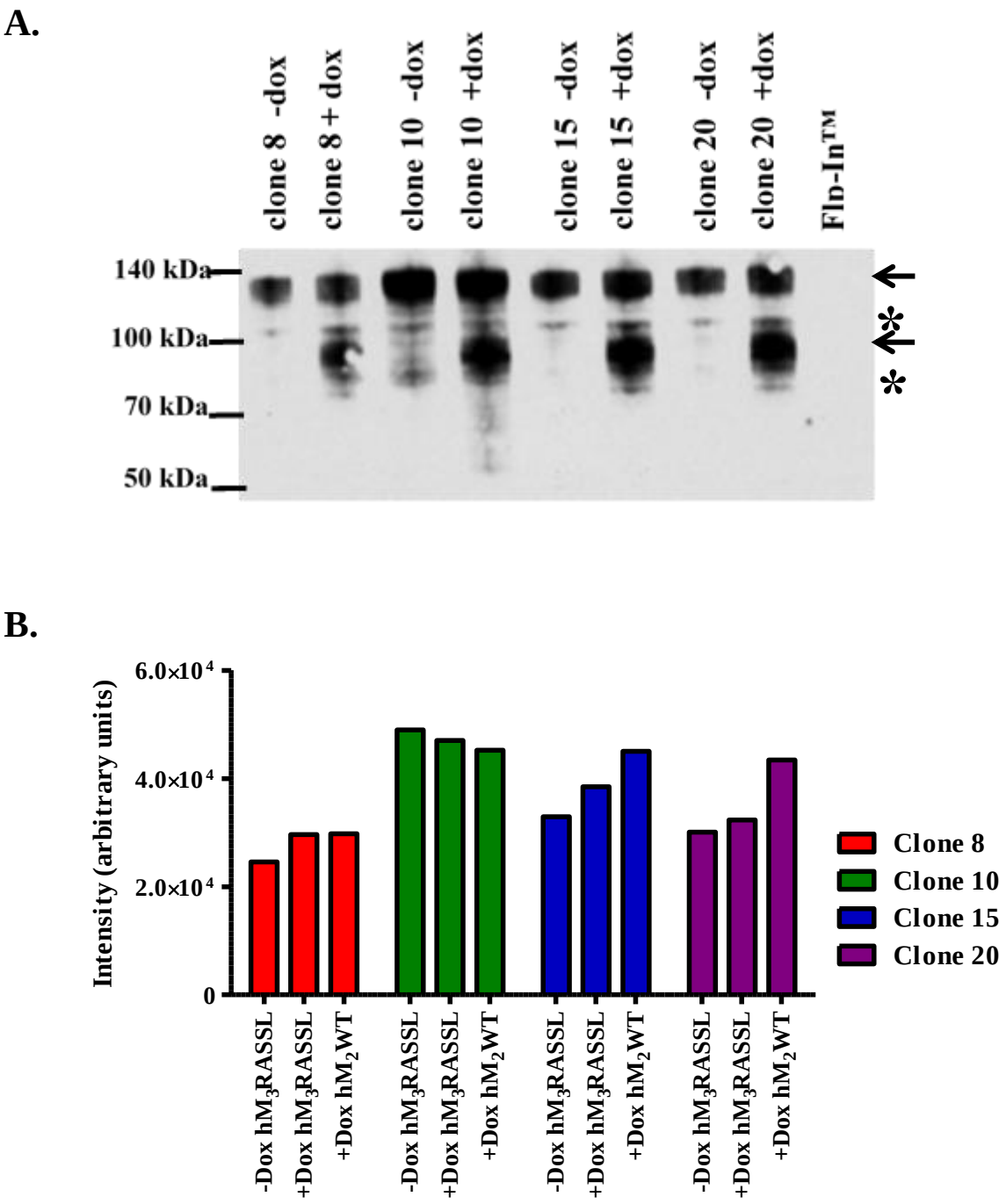

Figure 3.13 Immuno-detection of VSV-SNAP-hM$_2$WT and HA-CLIP-hM$_3$RASSL in the different clonal cell lines using anti-SNAP/CLIP antibody. (A) Lysate samples prepared from the four different clonal cell lines were immuno-blotted against the anti-SNAP/CLIP antiserum to allow detection of both receptors and to compare expression levels of receptors between the different cell lines. In the absence of doxycycline only the constitutive receptor HA-CLIP-hM$_3$RASSL was expressed with the glycosylated version seen just below 140 kDa (upper arrow) and un-glycosylated at 100 kDa (upper star). When cells were treated with 5 ng·ml^{-1} doxycycline the VSV-SNAP-hM$_2$WT expression was induced, allowing the detection of the glycosyoated polypeptide at around 80 kDa (lower arrow) and the un-glycosylated polypeptide with lower molecular mass (lower star). **(B)** The intensity of the doxycycline-induced VSV-SNAP-hM$_2$WT and the constitutively expressed HA-CLIP-hM3RASSL polypeptide bands was calculated and plotted for the different cell lines.

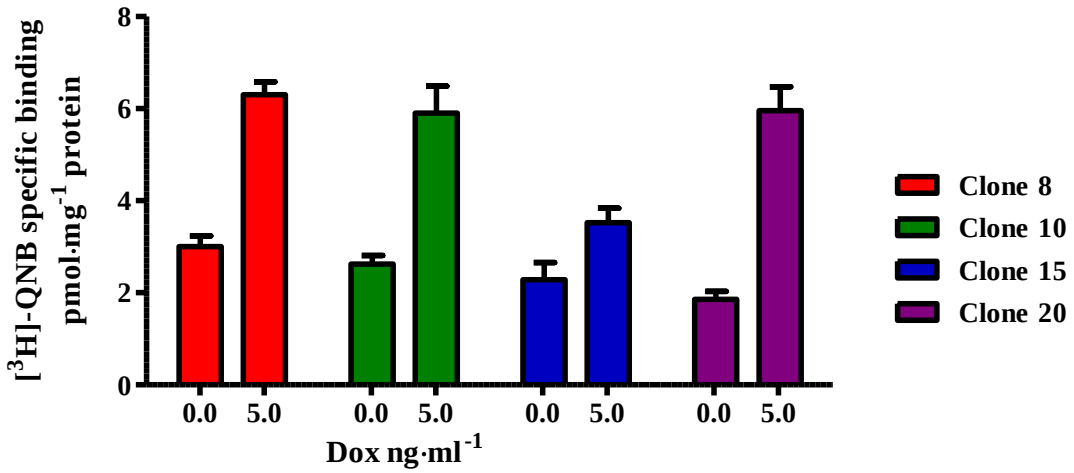

Figure 3.14 Radioligand binding to quantify total receptor expression using a single [^{3}H]-QNB concentration. Membrane preparations from the different clonal cell lines (treated or not with 5ng·ml^{-1} doxycycline for 24 hours) were used to determine specific binding of 16 nM [^{3}H]-QNB. Total receptor expression of HA-CLIP-hM_3RASSL and VSV-SNAP-hM_2WT was determined. (This is a representative experiment carried out in triplicates)

A.

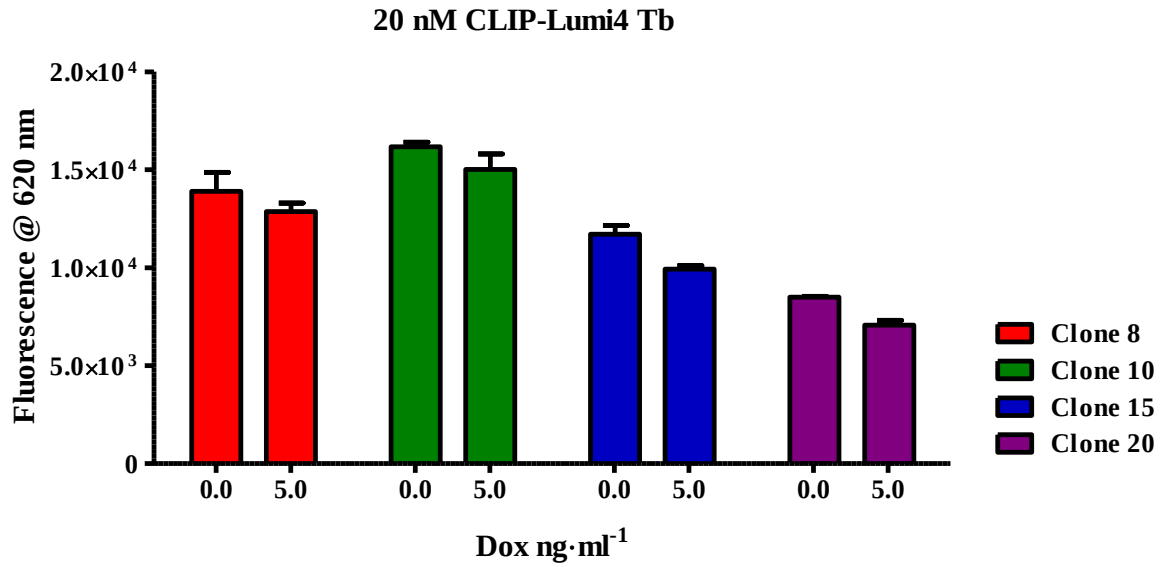

B.

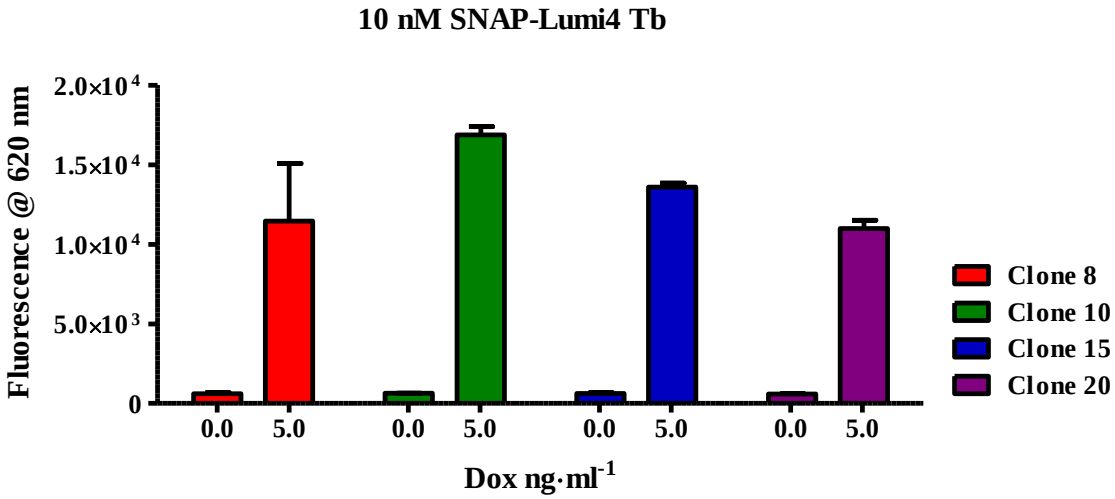

Figure 3.15 Fluorescence measurements at 620 nm detected expression of VSV-SNAP-hM$_2$WT and HA-CLIP-hM$_3$RASSL in the clonal cell lines. **(A)** 20 nM CLIP-Lumi4 Tb was used to label the different clonal cell lines in the presence and absence of doxycycline. The fluorescence readings at 620 nm corresponded to the expression levels of the CLIP-tagged constitutively expressed hM$_3$RASSL. **(B)** 10 nM SNAP-Lumi4 Tb was used to label the same clonal cell lines, in separate wells, and the increase in fluorescence measurements from the wells with cells treated with doxycycline compared to the untreated ones, corresponded to the induction of theVSV-SNAP-hM$_2$WT receptor expression. (Data presented as Means ± SEM, n=3, experiments carried out in triplicates)

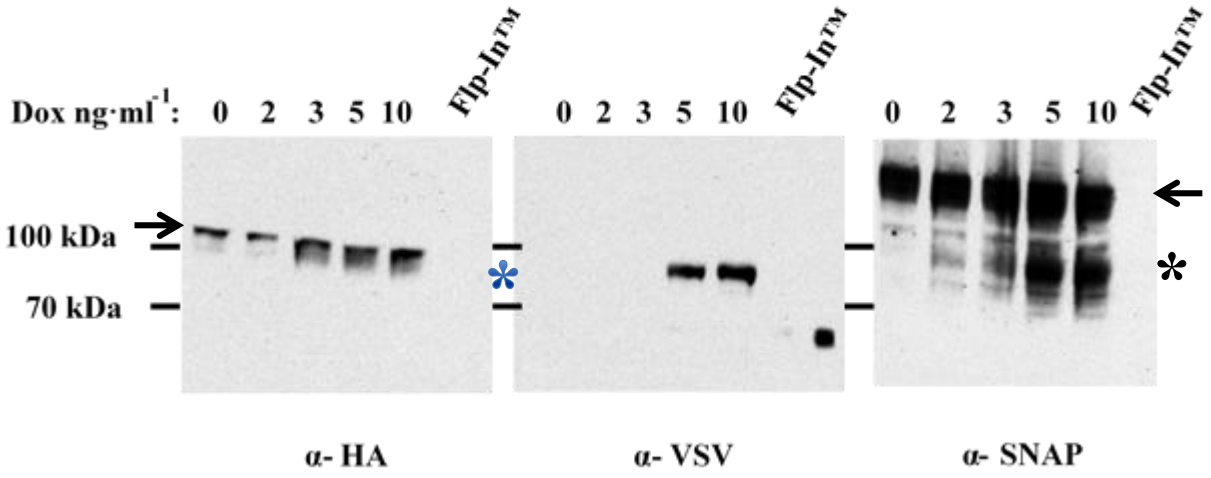

Figure 3.16 Immuno-detection of HA-CLIP-hM$_3$RASSL and VSV-SNAP-hM$_2$WT receptors in the cell line co-expressing the receptors. Lysates prepared from cells un-treated or treated with varying concentrations of doxycycline were resolved by SDS-PAGE and immuno-blotted with three different antisera. 10 µg of protein were loaded per well. The anti-HA antibody detected the non-glycosylated form of HA-CLIP-hM$_3$RASSL at around 100 kDa (arrow pointing rightwards). The anti-VSV antibody detected the non-glycosylated form of VSV-SNAP-hM$_2$WT at just above 70 kDa (blue star) and the anti-SNAP detected both the receptors, HA-CLIP-hM$_3$RASSL (arrow pointing leftwards) and VSV-SNAP-hM$_2$WT (star), in the two forms, glycosylated and non-glycosylated.

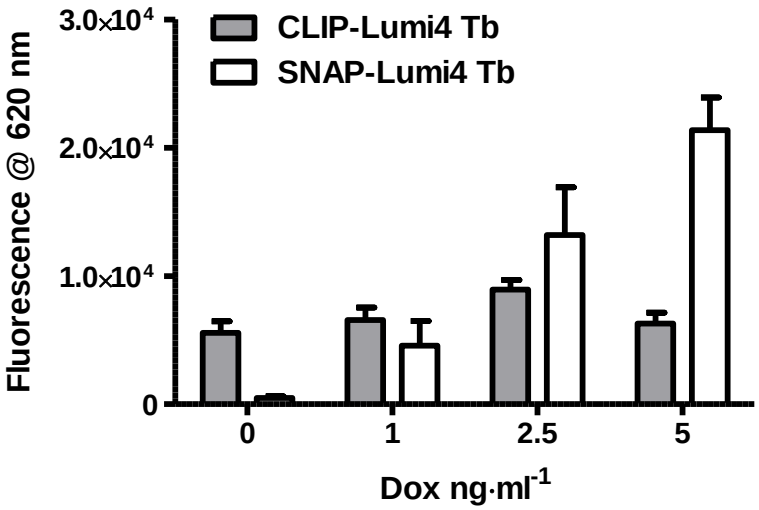

3.17 Detection of cell surface expression of HA-CLIP-hM$_3$RASSL and VSV-SNAP-hM$_2$WT receptors by monitoring fluorescence at 620 nm. Cells able of expressing both receptors were treated with varying concentrations of doxycycline and were labelled with CLIP-Lumi4 Tb (20 nM) or SNAP-Lumi4 Tb (10 nM) and fluorescence at 620 nm were measured. Data are Means ± SEM from n=8, except for 2.5 ng·ml^{-1} dox where n=6, experiments in duplicates).

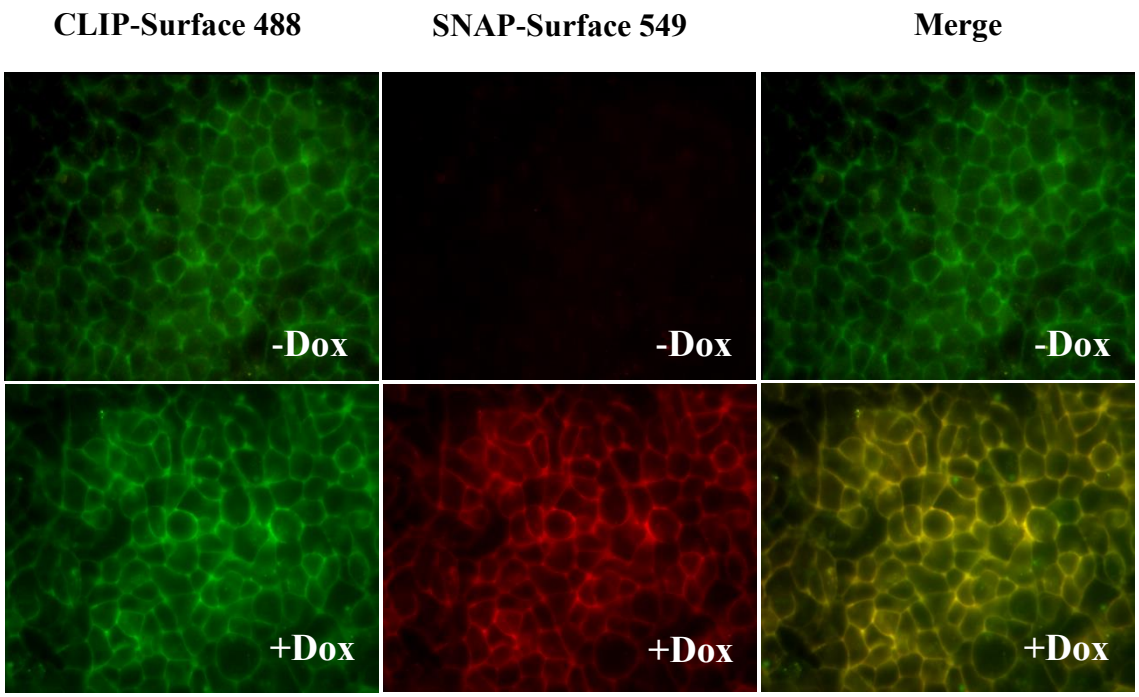

Figure 3.18 Detection of receptors at cell surface using epi-fluorescence imaging. Cells capable of expressing both receptors were grown on cover slips, in the absence or presence of 5 ng·ml^{-1} doxycycline for 24 hours. The HA-CLIP-hM_3RASSL (CLIP-Surface 488, Green) was expressed in cells untreated or treated with doxycycline. The VSV-SNAP-hM_2WT (SNAP-Surface 549, Red) expression was initiated only upon doxycycline addition. When both receptors were co-expressed the receptors displayed co-localisation at the cells surface as the merging of the two channels suggest.

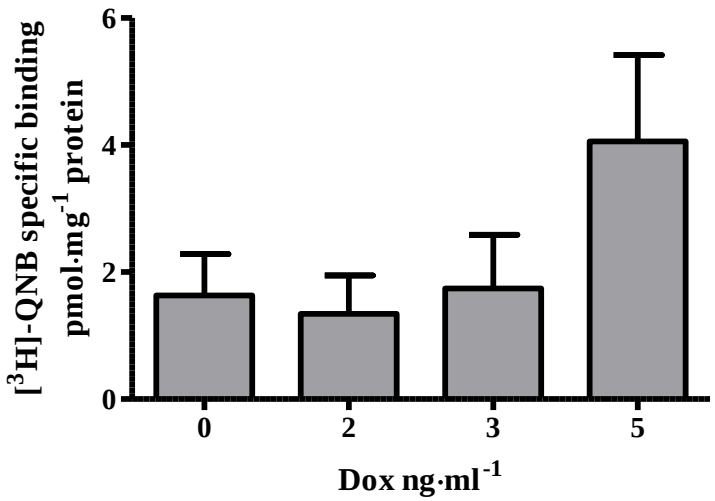

Figure 3.19 Quantification of total HA-CLIP-hM$_3$RASSL expression by radioligand binding. Membranes prepared cells capable of expressing both receptors were treated with various concentrations of doxycycline and were employed in determining the specific binding to a single saturating concentration of the muscarinic radioligand [^{3}H]-QNB (radioligand range used was between 16 nM-21.6 nM. Data are Means ± SEM for n=4, experiments in triplicates).

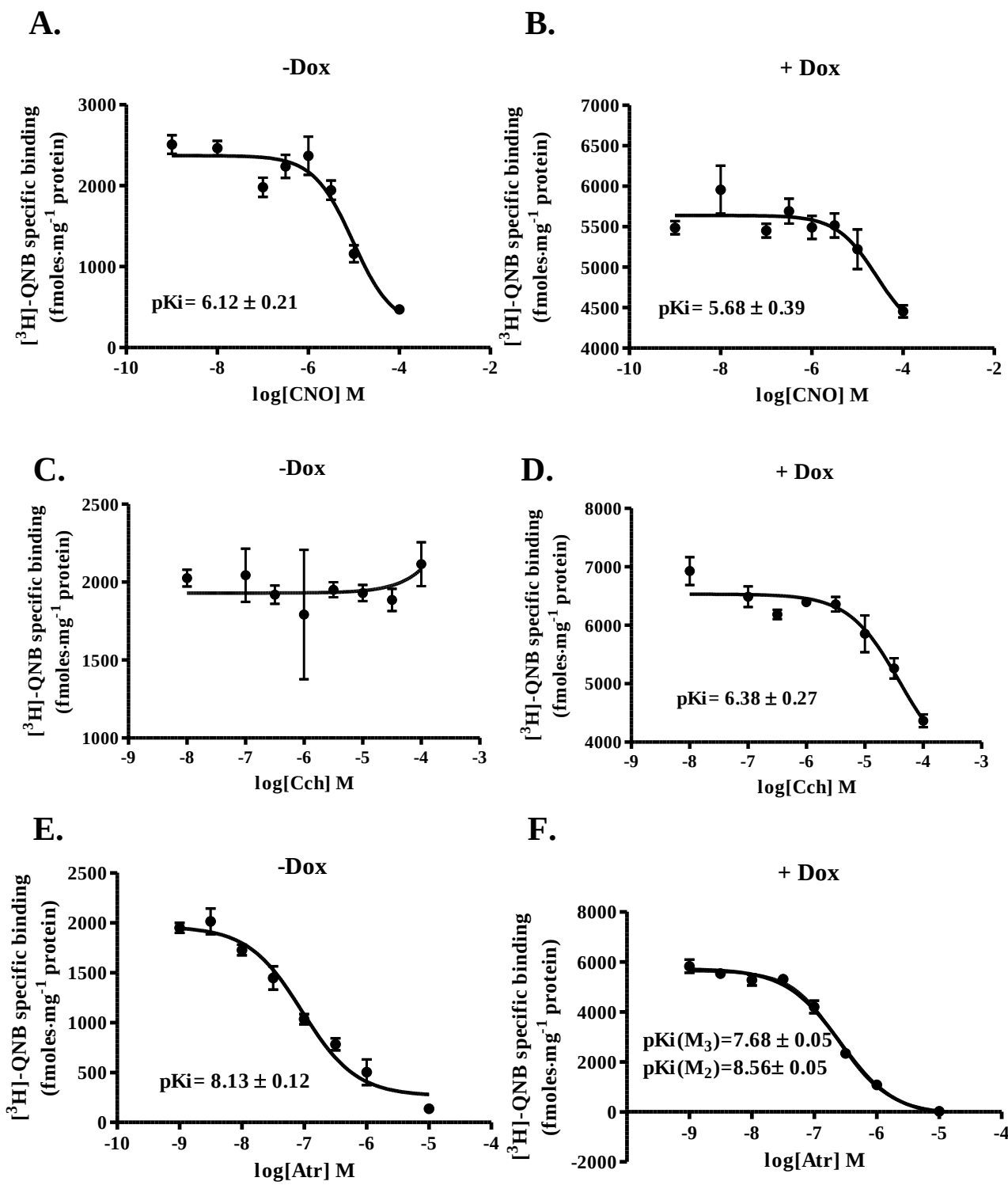

Figure 3.20 Competition binding determined the affinity of ligands for the receptors. Data shown in A-F are individual experiments using 5 µg protein per reaction and a single near saturating concentration of [^{3}H]-QNB (28.1 nM). Ligands were added to the reactions at increasing concentrations in samples prepared from cells either treated or not with 5 ng·ml^{-1} doxycycline. In samples where only the HA-CLIP-hM$_3$RASSL is expressed **(A)** CNO successfully out-competed the radioligand with pK_i = 6.12 ± 0.21. **(B)** In the presence of both receptors CNO showed a slightly different affinity with pK_i = 5.68 ± 0.39. (C) Carbachol did not bind to the HA-CLIP-hM$_3$RASSL receptor, **(D)** but only to the doxycycline inducedVSV-SNAP-hM$_2$WT with pK_i = 6.38 ± 0.27. **(E)** The antagonist

atropine could bind to the HA-CLIP-hM_3RASSL when expressed alone with a high affinity (pK_i = 8.13 ± 0.12) and **(F)** atropine also demonstrated binding to both receptors when they were co-expressed. This led to the observation of two different affinity measurements for atropine; one that corresponded to the M_3 (pK_i =7.68 ± 0.05) and a second that corresponded to the M_2 (pK_i = 8.56 ±0.05). The data from the competition binding assays were analysed using a two-site fit analysis for samples that contained both receptor populations and one-site fit analysis for the samples with only one receptor on Graph Pad software.

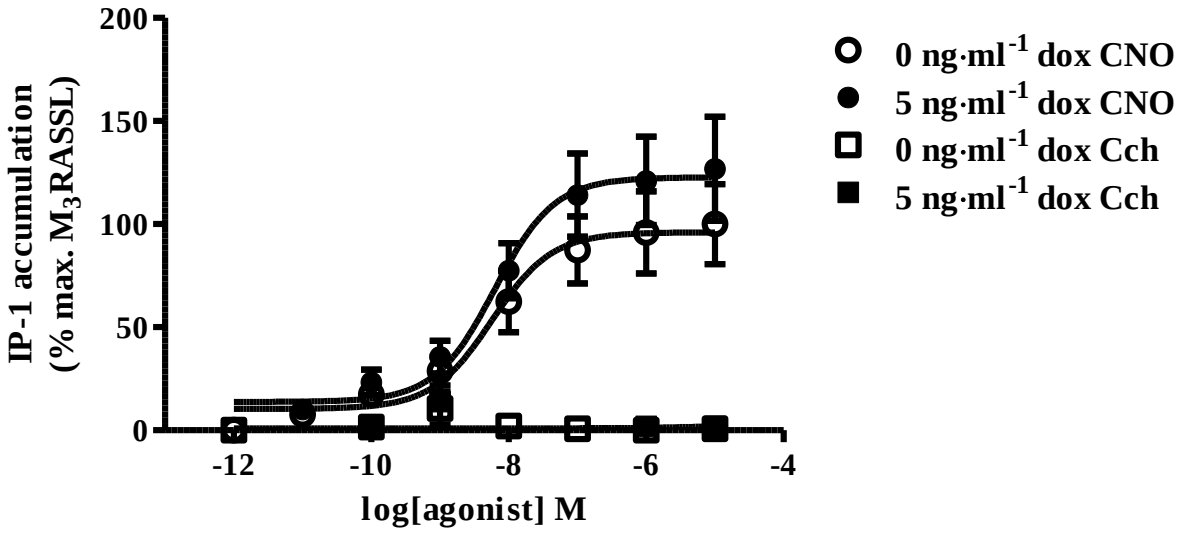

Figure 3.21 CNO-mediated hM$_3$RASSL activation results in IP1 accumulation in cells co-expressing HA-CLIP-hM$_3$RASSL and VSV-SNAP-hM$_2$WT. Cells treated with doxycycline to allow co-expression of VSV-SNAP-hM$_2$WT alongside the constitutive HA-CLIP-hM$_3$RASSL were employed to measure the levels of IP1. The synthetic ligand CNO potently increased the IP1 levels in the absence of VSV-SNAP-hM$_2$WT (0 ng·ml^{-1} dox) with pEC$_{50}$ (-dox) = 8.2 ± 0.3. The potency of CNO remained unaltered in the presence of both receptors (+5 ng·ml^{-1} dox) with pEC$_{50}$= 8.2± 0.27. There was a trend towards an increase in the efficacy of CNO but it was not statistically significant (P>0.5). Data presented as Means ± SEM, n=5, experiments in triplicates. P value was obtained by comparing the –dox to the +dox data upon treatment with CNO, using a two-paired t-test.

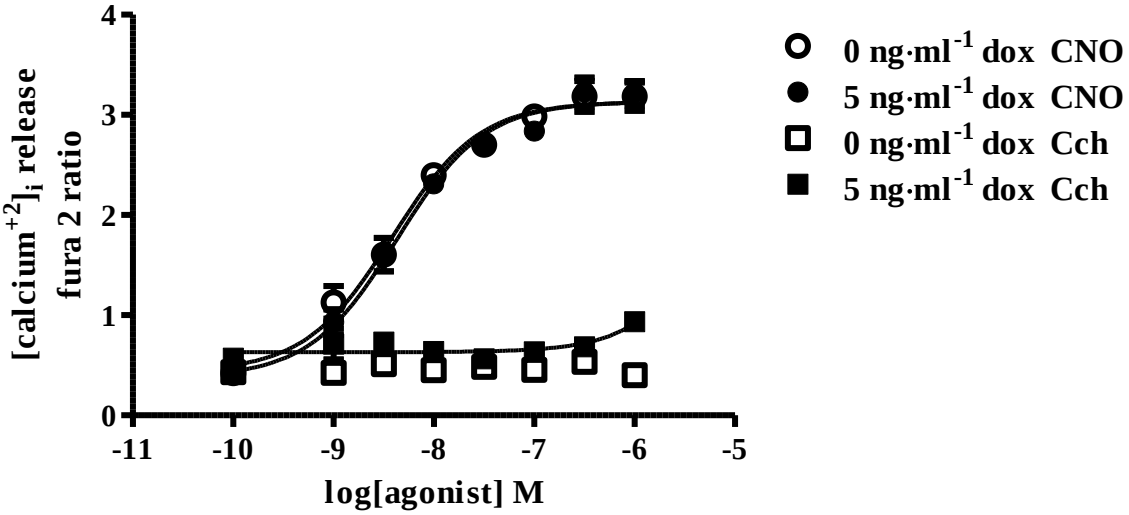

Figure 3.22 Intracellular calcium ion mobilisation in response to CNO-mediated activation of HA-CLIP-hM$_3$RASSL. Cells seeded in 96 well plates were treated or not with doxycycline to allow co-expression of VSV-SNAP-hM$_2$WT and HA-CLIP-hM$_3$RASSL. Cells were then labelled with 3μM fura 2 AM before addition of ligands and intracellular calcium concentration was measured after treatment with varying concentrations of carbachol (Cch) or CNO. The CNO mediated activation of HA-CLIP-hM$_3$RASSL receptor was responsible for the potent release of calcium ions (pEC$_{50}$ = 8.4± 0.08). The presence of VSV-SNAP-hM$_2$WT (+dox) did not affect neither the efficacy nor the potency of CNO in inducing calcium release through G$_{q/11}$ coupling activation (pEC$_{50}$ = 8.3 ± 0.06). Data presented as Means ± Range, n=2, experiments in triplicates.

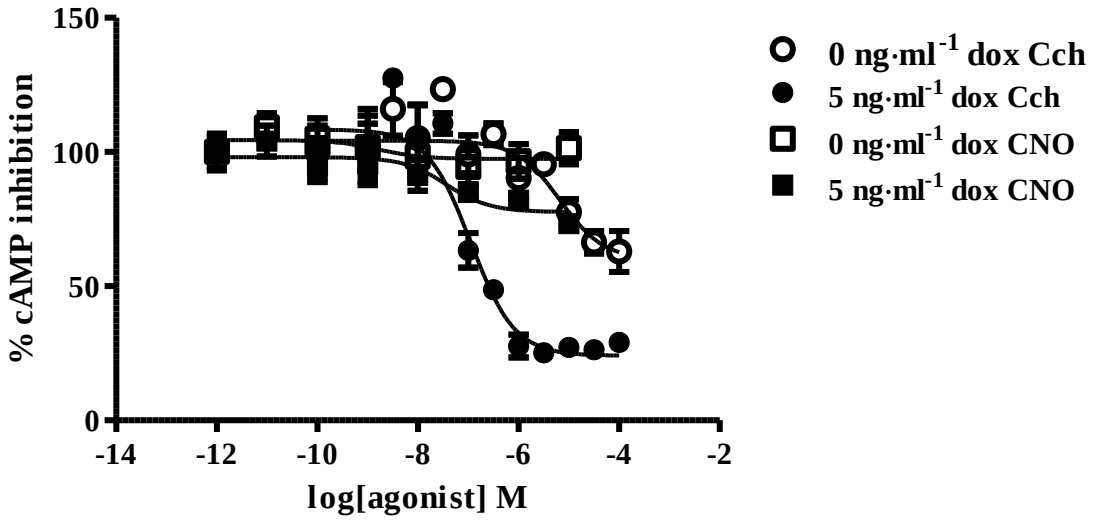

Figure 3.23 Reduction of cellular cAMP levels in response to carbachol-mediated activation of VSV-SNAP-hM$_2$WT through G$_{i/o}$ coupling. Cells able of co-expressing both receptors were treated or not with 5 ng·ml^{-1} doxycycline and were employed to measure the carbachol-mediated inhibition of forskolin-induced activation of adenylyl cyclase. Carbachol was able to potently (pEC$_{50}$= 6.9 ± 0.1, Means ± SEM, n=3, experiments in triplicates) inhibit the activation of adenylyl cyclase and thus, reduce the levels of cAMP in cells treated with 5 ng·ml^{-1} doxycycline. Carbachol showed no effect in the absence of the VSV-SNAP-hM$_2$WT receptor. No adenylyl cyclase inhibition was detected in response to CNO treatment and thus levels of cAMP were maintained unaltered.

Chapter 4

Analysis of hM_2WT and hM_3RASSL receptor complexes at the surface of live cells

4.1 Introduction

Class A GPCRs, in their monomeric form, may bind to and activate their corresponding G proteins (Whorton *et al.,* 2008), but there is accumulation of evidence suggesting that they may also exist and function as oligomers (Milligan, 2009; Javitch, 2004). There is growing evidence that supports the important role of oligomerisation in signalling, pharmacology and function of class A GPCRs (Milligan, 2013; Milligan *et al.,* 2004; Angers *et al.,* 2002; Ferre *et al.,* 2014; Herrick-Davis, 2013).

M_2 and M_3 muscarinic acetylcholine receptors, members of class A family of GPCRs, are co-expressed and they demonstrate a pattern of co-localisation at the cell membrane of native tissues of the central nervous system, such as striatum, hippocampus, cerebral cortex, thalamus, hypothalamus and cranial nerve nuclei (Pan *et al.,* 2008; Levey *et al.,* 1991; Wess, 2004), supporting the role of muscarinic receptors in cognition, memory and learning. M_2 and M_3 receptor subtypes are also co-expressed in the smooth muscle of the intestine, ileum, airway, iris, and bladder (Eglen *et al.,* 1994; Uchiyama and Chess-Williams, 2004; Wess, 2004), a fact that implies an important role of muscarinic receptors in the contraction of smooth muscle (Eglen *et al.,* 1996; Caulfield, 1993). M_2 receptor is also expressed in the heart, where it appears to play a role in controlling cardiac myocyte contraction (Caulfield, 1993; Wess, 2004). Saliva secretion (Matsui *et al.,* 2000) and insulin secretion (Gautam *et al.,* 2007) are functions that are thought to be mediated by the M_3 receptor. Any possible interactions between the two muscarinic subtypes, M_2 and M_3, could be of therapeutic importance. Therefore, a more thorough insight into the heteromerisation between M_2 and M_3 could be useful in terms of drug discovery. The interaction between M_2 and M_3 receptors has been demonstrated previously, by saturation BRET experiments, in live transfected HEK 293 cells (Goin and Nathanson, 2006). The analysis of $BRET_{50}$ values, obtained from BRET saturation curves, also showed the existence of high affinity homomers of M_1, M_2 and M_3 as well as a population of M_1-M_2, M_1-M_3 heteromers alongside with the M_2-M_3 heteromers, in the same cells (Goin and Nathanson, 2006). Other examples of muscarinic receptors in dimeric, or even higher oligomeric, forms have been reported (Hu *et al.,* 2013, Alvarez-Curto *et al.,* 2010, Patowary *et al.,* 2013, Herrick-Davis *et al.,* 2015). The existence of predominant tetrameric rhomboidal complex structures of the M_3 receptor has been demonstrated by spectrally resolved FRET (Patowary *et al.,* 2013). The oligomeric profile of the M_3 receptor was also supported by BRET data and structural /modelling studies (McMillin *et al.,* 2011), by disulphide cross-linking (Hu *et al.,* 2013), as well as by FRET assays (Alvarez-Curto *et al.,* 2010). The M_2 receptor was also shown to predominantly exist in tetrameric form,

determined by a quantitative FRET assessment (Pisterzi *et al.*, 2010). The existence of the tetrameric form of M_2 was supported by radioligand binding experiments, using reconstituted monomeric and tetrameric forms of the receptor (Redka *et al.*, 2014).

The focus of this chapter was to study the oligomerisation of muscarinic acetylcholine M_2 and M_3 receptors. More specifically, the interest was focused on using htrFRET to detect the formation of M_2 and M_3 homomers, in live cells, expressing one of the receptors, in a doxycycline inducible manner, and the co-existence of receptor homomers with M_2-M_3 heteromers, in cells expressing both the receptors. The co-existence of M_2 and M_3 heteromers alongside with the corresponding homomers has been demonstrated here, using htrFRET in combination with Tag-lite® technology, involving the SNAP/CLIP specific labelling of the N-terminally tagged receptors.

The lack of subtype selective ligands, due to the high sequence homology in the orthosteric binding pocket of muscarinic receptors, directed my approach towards the use of a genetically engineered version of M_3 receptor, which is unresponsive to the classical orthosteric muscarinic agonists, but is activated by the synthetic ligand CNO (Armbruster *et al.*, 2007; Alvarez-Curto *et al.*, 2011). The use of the hM_3RASSL allowed the differential activation of the two receptors in question, hM_2WT and hM_3RASSL, when these were co-expressed at the surface of the same cells. In addition, the simultaneous activation of the two receptors enabled the assessment of the possible effects of oligomerisation on receptor signalling, via monitoring the inhibition of cyclic adenosine monophosphate (cAMP) levels (due to G_i coupling of M_2) and the accumulation of inositol monophosphates (IP-1) levels, as well as the mobilisation of intracellular calcium ions (due to G_q coupling of M_3).

Aims of this chapter

- Detection of VSV-SNAP-hM_2WT and HA-CLIP-hM_3RASSL homomers at the surface of cells expressing each of the receptors, by htrFRET.
- Simultaneous detection of homomers and heteromers of VSV-SNAP-hM_2WT and HA-CLIP-hM_3RASSL receptors, in cells expressing both the receptors, by htrFRET.
- Evidence of oligomerisation by biochemical approaches such as Blue Native PAGE and co-immunoprecipitation.
- Consequences of receptor oligomerisation on receptor pharmacology and function.

4.2 Homomers of hM$_2$WT and hM$_3$RASSL receptors at the surface of live cells

Flp-In™ T-REx™-293 stable cell lines expressing either VSV-SNAP-hM$_2$WT or HA-CLIP-hM$_3$RASSL were characterised and the doxycycline concentrations at which the receptor expression levels were similar between the different cell lines were determined (see Table 4.1 summarising the doxycycline concentrations derived from results in Chapter 3). htrFRET experiments were performed that allowed the detection of VSV-SNAP-hM$_2$WT and HA-CLIP-hM$_3$RASSL homomers.

Cell line expressing:	**[Doxycycline] (ng·ml^{-1})**
VSV-SNAP-hM$_2$WT	**5**
HA-CLIP-hM$_3$RASSL	**10**
VSV-SNAP-hM$_2$WT(i)/ HA-CLIP-hM$_3$RASSL(c)	**5**

Table 4.1 Doxycycline concentrations used to induce receptor expression in the different cell lines. 5 ng·ml^{-1} doxycycline was added to one cell line to induce VSV-SNAP-hM$_2$WT expression. Similar levels of HA-CLIP-hM$_3$RASL expression were achieved with 10 ng·ml^{-1} doxycycline in the second cell line. The concentration of doxycycline that allowed the co-expression of the inducible VSV-SNAP-hM$_2$WT and the constitutively expressed HA-CLIP-hM$_3$RASSL, in similar levels, was 5 ng·ml^{-1}. Doxycycline concentrations were determined by radioligand binding, fluorescence measurements and immuno-detection of the receptors as described in Chapter 3.

Labelling of live cells with cell impermeant htrFRET compatible substrate pairs (donor and acceptor) was carried out and the protein-protein interactions were determined by monitoring the FRET signal at 665 nm. The combination of htrFRET donor and acceptor pair was selected according to the tagged-receptor fusion being expressed from each cell type. A schematic representation explaining the labelling approach and detection of the 665 nm signal is shown in Figure 4.1. The detection of oligomers was carried out by monitoring the FRET signal at 665 nm, upon excitation of the donor at 337 nm. The terbium cryptate donors, upon excitation at 337 nm, emit at 620 nm which can in turn excite the red acceptor species and these subsequently emit at 665 nm.

The cells inducibly expressing VSV-SNAP-hM_2WT upon treatment with 5 ng·ml^{-1} doxycycline, were labelled with 5 nM SNAP-Lumi4 Tb (donor) and varying concentrations of SNAP-Red (acceptor) and homomers of VSV-SNAP-hM2WT were detected (Figure 4.2). The cells inducibly expressing HA-CLIP-hM_3RASSL upon treatment with 10 ng·ml^{-1} doxycycline were labelled with 10 nM CLIP-Lumi4 Tb (donor) and varying concentrations of CLIP-Red (acceptor) and homomers were detected (Figure 4.3).

When examining homomer formation, the substrates used for the labelling bind to the same receptor species, therefore, when analysing the FRET results, the data at 665 nm were plotted against a logarithmic scale of acceptor concentration, to allow fitting the data to a Gaussian equation and the generation of a bell-shaped curve. The position of the peak of the bell shaped curve corresponded to the optimum donor/acceptor ratio that allowed the detection of the homomers. Theoretically, the peak of the curve indicates that 50 % of the labelled cell surface receptors were labelled with the donor species and 50 % were labelled with the acceptor species.

Homomers were not detected at the surface of cells that were not treated with doxycycline i.e. when receptors were not expressed. The minus doxycycline control was a very helpful way of determining homomer formation and allowing the determination of specific FRET signal, by subtracting the non- specific signal (-Dox) from the total FRET signal (+Dox). In order to determine the bystander FRET a different approach was followed that involved the use of a cell line inducibly expressing the VSV-SNAP-CD86 receptor. The use of the cell surface receptor CD86 that is naturally expressed on antigen presenting cells and only exists in a monomeric state (James *et al.*, 2007; Girard *et al.*, 2014) was found very useful as a negative control for oligomerisation, despite the structural differences compared to 7 TM receptors such as muscarinic acetylcholine receptors. A cell line able to inducibly express a modified version of the CD86 receptor was employed in htrFRET experiments. The VSV-SNAP-CD86 receptor fusion was used alongside the VSV-SNAP-hM_2WT to allow me to distinguish between real homomeric VSV-SNAP-hM_2WT interactions and bystander FRET signal obtained from the strictly monomeric CD86 receptor (Figure 4.4). The VSV-SNAP-CD86 receptor was expressed at the cell surface when cells were treated with doxycycline. The total expression profile of the VSV-SNAP-CD86 was demonstrated by subjecting lysates prepared from cells treated with varying doxycycline concentrations, by SDS-PAGE analysis and Western blot using an anti-SNAP antiserum (4.4 A). Cell surface expression of the receptor was measured by monitoring the fluorescence at 620 nm, of doxycycline treated cells, labelled with 5 nM of SNAP-Lumi4 Tb (Figure 4.4 B). A

comparison between the expression profiles of the VSV-SNAP-hM_2WT and VSV-SNAP-CD86 receptors is shown in Figure 4.4 C, demonstrating the concentration of doxycycline used to achieve similar expression levels between the two receptors in the two cell lines i.e. 2 ng·ml^{-1} doxycycline led to expression of CD86 at levels similar to hM_2WT when the VSV-SNAP-hM_2WT expressing cell line was treated with 5 ng·ml^{-1} doxycycline. Achieving similar expression levels was essential in comparing the htrFRET at 665 nm results obtained from the two receptors i.e. their ability to form oligomers (Figure 4.4 D). The two cell lines, expressing each of the receptors, were labelled with the same combination of htrFRET compatible donor/acceptor pair e.g. 5 nM SNAP-Lumi4 Tb and varying concentrations of SNAP-Red. The VSV-SNAP-CD86 did not seem to generate a bell-shaped curve comparable to that obtained from VSV-SNAP-hM_2WT. This suggested the lack of oligomer formation in CD86 receptor, as expected, and confirmed the bell shaped curve obtained from hM_2WT was not due to artefacts or random collision, but due to actual receptor oligomerisation.

4.3 Co-existence of homomers and heteromers of hM_2 and hM_3 when both receptors are co-expressed

Having established the formation of receptor homomers in Flp-In™ T-REx™-293 cell lines expressing each receptor individually, an important question to be addressed was whether the homomers of hM_2 and hM_3 receptors co-existed with the hM_2/hM_3 heteromers, when the two receptors were co-expressed. The htrFRET approach was employed, using cells able to express both receptors. Characterisation of this cell line enabled the determination of the doxycycline concentration (5 ng·ml^{-1}) that allowed the expression of both the inducibly expressed VSV-SNAP-hM_2WT receptor with the constitutive expressed HA-CLIP-hM_3RASSL in amounts relatively close to the physiological ones (see Chapter 3, section 3.3).

To assess the formation of homomers of VSV-SNAP-hM_2WT and HA-CLIP-hM_3RASSL at the surface of this cell line, cells were either co-labelled with 5 nM SNAP-Lumi4 Tb and varying concentrations of SNAP-Red (Figure 4.5 A) or 10 nM CLIP-Lumi4 Tb and varying concentrations of CLIP-Red (Figure 4.5 B), respectively. These cells, labelled with SNAP-Lumi4 Tb/SNAP-Red in the absence of doxycycline treatment did not demonstrate formation of hM_2WT homomers, which were only observed after treatment with 5 ng·ml^{-1} dox, detected as htrFRET signal at 665 nm (Figure 4.5 A). On the other hand, when the same cells were used for detection of hM_3RASSL homomers, following CLIP-Lumi4 Tb/

CLIP-Red co-labelling, without treatment with doxycycline, hM_3RASSL homomeric interactions were detected, and were maintained unchanged, in cells treated with doxycycline (Figure 4.5 B). Neither the signal at 665 nm nor the shape of the curve had changed, suggesting that the HA-CLIP-hM_3RASSL homomers remained unaffected by the presence of the inducible receptor VSV-SNAP-hM_2WT homomers.

To allow detection of heteromers between the VSV-SNAP-hM_2WT and HA-CLIP-hM_3RASSL, when both receptors were co-expressed at the surface of the same cells upon addition of doxycycline, a different combination of the htrFRET labelling donor/acceptor substrates was utilised (Figure 4.6). SNAP-Lumi4 Tb was used as a donor and CLIP-Red was used as an acceptor. An increase in fluorescence emission at 665 nm was detected, consistent with the presence of hM_2WT/hM_3RASSL heteromers. Equivalent results were obtained when the reverse combination of donor/acceptor was used. Heteromers were also detected when cells were labelled with CLIP-Lumi4 Tb as a donor and SNAP-Red as an acceptor. The htrFRET experiments to detect co-existence of homomers and heteromers in the same cell line when both receptors were co-expressed were carried out simultaneously.

4.4 Oligomeric complexes detected by Blue Native (BN) - PAGE and co-immunoprecipitation (Co-IP).

In addition to the htrFRET experiments, other more classic biochemical approaches were utilised to assess the formation of oligomeric complexes of the receptors in question. These included BN-PAGE and Co-IP. Various possibilities for oligomeric arrangements between the receptors may exist, either homomeric or heteromeric. Some of the possible arrangements, with their estimated sizes, are included in Figure 4.7, showing mostly dimers and tetramers. The reason mostly dimers and tetramers were taken into account was the reported preference of both receptors to exist in a tetrameric arrangement as homomers, with pharmacology data supporting M_2 tetramer formation (Redka *et al.*, 2014) and the suggested tetrameric rhomboidal homomeric arrangement of M_3 (Patowary *et al.*, 2013).

Blue Native PAGE was carried out (Figure 4.8) using lysates prepared from the cell line able to express both the receptors. Cells were treated or not with doxycycline to allow co-expression of both receptors or expression of only the constitutive HA-CLIP-hM_3RASSL. This allowed the detection of a number of potential oligomeric complexes with their estimated molecular masses, using anti-SNAP/CLIP and anti-VSV antibodies. Lysates prepared from cells not treated with doxycycline demonstrated HA-CLIP-hM_3RASSL

polypeptide appearing at about 400-480 kDa, consistent with a tetrameric arrangement of the receptor, as detected with the anti-SNAP/CLIP antibody. Upon treatment with doxycycline, the VSV-SNAP-hM_2WT receptor was expressed, and the appearance of much more intense polypeptide bands ranging from around 100-480 kDa were detected (although not clear) using an anti-SNAP/CLIP antibody. A polypeptide band above 240 kDa that was detected using the anti-VSV antibody, could suggest interactions between hM_2WT and hM_3RASSL receptors in a tetrameric arrangement. A second band seen at above 146 kDa could correspond to the homodimeric arrangement of VSV-SNAP-hM_2WT or a hetero-dimeric formation between hM_2WT/hM_3RASSL, while a more intense band at around 100 kDa could represent the monomers of VSV-SNAP-hM_2WT. Combinations such as 3 x hM_3RASSL/ 1 x hM_2WT (estimated size at 380 kDa) or 2 x hM_3RASSL/ 2 x hM_2WT (estimated size at 360 kDa) or even 1 x hM_3RASSL/ 3 x hM_2WT (estimated size at 340 kDa) could exist, but are not easily detected by the anti-SNAP/CLIP antibody. Treatment of the lysates with 1% SDS (reducing conditions) resulted in lower molecular mass polypeptide bands that could correspond to existence of monomers of HA-CLIP-hM_3RASSL and monomers of VSV-SNAP-hM_2WT. The anti-SNAP antiserum was not able to distinguish between the two receptors but the use of anti-VSV antibody managed to locate VSV-SNAP-hM_2WT presence at the polypeptides seen at 480 kDa and between 480-240 kDa, an observation that could be consistent with the presence of hM_2WT in a heteromeric complex with hM_3RASSL, in various combinations e.g. 3 x hM_3RASSL/1 x hM_2WT (estimated at 380 kDa), 2 x hM_3RASSL/ 2 x hM_2WT (estimated at 360 kDa), 1 x hM_3RASSL/ 3 x hM_2WT (estimated at 340 kDa) and in a homo-tetrameric form e.g. 4 x hM_2WT (estimated at 320 kDa). The polypeptide band seen at around 146 kDa could possibly suggest the existence of the hM_2WT in a homo-dimer (2 x hM_2WT, estimated at 160 kDa) or a hetero-dimer 1 x hM_3RASSL/ 1 x hM_2WT (estimated at 180 kDa). Treatment with 1% SDS resulted in the reduction of the sizes of the polypeptides to an intense band seen using either anti-SNAP/CLIP or anti-VSV antibodies, at just above 146 kDa, possibly suggesting the dissociation of the tetrameric forms to dimeric ones. In addition, a less intense polypeptide band was seen at above 66 kDa possibly corresponding to the monomers of hM_2WT (expected molecular mass approximately 80 kDa). Although, the sizes of the polypeptide bands seen on the blot were close to the estimated sizes of some of the expected oligomeric arrangements, we have to take into consideration the expected error in protein size estimation, when carrying out a BN-PAGE (Ward *et al.*, 2013; Wittig *et al.*, 2006).

The use of VSV and HA tag-receptor fusions allowed the performance of co-immunoprecipitation experiments, to assess potential VSV-SNAP-hM_2WT/HA-CLIP-hM_3RASSL heteromeric interactions in cells able to co-express both receptors (Figure 4.9). Cells were treated with 5 $ng \cdot ml^{-1}$ doxycycline and 6 μM tunicamycin and the treatments were stopped at several time points. Tunicamycin is a mixture of antibiotics that inhibit N-glycosylation in early stages of protein synthesis. Cells treated with tunicamycin are expected to express only the non-glycosylated version of proteins/receptors synthesised after tunicamycin treatment, and these appear as lower molecular mass bands when analysed on a Western blot, compared to the N-glycosylated version of the proteins synthesised prior to tunicamycin addition (see Chapter 3, section 3.2 and Figure 3.5). Cells were lysed using a relatively mild detergent dodecyl maltoside (DDM) containing lysis buffer that allows solubilisation of the proteins whilst preserving protein-protein interactions.

Lysates of cells were immuno-precipitated with anti-VSV. Immuno-precipitated samples were then resolved by SDS-PAGE and immuno-blotted with an anti-HA antibody to detect co-immunoprecipitation of HA-CLIP-hM_3RASSL. As induction of expression of VSV-SNAP-hM_2WT requires a significant period of time after addition of doxycycline, co-immunoprecipitation was only observed at the later time points (after 8 hours). As shown in Figure 3.3 (see Chapter 3), anti-HA is only able to identify the non-N-glycosylated form of HA-CLIP-hM_3RASSL. This is why experiments were performed in tunicamycin-treated cells.

The immunoprecipitation of VSV-SNAP-hM_2WT with anti-VSV antibodies resulted in the co-immunoprecipitation of anti-HA immuno-reactivity, corresponding to HA-CLIP-hM_3RASSL, only after treatment with doxycycline, thus when both receptors were co-expressed (Figure 4.9). The co-immunoprecipitation data do not demonstrate the existence of direct interactions but only imply the interaction of hM_3RASSL with hM_2WT. The inability of anti-HA antibody to efficiently detect the glycosylated version of HA-CLIP-hM_3RASSL is the reason that a band was not detected in the sample prepared from cells expressing both receptors in the absence of tunicamycin.

The biochemical results support the presence of oligomeric complexes, both homomeric and heteromeric in nature, and support the data obtained from the htrFRET experiments, suggesting that the htrFRET signal at 665 nm demonstrates the proximity of hM_2WT and hM_3RASSL within either homomeric or heteromeric interactions.

4.5 Oligomerisation in signalling and function

Once the existence of heteromers between VSV-SNAP-hM_2WT and HA-CLIP-hM_3RASSL at the surface of live cells was confirmed and once the conditions in which heteromerisation was achieved were established, it was important to assess whether heteromerisation affected the signalling and/or the function of the receptors. The key signalling pathways of the hM_2WT and hM_3RASSL receptors were described in Chapter 3 (see section 3.3). Briefly, hM_2WT, upon agonist-mediated activation, binds to and activates $G_{i/0}$ protein-dependent signalling pathways which involve inhibition of adenylate cyclase that leads to decreased levels of cAMP. On the other hand, the hM_3RASSL, upon CNO-mediated activation, binds to and activates $G_{q/11}$ proteins in a way similar to that of the hM_3WT receptor. Activation of $G_{q/11}$ dependent pathways involve the sequential activation of phospholipase Cβ (PLCβ), which in turns catalyses the formation of inositol 1,4,5-trisphosphate (IP_3) and diacylglycerol (DAG) from phosphatidylinositol 4,5-bisphosphate (PIP_2). IP_3 acts on IP_3 receptors in the Endoplasmic reticulum (ER) and induces release of calcium ions. DAG while still bound on the membrane acts to activate protein kinase C (PKC) (see Chapter 3, Figure 3.10).

In order to assess the role of oligomerisation in receptor function and signalling, the data already obtained from functional experiments (Figures 3.21, 3.22 and 3.23) were re-examined and discussed, while taking into consideration the existence of hM_2WT/hM_3RSSL heteromers. Cells able to co-express both receptors were treated or not with doxycycline and were employed to measure CNO-mediated increase in levels of inositol monophosphates (IP-1). There was a trend towards an increase in the efficacy of CNO in the presence of heteromers (+Dox), but it was not significant. The potency of CNO remained unaltered either in the absence of heteromers with pEC_{50} (-dox) = 8.2 ± 0.3 or in the presence of heteromers pEC_{50} (+dox) = 8.2 ± 0.27 (see Figure 3.21). Cells treated or not with doxycycline, were employed to measure the carbachol-mediated inhibition of forskolin mediated cAMP levels. Carbachol was able to potently (pEC_{50}=6.9 ±0.1) inhibit the levels of cAMP, in live cells, at conditions where the existence of heteromers was confirmed (+Dox). The presence of hM_2WT/hM_3RASSL heteromers did not seem to affect the hM_2WT mediated inhibition of cAMP levels (Figure 3.23).

4.6 Discussion

One of the main aims of this chapter was to detect the existence of oligomeric interactions of VSV-SNAP-hM_2WT and HA-CLIP-hM_3RASSL receptors that exist either in a homomeric or heteromeric arrangement. In cells stably expressing one of the receptors, upon treatment with the antibiotic doxycycline, detection of VSV-SNAP-hM_2WT or HA-CLIP-hM_3RASSL homomers was monitored by htrFRET. Homomeric interactions were not detected from cells in the absence of doxycycline, suggesting that the bell shaped curves obtained from doxycycline treated cells were due to receptor homomers. Although, that was a useful assay control, a negative oligomerisation control was required. For this reason the CD86 receptor that exists in a monomeric state at the surface of live cells (Girard *et al.,* 2014, James *et al.,* 2007), was used as a negative oligomerisation control. The cell line inducibly expressing the VSV-SNAP-CD86 upon treatment with doxycycline was used for labelling with 10 nM SNAP-Lumi4 Tb and varying concentrations of SNAP-Red and the FRET signal at 665 nm was monitored. The characteristic bell-shaped curve suggesting oligomerisation was absent in the case of CD86 receptor, when the data were compared to those obtained for the hM_2WT receptor. The result obtained from cells expressing the CD86 receptor clearly demonstrated the lack of oligomer formation and thus allowed the determination of bystander FRET levels. In conclusion, the bell-shaped curves obtained from VSV-SNAP-hM_2WT expressing cells were due to oligomerisation rather than random receptor-receptor interactions. The presence of VSV-SNAP-hM_2WT and HA-CLIP-hM_3RASSL homomers was consistent with previous reports on formation of M_2/M_3 heteromers from the literature (Goin and Nathanson, 2006).

The existence of the htrFRET signal at 665 nm indicated the close proximity between the receptors and this was interpreted as receptor oligomerisation. The nature of resonance energy transfer techniques does not allow concluding on the order of the receptor interactions (e.g. dimeric, tetrameric or higher order oligomeric) but only supports the existence of receptors being in close proximity that could be organised in an oligomeric complex.

The concentrations of the substrates used in the htrFRET experiments were not enough to fully saturate the tagged receptors. One of the main reasons for using sub-saturation concentrations had to do with high cost of the substrates. Although, only part of the cell surface expressed receptors was labelled using sub-saturation concentrations (nano molar level) of the substrates, FRET signals that corresponded to oligomeric interactions between the receptors were efficiently detected. Similar experiments carried out by others, using

the same technology and labelling substrates to monitor htrFRET as a means to detect homomers and heteromers of receptors in live cells, included use of higher concentrations of the donors and acceptors at the micro molar level (Doumazane *et al.,* 2011). Despite the use of sub-saturating substrate concentrations, the main idea was to have a population of the cell surface expressed receptors labelled, and theoretically by using the same doxycycline concentrations to achieve equal receptor expression between the experiments, and by using the same substrate concentrations to allow relatively equal labelling, allowed the assumption that the labelled receptor population was relatively equal between the experiments. Thus, detection of oligomers was considered consistent throughout the experiments.

Confirmation of the existence of oligomeric interactions between the co-expressed VSV-SNAP-hM_2WT and HA-CLIP-hM_3RASSL receptors was offered by a set of biochemical experiments, such as BN-PAGE and co-IP. In summary, co-existence of oligomers when both receptors were present was in agreement with the literature on muscarinic receptors and other GPCRs (Pou *et al.,* 2012; Maggio *et al.,* 1993; Goin and Nathanson, 2006). The htrFRET and biochemical data supported the formation of oligomers of muscarinic receptors are in agreement with the notion that class A GPCRs may form constitutive oligomers (Bouvier and Hebert, 2014).

The last important matter that was assessed in this chapter concerned the possible effects of oligomerisation on receptor signalling and function. There is evidence that propose that GPCR oligomerisation can affect the pharmacology and/or signalling transduction (Gonzalez-Maeso, 2011; Milligan, 2013). Data supporting the signalling cross-talk between the muscarinic M_2 and M_3 receptors were presented previously, suggesting a synergistic activation of ERK 1/2 signalling, following agonist-mediated co-activation of M_2 and M_3 when both receptors were co-expressed, in CHO cells (Hornigold *et al.,* 2003). In order to assess the role of oligomerisation in receptor signalling, the activation of G-proteins and downstream signalling was examined, upon agonist treatment, in the presence of heteromers in the cell line that co-expressed both receptors. There was a trend towards an increase in the efficacy of CNO in increasing the hM_3RASSL mediated inositol phosphate (IP1) levels, in the presence of heteromers while the efficacy of CNO was not affected. The potency of CNO remained unaltered in the absence of heteromers. Carbachol activation of the doxycycline induced VSV-SNAP-hM_2WT, in the presence of the constitutively expressed HA-CLIP-hM_3RASSL, demonstrated the expected inhibition of forskolin-induced cAMP levels that follows activation of $G_{i/o}$ coupling. Therefore, we can conclude that oligomerisation did not affect the signalling of the receptors in question. The

possible reason we did not detect a synergistic effect on signalling similar to that seen by Hornigold *et al.*, (2003) has to do with the different approaches followed in terms of receptor activation. Signalling cross-talk was observed when M_2 and M_3 receptors were co-activated by an agonist, whereas, in the functional assays carried out during this project, each receptor was activated separately and each signalling pathway was assessed individually. Another reason may involve the use of different cell lines and more importantly the use of a mutated version of hM_3 receptor, the hM_3RASSL. The hM_3RASSL, although, it binds to and activates the $G_{q/11}$ dependent pathway, it might be demonstrating a different behaviour, in terms of signalling cross-talk, compared to the wild type receptor.

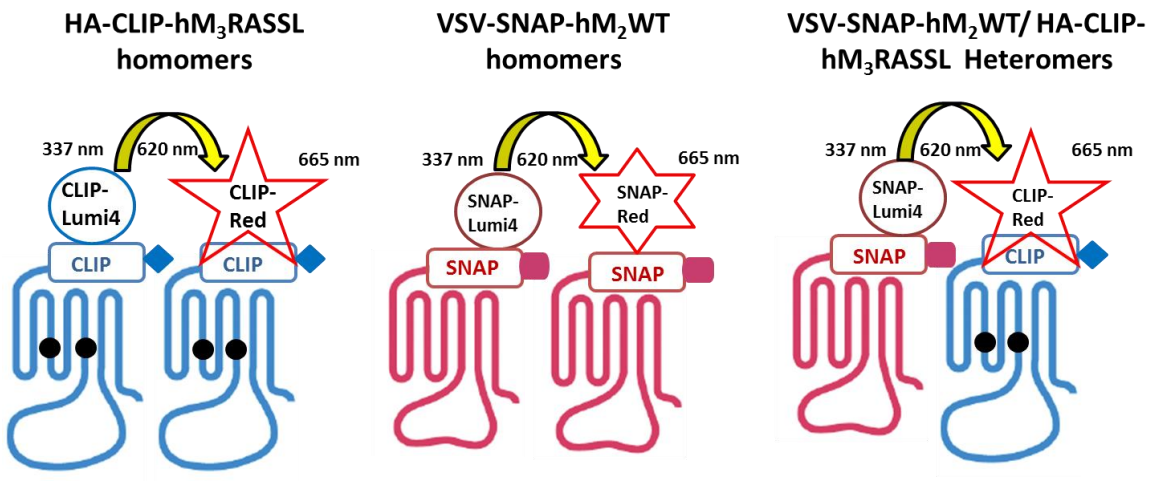

Figure 4.1 Schematic representation of hM_2 and hM_3 oligomers. Tag-lite® technology combines the use of SNAP and CLIP tags fused to the N-terminus of the receptor, together with htrFRET. The SNAP and CLIP tags are specifically and covalently labelled with benzyl guanine/cytosine derivative substrates such as SNAP-Lumi4 Tb and CLIP-Lumi4 Tb, respectively, which emit at 620 nm, following excitation at 337 nm and are used as donors. SNAP-Red and CLIP-Red which emit at 665 nm, following excitation at 620 nm, are used as acceptors. The use of an engineered version of the hM_3 receptor (hM_3RASSL), modified within the 3rd and 5th transmembrane domains (●Y149C and ●A239G) allowed the selective activation of the hM_3RASSL with the synthetic ligand clozapine-N-oxide (CNO), independently from the hM_2WT receptor, when co-expressed. The receptors are also N-terminally tagged with HA and VSV-G.

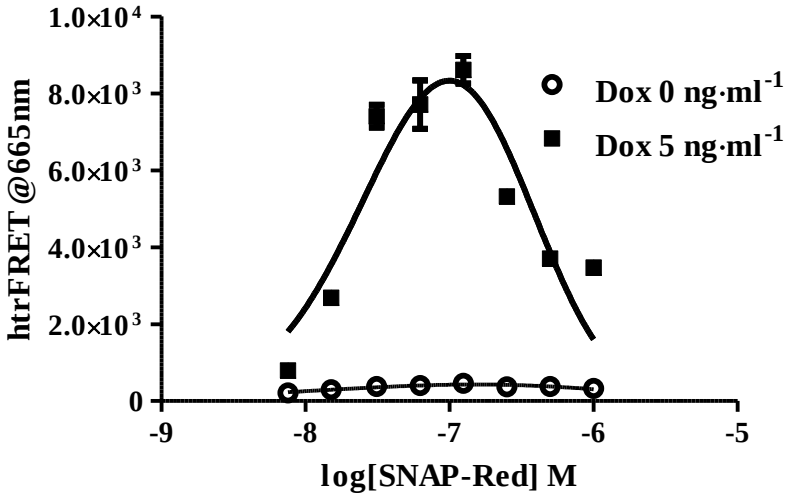

Figure 4.2 Homomers of VSV-SNAP-hM$_2$WT at the surface of live cells expressing the receptor. Cells able to express VSV-SNAP-hM$_2$WT in a doxycycline induced manner, were untreated (no dox) or treated with 5 ng·ml^{-1} dox, for 24 hours. After cells were plated in 96 well FRET-compatible plates, they were subjected to co-labelling with a combination of 5 nM SNAP Lumi4 Tb (energy donor) and varying concentrations of SNAP-Red (energy acceptor). Following excitation at 337 nm, fluorescence emission at 665 nm was monitored, which corresponded to the htrFRET signal. The non-specific signal obtained from doxycycline untreated cells was used as the basal signal, and was subtracted from the total (obtained from doxycycline treated cells), to calculate the specific htrFRET. The peak signal indicated the optimal energy donor/acceptor ratio concentrations e.g. 5 nM SNAP Lumi4 Tb (donor)/ 100 nM SNAP-Red (acceptor).

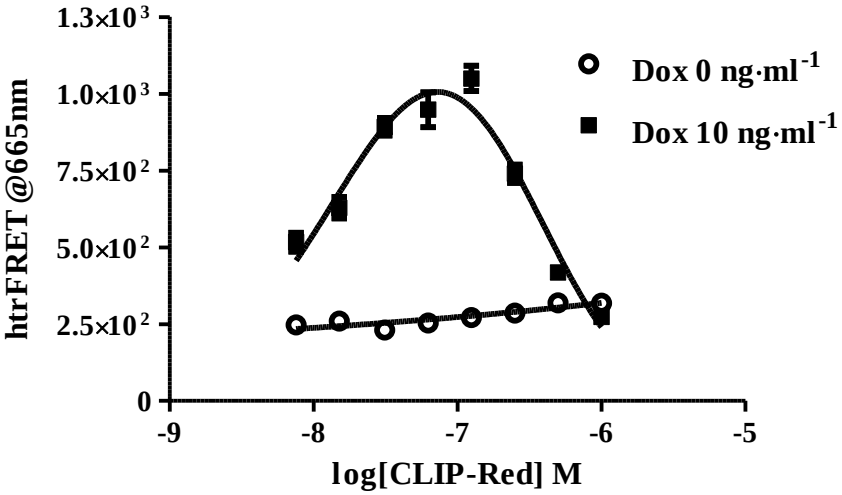

Figure 4.3 Homomers of HA-CLIP-hM$_3$RASSL at the surface of live cells expressing the receptor. Cells able to express the HA-CLIP-hM$_3$RASSL in a doxycycline dependent manner, were untreated (0 ng·ml^{-1} doxycycline) or treated (with 10 ng·ml^{-1} doxycycline), for 24 hours. After cells were plated in a 96 well FRET-compatible plate, they were subjected to co-labelling with 10 nM CLIP Lumi4Tb (energy donor) and varying concentrations of CLIP-Red (energy acceptor). Following excitation at 337 nm, the fluorescence emission at 665 nm, corresponding to the htrFRET signal was monitored. The non-specific signal obtained from doxycycline untreated cells was used as the basal signal, and was subtracted from the total (obtained from doxycycline treated cells), to calculate the specific htrFRET. The peak signal indicated the optimal energy donor/acceptor ratio concentrations e.g. 10 nM CLIP Lumi4 Tb (donor)/ 100 nM CLIP-Red (acceptor).

A.

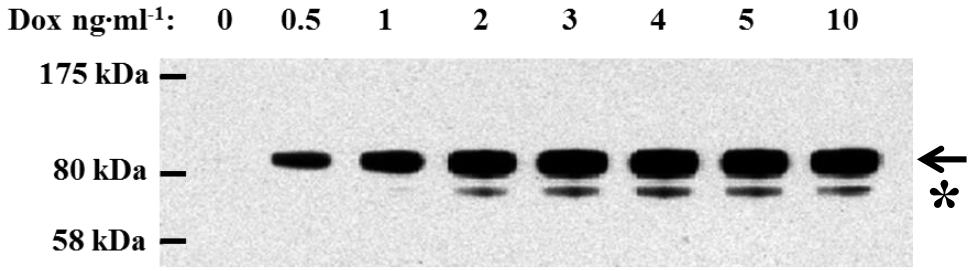
Dox ng·ml-1: 0 0.5 1 2 3 4 5 10
175 kDa
80 kDa
58 kDa
*

B.

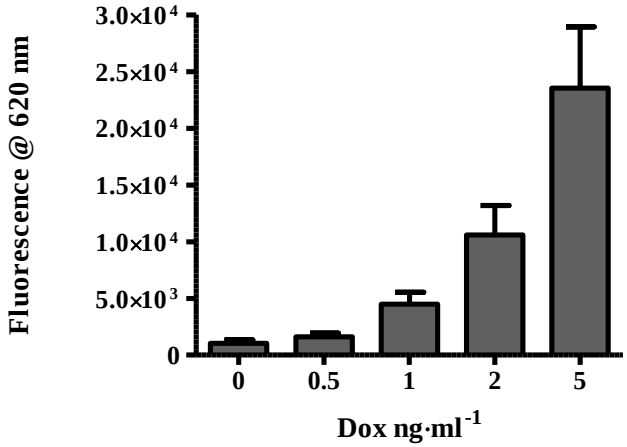
Fluorescence @ 620 nm
3.0×10^4
2.5×10^4
2.0×10^4
1.5×10^4
1.0×10^4
5.0×10^3
0
0 0.5 1 2 5
Dox ng·ml-1

C.

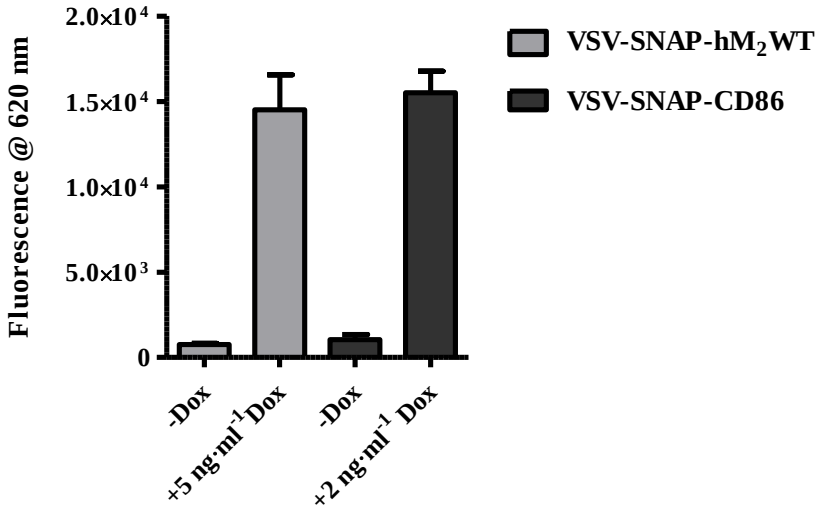
Fluorescence @ 620 nm
2.0×10^4
1.5×10^4
1.0×10^4
5.0×10^3
0
VSV-SNAP-hM2WT
VSV-SNAP-CD86
-Dox
+5 ng·ml-1 Dox
-Dox
+2 ng·ml-1 Dox

D.

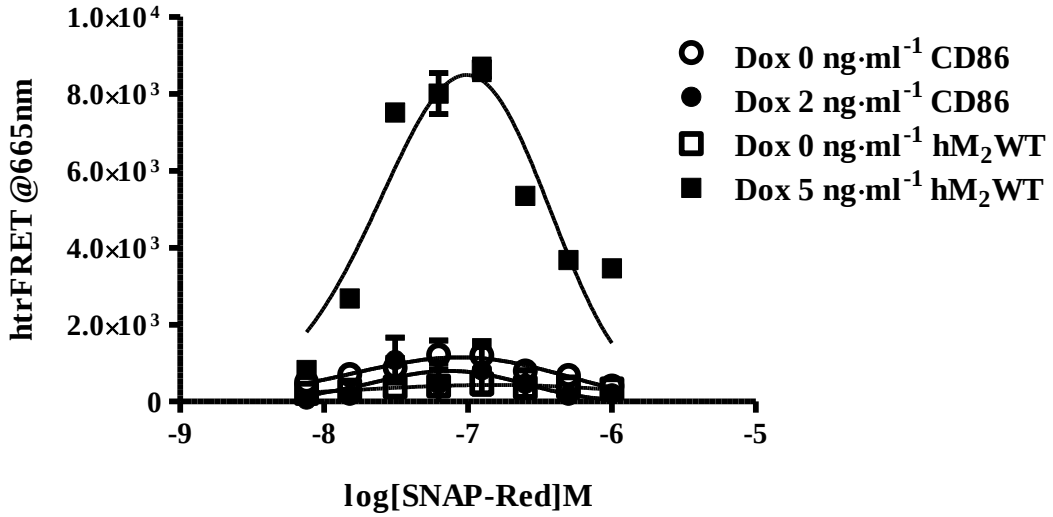

Figure 4.4 Negative control for oligomerisation (A) Total expression of VSV-SNAP-CD86, detected as 80 kDa polypeptide bands (arrow) using anti-SNAP/CLIP antiserum against lysates prepared from cells inducibly expressing the receptor upon treatment with varying concentrations of doxycycline. The non-glycosylated poypeptides appear at just belw 80 kDa (star). **(B)** VSV-SNAP-CD86 cell surface expression, by measuring fluorescence at 620 nm, following labelling of live doxycycline induced cells with 10 nM SNAP-Lumi4 Tb. **(C)** Comparison of the expression profiles between VSV-SNAP-hM_2WT and VSV-SNAP-CD86. **(D)** VS-SNAP-CD86 acting as a negative oligomerisation control, based on the inability to form a bell shape curve, compared to the VSV-SNAP-hM_2WT forming homomers in Figure 4.2.

A.

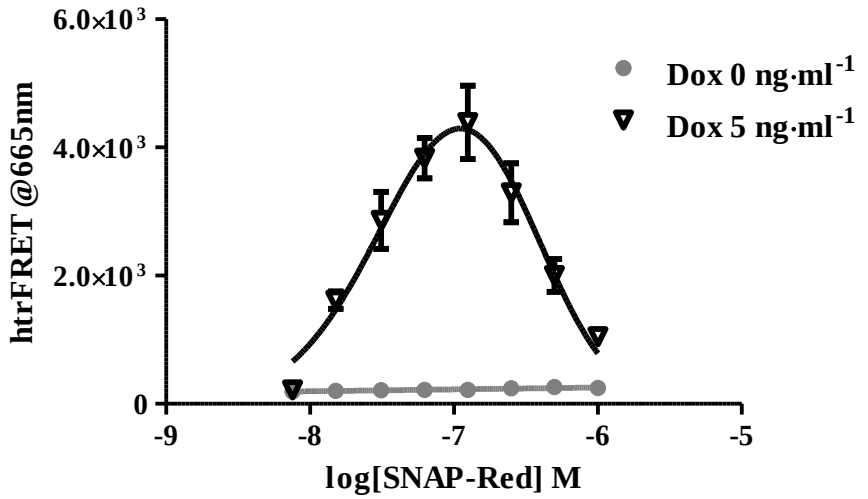

B.

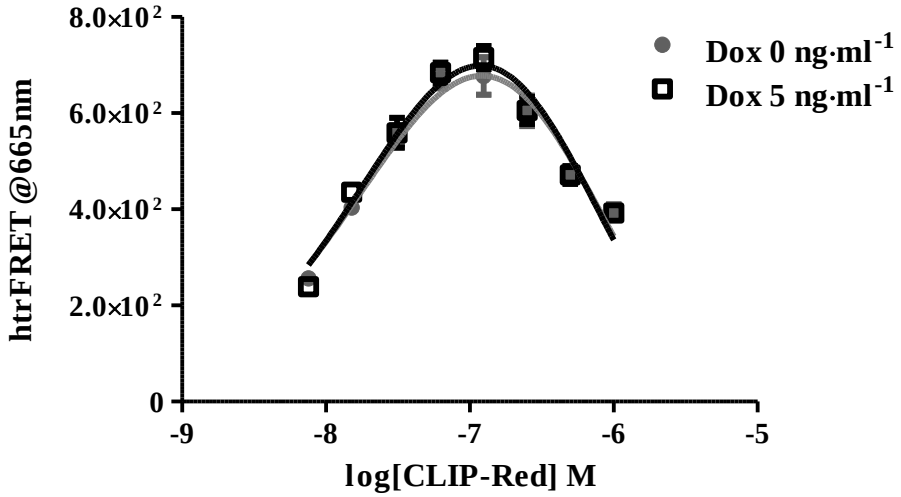

Figure 4.5 Homomers of VSV-G-SNAP-hM$_2$WT and HA-CLIP-hM$_3$RASSL co-exist at the surface of live cells expressing both receptors. Cells able to express the VSV-SNAP-hM$_2$WT receptor in a doxycycline dependent manner while constitutively expressing the HA-CLIP-hM$_3$RASSL receptor, were untreated (0 ng·ml^{-1} doxycycline) or treated(with 5 ng·ml^{-1} doxycycline) for 24 hours. **(A)** Cells were co-labelled with 5 nM SNAP Lumi4 Tb (energy donor) and varying concentrations of SNAP-Red (energy acceptor). **(B)** A different set of the same cell line was co-labelled with 10 nM CLIP Lumi4 Tb (energy donor) and varying concentrations of CLIP-Red (energy acceptor) and after excitation at 337 nm, the 665 nm htrFRET signal obtained, demonstrated the co-existence of VSV-SNAP-hM$_2$WT homomers and HA-CLIP-hM$_3$RASSL homomers at the cell surface when both receptors are co-expressed.

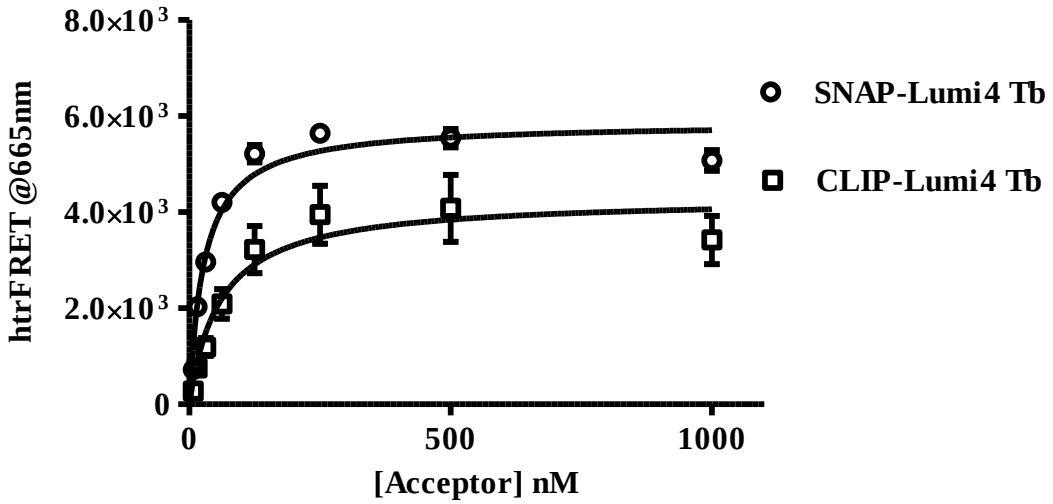

Figure 4.6 Heteromers between co-expressed HA-CLIP-hM$_3$RASSL and VSV-SNAP-hM$_2$WT receptors at the surface of live cells expressing both the receptors. Cells expressing both receptors were co-labelled with combinations of either SNAP Lumi4 Tb/CLIP-Red (circles) or CLIP Lumi4 Tb/SNAP-Red (squares). After excitation at 337 nm htrFRET signal at 665 nm was obtained. The htrFRET analysis suggested that heteromers between HA-CLIP-hM$_3$RASSL and VSV-SNAP-hM$_2$WT exist at the surface of live cells, when both receptors are co-expressed.

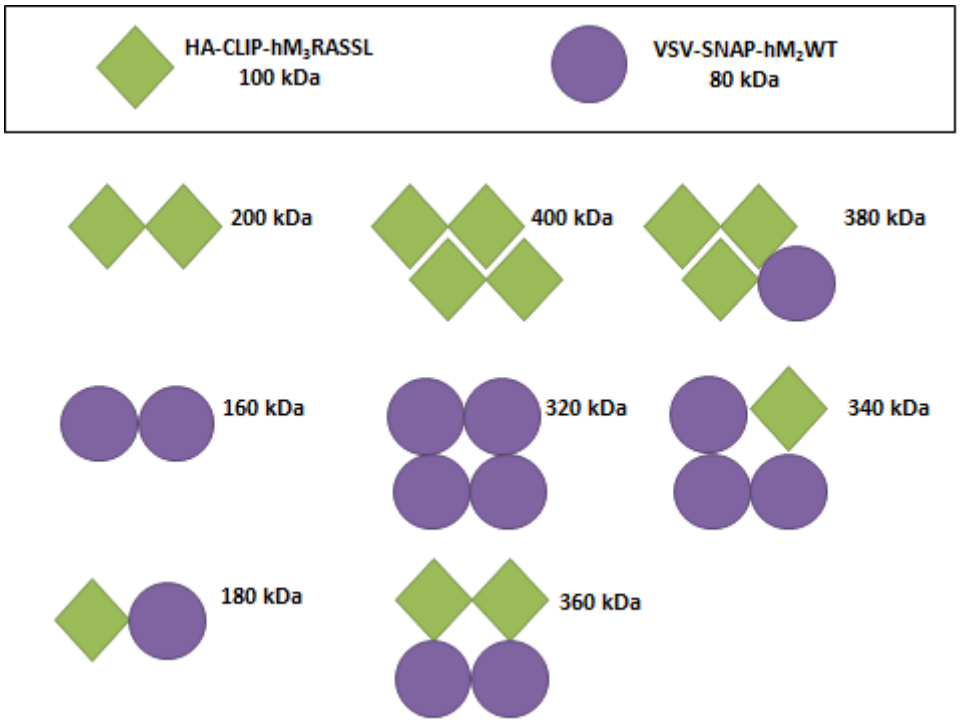

Figure 4.7 Sizes of the possible hM_2WT or hM_3RASSL homomeric and heteromeric complexes that may be formed. Some of the possible combinations of the oligomeric complexes were considered in this figure, and the possible molecular masses were estimated, to allow easier identification of any oligomeric complexes demonstrated on a Blue Native PAGE.

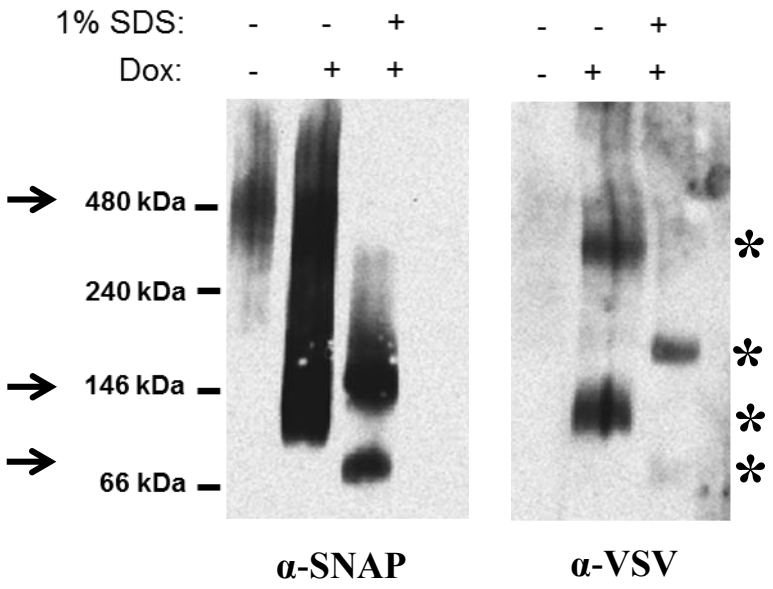

Figure 4.8 Blue Native PAGE demonstrating the different oligomeric complexes between the co-expressed HA-CLIP-hM$_3$RASSL and VSV-SNAP-hM$_2$WT. Cells expressing the HA-CLIP-hM$_3$RASSL (constitutively) and the VSV-SNAP-hM$_2$WT (in a doxycycline dependent manner), were treated with 5 ng·ml^{-1} doxycycline (+ Dox) or without (-Dox). Lysates prepared from these cells were extracted with dodecyl maltoside (DDM) and were subjected to Blue Native PAGE, either directly or following addition of 1% SDS, which were further processed to allow immune-detection using anti-SNAP/CLIP and anti-VSV antibodies.The upper arrow (pointing rightwards) at approximately 480 kDa indicates a possible tetrameric organisation of the HA-CLIP-hM$_3$RASSL.The middle arrow indicates possible dimeric arrangement of HA-CLIP-hM$_3$RASSL homomers or hM$_3$RASS/hM$_2$WT heteromers, that were not reduced to their monomeric forms upon addition of SDS. The lower arrow indicates the monomeric form of VSV-SNAP-hM$_2$WT. The stars at the second panel aim to point out the presence of VSV-SNAP-hM$_2$WT receptor in various heteromeric, homomeric or monomeric forms of the receptor.

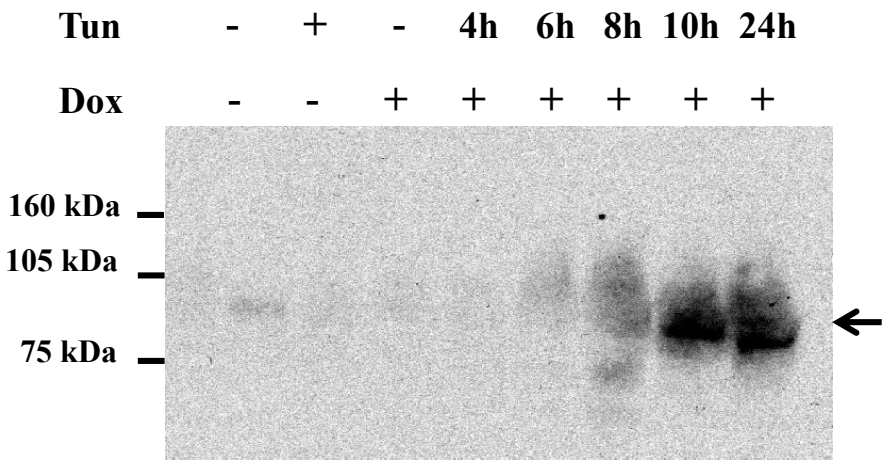

Figure 4.9 Co-immunoprecipitation confirms interaction between VSV-SNAP-hM$_2$WT and HA-CLIP-hM$_3$RASSL receptors when co-expressed. Cells treated or not with 5 ng·ml^{-1} doxycycline, were subjected to lysate preparation after co-treatment with 6 µM tunicamycin. The VSV-SNAP-hM$_2$WT receptor was immuno-precipitated from the lysate by incubation with VSV-conjugated agarose beads, and co-precipitation of HA-CLIP-hM$_3$RASSL was assessed by using anti-HA antiserum and Western blotting. Co-immunoprecipitation of the two receptors was observed (arrow indicating the presence of HA-CLIP-hM$_3$RASSL interacting with VSV-SNAP-hM$_2$WT) in the samples from cells treated with both doxycycline and tunicamycin for at least 8 h, with the intensity of the bands increasing with time of treatment. No specific polypeptide bands were observed in the samples treated only with doxycycline but not with tunicamycin.

Chapter 5

Ligand-mediated regulation of mAChR oligomerisation

5.1 Introduction

The co-existence of hM_2WT/hM_3RASSL heteromers with individual receptor homomers of hM_2WT and hM_3RASSL, at the surface of live cells expressing both receptors, was demonstrated by htrFRET and biochemical experiments as described in Chapter 4. These observations were in agreement with previous studies in which muscarinic receptors had been demonstrated to have a capacity to form oligomers (Goin and Nathanson, 2006; Alvarez-Curto *et al.,* 2010; Hu *et al.,* 2012; Patowary *et al.,* 2013). Other class A GPCRs have also been shown to form oligomers, e.g. dopamine receptors (Pou *et al.,* 2012) and opioid receptors (Gomes *et at.,* 2013).

An important question that remains to be addressed involves the potential of ligands to regulate the oligomeric state of muscarinic receptors. This may provide information that can be useful in drug discovery, in terms of drug selectivity improvement. Targeting receptor oligomers rather than the monomeric form of receptors (Angers et al., 2002; Milligan, 2013) is a concept arising from the suggestion that oligomerisation may confer novel pharmacology to the receptors, resulting from binding site interactions within an oligomeric complex (Smith and Milligan, 2010; Chun *et al.,* 2013).

Several observations have been previously reported in terms of ligand regulation of GPCR oligomerisation. The first BRET-based assay that documented the existence of homomers of β_2-adrenoceptors, demonstrated an increase in the energy transfer upon addition of the selective agonist isoproterenol, which was interpreted as an increase in oligomeric receptor interactions (Angers *et al.,* 2000). In another BRET-based study, constitutive δ-opioid receptor homomers were unaltered upon agonist treatment, implying a lack of agonist mediated regulation of this oligomer (McVey *et al.,* 2001). Studies on the CXCR1 and CXCR2 receptors forming homomers and heteromers as detected by FRET, demonstrated that upon ligand (CXCL8) activation of the receptors, the heteromeric complexes were altered whereas the homomeric profile of both receptors was stabilised (Martinez-Muñoz *et al.,* 2009). By contrast, a BRET-based approach used to study CXCL8-mediated regulation of CXCR1 and CXCR2 did not show any changes either in homomerisation or heteromerisation (Wilson *et al.,* 2005). The above examples point out the importance of the methodology used to study receptor oligomerisation and in addition, these examples suggest that different receptors may demonstrate different oligomerisation profiles and varied stability in the presence of ligands.

The literature on muscarinic receptors offers contradictory observations in terms of ligand regulation of oligomerisation. Specifically, the M_1 receptor was shown to exist as a

monomer, dimer or higher order oligomer (Marquer *et al.,* 2010). Hern *et al.,* (2010) demonstrated that about 30% of the M_1 receptor exists as a dimer, at any given time, and there is a dynamic interchange between monomers and dimers, detected by total internal reflection fluorescence imaging (TIRFM) at single cell level (Hern *et al.,* 2010). Constitutive M_1 receptor dimers seem to be stabilised upon treatment with the M_1-selective allosteric ligand, MT7, as demonstrated by Western blotting and native PAGE electrophoresis as well as by FRET and BRET based assays (Marquer *et al.,* 2010). In an *in vitro* study using insect cells and isolated membranes the orthosteric muscarinic antagonist QNB was shown to confer stability to pre-existing M_2 oligomers (Park and Wells, 2003). In addition, the muscarinic antagonist pirenzepine promoted M_1 dimerisation in live cells as observed by fluorescence correlation spectroscopy (Ilien *et al.,* 2009). Ilien *et al.,* (2009) suggested that in the absence of ligand, the M_1 predominantly existed as a monomer and it formed oligomers upon addition of pirenzepine (Ilien *et al.,* 2009). Detection of M_3 homo-dimers was enabled by using cysteine substituted mutants of the rat M_3 receptor in disulphide cross-linking experiments and Western blotting, where an increase in the formation of M_3 oligomeric complexes was observed upon addition of carbachol (Hu *et al.,* 2012). Quantitative BRET analysis using cells expressing M_1, M_2 or M_3 receptors showed the existence of homomers and saturation BRET analysis in cells co-expressing two of the receptors at a time demonstrated the presence of heteromers between M_1-M_2, M_2-M_3 and M_1-M_3. No effect was detected in the oligomeric status of homomers or heteromers upon carbachol treatment (Goin and Nathanson, 2006). Lack of significant effect of agonist induced receptor stimulation on M_3 receptor oligomerisation was shown by SDS-PAGE and Western blot analysis of membrane extracts from COS-7 cells expressing a mutant M_3 lacking most of the third intracellular loop domain (Zeng and Wess, 1999). In a more recent study, carbachol modified the homomeric status of M_3 receptor as detected by an increase in the htrFRET signal upon addition of agonist, possibly due to carbachol-mediated conformational change in the receptor (Alvarez-Curto *et al.,* 2010).

The detection of ligand-mediated changes in the oligomeric profile of GPCRs is a debated field of research and no conclusions have been reached for the overall GPCR family, since each member has demonstrated a unique oligomeric profile that is not easily applied to another member of the GPCR group (Pfleger and Eidne, 2005).

The approach described in this chapter in order to detect possible ligand-mediated effects on oligomerisation, involved a kinetic htrFRET method following addition of various

muscarinic ligands and the monitoring of the FRET signal at several time points. The donor/acceptor ratio was calculated and was plotted against time. SNAP- or CLIP-Lumi4 Tb was used as a donor in combination with the corresponding Red acceptor, in the dual labelling experiments. Combinations of red and green acceptors were used in the multiplex (triple) labelling of live cells, which allowed for the simultaneous detection of changes in homomer and heteromer status.

Aims of this chapter

To:

- Utilise htrFRET to assess whether muscarinic ligands can regulate homomeric and heteromeric profile of VSV-SNAP-hM_2WT and HA-CLIP-hM_3RASSL receptors.
- Use multiplex labelling to simultaneously detect more than one change in the system.
- Examine the role of receptor internalisation in oligomerisation upon agonist-mediated receptor activation.

5.2 Carbachol mediates a decrease in M_2/M_3 heteromers with a simultaneous increase in M_2/M_2 homomerisation.

To assess the regulation of receptor oligomerisation by ligands, kinetic htrFRET experiments were carried out using a selection of muscarinic ligands on the previously described cell lines expressing the SNAP/CLIP tagged receptors.

A summary of the donor/ acceptor concentrations that allowed for detection of oligomers are listed in Table 5.1.

Donor/ acceptor concentrations (nM)	Oligomer detected
SNAP-Lumi4 Tb (5 nM) / SNAP-Red (100 nM)	**hM_2WT/hM_2WT homomer**
CLIP-Lumi4 Tb (10 nM) / CLIP-Red (100 nM)	**hM_3RASSL/hM_3RASSL homomer**
SNAP-Lumi4 Tb (5 nM) / CLIP-Red (100 nM)	**hM_2WT/hM_3RASSL heteromer**
CLIP-Lumi4 Tb (10 nM) / SNAP-Red (125 nM)	**hM_2WT/hM_3RASSL heteromer**

Table 5.1 Optimum donor/acceptor concentrations that allowed detection of oligomers. The concentrations of substrates were obtained from the bell shape Gaussian curves (for homomers) and saturation curves (for heteromers) following co-labelling of live cells with a fixed concentration of donor and varying concentrations of acceptor. The concentrations of the donors and acceptors were determined by the peaks of the bell shaped curves in the case of homomers and the saturation point in the case of heteromers, where the optimum observation of oligomers was detected (see Chapter 4).

The selection of ligand concentrations used in the kinetic htrFRET assays was based on the K_i values for each ligand obtained from competition binding experiments in the presence of [^{3}H]-QNB (see Chapter 3, Tables 3.1 and 3.2). Following labelling of live cells with the htrFRET compatible substrates, set concentrations of the ligands were added to the assay one minute after performing the first reading on the plate reader. Measurements were recorded at several time points, over a 60 minute period. The 665/620 ratio was calculated and changes in this ratio were monitored in response to the different ligands added.

Live cells expressing both the receptors after treatment with 5 ng·ml^{-1} doxycycline, were labelled with CLIP-Lumi4 Tb and SNAP-Red. This substrate pair combination allowed detection of heteromers between VSV-SNAP-hM_2WT and HA-CLIP-hM_3RASSL. This showed a decrease in htrFRET, potentially reflective of a decrease in heteromers, in response to 1 mM carbachol and a decrease in response to the combination of 1 mM carbachol and 100 μM CNO but not to 100 μM CNO alone. Atropine (10 μM) had no effect on the heteromeric status of the receptors, as the profile of the kinetic htrFRET was similar to the one where no ligand was added (Vehicle: labelling medium containing 0.33% DMSO to maintain consistency between treatments) (Figure 5.1 A). A subsequent recording of the htrFRET on cells labelled with SNAP-Lumi4 Tb/SNAP-Red,

demonstrated an increase in the FRET signal and potentially in the formation of hM_2WT homomers in response to 1 mM carbachol or the combination of carbachol and CNO, but not to CNO alone, or to the antagonist atropine (Figure 5.1 B). Combining the two observations, a conclusion can be reached suggesting that carbachol-mediated occupation of hM_2WT receptor may disturb the oligomeric balance by causing an increase in the hM_2WT homomers and a simultaneous decrease in the heteromers i.e. a transition from heteromeric to homomeric organisation of the receptors. Interestingly, the kinetics of each change were found to be rather slow. The half time ($t_{1/2}$) of carbachol in decreasing the heteromer was 5.6 ± 3.2 minutes and the $t_{1/2}$ in increasing the homomers was 14.0 ± 3.8 minutes (Table 5.2). The synthetic ligand CNO did not lead to any alterations in the hM_2WT/hM_3RASSL heteromer formation.

The reverse donor/acceptor combination (SNAP-Lumi4 Tb/CLIP-Red) was also used to allow detection of changes within the hM_2WT/hM_3RASSL heteromer following ligand addition. Surprisingly, although this combination was successful in detecting VSV-SNAP-hM_2WT/HA-CLIP-hM_3RASSL heteromers, no significant changes were detected in the kinetic htrFRET upon carbachol addition, or upon addition of the combination of carbachol and CNO (Figure 5.1 C). The window was too small for any significant changes to be detected. The reason for this observation could be explained by the composition and size of the heteromer that could be affecting the orientation of the fluorophores within the complex. An example that points out the difference in the outcome on the kinetic htrFRET between the two sets of donor/acceptor pair combinations is shown in Figure 5.1 D with the CLIP-Lumi4 Tb/SNAP-Red pair resulting in a significant change in 665/620 ratio upon carbachol treatment (P=0.0013, two-paired t-test comparing ratio at time 0 minute versus time 40 minutes, upon treatment, n=3).

The homomeric profile of HA-CLIP-hM_3RASSL was also monitored in the cell line expressing both receptors. Cells treated or not with doxycycline were co-labelled with CLIP-Lumi4 Tb and CLIP-Red and the 665/620 ratio was monitored following ligand addition. There were no changes detected in the hM_3RASSL homomeric status, in response to any of the ligands, either in the absence (-Dox) or presence (+Dox) of hM_2WT (Figure 5.2 A and B, respectively). Overall, CNO did not have any effect on the oligomeric status of the receptors. There was an overall decline in the 665/620 ratio over time, even in the absence of ligands. This trend was observed in all kinetic experiments that involved the use of Tag-lite® technology, and it is considered to be the result of photo-bleaching of the substrates. Photo-bleaching was not detected in single point readings since the cells are

exposed to laser once, but it was detectable in sequential readings that involved multiple exposures of the substrates to light. Once the ligand-mediated changes on the oligomerisation profile of the receptors were observed by kinetic htrFRET it was important to address whether these changes were concentration dependent. Therefore, cells labelled with CLIP-Lumi4 Tb/SNAP-Red (detecting hM_2WT/hM_3RASSL heteromers) and SNAP-Lumi4 Tb/SNAP-Red (detecting hM_2WT homomers) were subjected to treatments with varying concentrations of carbachol, to allow the determination of the concentration-dependent fashion of oligomerisation changes (Figure 5.3). The choice of the 40 min time point to carry out the measurements was based on the fact that the changes were established at 40 min and were maintained for up to one hour. Carbachol potently decreased the formation of hM_2WT/hM_3RASSL heteromers (pIC_{50}= 5.2 ± 0.3) (Figure 5.3 A) and increased the formation of hM_2WT homomers (pEC_{50}= 5.5 ± 0.2) (Figure 5.3 B). Co-incubation with 10 μM atropine blocked the effects of carbachol in both cases. Incubation at 4˚C also inhibited the carbachol mediated decrease in heteromerisation and the increase in hM_2WT homomerisation, suggesting a possible involvement of receptor internalisation in the regulation of receptor oligomerisation.

The fluorescence at 620 nm was monitored using cells labelled only with Lumi4 Tb donor, to assess whether there were any changes at the cell surface receptor population in response to the ligand treatments (Figure 5.4). Cells treated with doxycycline to allow co-expression of both receptors, were labelled with 5 nM SNAP-Lumi4 Tb and were then subjected to ligand treatments while fluorescence at 620 nm was monitored for up to 60 minutes. There was a trend towards reduction in 620 nm signal upon treatment with 1 mM carbachol and with the combination of carbachol and CNO, but it was not significant (Figure 5.4 A). This small decline in the 620 nm signal could suggest a limited extend of internalisation of the hM_2WT receptors due to agonist-mediated activation. Cells labelled with 10 nM CLIP-Lumi4 Tb did not demonstrate any changes in the cell surface population of HA-CLIP-hM_3RASSL either when hM_3RASSL was expressed alone (-Dox) or when co-expressed with hM_2WT (+Dox) (Figure 5.4 B and C, respectively).

One limitation of the cellular system used to study the co-expressed receptors was that it did not allow the assessment of hM_2WT receptor alone, since VSV-SNAP-hM_2WT was only studied in the presence of the constitutively expressed HA-CLIP- hM_3RASSL. Therefore, a cell line inducibly expressing the VSV-SNAP-hM_2WT receptor was employed to carry out similar kinetic htrFRET experiments, offering a view of the behaviour of hM_2WT homomers in response to ligands in the absence of hM_3RASSL.

Cells capable of expressing VSV-SNAP-hM_2WT upon treatment with doxycycline were labelled with SNAP-Lumi4 Tb/SNAP-Red substrate pair, to allow detection of hM_2WT homomers and the 665/620 ratio was monitored over time (Figure 5.5). Carbachol (1 mM) produced an increase in the hM_2WT homomeric profile of the receptor with a $t_{1/2}$ =12.2 ± 0.8 minutes (Table 5.2). The combination of carbachol (1 mM) and CNO (100 μM) also led to an increase in hM_2WT homomerisation (Figure 5.5.A). The kinetics of this change were also relatively slow with a $t_{1/2}$ =22.0 ±7.0 minutes (Table 5.2), suggesting that the change might not be due to a conformational change, but rather due to recruitment of partners, or due to potential receptor internalisation. The fluorescence at 620 nm was also monitored, upon ligand addition, using cells labelled only with SNAP-Lumi 4 Tb. Treatment with carbachol demonstrated a trend towards a decrease in the 620 nm, suggesting a limited decrease in the cell surface population of the labelled VSV-SNAP-hM_2WT, potentially due to internalisation (Figure 5.5 B). The potent increase in the hM_2WT homomer formation caused by carbachol was also found to be concentration dependent with pEC_{50}= 5.20 ± 0.08. The agonist-mediated effect was inhibited by incubation at 4˚C (Figure 5.5 C).

Oligomer affected	$t_{1/2}$ (minutes) (1mM Cch)	$t_{1/2}$ (minutes) (Cch +CNO)
hM_2WT/hM_3RASSL in cells co-expressing both receptors	**5.6 ± 3.2**	**14.0 ± 3.8**
hM_2WT/hM_2WT in cells co-expressing both receptors	**10.5 ± 2.5**	**24.5 ± 4.5**
hM_2WT/hM_2WT in cells expressing hM_2WT	**12.2 ± 0.8**	**22.0 ± 7.0**

Table 5.2 Half time analysis of the kinetic htrFRET data. The half times ($t_{1/2}$) of agonists were calculated in order to measure the time required for each treatment to reduce the hM_2WT/hM_3RASSL heteromeric population to half its initial value or to double

hM_2WT homomers in cells that co-express the receptors and in cells that only express the VSV-SNAP-hM_2WT. The $t_{1/2}$ values were obtained from one phase decay analysis of kinetic htrFRET data. Data presented as Mean ± SEM, n=3.

Despite the changes observed in the hM_2WT/hM_3RASSL heteromer and hM_2WT homomer formation, there was no change observed within the hM_3RASSL homomers in response to ligands. In order to rule out the possibility of inefficient CLIP labelling (compared to the SNAP labelling) and any other interference originating from the cell line used, a different cell line was employed to assess ligand regulation of hM_3RASSL homomerisation (Figure 5.6). A cell line able to express VSV-SNAP-hM_3RASSL, in a doxycycline dependent manner (Figure 5.6 A) was used. Cells expressing the receptor were labelled with SNAP-Lumi4 Tb/SNAP-Red and homomers of VSV-SNAP-hM_3RASSL were detected at the surface of live cells (Figure 5.6 B). The synthetic ligand CNO was added but there were no significant changes detected in the hM_3RASSL homomer formation in kinetic htrFRET experiments (Figures 5.6 C and D). In conclusion, the hM_3RASSL homomer detected either using CLIP or SNAP tag labelling, in both cell lines used, remained unaffected by ligand mediated activation. Neither the increase in hM_2WT homomerisation nor the simultaneous decrease in the heteromers, when the two receptors were co-expressed, affected the profile and stability of hM_3RASSL homomers.

5.3 Multiplex labelling htrFRET confirms oligomerisation regulation mediated by carbachol and shows an effect of CNO on hM_3 homomeric arrangement.

The dynamics of oligomerisation is a term used to describe the formation of oligomers and dissociation into monomers, a process that is of great interest. The approach described in this section was intended to investigate the dynamics of oligomerisation between hM_2WT and hM_3RASSL receptors, using an agonist-mediated activation of receptors, in combination with the simultaneous measurement of htrFRET signal at two distinct wavelengths. The cell line able to express both receptors was treated with doxycycline to allow co-expression of VSV-SNAP-hM_2WT with the constitutively expressed HA-CLIP-hM_3RASSL at the surface of live cells. The receptors were labelled with one donor (Lumi4 Tb) and two different acceptors (green and red). The two different acceptors once excited, emitted at distinguishable wavelengths with the green emitting at 520 nm and the red at

665 nm (see diagram in Figure 4.1 B and Figure 5.7). This method allowed for the simultaneous detection of changes in two different sets of oligomeric arrangements i.e. heteromers and homomers, by utilising three different substrates to label a cell population. By using SNAP-Lumi4 Tb as donor and CLIP-Red with SNAP-Green as acceptors the changes in VSV-SNAP-hM_2WT/HA-CLIP-hM_3RASSL heteromers and VSV-SNAP-hM_2WT homomers were detected, respectively. Replacing the SNAP-Lumi4 Tb donor with CLIP-Lumi4 Tb while maintaining the same acceptors, CLIP-Red and SNAP-Green, allowed for changes in HA-CLIP-hM_3RASSL homomers and hM_2WT/hM_3RASSL heteromers to be detected, respectively (Figure 5.7).

Cells labelled with 5 nM SNAP-Lumi4 Tb/ 100 nM CLIP-Red / 100 nM SNAP-Green were subjected to ligand treatments for 40 minutes. Two measurements were taken, one at time 0 minute (prior to ligand addition) and one at 40 minutes (post ligand treatment). The 665/620 and 520/620 ratios, indicative of hM_2WT/hM_3RASSL heteromers and hM_2WT homomers, respectively, were calculated at both time points, for each treatment and statistics were performed to determine whether changes observed were significant. The P values were obtained by carrying out a two paired t-test comparing the ratio at time 0 minutes (untreated) versus time at 40 minutes (treated), for n=3 with each experiment carried out in triplicates.

The donor/acceptor ratio at time 0 min of each treated cell population was compared to the donor/acceptor ratio at time 40 minutes of the same treated cell set and a two tailed, paired t-test was performed for each set. The decrease in 665/620 ratio, corresponded to a significant reduction ($P= 0.04$) in the hM_2WT/hM_3RASSL heteromeric arrangement, in response to 1 mM carbachol (Figure 5.8 A). A significant increase in the 520/620 ratio ($P< 0.0001$) corresponded to an increase in the hM_2WT homomers, in response to carbachol. A significant decrease ($P= 0.006$) in the formation of hM_2WT homomers was also detected in response to 100 μM CNO, a change that was not previously observed in the dual labelling kinetic htrFRET experiments.

In a similar set of experiments the SNAP-Lumi4 Tb donor was replaced with 10 nM CLIP-Lumi4 Tb. The donor/acceptor ratio of 665/620 allowed the detection of an increase in the hM_3RASSL homomeric arrangement ($P= 0.03$), in response to the synthetic ligand CNO (Figure 5.9 A). This increase was only observed in cells that were not treated with doxycycline, thus in the absence of hM_2WT receptor and therefore in the absence of heteromers (Figure 5.9 A). There was no effect detected due to CNO- mediated activation

of hM_3RASSL, in the presence of hM_2WT (Figure 5.9 B). The changes in the hM_2WT/hM_3RASSL heteromeric arrangement, when CLIP-Lumi4 Tb was used as donor were monitored by measuring the 520/620 ratio, in the presence of both receptors. The heteromeric organisation was significantly reduced (P= 0.0001) in response to 1 mM carbachol as shown in Figure 5.9 C.

5.4 Internalisation of receptors in response to agonists

The decrease in the heteromeric arrangement between hM_2WT/hM_3RASSL and the simultaneous increase in the hM_2WT homomerisation, in response to carbachol, along with the relatively slow kinetics of those changes, had led to the hypothesis that receptor internalisation might be playing a role in ligand-mediated oligomerisation. In addition, htrFRET experiments performed at 4˚C, which should inhibit receptor internalisation, blocked the ligand mediated changes in both homomers and heteromers (see Figure 5.4 A and B), suggesting receptor internalisation might be implicated in this process.

To explore receptor internalisation, the cell line co-expressing both the receptors was employed in epi-fluorescence imaging experiments. Cells were grown on cover-slips and were either treated or not with doxycycline. Cells were then co-labelled with cell impermeable fluorescent dyes and internalisation was monitored over a 40 minute period, in the presence of a set concentration of the ligands/treatments. The labelling was performed at least 16 hours post doxycycline induction by co-incubating the cells with 5 μM of each fluorescent dye, CLIP-Surface 488 (green) and SNAP-Surface 549 (red) for 30 minutes. Cells without pre-treatment with doxycycline were only labelled with CLIP-Surface 488, to label the constitutively expressed HA-CLIP-hM_3RASSL.

Carbachol did not have any effect on the hM_3RASSL receptor (green), but seemingly led to hM_2WT (Red) internalisation (Figure 5.10). When the two channels were merged, the co-localisation of the two receptors was observed at the cell surface before the addition of ligand (with a calculated Pearson's correlation co-efficient r^2= 0.815, derived from scatter plot) and then co-localisation was lost as hM_2WT was internalised due to carbachol-mediated activation. The Pearson's correlation coefficient calculated at 40 minutes was decreased to r^2= 0.533.

Addition of 100 μM CNO did not lead to either hM_3RASSL or hM_2WT receptor internalisation (Figure 5.11) with both the receptors remaining at the cell surface.

Similarly, addition of vehicle (HBSS containing 0.33% DMSO to maintain consistency) demonstrated the lack of internalisation for both receptors (Figure 5.12). In an attempt to study hM_3RASSL internalisation, in the absence of hM_2WT, cells not treated with doxycycline were used. In those cells neither addition of CNO nor carbachol showed any signs of receptor internalisation (Figure 5.13).

An alternative approach to assess the extent of receptor internalisation, in response to ligand treatment in live cells, involved the combination of SNAP/CLIP-Lumi4 Tb labelling of the receptors and the Tag-lite® internalisation buffer containing the ligand treatments. The internalisation buffer possesses spectral properties (able to emit at 520 nm upon excitation at 490 nm) compatible with the Lumi4 Tb donors and can be used as an energy acceptor for the internalisation FRET assay. Cells inducibly expressing the VSV-SNAP-hM_2WT and the HA-CLIP-hM_3RASSL in a constitutive manner were labelled with SNAP-Lumi4 Tb or CLIP-Lumi4 Tb for an hour, prior to application of the ligand treatments. The FRET signal between the Lumi4 Tb and internalisation buffer was monitored. The ratio was calculated as *(donor/acceptor channel) x* 10^4 with any changes observed in the 620/520 ratio corresponded to changes in receptor internalisation. The percentage of maximal internalisation was calculated.

Internalisation of VSV-SNAP-hM_2WT was mediated upon stimulation with 1 mM carbachol and also when 1mM carbachol was co-added with 100 μM CNO, in cells expressing both receptors. Vehicle and addition of 10 μM atropine did not result in receptor internalisation, as expected (Figure 5.14 A). In another set of cells, not treated with doxycycline, thus expressing only the constitutive HA-CLIP-hM_3RASSL, internalisation was observed in response to 100 μM CNO, but also when CNO was used in combination with 1 mM carbachol. The HA-CLIP-hM_3RASSL demonstrated some level of internalisation in the absence of ligands, and in the presence of the antagonist atropine (Figure 5.14 B). This could probably correspond to the basal signal or it could be originating from constitutive receptor internalisation. In cells expressing both receptors, HA-CLIP-hM_3RASSL internalised upon CNO stimulation, but when CNO was co-added with carbachol, the internalisation level dropped to values close to basal (Figure 5.14 C).

The contradicting results concerning hM_3RASSL internalisation between epi-fluorescence microscopy and Tag-lite® internalisation approaches were probably due to the difference in sensitivity between the two methods. The Tag-lite® internalisation is a more sensitive technique, allowing detection of changes more efficiently than epi-fluorescence

microscopy. The more efficient labelling of the receptors with the Lumi4 Tb substrates, using relative high concentrations reaching 100 nM for SNAP-Lumi4 Tb and 200 nM for CLIP-Lumi4 Tb (20 fold more than those used in the rest of htrFRET experiments) also contributed to the sensitivity of the internalisation assay compared to the epi-fluorescence microscopy.

5.5 Discussion

The key points of this chapter include the observation of the agonist mediated changes in oligomerisation organisation of the receptors demonstrated by dual and triple labelling kinetic htrFRET approaches. The decrease in the hM_2WT/hM_3RASSL heteromer and the simultaneous increase in the hM_2WT homomer, leaving the hM_3RASSL homomer unaffected, in response to the agonist carbachol, were detected using both the dual and triple labelling htrFRET. In cells inducibly expressing the VSV-SNAP-hM_2WT receptor alone, a similar increase in homomer formation was detected, demonstrating similar kinetics, in response to carbachol. In order to rule out the possibility of inefficient CLIP-labelling (compared to the very efficient SNAP labelling as suggested by Pou *et al.*, 2010) that may be interfering with the detection of changes in the hM_3RASSL homomerisation, a cell line expressing the VSV-SNAP-hM_3RASSL receptor alone was employed for dual labelling with SNAP-specific substrates and subsequent kinetic htrFRET experiments. This had led to the suggestion that CNO did not affect the homomerisation of hM_3RASSL. Surprisingly, when using the multiplex labelling approach, employing CLIP-Lumi4 Tb as an energy donor to study the simultaneous changes in the system, a significant increase in the hM_3RASSL homomer was detected in response to CNO, in the absence of hM_2WT. This increase in hM_3RASSL homomers was not detected in the presence of hM_2WT/hM_3RASSL heteromers. Another novel observation offered by the multiplex labelling approach, using SNAP-Lumi4 Tb as an energy donor, involved the detection of an increase in the hM_2WT homomer in response to CNO (Figure 5.8 B) that could be due to down-regulation of the heteromer organisation. A possible explanation for the more efficient detection of agonist mediated changes in oligomerisation, with multiplex labelling, could relate to the more efficient labelling of the receptors as more substrate was added to the receptors being studied, making the approach more sensitive in detecting those changes.

Resonance energy transfer methods allow the detection of the real time interactions between donor and acceptor species and suggest possible receptor-receptor interactions

without being able to distinguish between dimers or higher order oligomers. The changes in the htrFRET signals or the ratios upon ligand treatment could be due to conformational changes within pre-existing oligomers, rather than alterations in the number of oligomers or due to formation of new oligomeric complexes or breaking of pre-existing ones. Those conformational rearrangements mediated by ligands could be modifying the distance between the donor and acceptor species, without rearranging the oligomeric complex as a whole. That could explain the increase in hM_2WT homomers and the simultaneous decrease in the hM_2WT/hM_3RASSL heteromers, leaving the hM_3RASSL unaffected. The CNO mediated stimulation of hM_3RASSL may be modifying the distance between the donor/acceptor but not in an extent as to allow detection of changes in the homomer.

The carbachol mediated heteromer decrease and the simultaneous hM_2WT homomer increase were reversed upon incubation at 4˚C, suggesting possible involvement of receptor internalisation in the regulation of oligomerisation. The changes that were initially thought to be due to ligand-mediated actions could be a consequence of the hM_2WT internalisation rather than hM_2WT/hM_3RASSL heteromer down-regulation. According to the epi-fluorescence microscopy based internalisation experiments the hM_2WT receptor was readily internalised in response to carbachol treatment, leaving the hM_3RASSL at the cell surface. The hM_3RASSL demonstrated some degree of internalisation in response to CNO, detected by the Tag-lite® internalisation assay, possibly due to the higher sensitivity of the method compared to the low spatial resolution of light microscopy. These observations were in agreement with the suggestion by Zeng and Wess, (1999) that M_2 receptor undergoes agonist induced down-regulation to a higher extent than M_3 and that M_2 internalisation could be involved in the M_2/M_3 heteromer down-regulation (Zeng and Wess, 1999). The agonist mediated internalisation and down-regulation of hM_2WT receptor has also been suggested previously (Tsuga *et al.*, 1998; Schlador *et al.*, 2000), whereas the hM_3WT or hM_3RASSL receptor did not demonstrate a great degree of internalisation upon agonist treatment (Alvarez-Curto *et al.*, 2010).

To assess the role of internalisation in regulating receptor oligomerisation, a whole set of experiments could be planned for future work. An example could include the use of receptors that have been modified in order to develop non-internalising mutants, and those could be then used in combination with the Tag-lite® technology and htrFRET method, in a similar manner described in this chapter. A receptor modified in such a way as to confer inability to internalise could be useful in studying the role of internalisation in oligomer formation. Assessing the role of oligomerisation in trafficking and endoplasmic reticulum

(ER) export would also be advantageous in answering key questions on the receptor oligomerisation mechanism. In addition, assessing the conformational modifications within the oligomeric structure could be useful by performing intramolecular FRET experiments that could detect possible changes in the intramolecular domains in response to receptor activation in a similar manner that was described in Alvarez-Curto *et al.*, (2011).

A.

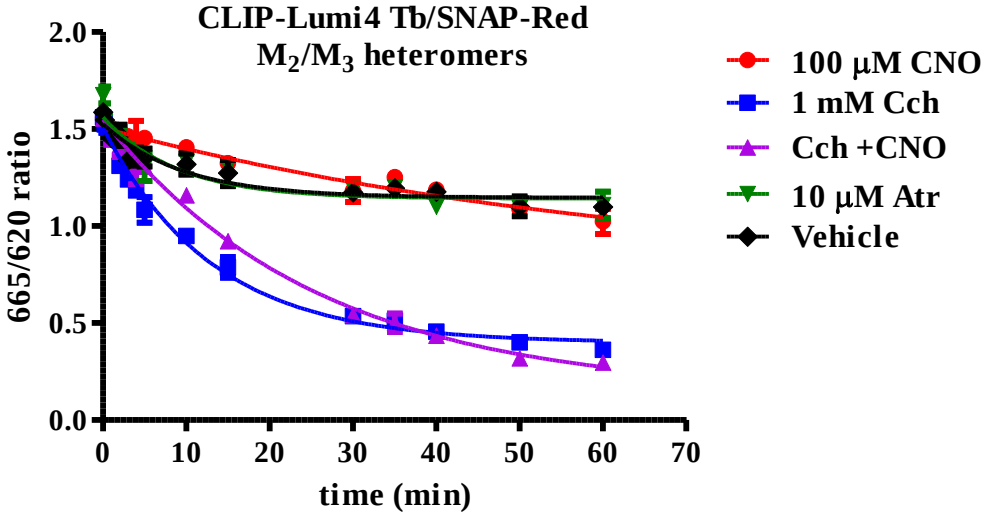
CLIP-Lumi4 Tb/SNAP-Red
M2/M3 heteromers
665/620 ratio
time (min)
100 µM CNO
1 mM Cch
Cch +CNO
10 µM Atr
Vehicle

B.

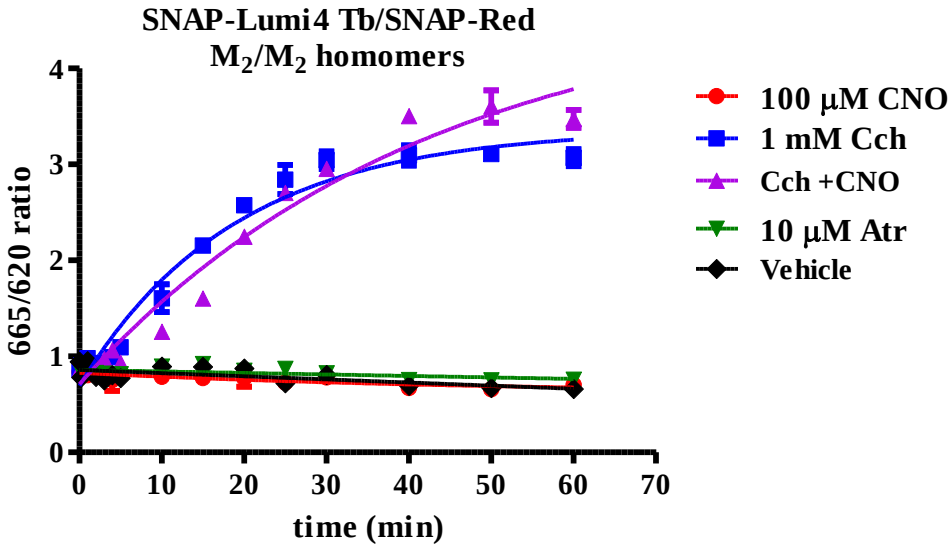
SNAP-Lumi4 Tb/SNAP-Red
M2/M2 homomers
665/620 ratio
time (min)
100 µM CNO
1 mM Cch
Cch +CNO
10 µM Atr
Vehicle

C.

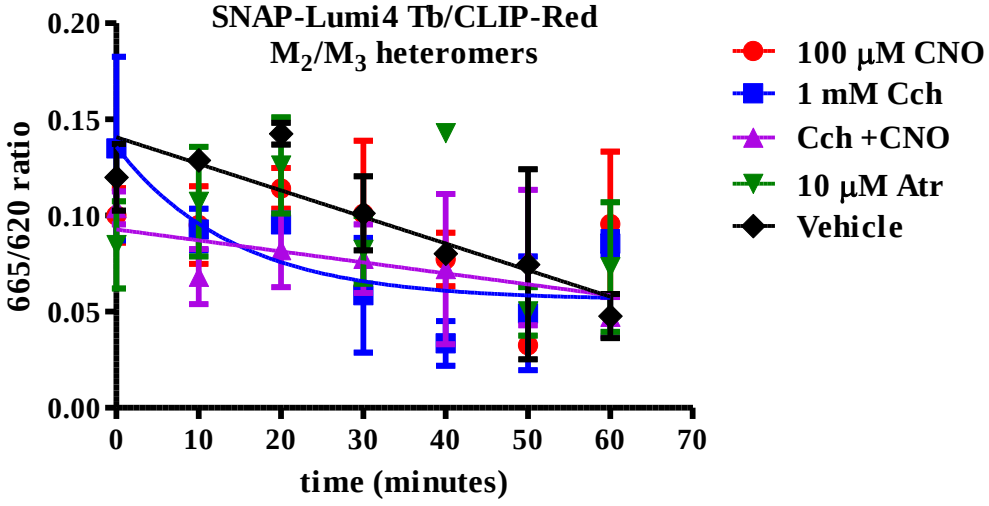
SNAP-Lumi4 Tb/CLIP-Red
M2/M3 heteromers
665/620 ratio
time (minutes)
100 µM CNO
1 mM Cch
Cch +CNO
10 µM Atr
Vehicle

D.

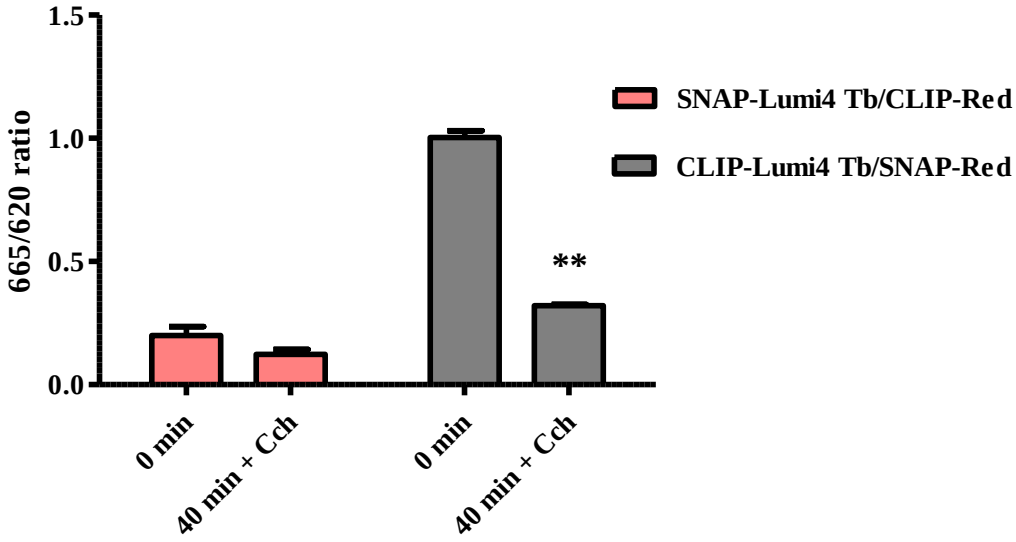

Figure 5.1 Carbachol mediated decrease in hM$_2$WT/hM$_3$RASSL heteromers and a simultaneous increase in hM$_2$WT homomers, by kinetic htrFRET. Cells expressing the VSV-SNAP-hM$_2$WT in a doxycycline inducible manner and the HA-CLIP-hM$_3$RASSL constitutively, were treated with 5 ng·ml^{-1} doxycycline for 24 hours and then subjected to co-labelling with **(A)** 10 nM CLIP-Lumi4 Tb and 125 nM SNAP-Red, and treated with a series of muscarinic ligands with the FRET ratio being monitored for 60 minutes. The heteromeric arrangement of VSV-SNAP-hM$_2$WT/HA-CLIP-hM$_3$RASSL was reduced in response to 1 mM carbachol and to the combination treatment of carbachol (1 mM) with CNO (100 μM). CNO alone did not have any effect on the heteromerisation nor did atropine and Vehicle (no ligand treatment; labelling medium containing 0.33% DMSO to maintain consistency). **(B)** Another set of doxycycline treated cells were co-labelled with 5 nM SNAP-Lumi4 Tb and 100 nM SNAP-Red to allow detection of VSV-SNAP-hM$_2$WT homomers. Treatment with 1 mM carbachol showed an increase in the homomer formation. The treatment combining both carbachol and CNO also resulted in an increase inVSV-SNAP-hM$_2$WT homomers. **(C)** Cells co-expressing the receptors were co-labelled with 5 nM SNAP-Lumi4 and 100 nM CLIP-Red to allow detection of VSV-SNAP-hM$_2$WT/HA-CLIP-hM$_3$RASSL heteromers. No significant changes in the kinetic htrFRET were detected upon ligand addition when using this donor/acceptor combination. Data in A, B and C are form a represenatative experiment carried out in triplicates. the experiment was repeated two more times but data could not be pooled together due to differences in 620 fluorescence. **(D)** Comparison between changes detected in VSV-SNAP-hM$_2$WT/HA-CLIP-hM$_3$RASSL heteromer in response to 1 mM Cch, of cells labelled with SNAP-Lumi4 Tb as donor and CLIP-Red as acceptor (pink bars) versus cells labelled with CLIP-Lumi4 Tb as donor and SNAP-Red as acceptor (grey bars). The reduction in VSV-SNAP-hM$_2$WT/HA-CLIP-hM$_3$RASSL heteromeric arrangement in response to 1 mM Cch was statistically significant (** P= 0.0013) when CLIP-Lumi4 Tb was used as donor and that was the reason for the choice of this donor/acceptor combination for the kinetic htrFRET experiments. P values were calculated by performing a two paired t-test, comparing the ratio at time 0 minutes(untreated) to time 40 minutes(treated), for n=3 (each experiment was carried out in triplicates).

A.

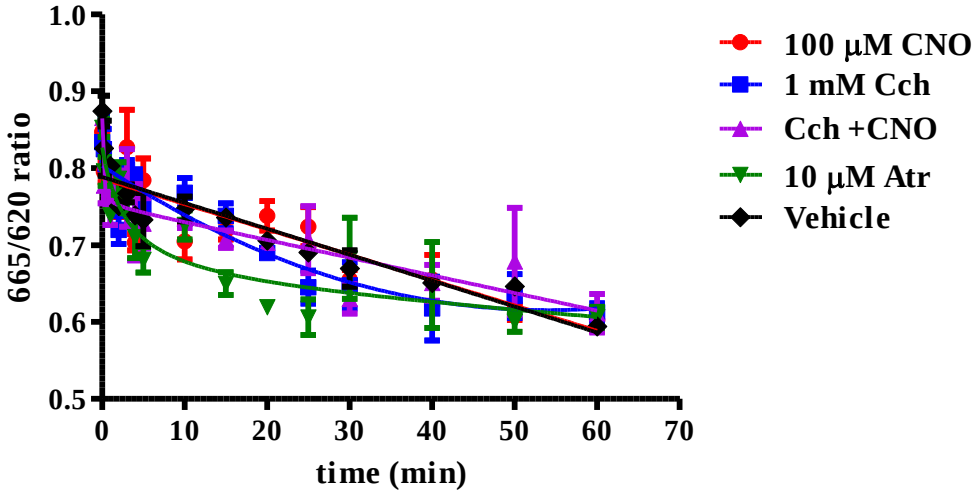

B.

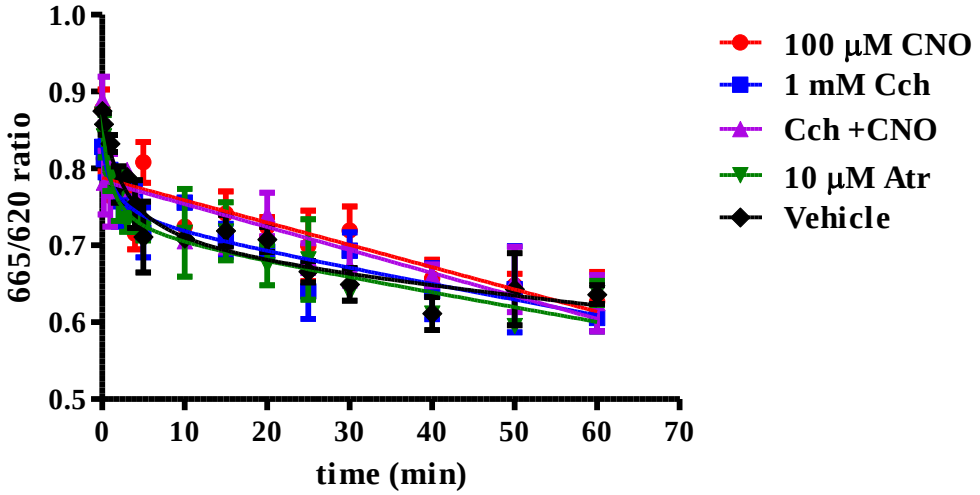

Figure 5.2 hM_3RASSL homomeric organisation is not affected by ligands either in the presence or absence of heteromers or hM_2WT homomers. (A) Cells either not treated with doxycycline or **(B)** treated with 5 ng·ml^{-1} doxycycline were labelled with 10 nM CLIP-Lumi4 Tb and 100 nM CLIP-Red to assess any changes within the HA-CLIP-hM_3RASSL homomers, upon addition of ligands. There was not a significant change observed in the 665/620 ratio, in response to any of the ligands added. There was a overall decline in the 665/620 ratio, that probably corresponds to the decrease in the 665 nm signal due to photo-bleaching.

A.

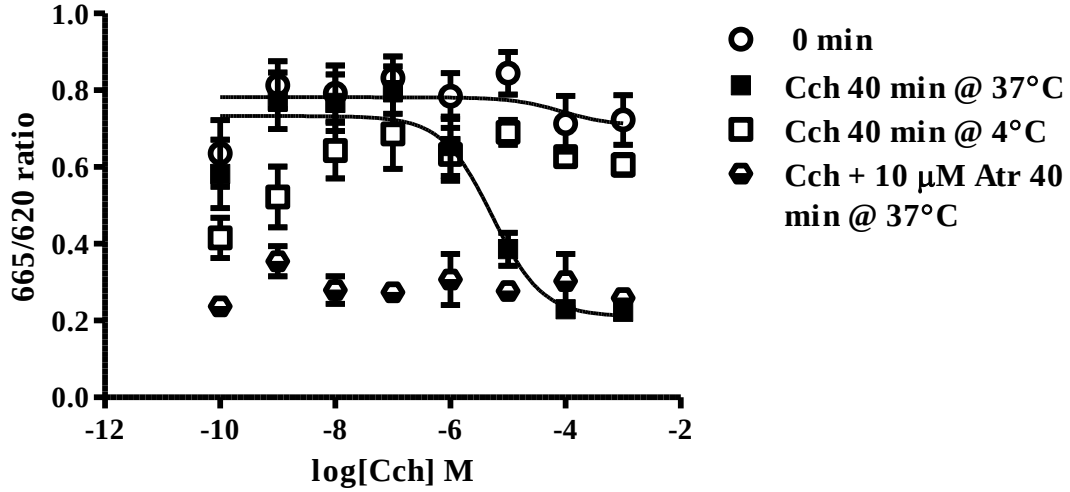

B.

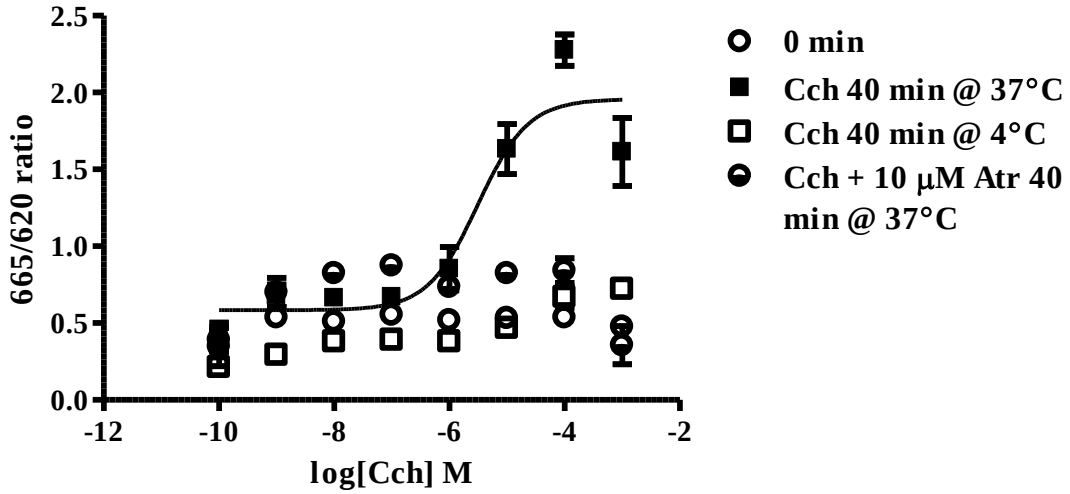

Figure 5.3 Effects of carbachol on oligomerisation are concentration dependent. Experiments involving addition of carbachol dose response concentrations were performed using cells treated with 5 $ng \cdot ml^{-1}$ doxycycline to allow co-expression of both VSV-SNAP-hM_2WT with the constitutively expressed HA-CLIP-hM_3RASSL. Measurements carried out twice, one at 0 minutes- before drug addition and one at 40 minutes-after drug addition. **(A)** The reduction in hM_2WT/hM_3RASSL heteromer in response to increasing concentrations of carbachol after 40 minutes treatment of cells co-labelled with 10 nM CLIP-Lumi4 Tb and 125 nM SNAP-Red led to an estimation of pIC_{50}= 5.3± 0.3. **(B)** Increase in the hM_2WT homomeric arrangement using cells co-labelled with 5 nM SNAP-Lumi4 Tb and 100 nM SNAP-Red, with calculated pEC_{50}= 5.5± 0.2. (Mean +/- SEM, n=4 for all treatments and n=2 for the treatments at 4˚C, experiments carried out in triplicate wells). The carbachol mediated effects were reversed when ligand treatments were carried out at 4˚C (open triangles). Co-incubation of carbachol with the muscarinic antagonist atropine reversed the increase in hM_2WT homomers.

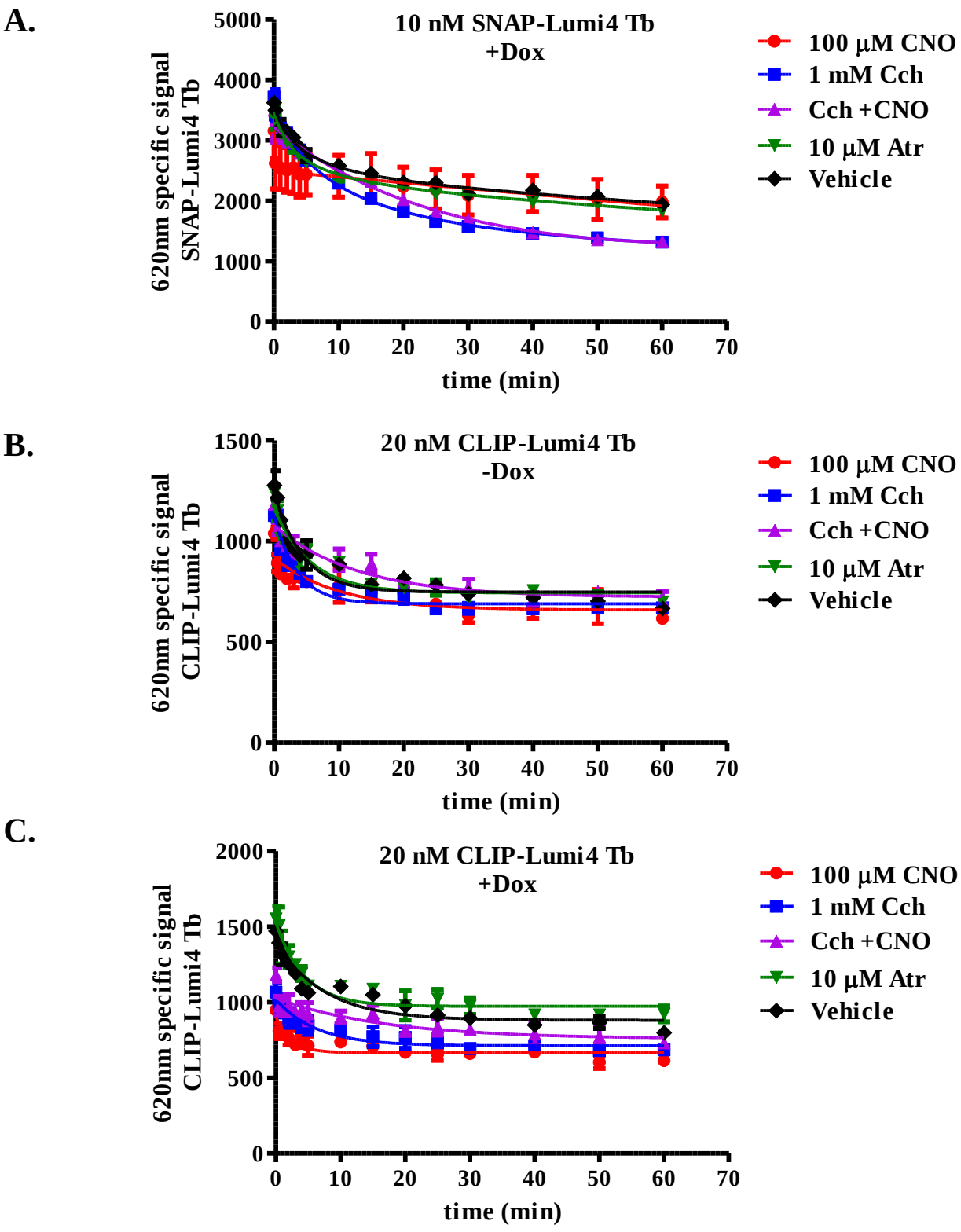

Figure 5.4 Monitoring cell surface receptor population upon ligand treatments. (A) Cells treated with 5 ng·ml^{-1} doxycycline to express both receptors were labelled with 10 nM SNAP-Lumi4 Tb and were then treated with ligands. A non- significant (P>0.05) trend towards a reduction in 620 nm fluorescence, corresponding to hM_2WT receptors was detected in response to carbachol. **(B)** Cells not treated with doxycycline and thus, expressing only the constitutive hM_3RASSL were labelled with 20 nM CLIP-Lumi4 Tb. Ligand treatments did not affect 620 nm signal. **(C)** Cells treated with 5 ng·ml^{-1}

doxycycline to express both receptors were labelled with 20 nM CLIP-Lumi4 Tb. No change in the 620 nm signal was detected upon ligand treatments.

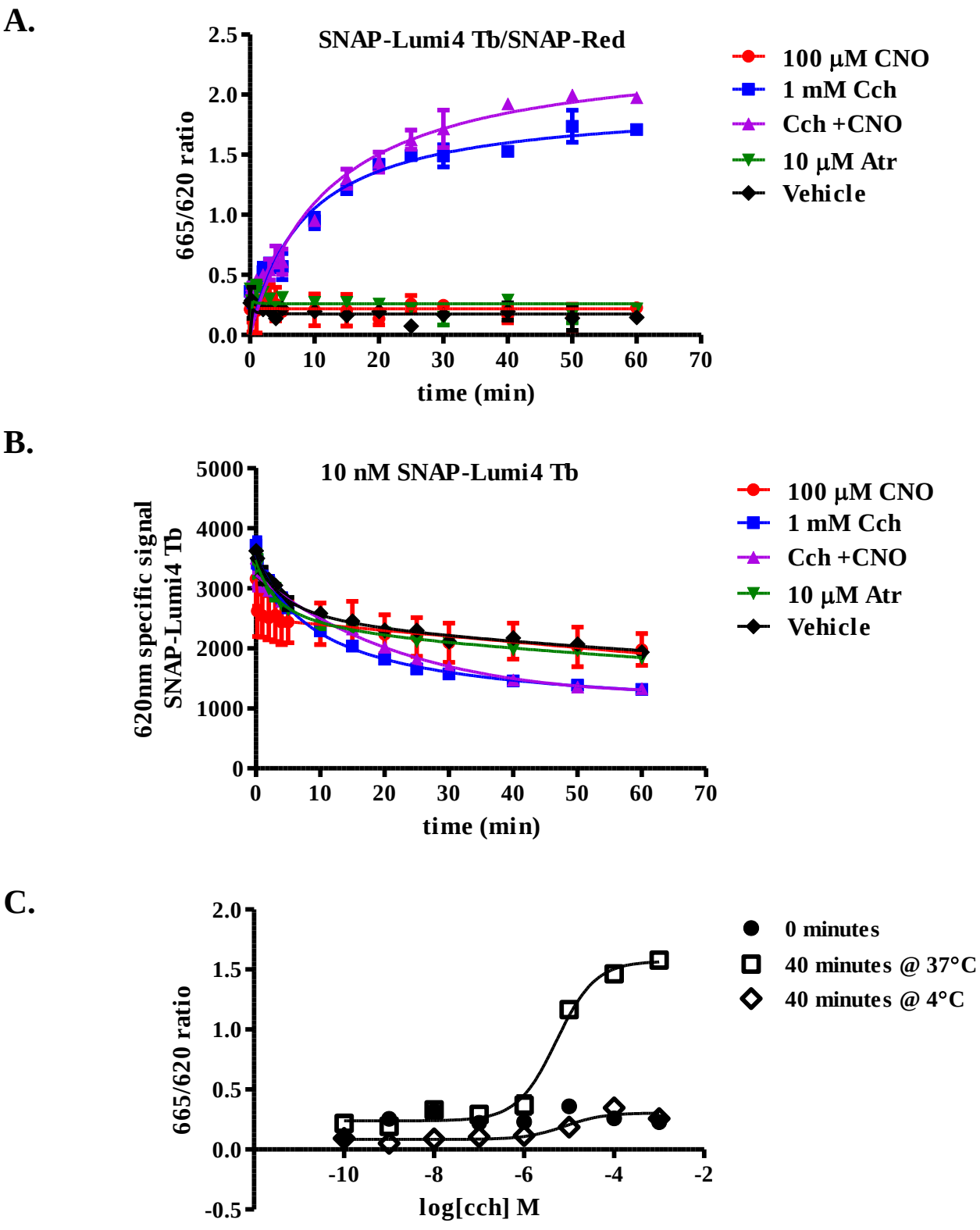

Figure 5.5 Ligand regulation of hM$_2$WT homomers in the absence of hM$_3$RASSL. Cells expressing VSV-SNAP-hM$_2$WT receptor alone upon doxycycline induction were used to assess the regulation of hM$_2$WT homomerisation in the absence of heteromers **(A)** Cells co-labelled with 5 nM SNAP-Lumi4 Tb and 100 nM SNAP-Red were employed in a kinetic htrFRET assay. There was an increase in homomeric profile in response to carbachol and in response to combination treatment of carbachol and CNO, with similar kinetics, while CNO alone had no effect on hM$_2$WT homomerisation. **(B)** Monitoring the

620 nm fluorescence after labelling of cells with 10 nM SNAP-Lumi4 Tb detected a trend towards a decrease in the cell surface hM_2WT population. **(C)** Cells co-labelled with 5 nM SNAP-Lumi4 Tb and 100 nM SNAP-Red demonstrated an increase in the homomerisation of VSV-SNAP-hM_2WT in response to carbachol which was concentration dependent (pEC_{50}= 5.28 ± 0.08) (Mean +/- SEM, n=4 for all treatments and Mean +/- Range, n=2 for treatments at 4˚C), and was completely abolished by incubation at 4˚C.

A.

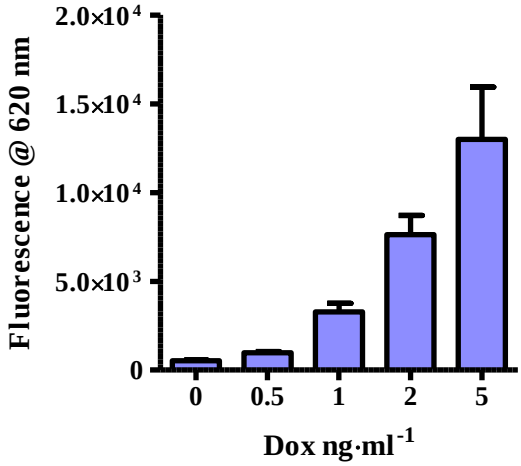
Fluorescence @ 620 nm
2.0×10⁴
1.5×10⁴
1.0×10⁴
5.0×10³
0
0
0.5
1
2
5
Dox ng·ml⁻¹

B.

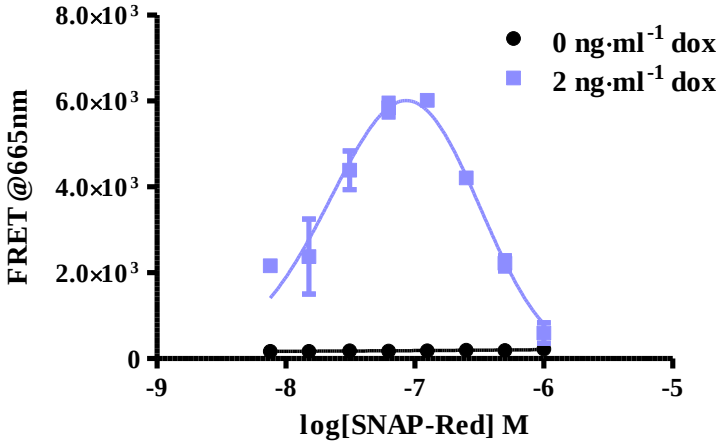
FRET @665nm
8.0×10³
6.0×10³
4.0×10³
2.0×10³
0
0 ng·ml⁻¹ dox
2 ng·ml⁻¹ dox
-9
-8
-7
-6
-5
log[SNAP-Red] M

C.

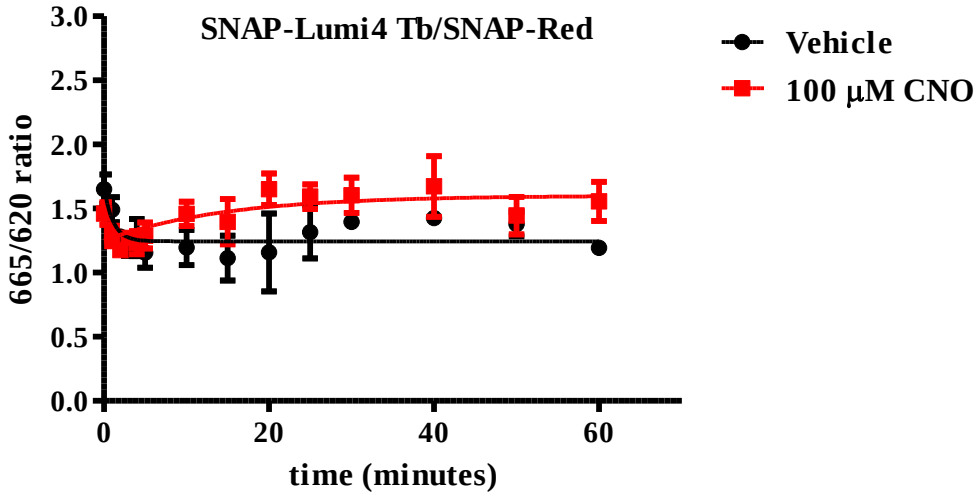
SNAP-Lumi4 Tb/SNAP-Red
665/620 ratio
3.0
2.5
2.0
1.5
1.0
0.5
0.0
0
20
40
60
time (minutes)
Vehicle
100 µM CNO

D.

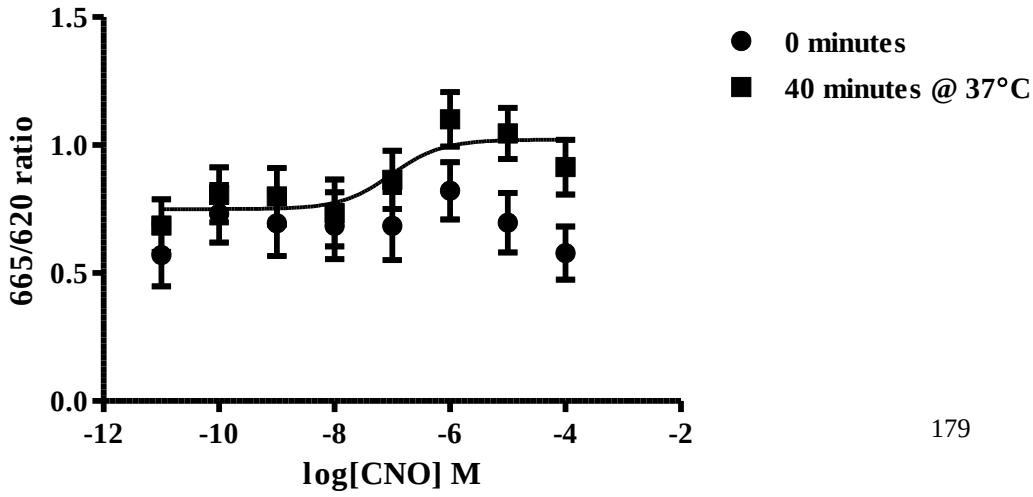
665/620 ratio
1.5
1.0
0.5
0.0
-12
-10
-8
-6
-4
-2
log[CNO] M
0 minutes
40 minutes @ 37°C

Figure 5.6 Assessing VSV-SNAP-hM$_3$RASSL receptor homomerisation. In order to assess the possible effect of the SNAP or CLIP tags on receptor oligomerisation a cell line was used able of expressing VSV-SNAP-hM$_3$RASSL after doxycycline induction. **(A)** Labelling of live cells stably expressing VSV-SNAP-hM$_3$RASSLdemonstrated an increase in receptor expression at the cell surface with increasing doxycycline concentrations. **(B)** Detection of VSV-SNAP-hM$_3$RASSL homomers at the cell surface of live cells following co-labelling with 5 nM SNAP-Lumi4 Tb and varying concentrations of SNAP-Red was in agreement with the existence of HA-CLIP-hM$_3$RASSL homomers. **(C)** The kinetic htrFRET showed no significant change in the homomerisation of the SNAP-tagged receptor, which is similar to that seen with the CLIP-tagged receptor. **(D)** No effect was detected following addition of increasing concentrations of CNO while monitoring the 665/620 ratio at set time points of 0 and 40 minutes.

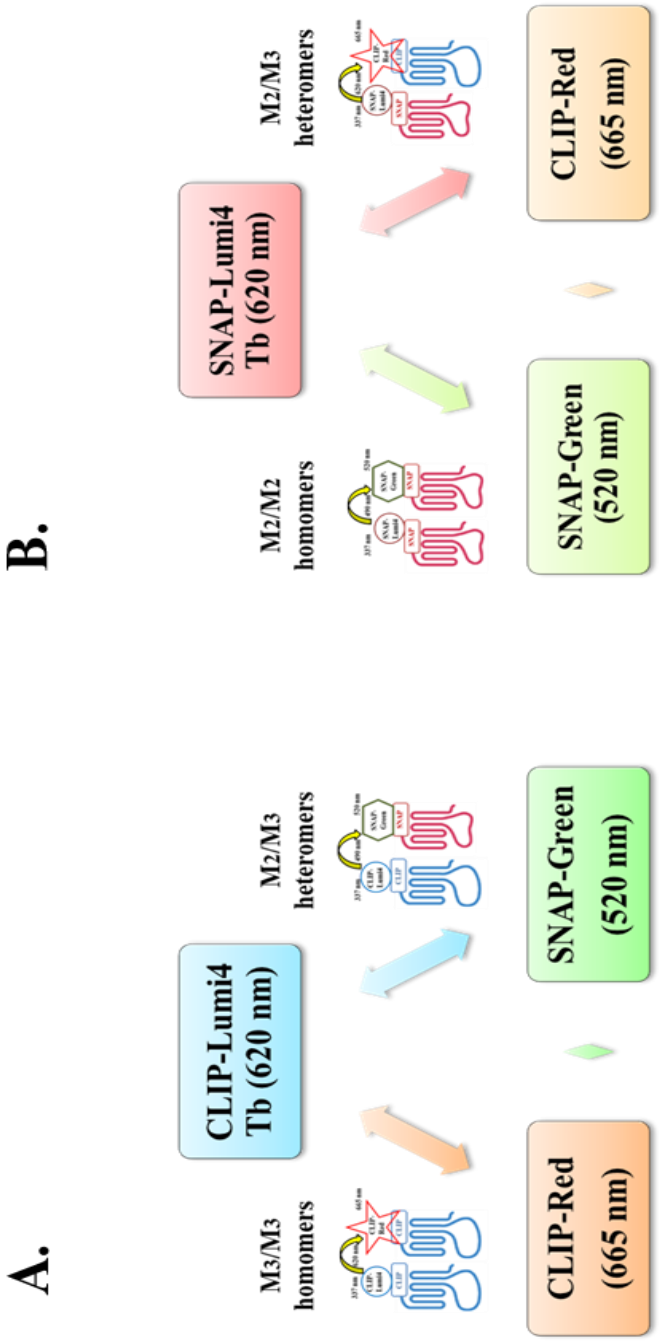

Figure 5.7 Schematic representation of multiplex (triple) labelling approach to detect simultaneous changes in receptor oligomerisation. This method utilises labelling of live cells with three different substrates, one donor (Lumi4 Tb) and two acceptor species (green and red). Lumi4 Tb donor emits at four different wavelengths, upon excitation at 337 nm. Emission at 490 nm excites the green acceptors which in turns emit at 520 nm. Emission at 620 nm excites the red acceptors that subsequently emit at 665 nm. The multiplex labelling was followed using **(A)** CLIP-Lumi4 Tb as a donor in combination with CLIP-Red and SNAP-Green acceptors to detect simultaneous changes in M_3/M_3 homomeric and M_2/M_3 heteromeric arrangements, respectively. **(B)** SNAP-Lumi4 Tb as donor with SNAP-Green and CLIP-Red acceptors to detect M_2/M_2 homomers and M_2/M_3 heteromers, respectively.

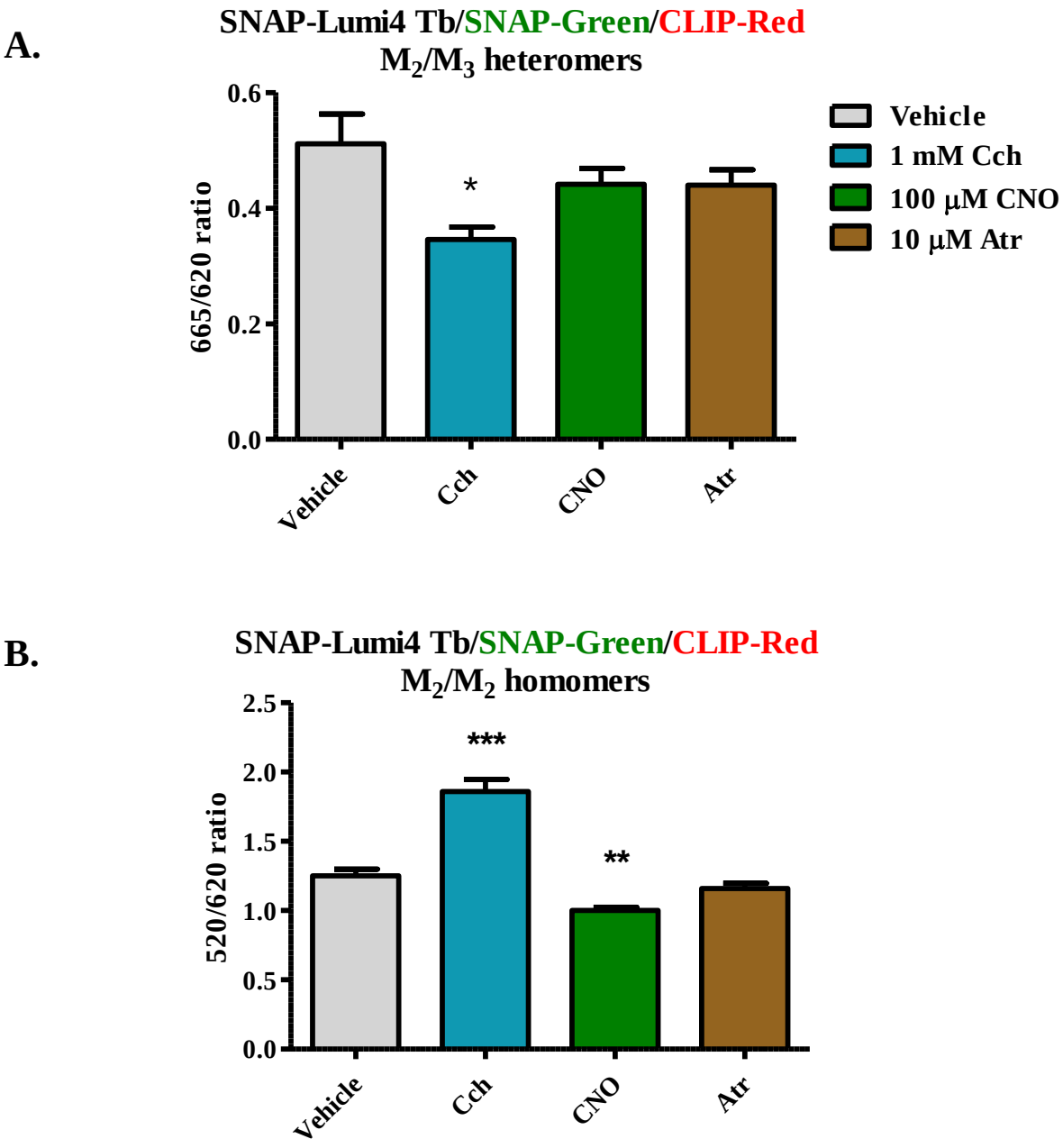

Figure 5.8 Triple labelling with SNAP-Lumi4 Tb as donor. Cells treated with doxycycline to enable co-expression of both VSV-SNAP-hM_2WT and HA-CLIP-hM_3RASSL receptors were labelled with three substrates; SNAP-Lumi4 Tb as donor and SNAP-Green and CLIP-Red as acceptors. Treatments with ligands were carried out for 40 minutes and the signal originating from the red emitting acceptor **(A)** was monitored at 665 nm, with the 665/620 ratio showing a decrease in the heteromer formation in response to 1 mM carbachol (* P= 0.04). **(B)** The signal from the green emitting acceptor was read at 520 nm and the 520/620 ratio was increased in response to 1 mM carbachol (*** P<0.0001), corresponding to an increase in the hM_2WT homomers, with a simultaneous decrease upon treatment with CNO (** P=0.006) suggesting a decrease in the homomeric arrangement of hM_2WT when the co-expressed hM_3RASSL was stimulated. (Mean +/- SEM, n=3, all experiments were carried out in triplicate points).

A.

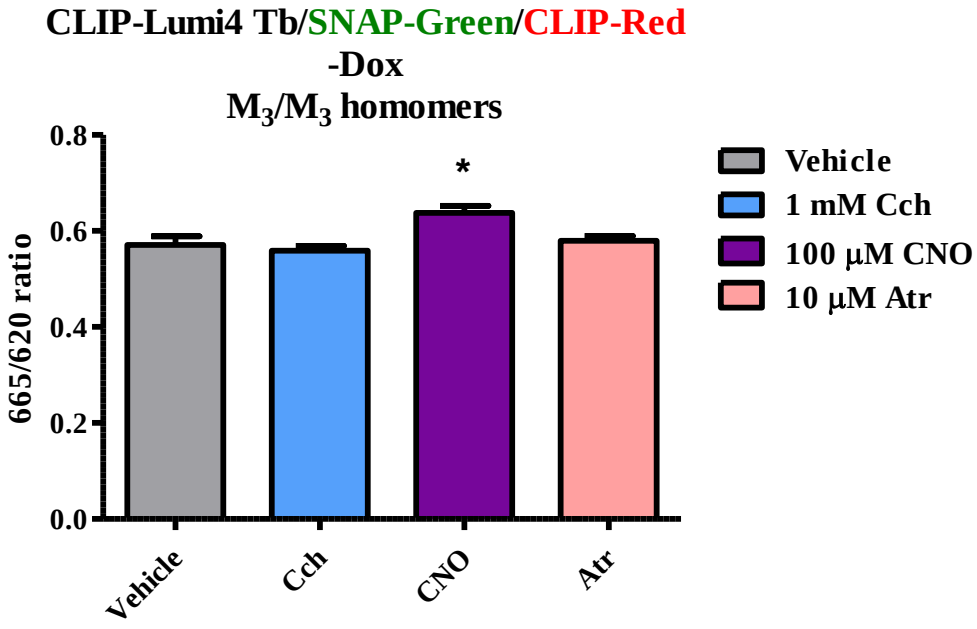
CLIP-Lumi4 Tb/SNAP-Green/CLIP-Red
-Dox
M3/M3 homomers
665/620 ratio
0.8
0.6
0.4
0.2
0.0
*
Vehicle
Cch
CNO
Atr
Vehicle
1 mM Cch
100 µM CNO
10 µM Atr

B.

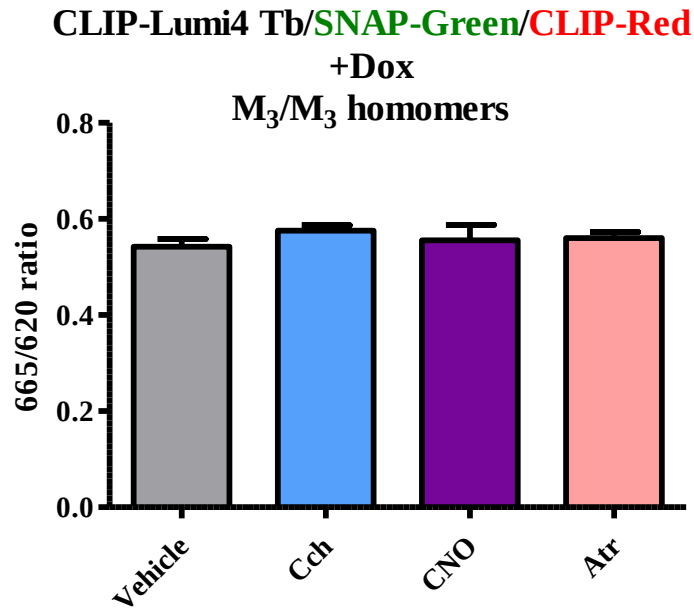
CLIP-Lumi4 Tb/SNAP-Green/CLIP-Red
+Dox
M3/M3 homomers
665/620 ratio
0.8
0.6
0.4
0.2
0.0
Vehicle
Cch
CNO
Atr

C.

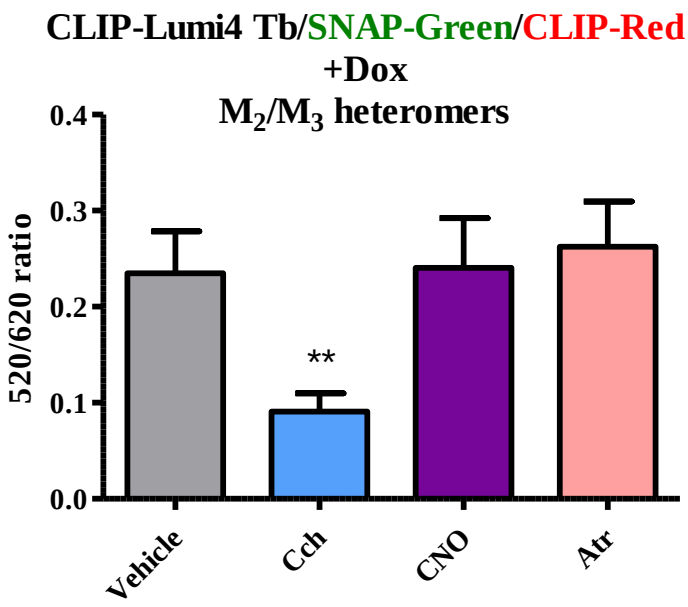

Figure 5.9 Triple labelling with CLIP-Lumi4 Tb as donor. Cells able of expressing both the receptors were either treated or not with doxycycline and were then labelled with three different substrates with CLIP-Lumi4 Tb acting as energy donor and SNAP-Green and CLIP-Red as acceptors. **(A)** Cells not treated with doxycycline, thus only expressing the constitutive HA-CLIP-hM_3RASSL, were labelled with the three substrates and then treated with ligands for 40 minutes with the signal at 665 nm being monitored. The treatment with CNO resulted in a significant increase in the hM_3RASSL homomeric arrangement (* P= 0.03). **(B)** Cells treated with 5 ng·ml^{-1} doxycycline, thus in the presence of VSV-SNAP-hM_2WT/HA-CLIP-hM_3RASSL heteromers did not demonstrate any changes in h$M3_R$ASSL homomeric arrangement. **(C)** The simultaneous monitoring of 520 nm fluorescence originating from the green acceptor, using cells treated with doxycycline demonstrated a decrease in the heteromeric profile of the receptors in response to carbachol (** P= 0.0001). P values were calculated by performing a two-paired t-test, comparing the ratios obtained from vehicle treated cells versus drug treated cells, 40 minutes after treatments. (Mean +/- SEM, n=3, all experiments were carried out in triplicate wells).

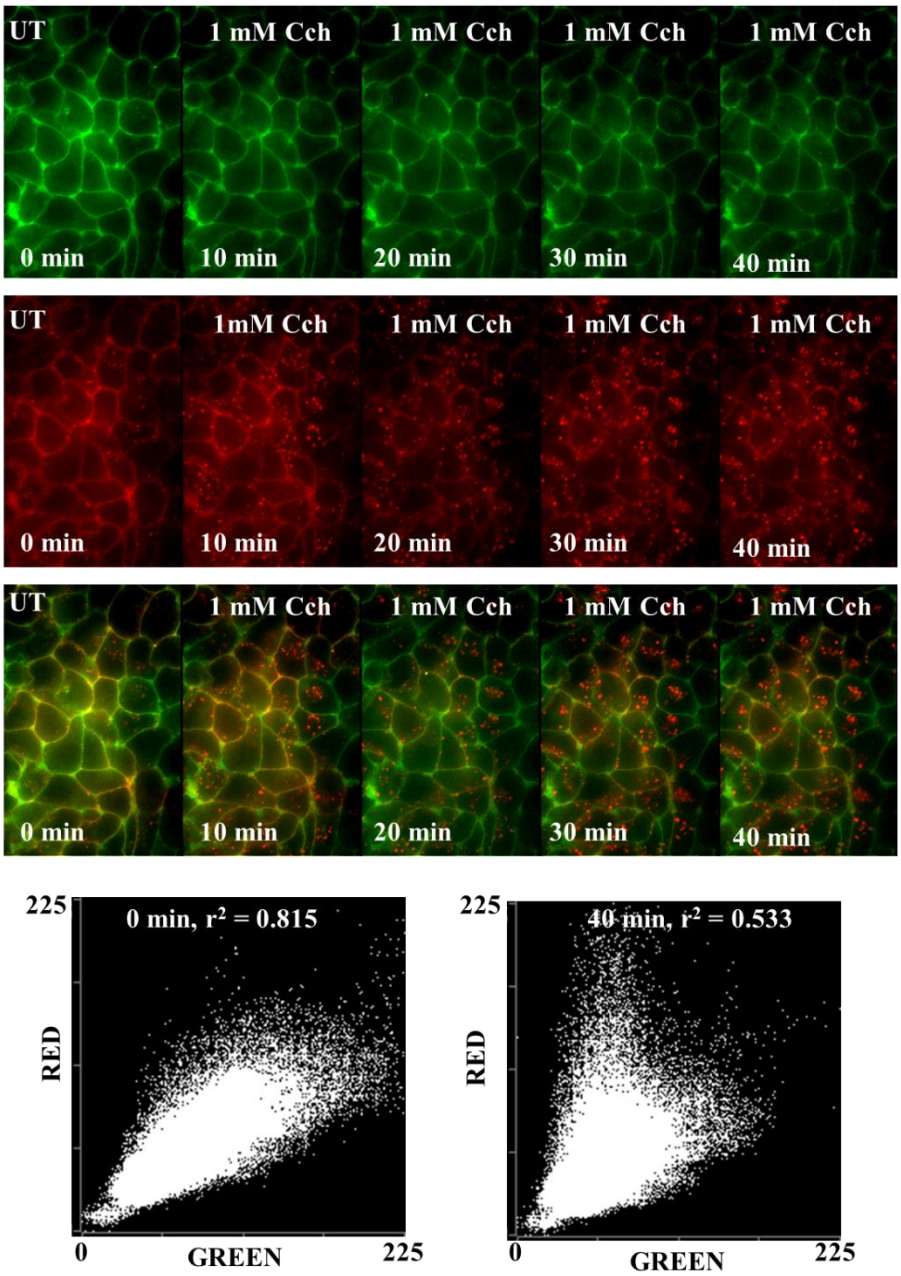

Figure 5.10 VSV-SNAP-hM$_2$WT receptor internalised in response to carbachol as detected by epi-fluorescence imaging. Live cells were plated on glass cover slips and treated with 5 ng·ml^{-1} doxycycline for at least 16 hours, thus able to express both the receptors, VSV-SNAP-hM$_2$WT and HA-CLIP-hM$_3$RASSL. Cells were co-labelled with cell impermeant fluorescent dyes, CLIP-Surface 488 and SNAP-Surface 549. Cells were then treated with 1 mM carbachol and images were captured to detect internalisation of the receptors. The green labelled hM$_3$RASSL did not show any internalisation, in response to carbachol, but the red labelled hM$_2$WT internalised upon stimulation with the agonist carbachol. Merging of the images allowed the detection of co-localisation of the two receptors that was lost upon stimulation and internalisation of hM$_2$WT. The Pearson's correlation coefficient was calculated from the scatter plots, demonstrating the initial co-localisation of the two differentially tagged receptors (r^2= 0.815) prior to treatment with the agonist and loss of co-localisation due to internalisation after 40 minutes of agonist treatment (r^2= 0.533).

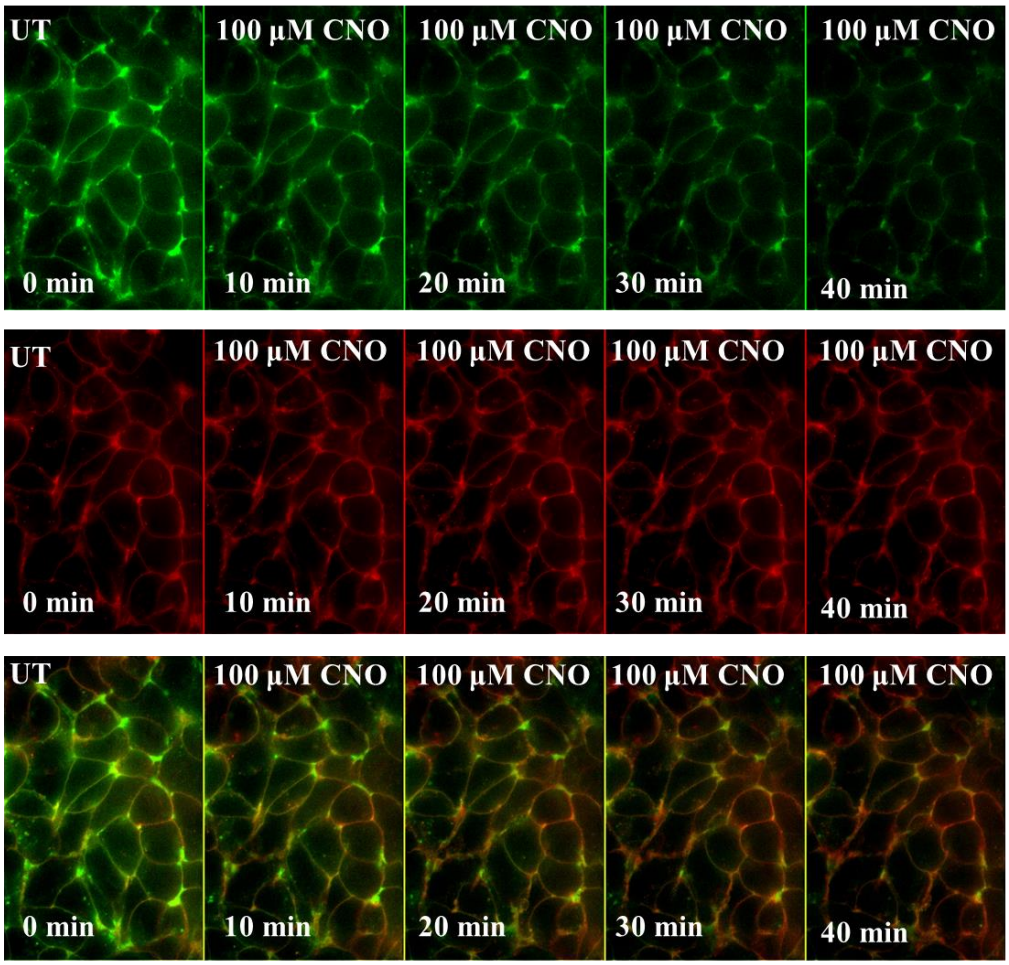

Figure 5.11 CNO does not mediate receptor internalisation. Live cells were plated on cover slips and treated with 5 ng·ml-1 doxycycline for at least 16 hours, to allow co-expression of both receptors. Cells were then co-labelled with cell impermeant fluorescent dyes, CLIP-Surface 488 and SNAP-Surface 549. Treatments with 100 µM CNO followed and images were captured at several time points to detect potential receptor internalisation. The green fluorescing hM_3RASL did not internalise upon stimulation with the synthetic ligand CNO, although it seemed that intensity was lost, possibly due to photo-bleaching. The red fluorescing hM_2WT receptor did not internalise upon addition of CNO.

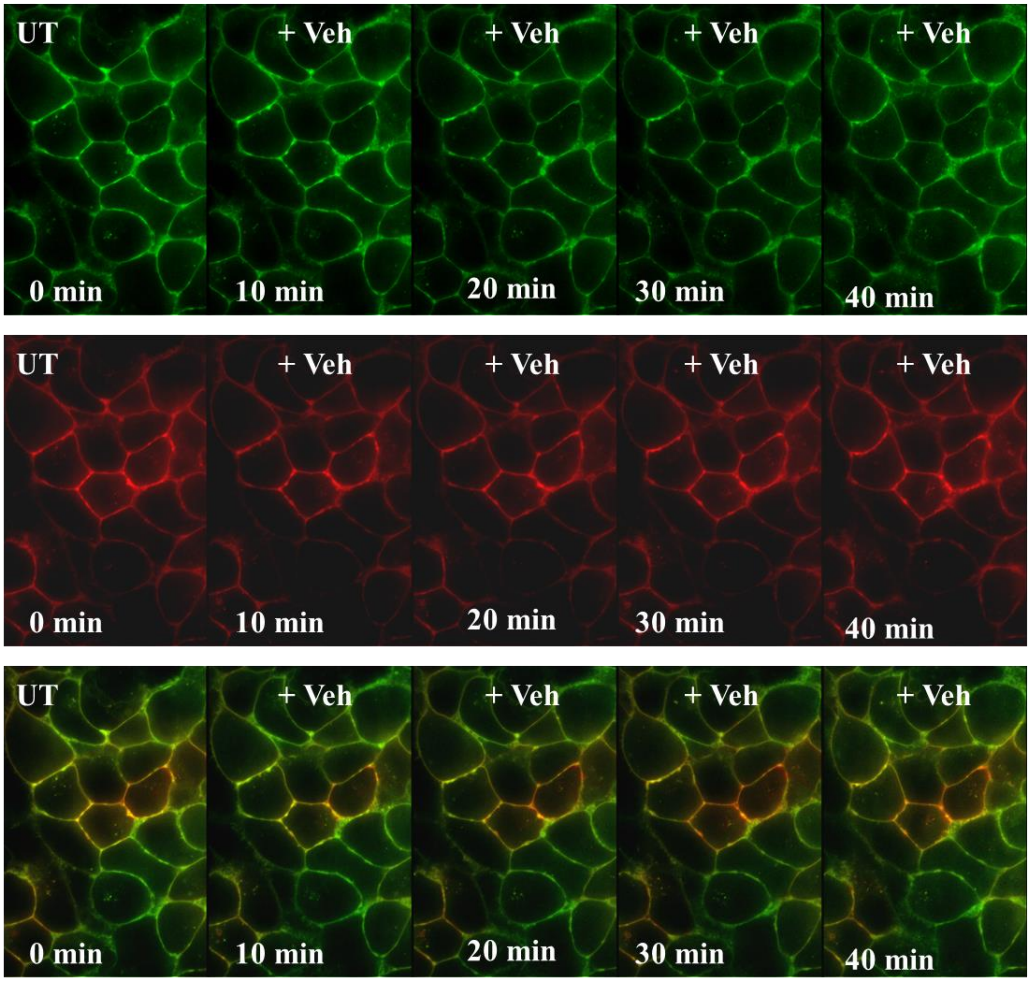

Figure 5.12 Epi-fluorescence microscopy using Vehicle as a control for internalisation experiments. Live cells were plated on cover slips and treated with 5 ng·ml-1 doxycycline for at least 16 hours, to allow co-expression of both receptors. Cells were then co-labelled with cell impermeable fluorescent dyes, CLIP-Surface 488 and SNAP-Surface 549, and were treated with HBSS (with 0.33% DMSO to maintain the consistency between treatments) acting as a vehicle for the assay. Addition of vehicle did not demonstrate any constitutive internalisation of either receptor.

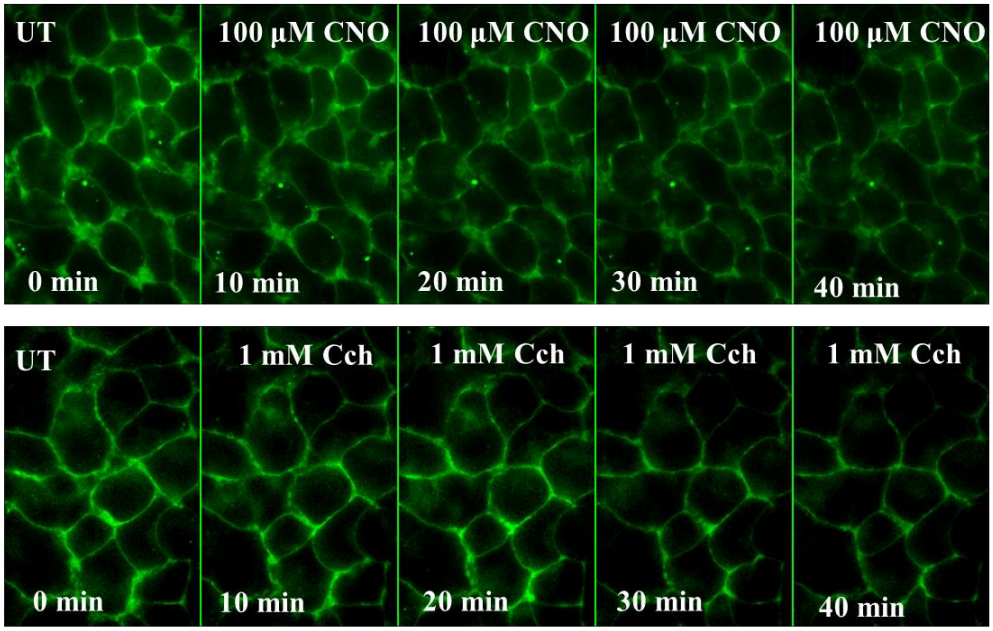

Figure 5.13 HA-CLIP-hM$_3$RASSL receptor does not internalise. Live cells were plated on cover slips, and were grown in the absence of doxycycline therefore cells were only constitutively expressing the HA-CLIP-hM$_3$RASSL receptor. Cells were labelled with CLIP-Surface 488 and images were captured prior and post treatments with either CNO or carbachol. The constitutively expressed HA-CLIP-hM$_3$RASSL did not demonstrate internalisation in response to either of the agonists.

A.

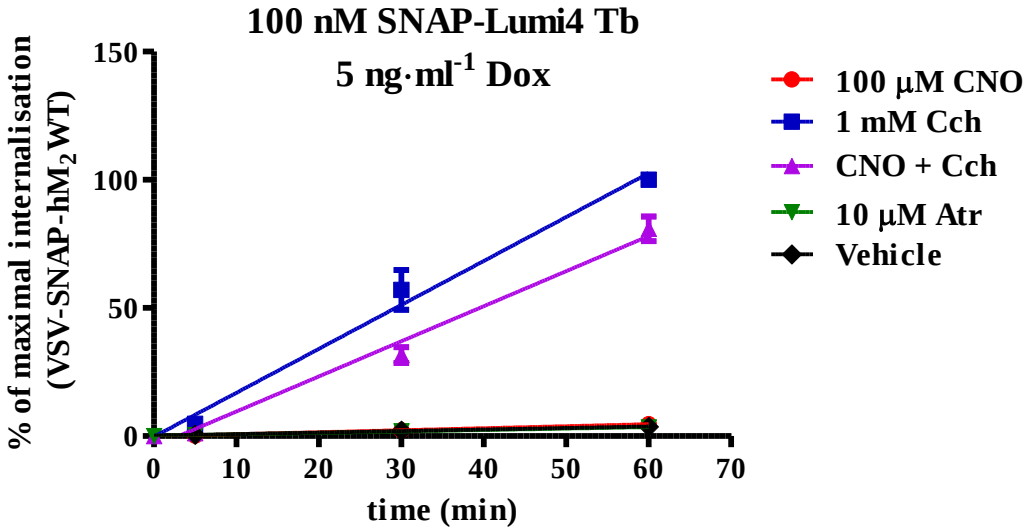
100 nM SNAP-Lumi4 Tb
5 ng·ml-1 Dox
% of maximal internalisation
(VSV-SNAP-hM2 WT)
time (min)
100 µM CNO
1 mM Cch
CNO + Cch
10 µM Atr
Vehicle

B.

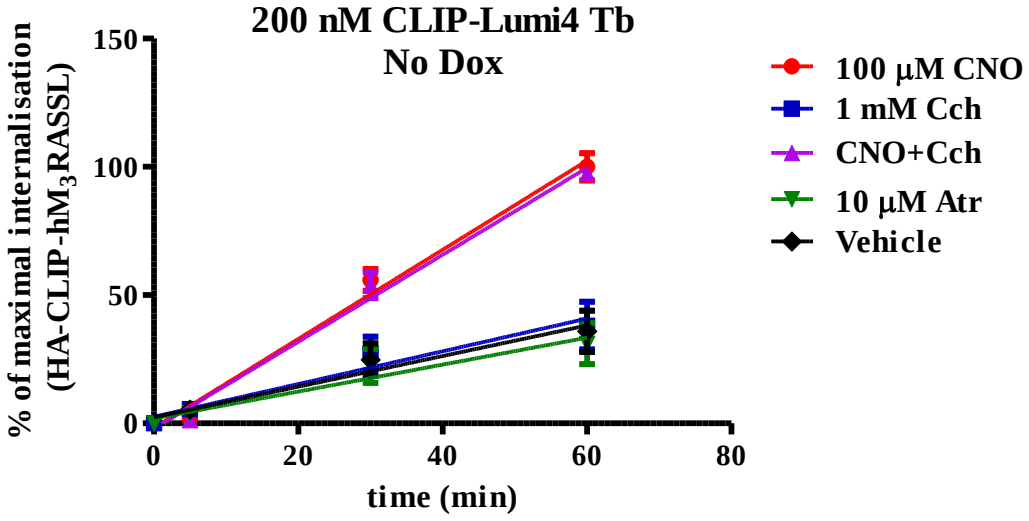
200 nM CLIP-Lumi4 Tb
No Dox
% of maximal internalisation
(HA-CLIP-hM3 RASSL)
time (min)
100 µM CNO
1 mM Cch
CNO+Cch
10 µM Atr
Vehicle

C.

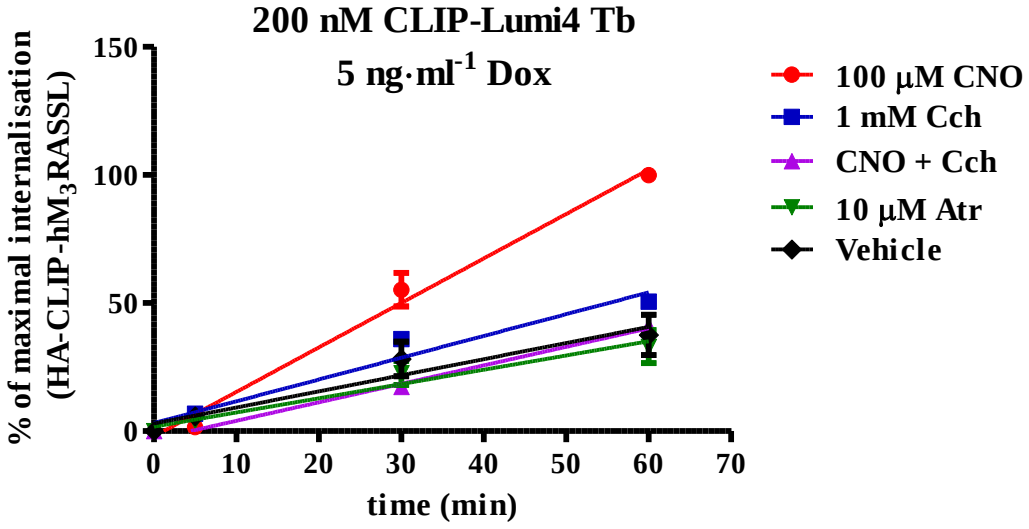
200 nM CLIP-Lumi4 Tb
5 ng·ml-1 Dox
% of maximal internalisation
(HA-CLIP-hM3 RASSL)
time (min)
100 µM CNO
1 mM Cch
CNO + Cch
10 µM Atr
Vehicle

Figure 5.14 Tag-lite® internalisation assay to assess ligand-mediated receptor internalisation. (A) Cells treated with 5 ng·ml^{-1} doxycycline to induce expression of both VSV-SNAP-hM_2WT and HA-CLIP-hM_3RASSL, were labelled with 100 nM SNAP-Lumi4 Tb and subsequently incubated with a mixture of Tag-lite® internalisation buffer and each of the ligand treatments. Fluorescence was monitored for up to 60 minutes. Carbachol and the combination of carbachol with CNO treatment promoted hM_2WT receptor internalisation which increased with time. **(B)** Cells not treated with doxycycline, able to express only the HA-CLIP-hM_3RASSL in a constitutive manner, were labelled with 200 nM CLIP-Lumi4 Tb and subsequently incubated with a mixture of Tag-lite® internalisation buffer with each of the treatments. CNO and the combination of CNO with carbachol treatment led to hM_3RASSL internalisation. **(C)** Cells expressing both the receptors were labelled with 200 nM CLIP-Lumi4 Tb and were then subjected to treatments. Internalisation of hM_3RASSL was detected in response to CNO, but not in response to the combination of CNO with carbachol. (Data shown as % of maximum internalisation, Mean ± Range, n=2).

Chapter 6

Final discussion

6. Discussion

The work presented in the context of this thesis confirms the previously demonstrated formation of homomers and heteromers between muscarinic receptor subtypes, in this case M_2 and M_3, at the surface of intact cells. A genetically engineered version of the human M_3 (HA-CLIP-hM_3RASSL) that was unable to bind and to respond to the endogenous muscarinic ligand acetylcholine or chemical analogues (i.e. carbachol) was used in combination with a form of the wild type human M_2 (VSV-SNAP-hM_2WT) to describe the receptor-receptor interactions, either homomeric or heteromeric, by htrFRET in combination with SNAP/CLIP tagging technology. The existence of oligomeric complexes was also confirmed by biochemical methods, such as Blue Native-PAGE and co-immunoprecipitation, using antibodies specific for the epitope VSV- and HA- tags that were fused at the N-termini of the receptors.

The most original finding here was the observation of ligand-induced alterations in the oligomeric profile of the receptors. Namely, upon VSV-SNAP-M_2WT specific stimulation with carbachol, pre-existing VSV-SNAP-hM_2WT/HA-CLIP-hM_3RASSL heteromeric organisation was reduced. At the same time, an increase in VSV-SNAP-hM_2WT homomeric profile was detected. These changes were ligand concentration-dependent and consistent with the extent of ligand occupancy of the receptor. Selective activation of HA-CLIP-hM_3RASSL with the synthetic ligand CNO did not result in significant changes in the oligomeric profile of either receptor homomers or heteromers. An alternative approach included triple labelling of the receptors i.e. one energy donor and two energy acceptors emitting at distinct wavelengths, provided interesting insight into the dynamics of interchange between homomers and heteromers upon ligand-mediated receptor stimulation. Ligand addition switched the balance from M_2/M_3 heteromers to M_2/M_2 homomers, but has left the M_3/M_3 homomers largely unaffected. Dissociation of the heteromers may have enhanced formation of M_2/M_2 oligomerisation and M_2 internalisation upon carbachol treatment. The inability to observe any changes in the M_3 homomeric arrangement could be due to the fact that M_3 receptors dissociating from the relatively transient heteromeric interaction remained at the plasma membrane and possibly interacted with other cellular components. It is known that the M_3 is able of forming tetramers that exist in a rhomboidal arrangement at the cell surface (Patowary *et al.*, 2013) and it could be that this is a more stable complex than the M_2/M_3 heteromeric arrangement.

According to the data obtained it may be proposed that ligand-mediated changes in the oligomeric profiles of the mAChRs favour heteromer-to-homomer transitions and this may

in general be a feature of homomers vs heteromers. Ligand-induced conformational changes in the muscarinic receptor M_2 activation possibly result in a more stable M_2/M_2 homomer that readily internalises. The dynamics of interchange between homomers and heteromers as observed by utilising a multiplex labelling approach and htrFRET detection of the oligomeric changes was helpful in confirming the simultaneous ligand-induced effects on oligomerisation. However, this approach was not sufficient to quantify the percentage of monomers/dimers/higher order oligomers in the system or to determine the exact arrangement of each oligomeric complex (dimer, tetramer or higher order oligomer), due to the limitations of RET-based techniques. In addition, there is still a need to resolve whether heteromers formed between M_2 and M_3 consist of heteromers of homodimers or other combinations of the receptors.

It is generally appreciated that identifying a consensus dimer interface or a common mechanism for dimer/oligomer formation could support the biological and functional relevance of GPCR oligomerisation (Lambert and Javitch, 2014). This seems to be very difficult given the diversity of observations in the field. Alternatively, it could be possible that different GPCRs act differently and that there is no consensus mechanism for oligomerisation. Investigation of oligomerisation could be focused on one GPCR type or a group of GPCRs. It is a possibility that every GPCR uses a unique mechanism, despite the obvious structural and functional similarities. It could as well be the case that every GPCR-GPCR complex, either homomeric or heteromeric, is behaving in a self-defined manner, and it could be this variation that defines the divergence in GPCR oligomerisation implications in receptor's functional and biological diversity, in a given cellular system or tissue/organ.

A common theme of receptor oligomerisation is the diversity of functions and ligand specificities that oligomerisation provides. The physical interactions between receptors result in an enlarged surface area that can have beneficial effects on the rate of reactions and orientation of the binding site through conformational changes conferred upon the receptors that enable ligand binding or promote subsequent interactions with other cellular components (Klemm *et al.,* 1998). Oligomerisation can result in altered signalling and pharmacology (Hiller *et al.,* 2013). Understanding the pharmacology of dimerisation/oligomerisation may lead to the development of ligands capable of selective targeting of GPCR dimers, thus providing an alternative approach in the treatment of diseases or conditions where GPCR oligomerisation is implicated. Initial attempts have led to the identification of certain ligands that possess two pharmacophores (bivalent ligands) able to interact at the binding sites of a receptor dimer (Hiller *et al.,* 2013). Development

and use of such ligands may provide new insight into the physiological importance of GPCR heteromerisation *in vivo*.

The lack of selective ligands for each muscarinic receptor subtype is a substantial limitation when it comes to selective receptor activation. This reflects the highly conserved orthosteric binding site between muscarinic receptor subtypes and it makes it very difficult to pharmacologically differentiate between muscarinic receptor sub-types. The generation of RASSLs and DREADDs offers great advantages in overcoming this drawback. The use of a RASSL version of M_3 receptor that can only be activated by the synthetic ligand, CNO, allowed the differential activation of the two receptors M_2 and M_3, when studying oligomerisation in a heterologous cellular system where both receptors were co-expressed.

Data collected from functional assays, in an attempt to investigate the role of receptor oligomerisation in signalling, suggested that formation of heteromers between VSV-SNAP-hM_2WT and HA-CLIP-hM_3RASSL did not affect the $G_{i/o}$ coupling-mediated pathway or $G_{q/11}$ coupling-dependent signalling. Interestingly, there was a trend towards an increase in the efficacy of CNO (not statistically significant) in increasing the IP1 levels upon M_3 stimulation, in the presence of heteromers, while at the same time the potency of the ligand remained unaffected. It could be explained as a result of receptor heteromerisation affecting the pharmacology of the protomers, or it could have resulted from signalling cross-talk that is independent of any physical interactions between the receptors. Signalling cross-talk between M_2 and M_3 receptors at the level of second messenger and ERK activation has been described previously. Hornigold *et al.,* (2003), reported that co-activation of M_2 and M_3 receptor sub-types in CHO cells resulted in a synergistic activation of ERK and also in increased IP_3 production compared to that seen in cells expressing only M_3 receptor (Hornigold *et al.,* 2003).

The use of htrFRET and SNAP/CLIP technology offers several advantages in the study of GPCR oligomerisation. Firstly, there is no disruption of the natural environment where oligomerisation takes place. Secondly, it allows detection of oligomerisation with the simultaneous monitoring of ligand-induced regulation of oligomerisation. Finally, htrFRET offers high signal-to-noise ratio. One of the main disadvantages of the htrFRET approach used in this project involves the high cost of the SNAP/CLIP technology reagents. In addition, the inability to estimate the exact size and composition of an oligomer is a limiting factor in the understanding of the oligomeric organisation of receptors. Another drawback involves the existence of 'bystander' FRET signal that originates from proteins that do not interact but still result in a FRET signal, which could be falsely interpreted as

real receptor-receptor interactions. An approach that can be used to confirm the dimerisation results obtained from an htrFRET based assay may involve the use of a negative oligomerisation control. Such a control could be a receptor that is known to be unable to form oligomeric complexes, existing in a monomeric form at the cell surface. Such a control could be used to determine bystander FRET signal and help distinguish real receptor -receptor interactions from random collisions. The cluster of differentiation 86 (CD86) receptor, a protein that is expressed on the surface of T cells and is implicated in numerous autoimmune diseases (Chang *et al.,* 2002) exists as a monomer (James *et al.,* 2007; Girard *et al.,* 2014) and this observation has been further validated by dual-colour fluorescence recovery after photo-bleaching (FRAP) microscopy, in live cells (Dorsch *et al.,* 2009). The tagging of the N-terminus of the CD86 receptor with SNAP tag has generated a fusion that was stably expressed in single stable Flp-In™ T-REx™-293 cells. Labelling of the expressed fusion at the surface of live cells with SNAP-Lumi4 Tb as donor and SNAP-Red as acceptor demonstrated the inability of CD86 receptor to dimerise/oligomerise. This observation suggests that the htrFRET signal originating from M_2 labelled receptors corresponds to real receptor interactions rather than random collisions (Aslanoglou *et al.,* 2015).

The use of Flp-In™ T-REx™-293 cells as a heterologous expression system offered certain advantages. Firstly, it ensured the trafficking and localisation of the expressed functional receptors at the cell surface and secondly, it allowed the manipulation of receptor expression, i.e. VSV-SNAP-hM_2W expression was induced by addition of doxycycline, while the HA-CLIP-hM_3RASSL was constitutively expressed at the cell surface. Expression of HA-CLIP-hM_3RASSL was unaffected by the presence or absence of doxycycline.

Reversal of the tagging of receptors could be a useful strategy to confirm the results obtained. Namely, the generation of a double stable cell line expressing both the VSV-SNAP-hM_3RASSL and HA-CLIP-hM_2WT receptors could be used in similar htrFRET experiments as future work.

The role of internalisation can be further investigated, as there was evidence that suggested receptor internalisation followed the ligand-mediated regulation of oligomerisation. The dissociation of M_2/M_3 heteromers was followed by an increase in M_2/M_2 homomers that internalised shortly after carbachol treatment. Further questions that still remain unanswered include whether the htrFRET signal obtained from the internalised M_2 receptors was due to the receptors being internalised as homomers or due to the close

proximity of M_2 protomers in endocytic vesicles. It has been suggested that the M_2 undergoes agonist-induced internalisation at a higher extent than M_3 receptor, proposing that most of the M_3 receptor population remains at the cell surface following ligand addition (Schlador *et al.,* 2000).

Experiments that would offer functional relevance of the M_2/M_3 heteromerisation *in vivo* could be advantageous in understanding the role of the heteromers in native tissues, organ or even whole organisms. M_2 and M_3 receptor sub-types are found in CNS and periphery, and they are co-expressed in smooth muscle cells (e.g. of the intestine and airway) with M_3 playing a direct role in smooth muscle contraction, while, M_2 affects smooth muscle contraction in an indirect manner, possibly through inhibiting the action of relaxants (Eglen *et al.,* 1996). The involvement of the two receptors in numerous disorders such as Alzheimer's disease, schizophrenia and cognitive impairment, makes them ideal targets for therapeutics. The understanding of the heteromerisation mechanism between these two receptors may lead to the development of novel therapeutic compounds able of recognising and binding to the oligomeric arrangement of the two receptors, rather than to the individual protomers, thereby regulating the oligomer-related signalling and function.

The work presented in this thesis could enhance the understanding in the field of ligand-mediated regulation of muscarinic acetylcholine receptors and provide a starting point that could potentially lead to the future development of novel therapeutics for the treatment of conditions where muscarinic receptor oligomerisation might be implicated.

References

Albizu, L., Cottet, M., Kralikova, M., Stoev, S., Seyer, R., Brabet, I., Roux, T., Bazin, H., Bourrier, E., Lamarque, L., Breton, C., Rives, M.L., Newman, A., Javitch, J., Trinquet, E., Manning, M., Pin, J.P., Mouillac, B. and Durroux, T. (2010) Time-resolved FRET between GPCR ligands reveals oligomers in native tissues. *Nature Chem. Biol.* **6:** 587-594

Alvarez-Curto, E., Ward, R. J., Pediani, J.D. and Milligan G. (2010) Ligand Regulation of the Quaternary Organization of Cell Surface M_3 Muscarinic Acetylcholine Receptors Analyzed by Fluorescence Resonance Energy Transfer (FRET) Imaging and Homogeneous Time-resolved FRET. *J. Biol. Chem.* **285:** 23318-23330

Alvarez-Curto, E., Prihandoko, R., Tautermann, C.S., Zwier, J.M., Pediani, J.D., Lohse, M.J., Hoffmann, C., Tobin, A.B., and Milligan, G. (2011). Developing chemical genetic approaches to explore G protein coupled receptor function: Validation of the use of a Receptor Activated Solely by Synthetic Ligand (RASSL). *Mol. Pharmacol.* **80:** 1033-1046

Angers, S., Salahpour, A., Joly, E., Hilairet, S., Chelsky, D., Dennis, M., and Bouvier, M. (2000) Detection of β2-adrenergic receptor dimerisation in living cells using bioluminescence resonance energy transfer (BRET). *PNAS.* **97:** 3684-3689

Angers, S., Salahpour, A., and Bouvier, M. (2002) Dimerization: an emerging concept for G protein-coupled receptor ontogeny and function. *Annu. Rev. Pharmacol. Toxicol.* **42:** 409-435

Armbruster, B.N., Li, X., Pausch, M.H., Herlitze, S., and Roth, B.L. (2007) Evolving the lock to fit the key to create a family of G protein-coupled receptors potently activated by an inert ligand. *Proc. Natl. Acad. Sci. USA* **104:** 5163-5168

Aslanoglou, D., Alvarez-Curto, E., Marsango, S. and Milligan, G. (2015) Distinct regulation of muscarinic acetylcholine M_2/M_3 heteromers and their corresponding homomers. *J. Biol. Chem.* **290:** 14785-14796

Bargmann, C.I. (1998). Neurobiology of the Caenorhabditis elegans genome. *Science* **282:** 2028–2033.

Bayburt, T.H., Vishnivetskiy, S.A., McLean, M.A., Morizumi, T, Huang, C.C., Tesmer, J.J., Ernst, O.P., Sligar, S.G., and Gurevich, V.V. (2011) Monomeric rhodopsin is sufficient for normal rhodopsin kinase (GRK1) phosphorylation and arrestin-1 binding. *J. Biol. Chem.* **286:** 1420-1428

Bazin, H., Preaudat, M., Trinquet, E., and Mathis, G. (2001) Homogeneous time resolved fluorescence resonance energy transfer using rare earth cryptates as a tool for probing molecular interactions in biology. *Spectrochim. Acta. A. Mol. Biomol. Spectrosc*. **57:** 2197-2211

Beech, D.J., Bernheim, L., and Hille, B. (1992). Pertussis toxin and voltage dependence distinguish multiple pathways modulating calcium channels of rat sympathetic neurons. *Neuron* **8:** 97-106

Billington, C.K., and Penn, R.B. (2002) M3 Muscarinic acetylcholine receptor regulation in the airway. *Am. J. Respir. Cell Mol. Biol.* **26:**269-272

Birdsall, N. J. M. (2010) Class A GPCR heterodimers: evidence from binding studies. *Cell* **31:** 499-508

Bockaert, J., and Pin, J.P. (1999) Molecular tinkering of G protein-coupled receptors: an evolutionary success. *EMBO J.* **18:** 1723-1729

Bodick, N.C., Offen, W.W., Levey, A.I., Cutler, N.R., Gauthier, S.G., Satlin, A., Shannon, H.E., Tollefson, G.D., Rasmussen, K., Bymaster, F.P., Hurley, D.J., Potter, W.Z. and Paul, S.M. (1997) Effects of xanomeline, a selective muscarinic receptor agonist, on cognitive function and behavioural symptoms in Alzheimer disease. *Arch. Neurol.* **54:** 465-473

Borroto-Escuela, D. O., García-Negredo, G., Garriga, P., Fuxe, K., and Ciruela, F. (2010) The M(5) muscarinic acetylcholine receptor third intracellular loop regulates receptor function and oligomerization. *Biochim. Biophys. Acta.* **1803:** 813-25

Bouvier, M., and Hebert, T.E. (2014) Cross talk proposal: Weighing the evidence for class A GPCR dimers, the evidence favours dimers. *J. Physiol.* **592:** 2439-2441

Brown, D.A., and Sihra, T.S. (2008) Presynaptic signaling by heterotrimeric G-proteins. *Handb. Exp. Pharmacol.* **2008:** 207-260.

Bruysters, M., Jongejan, A., Akdemir, A., Bakker, R.A., and Leurs, R. (2005) A G(q/11)-coupled mutant histamine H(1) receptor F435A activated solely by synthetic ligands (RASSL). *J. Biol. Chem.* **280:** 34741–34746

Bubser, M., Byun, N., Wood, M.R., and Jones, C.K. (2012) Muscarinic receptor pharmacology and circuity for the modulation of cognition. *Handbook of Experim. Pharmacol*. **208:** 121-166

Burstein, E.S., Spalding, T.A., Hill-Eubanks, D., and Brann, M.R. (1995) Structure-Function of muscarinic receptor coupling to G proteins. *J. Biol. Chem.* **270:** 3141-3146

Burstein, E.S., Spalding, T.A., Hill-Eubanks, D., and Brann, M.R. (1996) Structure-function of muscarinic receptor coupling to G proteins: Random saturation mutagenesis identifies a critical determinant of receptor affinity for G proteins. *J. Biol. Chem.* **270:** 3141-3146

Bymaster, F.P., McKinzie, D.L., Felder, C.C., and Wess, J. (2002) Use of M_1-M_5 Muscarinic receptor Knockout mice as novel tools to delineate the physiological roles of the muscarinic cholinergic system. *Neurochem. Research* **28:** 437-442

Calebiro, D., Nikolaev, V.O., Persani, L., and Lohse, M.J. (2010) Signaling by internalised G-protein-coupled receptors. *Trends Pharmacol. Sci.* **31:** 221-228

Calebiro, D., Rieken, F., Wagner, J., Sungkaworn, T., Zabel, U., Borzi, A., Cocucci, E., Zurn, A., and Lohse, M.J. (2013) Single-molecule analysis of fluorescently labelled G-protein-coupled receptors reveals complexes with distinct dynamics and organisation. *Proc. Natl. Acad. Sci. USA* **110:** 743-748

Chen, X., Choo, H., Huang, X-P., Yang, X., Stone, O., Roth, B.L., and Jin, J. (2015) The first structure-activity relationship studies for designer receptors exclusively activated by designer drugs. *ACS Chem. Neurosci.*

Cherezov, V., Rosenbaum, D.M., Hanson, M.A., Rasmussen, S.G., Thian, F.S., Kobilka, T.S., Choi, H.J., Kuhn, P., Weis, W.I., Kobilka, B.K., and Stevens, R.C. (2007) High-resolution crystal structure of an engineered human beta2-adrenergic G protein-coupled receptor. *Science* **318:** 1258-1265

Christopoulos, A., Grant, M.K.O., Ayoubzadeh, N., Kim, O.N., Sauerberg, P., Jeppesen, L., and El-Fakahany, E.E. (2001) Synthesis and pharmacological evaluation of dimeric muscarinic acetylcholine receptor agonists. *J. Pharmacol. Exp. Ther.* **298:** 1260-1268

Chun, L., Zhang, W.H., and Liu, J.F. (2012) Structure and ligand recognition of class C GPCRs. *Acta Pharmacol. Sin.* **33:** 312-323

Claeysen, S., Joubert, L., Sebben, M., Bockaert, J., and Dumuis, A. (2003) A single mutation in the 5-HT4 receptor (5-HT4-R D100(3.32)A) generates a Gs-coupled receptor activated exclusively by synthetic ligands (RASSL). *J. Biol. Chem.* **278:** 699–702

Clayton, A.H.A., and Chattopadyay, A. (2014) Taking care of bystander FRET in a crowded cell membrane environment. *J. Biophys.* **106:** 1227-1228

Conklin, B.R. (2007) New tools to build synthetic hormonal pathways. *Proc. Natl. Acad. Sci. USA* **104:** 4777-4778

Cottet, M., Faklaris, O., Maurel, D., Scholler, P., Doumazane, E., Trinquet, E., Pin, J.P., and Durroux, T. (2012) BRET and time-resolved FRET strategy to study GPCR oligomerisation: from cell lines toward native tissues. *Frontiers in Endocrinology* **3:** 1-14

Comps-Agrar, L., Kniazeff, J., Brock, C., Trinquet, E., and Pin, J-P. (2011) Stability of GABAB receptor oligomers revealed by dual TR-FRET and drug-induced cell surface targeting. *FASEB J.* **26:** 3430-3439

Cornea, A., Janovick, J.A., Maya-Nunez, G., and Conn, P.M. (2000) Gonadotropin releasing hormone microaggregation: rate monitored by fluorescence resonance energy transfer. *J. Biol. Chem.* **276:** 2153-58

Coward, P., Wada, G.H., Falk, M.S., Chan, S.D., Meng, F., Akil, H., and Conklin, B.R. (1998) Controlling signaling with a specifically designed Gi-coupled receptor. *Proc. Natl. Acad. Sci. USA* **95:** 352-357

Cvejic, S., and Devi, L.A. (1997) Dimerisation of the delta opioid receptor: implication for a role in receptor internalisation. *J. Biol. Chem.* **272:** 26959-26964

Davis, C.N., Risso Bradley, S., Schiffer, H.H., Friberg, M., Koch, K., Tolf, B-R., Bonhaus, D.W., and Lameh, J. (2009) Differential regulation of muscarinic M_1 receptors by orthosteric and allosteric ligands. *BMC Pharmacol.* **9:** 14

Degorce, F., Card, A., Soh, S., Trinquet, E., Knapik, G.P., and Xie, B. (2009) HTRF: A technology tailored for drug discovery-A review of theoretical aspects and recent applications. *Curr. Chem. Genomics* **3:** 22-32

De Lorme, K.C., Grant, M.K.O., Noetzel, M.J., Polson, S.B., and El-Fakahany, E.E. (2007) Long-Term Changes in the Muscarinic M1 Receptor Induced by Instantaneous Formation of Wash-Resistant Xanomeline-Receptor Complex. *J. Pharmacol. Exp. Ther.* **323:** 868-876

DeWire, S.M., Ahn, S., Lefkowitz, R.J., and Shenoy, S.K. (2007) Beta-arrestins and cell signaling. *Annu. Rev. Physiol.* **69:** 483-510

Dohlman, H.G., Thoraer, J., Caron, M.G., and Leftowitz, R.J. (1991) Model systems for the study of seven-transmembrane-segment receptors. *Annu. Rev. Biochem.* **60:** 653-88.

Dorsch, S., Klotz, K.N., Engelhardt, S., Lohse, M.J., and Bunemann, M. (2009) Analysis of receptor oligomerisation by FRAP microscopy. *Nat. Methods* **6:** 225-230

Doumazane, E., Scholler, P., Zwier, J.M., Trinquet, E., Rondard, P., and Pin, J.P. (2011) A new approach to analyse cell surface protein complexes reveals specific heterodimeric metabotropic glutamate receptors. *FASEB J.* **25:** 66-77

Eglen, R.M., Hedge, S.S., and Watson, N. (1996) Muscarinic receptor subtypes and smooth muscle function. *Pharmacol. Rev.* **48:** 531-565

Eglen, R.M., Reddy, W., Watson, N., and Challiss, R.A. (1994) Muscarinic acetylcholine receptor subtypes in smooth muscle. *Trends Pharmacol. Sci.* **15:** 114-119

Ellis, J., Pediani, J.D., Canals, M., Milasta, S., and Milligan, G. (2006) Orexin-1 receptor-cannabinoid CB1 receptor heterodimerisation results in both ligand-dependent and independent coordinated alterations of receptor localisation and function. *J. Biol. Chem.* **281:** 38812-28824

Emami-Nemini, A., Roux, T., Leblay, M., Bourrier, E., Lamarque, L., Trinquet, E., and Lohse, M.J. (2013) Time-resolved fluorescence ligand binding for G protein-coupled receptors. *Nat. Protoc.* **8:** 1307-1320

Ernst, O.P., Gramse, V., Kolbe, M., Hofmann, K.P., and Heck, M. (2007) Monomeric G protein-coupled receptor rhodopsin in solution activates its G-protein transducing at the diffusion limit. *Proc. Natl. Acad. Sci. USA* **104:** 10859-10864

Evron, T., Daigle, T.L., and Caron, M.G. (2012) GRK2: multiple roles beyond G protein-coupled receptor desensitisation. *Trends Pharmacol. Sci.* **33:** 154-164

Ferre, S., Casadó, V., Devi, L.A., Filizola, M., Jockers, R., Lohse, M.J., Milligan, M., Pin, J.P., and Guitart, X. (2014) G protein-coupled receptor oligomerisation revisited: Functional and pharmacological perspectives. *Pharmacol. Rev.* **66:** 413-434

Foster, D.J., Gentry, P.R., Lizardi-Ortiz, J.E., Bridges, T.M., Wood, M.R., Niswender, C.M., Sulzer, D., Lindsley, C.W., Xiang, Z., and Conn, P.J. (2014) M_5 receptor activation produces opposing physiological outcomes in Dopamine neurons depending on the receptor's location. *J. Neurosci.* **34:** 3252-3262

Fotiadis, D., Liang, Y., Filipek, S., Saperstein, D.A., Engel, A., and Palczewski, K. (2003) Atomic-force microscopy: rhodopsin dimers in native disc membranes. *Nature* **421:** 127-128

Förster, T. (1948) Zwischenmolekulare Energiewanderung und Fluoreszenz. *Ann. Phys. (Leipzig)* **2:** 55-75

Frederick, A.L., Yano, H., Trifilieff, P., Vishwasrao, H.D., Biezonski, D., Mészáros, J., Urizar, E., Sibley, D.R., Kellendonk, C., Sonntag, K.C., Graham, D.L., Colbran, R.J., Stanwood, G.D., and Javitch J.A. (2015) Evidence against dopamine D1/D2 receptor heteromers. *Mol Psychiatry [Epub ahead of print]*

Fredriksson, R., Lagerström, M.C., Lundin, L.G., and Schiöth, H.B. (2003) The G-protein coupled receptors in the human genome form five main families: phylogenetic analysis, paralogon groups, and fingerprints. *Mol. Pharmacol.* **63:** 1256–1272

Gautam, D., Han, S.J., Hamdan, F.F., Jeon, J., Li, B., Cui, Y., Mears, D., Lu, H., Deng, C., Heard, T., and Wess, J. (2006) A critical role for beta cell M3 muscarinic acetylcholine receptors in regulating insulin release and blood glucose homeostasis in vivo. *Cell Metab.* **3:** 449-461

Gautam, D., Ruiz de Azua, I., Li, J.H., Guettier, J.M., Heard, T., Cui, Y., Lu, H., Jou, W., Gavrilova, O., Zawalich, W.S. and Wess, J. (2010) Beneficial metabolic effects caused by persistent activation of beta-cell M_3 muscarinic acetylcholine receptors in transgenic mice. *Endocrinology* **151:** 5185-5194.

Gautier, A., Juillerat, A., Heinis, C., Correa, I.R., Kindermann, M., Beaufils, F., and Johnson, K. (2008) An engineered protein tag for multiprotein labeling in living cells. *Chem. Biol.* **15:** 128-136

Girard, T., Gaucher, D., El-Far, M., Breton, G., and Sékaly, R.P. (2014) CD80 and CD86 IgG domains are important for quaternary structure, receptor binding and co-signaling function. *Immunol. Lett.* **161:** 65-75

Goin, J. C., and Nathanson, N. M. (2006) Quantitative analysis of Muscarinic Acetylcholine receptor Homo- and Hetero-dimerisation in Live cells. *JBC.* **281:** 5416-5425

Gomes, I., Fujita, W., Gupta, A., Saldanha, A.S., Negri, A., Pinello, C., Roberts, E., Filizola, M., Hodder, P., and Devi, L. (2013) Identification of a μ-δ opioid receptor heteromer-biased agonist with antinociceptive activity. *PNAS.* **110(29):** 12072-12077

Gomes-Soler, M., Ahern, S., Fernandez-Duenas, V., and Ciruela, F. (2011) On the role of G protein-coupled receptors oligomerisation. *The Open Biol. J.* **4:** 47-53

González-Maeso, J. (2011) GPCR oligomers in pharmacology and signaling. *Molecular Brain* **4:** 20

Goddard, A.D., and Watts, A. (2012) Contributions of fluorescence techniques to understanding G protein-coupled receptor dimerisation. *Biophys. Rev.*

Goodman, O.B. Jr., Krupnick, J.G., Santini, F., Gurevich, V.V., Penn, R.B., Gagnon, A.W., Keen, J.H., and Benovic, J.L. (1996) Beta-arrestin acts as a clathrin adaptor in endocytosis of the beta2-adrenergic receptor. *Nature* **383:** 447– 450.

Grant, M.K.O., Noetzel, M.J., De Lorme, K.C., Jakubik, J., Dolezal, V., and El-Falkahany, E.E. (2010) Pharmacological Evaluation of the Long-Term Effects of Xanomeline on the M_1 Muscarinic Acetylcholine Receptor. *PLoS One* **5:** e15722

Guettier, J.M., Gautam, D., Scarselli, M., Ruiz de Azua, I., Li, J.H., Rosemond, E., Ma, X., Gonzalez, F. J., Armbruster, B.N., Lu, H., Roth, B.L., and Wess, J. (2009) A chemical-genetic approach to study G protein regulation of beta cell function in vivo. *Proc. Natl. Acad. Sci. USA* **106:** 19197-19202

Gouldson, P.R., Higgs, C., Smith, R.E., Dean, M.K., Gkoutos, G.V., and Reynolds, C.A. (2000) Dimerization and domain swapping in G-protein-coupled receptors: a computational study. *Neuropsychopharmacol.* **23:** 60-77

Gregory, K.J., Hall, N.E., Tobin, A.B., Sexton, P.M., and Christopoulos, A. (2010) Identification of orthosteric and allosteric site mutations in M2 muscarinic acetylcholine receptors that contribute to ligand-selective signalling bias. *J. Biol. Chem.* **285:** 7459-7474

Guo, W., Urizar, E., Kralikova, M., Mobarec, J.C., Shi, L., Filizola, M., and Javitch, J.A. (2008) Dopamine D2 receptors form higher order oligomers at physiological expression levels. *EMBO J.* 27: 2293-2304

Gurevich, V.V., and Benovic, J.L. (1993) Visual arrestin interaction with rhodopsin. Sequential multisite binding ensures strict selectivity toward light-activated phosphorylated rhodopsin. *J. Biol. Chem.* **268:** 11628-11638

Gurevich, V.V., and Gurevich, E.V. (2003) The new face of active receptor bound arrestin attracts new partners. *Structure* **11:** 1037-1042

Haga, K., Kruse, A.C., Asada, H., Yurugi-Kobayashi, T., Shiroishi, M., Zhang, C., Weis, W.I., Okada, T., Kobilka, B.K., Haga, T., and Kobayashi, T. (2012) Structure of the human M2 muscarinic acetylcholine receptor bound to an antagonist. *Nature* **482:** 547-551

Hamm, H.E. (2001) How activated receptors couple to G proteins. *Proc. Natl. Acad. Sci. USA* **98:** 4819-4821

Han, M., Gurevich, V.V., Vishnivetskiy, S.A., Sigler, P.B., and Schubert, C. (2001) Crystal Structure of -Arrestin at 1.9 A˚: Possible Mechanism of Receptor Binding and Membrane Translocation. *Structure* **9:** 869-880

Hanyaloglu, A.C., Seeber, R.M., Kohout, T.A., Lefkowitz, R.J., and Eidne, K.A. (2002) Homo- and hetero-oligomerization of thyrotropin-releasing hormone (TRH) receptor subtypes. Differential regulation of beta-arrestins 1 and 2. *J. Biol. Chem.* **277:** 50422-50430

Hasbi, A., O'Dowd, B.F., and George, S.R. (2011) Dopamine D1-D2 heteromer signalling pathway in the brain: emerging physiological relevance. *Mol. Brain* **4:**26

Hedge, S.S., Choppin, A., Bonhaus, D., Briaud, S., Loeb, M., Mon, T.M., Loury, D., and Eglen, R.M. (1997) Functional role of M_2 and M_3 muscarinic receptors in the urinary bladder of rats *in vitro* and *in vivo*. *Brit. J. Pharmacol.* **120:** 1409-1418

Hebert, T.E., Moffett, S., Morello, J-P., Loisel, T.P., Bichet, D.G., and Bouvier, M. (1996) A peptide derived from a beta$_2$-adrenergic receptor transmembrane domain inhibits both receptor dimerisation and activation. *J. Biol. Chem.* **271:** 16384-16392

Herrick-Davis, K., Grinde, E., Harrigan, T.J., and Mazurkiewicz, J.E. (2005) Inhibition of serotonin 5-Hydroxytryptamine2C receptor function through heterodimerization. *J. Biol. Chem.* **280:** 40144-40151

Herrick-Davis, K., Grinde, E., Cowan, A., and Mazurkiewicz, J.E. (2013) Fluorescence correlation spectroscopy analysis of serotonin, adrenergic, muscarinic, and dopamine receptor dimerization: the oligomer number puzzle. *Mol. Pharmacol.* **84:** 630-642.

Herrick-Davis, K., Grinde, E., Lindsley, T., Teitler, M., Mancia, F., Cowan, A., and Mazurkiewicz, J.E. (2015) Native serotonin 5-HT_{2C} receptors are expressed as homodimers in the apical surface of choroid plexus epithelial cells. *Mol. Pharmacol. Fast Forward*

Hern, J.A., Baig, A.H., Mashanov, G.I., Birdsall, B., Corrie, J.E.T., Lazareno, S., Molloy, J.E., and Birdsall, N.J.M. (2010) Formation and dissociation of M_1 muscarinic receptor dimers seen by total internal reflection fluorescence imaging of single cells. *Proc. Natl. Acad. Sci. USA* **107:** 2693-2698

Hill, C.A., Fox, A.N., Pitts, R.J., Kent, L.B., Tan, P.L., Chrystal, M.A., Cravchik, A., Collins, F.H., Robertson, H.M., and Zwiebel, L.J. (2002) G protein-coupled receptors in *Anopheles gambiae*. *Science* **298:** 176-178

Hille, B. (1992) G protein-coupled mechanisms and nervous signaling. *Neuron* **9:** 187-195

Hiller, C., Kuhhorn, J., and Gmeiner, P. (2013) Class A G-protein-coupled receptor (GPCR) dimers and bivalent ligands. *J. Med. Chem.* **56:** 6542-6559

Hollenstein, K., de Graaf, C., Bortolato, A., Wang, M.W., Marshall, F.H., and Stevens, R.C. (2014) Insights into the structure of class B GPCRs. *Trends Pharmacol. Sci.* **35:** 12-22

Hornigold, D.C., Mistry, R., Raymond, P.D., Blank, J.L., and Challiss, R.A.J. (2003) Evidence for cross-talk between M_2 and M_3 muscarinic acetylcholine receptors in the regulation of second messenger and extracellular signal-regulated kinase signalling pathways in Chinese hamster ovary cells. *Brit. J. Pharmacol*. **138:** 1340-1350

Hu, J., Thor, D., Zhou, Y., Liu, T., Wang, Y., McMillin, S. M., Mistry, R., Challiss, R.A.J., Constanzi, S., and Wess, J. (2012) Structural aspects of M3 Muscarinic acetylcholine receptor dimer formation and activation. *FASEB.* **26:** 1-13

Hu, J., Hu, K., Liu, T., Stern, M.K., Mistry, R., Challiss, R.A.J., Costanzi, S., and Wess, J. (2013) Novel structural and functional insights into M_3 muscarinic receptor Dimer/Oligomer formation. *J. Biol. Chem.* **288:** 34777-34790

Huang, J. Chen, S., Zhang, J.J., and Huang, X.Y. (2013) Crystal structure of oligomeric β1-adrenergic G protein-coupled receptors in ligand free basal state. *Nat. Struct. Mol. Biol.* **20:** 419-425

Hudson, B.D., Hebert, T.E., and Kelly, M.E.M. (2010) Physical and functional interaction between CB_1 cannabinoid receptor and β_2-adrenoceptor. *Br. J. Pharmacol.* **160:** 627-642

Hulme, E.C., Lu, Z.L., Saldanha, J.W., and Bee, M.S. (2003a) Structure and activation of muscarinic acetylcholine receptors. *Biochem. Soc. Trans.* **31:** 29–34

Hulme, E.C., Lu, Z.L., and Bee, M.S. (2003b) Scanning mutagenesis studies of the M1 muscarinic acetylcholine receptor. *Receptors Channels* **9:** 215-228

Ilien, B., Glasser, N., Clamme, J. P., Didier, P., Piemont, E., Chinnappan, R., Daval, S. B., Galzi, J. L., and Mely, Y. (2009) Pirenzepine promotes the dimerisation of Muscarinic M_1 receptors through a three step binding process. *J. Biol. Chem.* **284:** 19533-19543

Insel, P.A., Snead, A., Murray, F., Zhang, L., Yokouchi, H., Katakia, T., Kwon, O., Dimucci,D., and Wilderman, A. (2012). GPCR expression in tissues and cells: are the optimal receptors being used as drug targets? *Br. J. Pharmacol.* **165:** 1613-1616

Jaakola, V.P., Griffith, M.T., Hanson, M.A., Cherezov, V., Chien, E.Y., Lane, J.R., Ijzerman, A.P., and Stevens, R.C. (2008) The 2.6 angstrom crystal structure of a human A2A adenosine receptor bound to an antagonist. *Science* **322:** 1211-1217

Jain, S., Ruiz de Azua, I., Lu, H., White, M.F., Guettier, J-M., and Wess, J. (2013) Chronic activation of designer Gq-coupled receptor improves β cell function. *J. Clin. Invest.* **123:** 1750-1762

Jakubik, J., Haga, T., and Tucek, S. (1998) Effects of an agonist, allosteric modulator, and antagonist on guanosine-gamma[^{35}S]thiotriphosphate binding to liposomes with varying muscarinic receptor/G_o protein stoichiometry. *Mol. Pharmacol.* **54:** 899-906

Jakubik, J., and El-Fakahany, E.E. (2010) Allosteric modulation of muscarinic acetylcholine receptors. *Pharmaceuticals* **3:** 2838-2860

James, J.R., White, S.S., Clarke, R.W., Johansen, A.M., Dunne, P.D., Sleep, D.L., Fitzgerald, W.J., Davis, S.J., and Klenerman, D. (2007) Single-molecule level analysis of the subunit composition of the T cell receptor on live T cells. *Proc. Natl. Acad. Sci. USA* **104:** 17662-17667

Jastrzebska, B., Ringler, P., Palczewski, K., and Engel, A. (2013) The rhodopsin-transducin complex houses two distinct rhodopsin molecules. *J. Struct. Biol.* **182:** 164-172

Javitch, J.A. (2004) The Ants Go Marching Two by Two: Oligomeric Structure of G-Protein-Coupled Receptors. *Mol. Pharmacol.* **66:** 1077-1082

Javitch, J.A., Fu, D., Liapakis, G., and Chen, J. (1997) Constitutive activation of the β2-adrenergic receptor alters the orientation of its sixth membrane-spanning segment. *J. Biol. Chem.* **272:** 18546-18549

Jones, K.A., Borowsky, B., Tamm, J.A., Craig, D.A., Durkin, M.M., Dai, M., Yao, W.J., Johnson, M., Gunwaldsen, C., Huang, L.Y., Tangm C., Shen, Q., Salon, J.A., Morse, K., Laz, T., Smith, K.E., Nagarathnam, D., Noble, S.A., Branchek, T.A., and Gerald, C. (1998) $GABA_B$ receptors function as a heteromeric assembly of the subunits $GABA_BR1$ and $GABA_BR2$. *Nature* **396:** 674-679

Jordan, B.A., and Devi, L.A. (1999) G-protein-coupled receptor heterodimerisation modulates receptor function. *Nature* **399:** 697-700

Josefsson, L-G., and Rask, L. (1997) Cloning of a putative G-coupled receptor from Arabidopsis thaliana. *Eur. J. Biochem.* **249:** 415–420.

Kang, Y., Zhou, X.E., Gao, X., He, Y., Liu, W., Ishchenko, A., Barty, A., White, T.A., Yefanov, O., Han, G.W., Xu, Q., de Waal, P.W., Ke, J., Tan, M.H., Zhang, C., Moeller, A., West, G.M., Pascal, B.D., Van Eps, N., Caro, L.N., Vishnivetskiy, S.A., Lee, R.J., Suino-Powell, K.M., Gu, X., Pal, K., Ma, J., Zhi, X., Boutet, S., Williams, G.J., Messerschmidt, M., Gati, C., Zatsepin, N.A., Wang, D., James, D., Basu, S., Roy-Chowdhury, S., Conrad, C.E., Coe, J., Liu, H., Lisova, S., Kupitz, C., Grotjohann, I., Fromme, R., Jiang, Y., Tan, M., Yang, H., Li, J., Wang, M., Zheng, Z., Li, D., Howe, N., Zhao, Y., Standfuss, J., Diederichs, K., Dong, Y., Potter, C.S., Carragher, B., Caffrey, M., Jiang, H., Chapman, H.N., Spence, J.C., Fromme, P., Weierstall, U., Ernst, O.P., Katritch, V., Gurevich, V.V., Griffin, P.R., Hubbell, W.L., Stevens, R.C., Cherezov, V., Melcher, K., and Xu, H.E. (2015) Crystal structure of rhodopsin bound to arrestin by femtosecond X-ray laser. *Nature* **523:** 561-567.

Karnik, S.S., and Khorana, H.G. (1990) Assembly of functional rhodopsin requires a disulfide bond between cysteine residues 110 and 187. *J. Biol. Chem.* **265:** 17520-17524

Kaupmann, K., Malitschek, B., Schuler, V., Heid, J., Froestl, W., Mosbacher, J., Bischoff, S., Kulik, A., Shigemoto, R., Karschin, A., and Bettler, B. (1998) $GABA_B$-receptor subtypes assemble into functional heteromeric complexes. *Nature* **396:** 683-687

Kilpatrick, L.E., Humphrys, L.J., and Holliday, N.D. (2015) A G protein coupled receptor dimer imaging assay reveals selectively modified pharmacology of Neuropeptide Y Y1/Y5 receptor heterodimers. *Mol. Pharmacol.* ?????

Klemm, J.D., Schreiber, S.L., and Crabtree, G.R. (1998) Dimerization as a regulatory mechanism in signal transduction. *Annu. Rev. Immunol.* **16:** 569-592

Kobilka, B.K. (2007) G protein coupled receptor structure and activation. *Biochim. Biophys. Acta.* **1768:** 794-807

Kovoor, A., Celver, J., Abdryashitov, R.I., Chavrin, C., and Gurevich, V.V. (1999) Targeted construction of phosphorylation-independent β-arrestin mutants with constitutive activity in cells. *J. Biol. Chem.* **274:** 6831-6834

Kow, R.L., and Nathanson, N.M. (2012) Muscarinic receptors become crystal clear. *Nature* **482:** 480-481

Krejci, A., Michal, P., Jakubik, J., Ricny, J., and Dolezal, V. (2004) Regulation of signal transduction at M_2 muscarinic receptor. *Physiol. Res.* **53:** 131-140

Krejci, A., and Tucek, S. (2002) Quantitation of mRNAs for M_1 to M_5 subtypes of muscarinic receptors in rat heart and brain cortex. *Mol. Pharmacol.* **61:** 1267-1272

Kristiansen, K., Kroeze, W.K., Willins, D.L., Gelber, E.I., Savage, J.E., Glennon, R.A., and Roth, B.L. (2000) A highly conserved aspartic acid (Asp-155) anchors the terminal amine moiety of tryptamines and is involved in membrane targeting of the 5-HT(2A) serotonin receptor but does not participate in activation via a "salt-bridge disruption" mechanism. *J. Pharmacol. Exp. Ther.* **293:** 735–746

Kruse, A.C., Hu, J., Pan, A.C., Arlow, D.H., Rosenbaum, E., Green, H.F., Liu, T., Chae, P.S., Dror, R.O., Shaw, D.E., Weis, W.I., Wess, J., and Kobilka, B.K. (2012) Structure and dynamics of the M3 muscarinic acetylcholine receptor. *Nature* **482:** 552-556

Kruse, A.C., Ring, A.M., Manglik, A., Hu, J., Hu, K., Eitel, K., Hubner, H., Pardon, E., Valant, C., Sexton, P.M., Christopoulos, A., Felder, C.C., Gmeiner, P., Steyaert, J., Weis, W.I., Garcia, K.C., Wess, J., and Kobilka, B.K. (2013) Activation and allosteric modulation of a muscarinic acetylcholine receptor. *Nature* **504:**101-106.

Kruse, A.C., Ring, A.M., Manglik, A., Hu, J., Eitel, K., Hubner, H., Pardon, E., Valent, C., Sexton, P.M., Christopoulos, A., Felder, C.C., Gmeiner, P., Steyaert, J., Weis, W.I., Garcia, C., Wess, J., and Kobilka, B.K. (2013 a) Activation and allosteric modulation of a muscarinic acetylcholine receptor. *Nature* **504:** 101-106

Kruse, A.C., Weiss, D.R., Rossi, M., Hu, J., Hu, K., Eitel, K., Gmeiner, P., Wess, J., Kobilka, B.K., and Scoichet, B.K. (2013) Muscarinic receptors as model targets and antitargets for structure-based ligand discovery. *Mol. Pharmacol.* **84:** 528-540

Kruse, A.C., Jianxin, H., Kobilka, B.K., and Wess, J. (2014) Muscarinic acetylcholine receptor X-ray structure: potential implications for drug development. *Curr. Op. Pharmacol*. **16:** 24-30

Kunishima, N., Shimada, Y., Tsiji, Y., Sato, T., Yakamoto, M., Kumasaka, T., Nakanishi, S., Jingami, H., and Morikawa, K. (2000) Structural basis of glutamate recognition by a dimeric metabotropic glutamate receptor. *Nature* **407:** 971-977

Kurowski, P., Gawlak, M., and Szulczyk, P. (2015) Muscarinic receptor control of pyramidal neuron membrane potential in the medial prefrontal cortex (mPFC) in rats. *Neurosci.* **330:** 474-488

Lagerstrom, M.C., and Schioth, H.B. (2008) Structural diversity of G protein-coupled receptors and significance for drug discovery. *Nature Rev Drug Discover* **7:** 339-357

Lambert, N.A., and Javitch, J.A. (2014) Crosstalk opposing view: Weighing the evidence for class A GPCR dimers, the jury is still out. *J. Physiol.* **592:** 2443-2445

Lazareno, S., Popham, A., and Birdsall, N.J.M. (2002) Analogs of WIN 62,577 define a second allosteric site on muscarinic receptors. *Mol. Pharmacol.* **62:** 1492-1505

Lefkowitz, R.J., and Shenoy, S.K. (2005) Transduction of receptor signals by beta-arrestins. *Science* **308:** 512-7

Levey, A.I. (1993) Immunological localisation of m1-m5 muscarinic acetylcholine receptors in peripheral tissues and brain. *Life Sci.* **52:** 441-448

Levey, A.I., Kitt, C.A., Simonds, W.F., Proce, D.L., and Brann, M.R. (1991) Identification and Localization of Muscarinic Acetylcholine Receptor Proteins in Brain with Subtype-specific Antibodies. *J. Neurosci.* **11:** 3218-3226

Li, B., Scarselli, M., Knudsen, C.D., Kim, S.K., Jacobson, K.A., McMillin, S.M., and Wess, J. (2007) Rapid identification of functionally critical amino acids in a G protein-coupled receptor. *Nat Methods* **4:** 169–174

Liang, Y., Fotiadis, D., Filipek, S., Saperstein, D.A., Palczewski, K., and Engel, A. (2003) Organisation of the G protein-coupled receptors rhodopsin and opsin in native membranes. *J. Biol. Chem.* **278:** 21655-21662

Lin, Y., and Smrcka, A.V. (2011) Understanding molecular recognition by G protein βγ subunits on the path to pharmacological targeting. *Mol. Pharmacol.* **80:** 551-557

Lüscher, C., and Slesinger, P.A. (2010) Emerging roles for G protein-gated inwardly rectifying potassium (GIRK) channels in health and disease. *Nat. Rev. Neurosci.* **11:** 301-315

Luttrell, L.M., and Lefkowitz, R.J. (2002) The role of β-arrestins in the termination and transduction of G-protein-coupled receptor signals. *J. Cell Sci.* **115:** 455-464

Maggi, A., U'Prichard, D.C., and Enna, S.J. (1980) β-Adrenergic regulation of α_2-adrenergic receptors in the central nervous system. *Science* **207:** 645-647.

Maggio, R., Barbier, P., Fornai, F., and Corsini, G. U. (1996) Functional role of the third cytoplasmic loop in muscarinic receptor dimerisation. *J. Biol. Chem*. **49:** 31055-31060

Maggio, R., Barbier, P., Colelli, A., Salvadori, F., Demontis, G., and Corsini, G. U. (1999) G-protein-linked receptors: pharmacological evidence for the formation of heterodimers. *JPET*. **291:** 251-257

Maggio, R., Vogel, Z., and Wess, J. (1993) Coexpression studies with mutant muscarinic/adrenergic receptors provide evidence for intermolecular "cross-talk" between G-protein-linked receptors. *Proc. Natl. Acad. Sci. USA* **90:** 3103-3107

Malbon, C.C. (2005) G proteins in development. *Nat. Rev.* **6:** 689-701

Manglik, A., Kruse, A.C., Kobilka, T.S., Thian, F.S., Mathiesen, J.M., Sunahara, R.K., Pardo, L., Weis, W.I., Kobilka, B.K., and Granier, S. (2012) Crystal structure of the mu-opioid receptor bound to a morphinan antagonist. *Nature* **485:** 321-326

Margeta-Mitrovic, M.., Jan, Y. N., and Jan, L.Y. (2000) A trafficking checkpoint controls GABA(B) receptor heterodimerisation. *Neuron* **27:** 97-106

Martinez-Munoz, L., Lucas, P., Navarro, G., Checa, A.I., Franco, R., Martinez-A. C., Rodriguez-Frade, J.M., and Mellado, M. (2009) Dynamic regulation of CXCR1 and CXCR2 Homo- and Heterodimers. *J.Immunol.* **183:** 7337-7346

Marquer, C., Fruchart-Gaillard, C., Mourier, G., Grandjean, O., Girard, E., le Maire, M., Brown, S., and Servent, D. (2010) Influence of MT7 toxin on the oligomerisation state of the M_1 muscarinic receptor. *Biol. Cell* **102:** 409-420

Matsui, M., Motomura, D., Fujikawa, T., Jiang, J., Takahashi, S-I., Manabe, T., and Taketo, M.M. (2002) Mice Lacking M_2 and M_3 Muscarinic Acetylcholine Receptors Are Devoid of Cholinergic Smooth Muscle Contractions But Still Viable. *J. Neurosci.* **22:** 10627-10632

Maurel, D., Comps-Agrar, L., Brock, C., Rives, M.-L., Bourrier, E., Ayoub, M. A., Bazin, H., Tinel, N., Durroux, T., Prézeau, L., Trinquet, E., and Pin, J.-P. (2008) Cell surface protein-protein interaction analysis with combined time-resolved FRET and snap-tag technologies: application to GPCR oligomerization. *Nat. Methods* **5:** 561–567

May, L.T., Leach, K., Sexton, P.M., and Christopoulos, A. (2007) Allosteric modulation of G protein-coupled receptors. Annu. Rev. Pharmacol. Toxicol. **47:** 1-51

McVey, M., Ramsay, D., Kellett, E., Rees, S., Wilson, S., Pope, A.J., and Milligan, G. (2001) Monitoring receptor oligomerization using time-resolved fluorescence resonance energy transfer and bioluminescence resonance energy transfer: the human δ opioid receptor displays constitutive oligomerization at the cell surface which is not regulated by receptor occupancy. *J. Biol. Chem.* **276:** 14092-14099.

McMillin, S.M., Heusel, M., Liu, T., Costanzi, S., and Wess, J. (2011) Structural basis of M3 muscarinic receptor dimer/oligomer formation. *J. Biol. Chem.* **286:** 28584-28598

Milligan, G. (2004) Applications of bioluminescence and fluorescence resonance energy transfer to drug discovery at G protein-coupled receptors. *Eur. J. Pharm. Sci.* **21:** 397-40
Milligan, G. (2009) G protein-coupled receptor hetero-dimerisation: contribution to pharmacology and function. *Brit. J. Pharmacol*. **158:** 5-14

Milligan, G. (2013) The prevalence, maintenance, and relevance of G protein-coupled receptor oligomerization. *Mol. Pharmacol.* **84:** 158-169.

Milligan, G. (2013) The prevalence, maintenance, and relevance of G protein-coupled receptor oligomerization. *Mol. Pharmacol.* **84(1):** 158-169.

Milligan, G., Lopez-Gimenez, J., Wilson, S., and Carillo, J.J. (2004) Selectivity in the oligomerisation of G protein-coupled receptors. *Seminars in Cell and Develop. Biol.* **15:** 263-268

Milligan, G., and McGrath, J.C. (2009) GPCR theme editorial. *Br. J. Pharmacol.* **158:** 1-4

Morello, J.P., Salahpour, A., Laperriere, A., Bernier, V., Arthus, M.F., Lonergan, M., Petaja-Repo, U., Angers, S., Morin, D., Bichet, D.G., and Bouvier, M. (2000) Pharmacological chaperones rescue cell-surface expression and function of misfolded V2 vasopressin receptor mutants. *J. Clin. Invest.* **105:** 887– 895.

Mundell, S.J., and Benovic, J.L. (2000) Selective regulation of endogenous G protein-coupled receptors by arrestins in HEK293 cells. *J. Biol. Chem.* **275:** 12900-12908

Mustafa. S., See, H. B., Seeber, R. M., Armstrong, S. P., White, C. W., Ventura, S., Ayoub, M. A., and Pfleger, K. D. (2012) Identification and profiling of novel α1A-adrenoceptor-CXC chemokine receptor 2 heteromer. *J. Biol. Chem.* **287(16):** 12952-65

Nakajima, K., Jain, S., Ruiz de Azua, I., McMillin, S.M., Rossi, M., and Wess, J. (2013) Minireview: Novel Aspects of M_3 Muscarinic Receptor Signaling in Pancreatic β-Cells. *Mol. Endocrinol.* **27:** 1208-1216

Neves, S. R., Ram, P. T., and Iyengar, R. (2002) G protein pathways. *Science* **296:** 1636-1639

Norman, A.B., Eubanks, J.H., and Creese, I. (1989) Irreversible and quaternary muscarinic antagonists discriminate multiple muscarinic receptor binding sites in rat brain. *J. Pharmacol. and Experimental Therapeutics* **248:** 1116-1122

Novi, F., Stanasila, L., Giorgi, F., Corsini, G.U., Cotecchia, S., and Maggio, R. (2005) Paired activation of two components within muscarinic M_3 receptor dimers is required for recruitment of β-arrestin-1 to the plasma membrane. *J. Biol. Chem.* **280:** 19768-19776

Oakley, R.H., Laporte, S.A., Holt, J.A., Caron, M.G., and Barak LS. (2000) Differential affinities of visual arrestin, beta arrestin1, and beta arrestin2 for G protein-coupled receptors delineate two major classes of receptors. *J. Biol. Chem.* **275:** 17201-17210.

Pal, K., Melcher, K., and Xu, H.E. (2012) Structure and mechanism for recognition of peptide hormones by Class B G-protein-coupled receptors**.** *Acta Pharmacol. Sin.* **33:** 300-311

Palczewski, K. (2006) G protein-coupled receptor rhodopsin. *Annu. Rev. Biochem.* **75:** 743-767

Palczewski, K., Kumasaka, T., Hori, T., Behnke, C.A., Motoshima, H., Fox, B.A., Le Trong, I., Teller, D.C., Okada, T., Stenkamp, R.E., Yamamoto, M., and Miyano, M. (2000) Crystal structure of rhodopsin: a G protein-coupled receptor. *Science* **289:** 739-745

Pan, H.L., Wu, Z.Z., Zhou, H.Y., Chen, S.R., Zhang, H.M., and Li, D.P. (2008) Modulation of pain transmission by G protein-coupled receptors. *Pharmacol. Ther.* **117:** 141-161

Park, J.H., Scheerer, P., Hofmann, K.P., Choe, H.W., and Ernst, O.P. (2008) Crystal structure of the ligand-free G-protein-coupled receptor opsin. *Nature* **454:** 183-187

Park, P. S., and Wells, J. W. (2003) Monomers and oligomers of the M2 muscarinic cholinergic receptor purified from Sf9 cells. *Biochemistry.* **42(44):** 12960-71.

Patowary, S. Alvarez-Curto, E., Xu, T.R., Holz, J.D., Oliver, J.A., Milligan, G., and Raicu, V. (2013) The muscarinic M_3 acetylcholine receptor exists as two differently sized complexes at the plasma membrane. *Biochem. J.* **452:** 303-312

Pei, Y., Rogan, S.C., Yan, F., and Roth, B.L. (2008) Engineered GPCRs as tools to modulate signal transduction. *Physiology* **23:** 313-321

Pellisier, L.P., Barthet, G., Gaven, F., Cassier, E., Trinquet, E., Pin, J-P., Marin, P., Dumuis, A., Bockaert, J., Baneres, J.L., and Claeysen, S. (2011) G protein activation by serotonin type 4 receptor dimers: evidence that turning on two protomers is more efficient. *J. Biol. Chem.* **286:** 9985-9997

Petaja-Repo, U.E., Hogue, M., Laperriere, A., Bhalla, S., Walker, P., and Bouvier, M. (2001) Newly synthesized human delta opioid receptors retained in the endoplasmic reticulum are retrotranslocated to the cytosol, deglycosylated, ubiquitinated, and degraded by the proteasome. *J. Biol. Chem.* **276:** 4416-23.

Perez, D.M. (2005) From Plants to Man: The GPCR 'Tree of Life'. *Mol. Pharmacol.* **67:** 1383-1384

Perez, D.M., and Karnik, S.S. (2005) Multiple signaling states of G-protein-coupled receptors. *Pharmacol. Rev.* **57:** 147-161

Pin, J-P., Neubig, R., Bouvier, M., Devi, L., Filizola, M., Javitch, J.A., Lohse, M.J., Milligan, G., Palczewski, K., Parmentier, M., and Spedding, M. (2007) International Union of Basic and Clinical Pharmacology. LXVII. Recommendations for the recognition and nomenclature of G protein-coupled receptor heteromultimers. *Pharmacol. Rev.* **59:** 5-13

Pisterzi, L.F., Jansma, D.B., Georgiou, J., Woodside, M.J., Tai-Chieh, J., Angers, S., Raixu, V., Wells, J.W. (2010) Oligomeric size of the M_2 muscarinic receptor in live cells

as determined by quantitative fluorescence resonance energy transfer. *J. Biol. Chem.* **285:** 16723-16738

Pou, C., Mannoury la Cour, C., Stoddart, L. A., Millan, M., and Milligan, G. (2012) Functional homomers and heteromers of dopamine D_{2L} and D_3 receptors co-exist at the cell surface. *JBC.* **287:** 8864-8878

Raffa, R.B. (2009) The M5 muscarinic receptor as possible target for treatment of drug abuse. *J. Clin. Pharm. Ther.* **34:** 623-629

Rashid, A.J., O'Dowd, B.F., Verma, V., and George, S.R. (2007) Neuronal Gq/11-coupled dopamine receptors: an uncharted role for dopamine. *Trends Pharmacol. Sci*. **28:** 551-555

Rasmussen, S.G., DeVree, B.T., Zou, Y., Kruse, A.C., Chung, K.Y., Kobilka, T.S., Thian, F.S., Chae, P.S., Pardon, E., Calinski, D., Mathiesen, J.M., Shah, S.T., Lyons, J.A., Caffrey, M., Gellman, S.H., Steyaert, J., Skiniotis, G., Weis, W.I., Sunahara, R.K., and Kobilka, B.K. (2011) Crystal structure of the β2 adrenergic receptor-Gs protein complex. **Nature 477:** 549-555

Raufman, J.P., Samini, R., Shah, N., Khurana, S., Shan, J., Drachenberg, C., Xie, G., Wess, J., and Cheng, K. (2008) Genetic ablation of M_3 muscarinic receptors attenuates murine colon epithelial cell proliferation and neoplasia. *Cancer Res.* **68:** 3573-3578

Redfern, C.H., Coward, P., Degtyarev, M.Y., Lee, E.K., Kwa, A.T., Hennighausen, L., Bujard, H., Fishman, G.I., and Conklin, B.R. (1999) Conditional expression and signaling of a specifically designed Gi-coupled receptor in transgenic mice. *Nat. Biotechnol.* **17:** 165–169

Redka, D.S., Monzumi, T., Elmslie, G., Paranthaman, P., Shivnaraine, R.V., Ellis, J., Ernst, O.P., and Wells, J.W. (2014) Coupling of G proteins to reconstituted monomers and tetramers of the M_2 muscarinic receptor. *J. Biol. Chem.* **289:** 24347-24365

Rivero-Muller, A., Chou, Y.Y., Ji, I., Lajic, S., Hanyaloglu, A.C., Jonas, K., Rahman, N., Ji, T.H., and Huhtaniemi, I. (2010) Rescue of defective G protein-coupled receptor

function in vivo by intermolecular cooperation. *Proc. Natl. Acad. Sci. USA* **107:** 2319-2324

Rocheville, M., Lange, D.C., Kumar, U., Patel, S.C., Patel, R.C., and Patel, Y.C. (2000a) Receptors for dopamine and somatostatin: formation of hetero-oligomers with enhanced functional activity. *Science* **288:** 154-157

Rocheville, M., Lange, D.C., Kumar, U., Sasi, R., Patel, R.C., and Patel, Y.C. (2000b) Subtypes of the somatostatin receptor assemble as functional homo- and heterodimers. *J. Biol. Chem.* **275:** 7862-7869

Rogan, S.C., and Roth, B.L. (2011) Remote control of Neuronal signaling. *Pharmacol. Rev*. **63:** 291-315

Rosenbaum, D. M., Cherezov, V., Hanson, M.A., Rasmussen, S.G., Thian, F.S., Kobilka, T.S., Choi, H.J., Yao, X.J., Weis, W.I., Stevens, R.C., and Kobilka, B.K. (2007) GPCR engineering yields high-resolution structural insights into β_2-adrenergic receptor function. *Science* **318:** 1266-1273

Ruprecht, J.J., Mielke, T., Vogel, R., Villa, C., and Schertler, G.F. (2004) Electron crystallography reveals the structure of metarhodopsin I. *EMBO J.* **23:** 3609-3620

Sadja, R., Alagem, N., and Reuveny, E. (2003) Gating of GIRK channels: Details of an intricate membrane-delimited signaling complex. *Neuron* **39:** 9-12

Salahpour, A., Angers, S., Mercier, J.E., Lagace, M., Marullo, S., and Bouvier, M. (2004) Homodimerisation of the beta2-adrenergic receptor as a prerequisite for cell surface targeting. *J. Biol. Chem.* **279:** 33390-33397

Sartania, N., Appelbe, S., Pediani, J.D., and Milligan, G. (2007) Agonist occupancy of a single monomeric element is sufficient to cause internalization of the dimeric β_2-adrenoceptor. *Cell Signal.* **19:** 1928-1938

Scearce-Levie, K., Coward, P., Redfern, C.H., and Conklin, B.R. (2001) Engineering receptors activated solely by synthetic ligands (RASSLs). *Trends Pharmacol Sci.* **22:** 414–420.

Scearce-Levie, K., Lieberman, M.D., Elliott, H.H., and Conklin, B.R. (2005) Engineered G protein-coupled receptors reveal independent regulation of internalization, desensitization and acute signaling. *BMC Biol.* **3:** 3

Schlador, M.L., Grubbs, R.D., and Nathanson, N.M. (2000). Multiple topological domains mediate subtype-specific internalization of the M2 muscarinic acetylcholine receptor. *J. Biol. Chem.* **275:** 23295-23302

Shukla, A.K., Manglik, A., Kruse, A.C., Xiao, K., Reis, R.I.,Tseng, W-C., Staus, D.P., Hilger, D., Uysal, S., Huang, L-Y., Paduch, M., Tripathi-Shukla, P., Koide, A., Koide, S., Weis, W.I., Kossiakoff, A.A., Kobilka, B.K., and Lefkowitz, R.J. (2013) Structure of active β-arrestin1 bound to a G protein-coupled receptor phosphopeptide. *Nature* **497:** 137-141

Spengler, D., Waeber, C., Pantaloni, C., Holsboer, F., Bockaert, J., Seeburg, P.H., and Journo, L. (1993) Differential signal transduction by five splice variants of the PACAP receptor. *Nature (Lond.)* **365:** 170-175

Srinivasan, S., Santiago, P., Lubrano, C., Vaisse, C., and Conklin, B.R. (2007) Engineering the melanocortin-4 receptor to control constitutive and ligand-mediated G(S) signaling in vivo. *PLoS ONE* **2:** e668

Srinivasan, S., Vaisse, C., and Conklin, B.R. (2003) Engineering the melanocortin-4 receptor to control G(s) signaling in vivo. *Ann. N.Y. Acad. Sci.* **994:** 225–232

Strader, C.D., Gaffren, T., Sugg, E.E., Rios Candelore, M., Keys, R., Patchett, A.A., and Dixon, R.A.F. (1991) Allele specific activation of genetically engineered receptor. *J. Biol. Chem.* **266:** 5-8

Sunahara, R.K., and Taussig, R. (2002) Isoforms of mammalian adenylyl cyclase: multiplicities of signaling. *Mol. Interv.* **2:** 168-184

Sur, C., Mallorga, P.J., Wittmann, M., Jacobson, M.A., Pascarella, D., Williams, J.B., Brandish, P.E., Pettibone, D.J., Scolnick, E.M., and Conn, P.J. (2003) N-desmethylclozapine, an allosteric agonist at muscarinic 1 receptor, potentiates N-methyl-$_D$-aspartate receptor activity. *Proc. Natl. Acad. Sci. USA* **100:** 13674-13679

Sweger, E.J., Casper, K.B., Scearce-Levie, K., Conklin, B.R., and McCarthy, K.D. (2007) Development of hydrocephalus in mice expressing the G(i)-coupled GPCR Ro1 RASSL receptor in astrocytes. *J. Neurosci.* **27:** 2309-2317

Terrillon, S., and Bouvier, M. (2004) Roles of G-protein-coupled receptor dimerisation. *EMBO Reports* **5:** 30-34

Terrillon, S., Durroux, T., Mouillac, B., Breit, A., Ayoub, M.A., Taulan, M., Jockers, R., Barberis, C., and Bouvier, M. (2003) Oxytocin and vasopressin V1a and V2 receptors form constitutive homo- and heterodimers during biosynthesis. *Mol. Endocrinol.* **17:** 677-691

Terrillon, S., Barberis, C., and Bouvier, M. (2004) Heterodimerisation of V1a and V2 vasopressin receptors determines the interaction with beta-arrestin and their trafficking patterns. *Proc. Natl. Acad. Sci. USA* **101:** 1548-1553

Tobin, A.B., and Budd, D.C. (2003) The anti-apoptotic response of the Gq/11-coupled muscarinic receptor family. *Biochem. Soc. Trans.* **31:** 1182-1185

Traynor, J.R., and Neubig, R.R. (2005) Regulators of G protein signaling and drugs of abuse. *Mol. Interv.* **5:**30-41

Trinquet, E., and Mathis, G. (2006) Fluorescent technologies for the investigation of chemical libraries. *Mol. BioSyst.* **2:** 380-387

Tsutsui, K., and Shichida, Y. (2010). Multiple functions of Schiff base counterion in rhodopsins. *Photochem. Photobiol. Sci.* **9:** 1426-1434.

Tsukamoto, H., Sinha, A., DeWitt, M., and Farrens, D.L. (2010) Monomeric rhodopsin is the minimal functional unit required for arrestin binding. *J. Mol. Biol*. **399:** 501-511

Tsuga, H., Kameyama, K., Haga, T., Lameh, J., and Sadee, W. (1998) Internalization and downregulation of human muscarinic acetylcholine receptor m2 subtypes. Role of third intracellular m2 loop and G protein-coupled receptor kinase 2. *J. Biol. Chem.* **273:** 5323-5330

Uchiyama, T., and Chess-Williams, R. (2004) Muscarinic receptor subtypes of the bladder and gastrointestinal tract. *J. Smooth Muscle Res.* **40:** 237-247

van der Westhuizen, E.T., Valant, C., Sexton, P.M., and Christopoulos, A. (2015) Endogenous allosteric modulators of G protein-coupled receptors. *J. Pharmacol. Exp. Ther.* **353:** 246-260

Vassart, G. (2010) An in vivo demonstration of functional G protein-coupled receptor dimers. *Proc. Natl. Acad. Sci. USA* **107:** 1819-1820

Venkatakrishnan, A.J., Deupi, X., Lebon, G., Tate, C.G., Schertler, G.F., and Babu, M.M. (2013) Molecular signatures of G-protein-coupled receptors. *Nature* **494:** 185-194

Vernier, P., Cardinaud, B., Valdenaire, O., Philippe, H., and Vincent, J.D. (1995) An evolutionary view of drug-receptor interaction: the bioamine receptor family. *Trends Pharmacol. Sci.* **16**: 375-381

Versele, M., Lemaire, K., and Thevelain, J.M. (2001) Sex and sugar in yeast: two distinct GPCR systems. *EMBO Rep.* **2:** 574-579

Vilardaga, J. P., Bunemann, M., Krasel, C., Castro, M., and Lohse, M. J. (2003) Measurement of the millisecond activation switch of G protein-coupled receptors in living cells. *Nature Biotechnol.* **21:** 807-812

Vilardaga, J.P., Hayes, S.C., Levin, M.E., and Muto, T. (2009) Creating a strategy for progress: a contextual behavioural science approach. *Behav. Anal.* **32:** 105-133

Wang, D., Sun, X., Bohn, L.M., and Sadee, W. (2005) Opioid receptor Homo- and Heterodimerisation in living cells by quantitative Bioluminescence Resonance Energy Transfer. *Mol. Pharmacol.* **67:** 2173-2184

Warne, T., Serrano-Vega, M.J., Baker, J.G., Moukhametzianov, R., Edwards, P.C., Henderson, R., Leslie, A.G., Tate, C.G., and Schertler, G.F. (2008) Structure of a beta1-adrenergic G-protein-coupled receptor. *Nature* **454:** 486-491

Weiner, D.M., Levey, A.I., and Brann, M.R. (1990) Expression of muscarinic acetylcholine and dopamine receptor mRNAs in rat basal ganglia. *Proc. Natl. Acad. Sci. USA* **87:** 7050-7054

Wess, J. (1998) Molecular basis of receptor/G-protein-coupling selectivity. *Pharmacol Ther.* **80:** 231-264.

Wess, J. (2004) Muscarinic acetylcholine receptor knockout mice: novel phenotypes and clinical implications. *Annu. Rev. Pharmacol. Toxicol.* **44:** 423-450

Wess, J. (2012) Novel muscarinic receptor mutant mouse models. **Handb. Exp. Pharmacol**. **208:** 95-117

Wess, J., Eglen, R.M., and Gautam, D. (2007) Muscarinic acetylcholine receptors, mutant mice provide new insights for drug development. *Nat. Rev. Drug Discov.* **6:** 721-733

Wettschureck, N., and Offermanns, S. (2005) Mammalian G proteins and their cell type specific functions. *Physiol. Rev.* **85:** 1159–1204.

Wheatley, M., and Hawtin, S.R. (1999) Glycosylation of G protein coupled receptors for hormones central to normal reproductive functioning: its occurrence and role. *Human Reproduct. Update.* **5:** 356-364

White, J.H., Wise, A., Main, M.J., Green, A., Fraser, N.J., Disney, G.H., Barnes, A.A., Emson, P., Foord, S.M., and Marshall, F.H. (1998) Heterodimerisation is required for the formation of a functional $GABA_B$ receptor. *Nature* **396:** 679-682

Whorton, M.R., Jastrzebska, B., Park, P.S., Fotiadis, D., Engel, A., Palczewski, K., and Sunahara, R.K. (2008) Efficient coupling of transducin to monomeric rhodopsin in a phospholipid bilayer. *J. Biol. Chem.* **283:** 4387- 4394

Wilson, S., Wilkinson, G., and Milligan, G. (2005) The CXCR1 and CXCR2 receptors form constitutive homo- and heterodimers selectively and with equal apparent affinities. *J. Biol. Chem*. **280:** 28663-28674

Wu, B., Chien, E.Y., Mol, C.D., Fenalti, G., Liu, W., Katrtich, V., Abagyan, R., Broon, A., Wells, P., Bi, F.C., Hamel, D.J., Kuhn, P., Handel, T.M., and Cherezov, R.C. (2010) Structures of the CXCR4 chemokine GPCR with small molecule and cyclic peptide antagonists. *Science* **330:** 1066-1071

Wu, H., Wacker, D., Mileni, M., Katritch, V., Han, G.W., Vardy, E., Liu, W., Thomson, A.A., Huang, X.P., Carroll, F.I., Mascarella, S.W., Westkaemper, R.B., Mosier, P.D., Roth, B.L., Cherezov, V., and Stevens, R.C. (2012) Structure of the human κ-opioid receptor in complex with JDTic. *Nature* **485:** 327-332

Xu, J., He, J., Castleberry, A.M., Balasubramanian, S., Lau, A.G., and Hall, R.A. (2003) Heterodimerization of alpha 2A- and beta 1-adrenergic receptors. J. Biol. Chem. **278:** 10770-10777

Xu, T-R., Ward, R.J., Pediani, J.D., and Milligan, G. (2011) The orexin OX_1 receptor exists predominantly as a homodimer in the basal state: potential regulation of receptor organisation by both agonist and antagonist ligands. *Biochem. J.* **439:** 171-183

Yamada, M., Lamping, K.G., Duttaroy, A., Zhang, W., Cui, Y., Bymaster, F.P.., McKinzie, D.L., Felder, C.C., Deng, C-X., Faraci, F.M., and Wess, J. (2001) Cholinergic dilation of cerebral blood vessels is abolished in M5 muscarinic acetylcholine receptor knockout mice. *Proc. Natl. Acad. Sci. USA.* **98:** 14096-14101

Yan, Z., Flores-Hernandez, J., and Surmeier, D.J. (2001) Coordinated expression of muscarinic receptor messenger RNAs in striatal medium spiny neurons. *Neurosci.* **103:** 1017-1024

Zeng, F.Y., Hopp, A., Soldner, A., and Wess, J. (1999) Use of a disulfide cross-linking strategy to study muscarinic receptor structure and mechanisms of activation. *J. Biol. Chem.* **274:** 16629-16640.

Zeng, F.Y. and Wess, J. (1999) Identification and molecular characterisation of m3 muscarinic receptor dimers. *J. Biol. Chem.* **274:** 19487-19497

Zhang, W., Yamada, J., Gomeza, A.S., Basile, J., and Wess, J. (2002) Multiple muscarinic acetylcholine receptor subtypes modulate striatal dopamine release, as studied with M1-M5 muscarinic receptor knock-out mice. *J. Neurosci.* **22:** 6347-6352

Zhou, X.E., Melcher, K., and Xu, H.E. (2012) Structure and activation of rhodopsin. *Acta Pharmacol. Sin.* **33:** 291-299

Additional material

The following paper was published as a result of the studies carried out for this thesis.